

Superconducting phases of *f*-electron compounds

Christian Pfeleiderer*

Physik Department E21, Technische Universität München, D-85748 Garching, Germany

(Published 25 November 2009)

Intermetallic compounds containing *f*-electron elements display a wealth of superconducting phases, which are prime candidates for unconventional pairing with complex order parameter symmetries. For instance, superconductivity has been found at the border of magnetic order as well as deep within ferromagnetically and antiferromagnetically ordered states, suggesting that magnetism may promote rather than destroy superconductivity. Superconducting phases near valence transitions or in the vicinity of magnetopolar order are candidates for new superconductive pairing interactions such as fluctuations of the conduction electron density or the crystal electric field, respectively. The experimental status of the study of the superconducting phases of *f*-electron compounds is reviewed.

DOI: [10.1103/RevModPhys.81.1551](https://doi.org/10.1103/RevModPhys.81.1551)

PACS number(s): 74.20.Mn, 74.70.Tx

CONTENTS

I. Introduction	1552	2. URhGe	1586
A. Superconductivity versus magnetism	1552	B. Border of ferromagnetism	1588
B. Road map to superconducting phases	1555	1. UCoGe	1588
II. Interplay of Antiferromagnetism and Superconductivity	1556	2. UIr	1588
A. Border of antiferromagnetism	1556	3. Note on <i>d</i> -electron ferromagnets	1589
1. The series CeM_2X_2	1556	IV. Emergent Classes of Superconductors	1589
a. $CeCu_2Si_2$ and $CeCu_2Ge_2$	1557	A. Noncentrosymmetric superconductors	1589
b. $CePd_2Si_2$ and $CeNi_2Ge_2$	1559	1. $CePt_3Si$	1591
c. $CeRh_2Si_2$	1560	2. $CeMX_3$	1594
2. The series $Ce_nM_mIn_{3n+2m}$	1560	a. $CeRhSi_3$	1594
a. $CeIn_3$	1562	b. $CeIrSi_3$	1595
b. Introduction to $CeMIn_5$	1563	c. $CeCoGe_3$	1595
c. $CeCoIn_5$	1563	3. UIr	1596
d. $CeRhIn_5In$	1565	B. Superconductivity near electron localization	1597
e. $CeIrIn_5$	1566	1. Border of valence transitions	1597
f. Ce_2RhIn_8	1567	2. Plutonium- and neptunium-based systems	1597
g. Substitutional doping in $Ce_nM_mIn_{3n+2m}$	1567	a. $PuCoGa_5$ and $PuRhGa_5$	1598
h. Common features and analogies	1568	b. $NpPd_5Al_2$	1600
3. Miscellaneous Ce systems	1569	C. Border of polar order	1601
a. $CeNiGe_3$	1569	1. $PrOs_4Sb_{12}$	1601
b. $Ce_2Ni_3Ge_5$	1570	2. $PrRu_4P_{12}$	1604
c. $CePd_5Al_2$	1570	V. Multiple Phases	1604
B. Coexistence with antiferromagnetism	1570	A. Order parameter transitions	1604
1. Large-moment antiferromagnets	1570	1. Superconducting phases of UPt_3	1604
a. UPd_2Al_3	1571	2. Further candidates	1605
b. UNi_2Al_3	1574	a. $CeCu_2Si_2$	1605
c. $CePt_3Si$	1576	b. $CeNi_2Ge_2$	1605
2. Small moment antiferromagnets	1576	c. $CeIrIn_5$	1605
a. UPt_3	1576	d. UPd_2Al_3	1605
b. URu_2Si_2	1578	e. URu_2Si_2	1606
C. The puzzling properties of UBe_{13}	1580	f. UBe_{13}	1606
III. Interplay of Ferromagnetism and Superconductivity	1581	g. UGe_2	1606
A. Superconducting ferromagnets	1581	h. URhGe	1606
1. UGe_2	1581	i. $CePt_3Si$ and $CeMX_3$	1606
		j. $PrOs_4Sb_{12}$	1606
		B. Textures	1607
		1. Fulde-Ferrell-Larkin-Ovchinnikov states	1607
		2. Magnetic domains versus flux lines	1609
		VI. Perspectives	1609
		Acknowledgments	1610
		References	1610

*christian.pfleiderer@frm2.tum.de

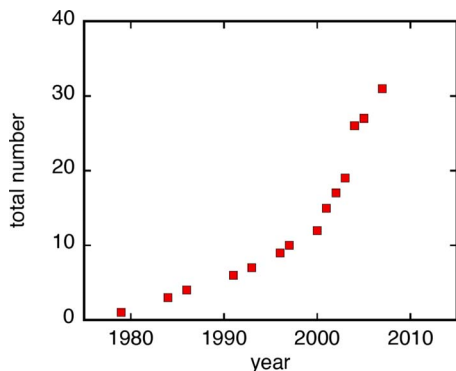


FIG. 1. (Color online) Evolution of the total number of *f*-electron heavy-fermion superconductors. Systems included in this plot and covered in this review: 1979, CeCu₂Si₂; 1984, UBe₁₃ and UPt₃; 1986, URu₂Si₂; 1991, UPd₂Al₃ and UNi₂Al₃; 1993, CeCu₂Ge₂; 1996, CePd₂Si₂ and CeNi₂Ge₂; 1997, CeIn₃; 2000, CeRhIn₅ and UGe₂; 2001, CeIrIn₅, CeCoIn₅, and URhGe; 2002, PuCoGa₅ and PrOs₄Sb₁₂; 2003, Ce₂RhIn₈ and PuRhGa₅; 2004, CeNiGe₃, Ce₂Ni₃Ge₅, UIr, PrRu₄P₁₂, CePt₃Si, CeIrSi₃, and CeRhSi₃; 2005, PrRu₄Sb₁₂; 2007, UCoGe, NpPd₅Al₂, CeCoGe₃, and CePd₅Al₂.

I. INTRODUCTION

Superconductivity was discovered almost a century ago, yet unexpected and fascinating new variants of this same old theme are being found at an increasing pace. This is due to great technical advances in materials preparation and an increasingly more systematic screening of new compounds. Prior to the late 1970s all known superconductors could be accounted for in terms of a condensate of Cooper pairs, with the Cooper pairs forming due to electron-phonon interactions. With the discovery of the superfluid phases of ³He this understanding began to change in two ways (Osheroff *et al.*, 1972; Vollhardt and Wölfle, 1990). First, ³He provided an example of non-electron-phonon-mediated pairing. Second, it provided an example of a superfluid condensate that breaks additional symmetries. The discovery of heavy-fermion superconductivity as a prime candidate for complex order parameter symmetries and non-electron-phonon-mediated pairing in *f*-electron compounds nearly three decades ago was long recognized as an important turning point in the history of superconductivity. However, progress in heavy-fermion superconductivity until not long ago was slow.

In recent years the superconductivity in the cuprates, ruthenates, cobaltates, pyrochlores, and iron pnictides in particular has received great attention. However, a spectacular series of discoveries and developments in *f*-electron superconductors took place at the same time. While in the first 12 years following the discovery of heavy-fermion superconductivity in CeCu₂Si₂ only five more heavy-fermion superconductors were identified, more than 25 additional systems have been found in the past 15 years (see Fig. 1). By now over 30 systems are known, about half of which were discovered in the past five years alone. This illustrates the recent increase in

the speed of development of the field of *f*-electron superconductivity.

There is now growing appreciation that superconducting phases of *f*-electron compounds frequently exist at the borders of competing and coexisting forms of electronic order. For the majority of systems, including the original heavy-fermion superconductors, an interplay with antiferromagnetism is observed. However, there are also several examples of superconductivity that coexists with ferromagnetism. Further examples include superconductivity at the border of polar order and near electron localization transitions. Finally, several heavy-fermion superconductors have even been discovered with noncentrosymmetric crystal structures and coexistent antiferromagnetic order. The large variety of systems found so far establishes unconventional *f*-electron superconductivity as a rather general phenomenon. It also suggests the existence of further unimagined forms of superconductivity.

The objective of this review is to give a status report on the experimental properties of the candidates for unconventional *f*-electron superconductivity. For a long time the search for a unified microscopic theory of *f*-electron superconductivity has been hampered by the large differences among the small number of known systems. Although the increasing number of systems has allowed great progress in theoretical understanding, a critical discussion of the theoretical scenarios is well beyond the length constraints of the present review. For reviews of selected compounds and theoretical scenarios we refer to Grewe and Steglich (1991); Sigrist and Ueda (1991); Sauls (1994); Mineev and Samokhin (1999); Joynt and Taillefer (2002); Sigrist (2005); Thalmeier and Zwicknagl (2005); Thalmeier *et al.* (2005); Flouquet (2006); Flouquet *et al.* (2006); Maple *et al.* (2008).

The outline of this paper is as follows. The Introduction (Sec. I) presents a short account of conventional superconductivity and its interplay with magnetism, Fermi liquid quasiparticle interactions, and advances in materials preparation. In Sec. II we address the interplay of antiferromagnetism and superconductivity. Section III is concerned with ferromagnetism and superconductivity, while we review the properties of emergent classes of new superconductors, discovered recently, in Sec. IV. Finally, in Sec. V, we summarize evidence for multiple superconducting phases in UPt₃ and tentative indications for such behavior in other systems as well as evidence for the formation of textures. We conclude with a short section on the general perspectives of this field.

A. Superconductivity versus magnetism

Superconductors are so called because they are perfect electrical conductors. However, in contrast to ideal conductors, superconductors display, as their second defining property, perfect diamagnetism, i.e., in the superconducting state sufficiently low applied magnetic fields are spontaneously expelled. The flux expulsion identifies superconductivity as a thermodynamic phase.

The two defining properties of superconductors, notably perfect conductivity and perfect diamagnetism, were discovered by Onnes in 1911 (1911a, 1911b, 1911c) and Meissner and Ochsenfeld in 1933, respectively, but it was not until 1957 that Bardeen, Cooper, and Schrieffer (BCS) proposed a remarkably successful theoretical framework (Bardeen *et al.*, 1957). There is a large number of introductory and advanced level textbooks and review papers on this topic, e.g., Parks, 1969; Tinkham, 1969; Gennes, 1989; Waldram, 1996; Sigrist, 2005. BCS theory identifies superconductivity as the quantum-statistical condensation of so-called Cooper pairs, which are bound pairs of quasiparticle excitations in a Fermi liquid. For a simple Hamiltonian describing attractively interacting quasiparticles in a conduction band, it is possible to show the formation of an excitation gap Δ in the quasiparticle spectrum at the Fermi level E_F .

A superconducting transition exists for quasiparticle systems with both attractive and repulsive components of the quasiparticle interactions (Morel and Anderson, 1962). For instance, in the presence of electron-phonon interactions the Coulomb repulsion of conduction electrons is screened and exhibits a retarded attractive interaction component below the Debye frequency. Physically speaking, the electrons avoid the bare Coulomb repulsion and attract each other in terms of a polarization trace that decays slowly as compared with the travel speed of the electrons. The mathematical form of T_s is essentially the same as for purely attractive interactions, but the Coulomb interaction enters in a renormalized form. The same is also true when the full retarded solution is followed in the Eliashberg strong-coupling formalism (Eliashberg, 1960), which leads to the MacMillan form of T_s (MacMillan, 1968; Allen and Dynes, 1975). We return to more complex quasiparticle interactions of strongly correlated electron systems in Sec. I.B.

The experimental characteristics of conventional superconductors derive from the formation of an isotropic gap at the Fermi surface. This implies that bulk properties such as the specific heat show an exponential temperature dependence below T_s and, in the weak-coupling limit, an anomaly $\Delta C/\gamma T_s=1.43$. At the heart of the theory the superconducting state is the formation of quantum-mechanical phase coherence, as seen in several microscopic probes. For instance, the NMR spin-lattice relaxation rate shows coherence effects such as the Hebel-Slichter peak and an exponential freezing out below T_s (for a pedagogical discussion with examples, see Tinkham, 1969; Waldram, 1996). The rigidity of the superconductivity against external perturbations is expressed by the phase stiffness of the superconducting condensate, as measured by the coherence length ξ . The length scale of the variations in the superconducting order parameter is expressed by the Pippard or Ginzburg-Landau coherence length.

When electron-phonon coupling is taken into account, the resulting screened retarded quasiparticle interactions are short ranged, representing essentially contact interactions. For the corresponding Cooper pair wave function, which is composed of the product of an orbital

and a spin contribution, this implies that the orbital contribution has to be in the $l=0$ channel (no angular momentum) and the spin part has to have spin-singlet character ($s=0$, opposing spin directions). Otherwise the range of the attractive interaction component is shorter than the average distance apart of the electrons.

Characteristic length scales that determine the way applied magnetic fields suppress superconductivity are the coherence length ξ , on the one hand, and the penetration depth λ , on the other hand. If the ratio $\kappa = \lambda/\xi$ exceeds $1/\sqrt{2}$ the energy density of the surface separating the normal and superconducting states becomes negative, and the superconducting state is referred to as being type II. Here magnetic field penetrates in flux lines carrying the flux quantum $\Phi_0=h/2e$ (Abrikosov, 1952). The flux lines are organized in a lattice with a geometry that minimizes the ground state energy. All the compounds addressed in this review are strong type-II superconductors and the morphology of the flux line lattice yields information on the nature of the superconductivity; for recent work in pure Nb see Laver *et al.* (2006); Mühlbauer, Pfeleiderer, *et al.* (2009).

Microscopically, applied magnetic fields suppress superconductivity by interacting with either the orbital or the spin momentum. For pure orbital limiting the upper critical field $H_{c2}^{\text{orb}}(T \rightarrow 0) = \Phi_0/(2\pi\xi^2)$ is connected with the initial slope of H_{c2}^{orb} near T_s as $H_{c2}^{\text{orb}}(T \rightarrow 0) = -0.7dH_{c2}/dT|_{T_s}$ (Saint-James *et al.*, 1969). This is in contrast to pure Pauli limiting of the upper critical field, which is related to T_s as $H_{c2}^{\text{Pauli}}(T \rightarrow 0) = 1.84T_s$, where H is in T and T_s is in K (Chandrasekhar, 1962; Clogston 1962). The ratio of orbital to Pauli limiting is expressed by the Maki parameter $\alpha = \sqrt{2}H_{c2}^{\text{Pauli}}/H_{c2}^{\text{orb}}$ (Saint-James *et al.*, 1969). It is also known that the transition at H_{c2} for pure Pauli limiting becomes first order below $T^{\text{f}} = 0.56T_s$ (Saint-James *et al.*, 1969; Ketterson and Song, 1999).

Since the early days of research in superconductivity, the effect of internal magnetic fields (e.g., exchange fields) on the superconductivity was of much interest. Theoretical work suggested that static or dynamic internal magnetic fields would prevent superconductivity (Ginzburg, 1957; Berk and Schrieffer, 1966). In the limit of extreme purity and pure Pauli limiting, i.e., large values of α , a novel state was predicted to be possible, which consists of real-space modulations of superconductivity with a weakly spin-polarized normal state (Fulde and Ferrell, 1964; Larkin and Ovchinnikov, 1965). We return to the experimental status of this so-called Fulde-Ferrell-Larkin-Ovchinnikov (FFLO) phase in *f*-electron systems in Sec. V.B.1.

Experimentally the question of internal magnetic fields in superconducting materials was at first followed up in studies of binary and pseudobinary systems with rare-earth impurities (R) such as $\text{La}_{1-x}\text{R}_x$ and $\text{Y}_{1-x}\text{R}_x\text{Os}_2$ (Matthias *et al.*, 1958b). Early studies suffered from metallurgical complexities due to clustering and glassy types of magnetic order and were somewhat inconclusive. They motivated more detailed studies,

however, which led to a fairly advanced understanding of paramagnetic impurities in superconductors. Reviews have been given in, e.g., [Maple \(1976, 1995, 2005\)](#); [White and Geballe \(1979\)](#). Overall it was accepted that magnetic impurities are detrimental to superconductivity, while it was also appreciated that conventional superconductivity is fairly insensitive to nonmagnetic defects ([Anderson, 1959](#)).

These studies have shown that the rate of suppression of T_s is highest in the middle of the rare-earth series ([Matthias *et al.*, 1958b](#); [Maple, 1970](#)), consistent with the strongest pair breaking due to magnetic exchange interactions ([Herring, 1958](#); [Suhl and Matthias, 1959](#); [Abrikosov and Gor'kov, 1961](#)). An exception is Ce, which causes an anomalously large depression of T_s due to the strong hybridization of the *f* electrons with the conduction electrons. A more detailed understanding of magnetic impurity effects on superconductors requires an understanding of the properties of magnetic moments that are dissolved in a nonmagnetic host. In the Kondo effect, the conduction electrons hybridize with the magnetic moment, eventually forming a screening cloud below a characteristic temperature T_K , the Kondo temperature (for an introduction see, e.g., [Hewson, 1993](#)). Alternatively, the moment may be quenched by low-lying crystal fields. While the former leads to strong Cooper pair breaking, the latter reduces its effects.

Pioneering studies of $\text{Ce}_{1-x}\text{La}_x\text{Al}_2$ revealed the presence of Kondo screening with a Kondo temperature $T_K \sim 0.2$ K ([Maple and Fisk, 1968](#); [Felsch and Winzer, 1973](#); [Andrei, 1982](#)). $\text{Ce}_{1-x}\text{La}_x\text{Al}_2$ displays reentrant superconductivity ([Riblet and Winzer, 1971](#); [Maple *et al.*, 1972](#)) i.e., the superconducting transition at T_{s1} is followed by a second characteristic temperature $T_{s2} < T_{s1}$ below which superconductivity vanishes again. The re-entrance may be understood as resulting from an increasing strength of the pair breaking of the paramagnetic impurities with decreasing temperature because $T_K < T_s$ ([Müller-Hartmann and Zittartz, 1971](#)). The strength of pair breaking due to Kondo screening was also studied in high-pressure experiments on $\text{La}_{1-x}\text{Ce}_x$ alloys, where the superconductivity vanishes in a finite pressure interval for $x=0.02$ as the Kondo temperature increases under pressure ([Maple *et al.*, 1972](#)). As a side effect of the detailed studies of $\text{Ce}_{1-x}\text{La}_x\text{Al}_2$ it was also recognized that even pure CeAl_2 displays a Kondo effect, thus qualifying as perhaps the first example of a Kondo lattice ([van Daal and Buschow, 1969](#); [Maple, 1969](#); [Buschow and van Daal, 1970](#)). The effect of crystal electric fields (CEFs) in removing the magnetic moment was studied in the series $\text{La}_{1-x}\text{Pr}_x\text{Tl}_3$, where superconductivity vanishes only slowly, because the crystal fields reduce the pair breaking strength with increasing x ([Bucher *et al.*, 1972](#)).

In contrast to a purely competitive form of superconductivity and magnetism, doping studies in the series $\text{Ce}_{1-x}\text{Gd}_x\text{Ru}_2$ also suggested the possibility of coexistence of superconductivity and magnetism in small parameter regimes ([Matthias *et al.*, 1958a](#); [Hein *et al.*, 1959](#);

[Phillips and Matthias, 1961](#)). By the late 1970s two series of compounds had been discovered that display such an extremely delicate balance of superconductivity and magnetism intrinsically, notably RRh_4B_4 , where *R* is a rare earth, and the Chevrel phases such as DyMo_6S_8 ([Fertig *et al.*, 1977](#); [Ishikawa and Fischer, 1977](#); [Moncton *et al.*, 1977](#); [Bulaevskii *et al.*, 1985](#)). These compounds are frequently referred to as magnetic superconductors. As a key feature T_s in these systems is always larger than the magnetic ordering temperature.

The interplay of magnetism and superconductivity is exemplified by $\text{Er}_{1-x}\text{Ho}_x\text{Rh}_4\text{B}_4$, in which the onset of ferromagnetism destroys superconductivity. In a small temperature interval for small x magnetic order succeeds in coexisting with superconductivity by formation of a modulated state. This firmly suggests that superconductivity and magnetism are antagonistic forms of order. However, for selected antiferromagnetic members of this series a constructive interplay of magnetism and superconductivity can be inferred from an increase in H_{c2} below T_N . In contrast to the systems reviewed here, in the series $\text{Er}_{1-x}\text{Ho}_x\text{Rh}_4\text{B}_4$ superconductivity and magnetism may be viewed as residing in separate microscopic subsystems. Comprehensive reviews of this field may be found in [Fischer and Maple \(1982\)](#); [Maple and Fischer \(1982\)](#); [Fischer \(1990\)](#).

As a side remark, these compounds also provided the first hints of the Jaccarino-Peter effect ([Jaccarino and Peter, 1962](#)), an enhancement of the superconductivity when an applied field cancels any internal magnetic fields. In recent years further compounds have been discovered with coexistence in separate subsystems, notably the ruthenocuprates ([Otzschi *et al.*, 1999](#); [Frazer *et al.*, 2001](#); [Klamut *et al.*, 2001](#)) and the borocarbides $\text{RNi}_2\text{B}_2\text{C}$ ($R=\text{Gd-Lu, Y}$) ([Mazumdar and Nagarajan, 2005](#); [Budko and Canfield, 2006](#)).

The possibility of unconventional superconducting order parameter symmetries had been anticipated theoretically when the superfluid phases of ^3He were discovered; reviews may be found in [Leggett \(1975\)](#); [Wheatly \(1975\)](#); [Vollhardt and Wölfle \(1990\)](#). In particular, ^3He provided a first example of a constructive interplay of superconductivity and the magnetic properties of the system. Theoretically it had been suggested that ferromagnetic fluctuations may mediate superconductive pairing ([Layzer and Fay, 1971](#); [Fay and Appel, 1977](#)) and that superconductivity may even exist in itinerant ferromagnets ([Fay and Appel, 1980](#)). However, for a long time there was no evidence supporting this suggestion in real materials.

During the 1970s advances were also made in the understanding of intermediate-valence compounds; see, e.g., [Buschow \(1979\)](#) and [White and Geballe \(1979\)](#). As a key feature nonmagnetic members of this group of materials exhibit enhanced Fermi liquid coefficients such as the linear specific heat $\gamma=C/T$ or quadratic temperature dependence of the resistivity $A=\Delta\rho/T^2$. A number of compounds, such as CeAl_3 , even displayed particularly strong renormalization effects of the Fermi liquid coef-

ficients (Andres *et al.*, 1975). These are known as heavy-fermion systems. Among these, superconductivity was observed for the first time in CeCu₂Si₂ (Steglich *et al.*, 1979). The large specific heat anomaly of CeCu₂Si₂ at the superconducting transition immediately suggested that strongly renormalized quasiparticle excitations take part in the pairing. Moreover, under small changes in stoichiometry the ground state of CeCu₂Si₂ was found to become magnetically ordered. This vicinity to magnetic order suggested an important role of magnetic correlations in the superconductive pairing.

The discovery of heavy-fermion superconductivity created intense experimental and theoretical effort. For early reviews see (Stewart *et al.*, 1984; Grewe and Steglich, 1991). However, in the first 12 years following the discovery of superconductivity in CeCu₂Si₂ (Steglich *et al.*, 1979) only five more heavy-fermion superconductors were discovered [UBe₁₃ (Bucher *et al.*, 1975), UPt₃ (Stewart *et al.*, 1984), URu₂Si₂ (Schlabitz *et al.*, 1984, 1986; Maple *et al.*, 1985; Palstra *et al.*, 1985), UPd₂Al₃, and UNi₂Al₃ (Geibel, Schank, Thies, *et al.*, 1991; Geibel, Thies, Kazorowski, *et al.*, 1991)]. Because the microscopic details of these systems proved to be remarkably different, a unified theoretical understanding turned out to be a challenge.

B. Road map to superconducting phases

In recent years several factors have proved to be almost universally important in the search for further examples of superconducting phases of *f*-electron compounds: first, an improved appreciation of the quasiparticle interactions in Fermi liquids; second, the experimental ability to tune these interactions in pure metallic systems in a controlled manner by means of a nonthermal control parameter such as pressure, stress, or magnetic field; and third, and most important, great advances in materials preparation. In the following we discuss these developments.

A simple plausibility argument shows that the superconductive pairing in heavy-fermion systems is probably not driven by electron-phonon interactions and that the order parameter is most likely unconventional, i.e., the order parameter breaks additional symmetries. Given the importance of retardation for electron-phonon-mediated pairing and the local character of the interaction, it is helpful to keep in mind that the travel speed of a quasiparticle excitation in heavy-fermion systems typically is reduced by nearly three orders of magnitude. Thus the effects of repulsive quasiparticle interaction components for a conventional pairing symmetry ($l=0$ and $s=0$) can no longer be avoided. However, the repulsive components of the interactions may be avoided in higher angular momentum and spin states of the Cooper pairs.

A systematic search for novel forms of superconductive pairing interactions and pairing symmetries hence requires a systematic quantitative determination of the quasiparticle interactions in the presence of strong elec-

tronic correlations. A search also requires very clean samples since unconventional pairing tends to be extremely sensitive to nonmagnetic defects. As a rule of thumb, the charge carrier mean free path needs to be substantially larger than the coherence length for superconductivity to occur.

Quite generally the quasiparticle interactions may be expressed in terms of the generalized dynamical response function of the system. For instance, in systems at the border of magnetic order this is expressed in terms of the wave-vector- (ω) and frequency- (\vec{q}) dependent magnetic susceptibility $\chi(\vec{q}, \omega)$; for a pedagogical introduction see Lonzarich (1997). Experimentally, quasiparticle excitation spectra and the related interaction potentials may be explored in quantum oscillatory studies. Careful comparison of the experimentally observed quasiparticle enhancements with the response function determined in, neutron scattering allows the development of a simple description of the generalized quasiparticle interactions.

A program of this kind was first systematically carried out in the 1980s for weakly and nearly magnetic transition-metal compounds and selected *f*-electron systems. For reviews of this work see Lonzarich (1980, 1987, 1988). More recent reviews of quantum oscillatory studies may be found in Onuki 1993; Onuki and Hasegawa (1995); Settai, Takeuchi, *et al.* (2007). An important aspect of the early work was that it became possible at the same time to calculate quantitatively the magnetic ordering temperature of weakly magnetic itinerant-electron systems (Lonzarich and Taillefer, 1985; Moriya, 1985). This paved the way for a quantitative analysis of superconducting pairing interactions in weakly ferromagnetic and antiferromagnetic compounds (see, e.g., Dungate, 1990), and eventually allowed an educated guess at which systems to study; see also Monthoux *et al.* (2007).

The quasiparticle interactions were finally tuned by means of high hydrostatic pressures in pure samples. The experiments served to clarify two questions: first, to identify possible examples of magnetically mediated superconductivity (for early attempts see, e.g., Cordes *et al.*, 1981) and second, to investigate the nature of the metallic state in the vicinity of a quantum critical point. We note that quantum phase transitions, quite generally, are defined as phase transitions that are driven by quantum fluctuations. In practice this means that quantum phase transitions are zero-temperature second-order phase transitions. It transpires that quantum phase transitions represent an extremely rich field of condensed matter physics. For reviews see Hertz, (1976); Sachdev, (1999); Stewart (2001, 2006); Vojta (2003); Belitz *et al.*, (2005); Löhneysen *et al.* (2007). In recent years this definition has been relaxed somewhat, and zero temperature phase transitions in general are referred to as quantum phase transitions (Pfeleiderer, 2005).

Besides the advances in understanding the metallic state in the presence of strong electronic correlations, advances have also been achieved in the experimental techniques; for a recent review in *5f* states in actinides,

see Moore and van der Laan (2009). Studies under extreme conditions such as very low temperatures, high pressures, and high magnetic fields are now routinely possible in numerous laboratories.

Most important, however, are major improvements in materials preparation, for instance, by purification of the starting elements. Electrotransport of uranium under ultrahigh vacuum was found to be extremely efficient in removing impurities such as Fe and Cu (Fort, 1987; Haga *et al.*, 1998). Electrotransport in combination with annealing under ultrahigh vacuum has also been used to promote the formation of large single-crystal grains and improve the sample quality (Schmidt and Carlson, 1976; Haga *et al.*, 2007; Matsuda *et al.*, 2008). For the growth of high-vapor-pressure compounds a closed crucible annealing technique was developed (Assmus *et al.*, 1984). In many materials the combination of ultrahigh vacuum with an inert gas atmosphere is sufficient to obtain large high-quality single crystals (McDonough and Huxley, 1995). This cannot be underestimated given that both the rare earth and actinide elements readily react, especially with oxygen, hydrogen, and nitrogen. Advances in the understanding of the phase diagrams of binary and ternary compounds have motivated the improvement and extensive use of techniques such as traveling-solvent float zoning or the controlled use of flux methods in the skutterudites or the series of $Ce_nM_mIn_{3n+2m}$ compounds. Finally, in recent years, an increasing number of groups have explored the use of optical floating-zone furnaces for the growth of intermetallic compounds (see, e.g., Souptel *et al.*, 2007). For example, large single crystals of UNi_2Al_3 (Mihalik *et al.*, 1997) and of URu_2Si_2 (see, e.g., Pfeleiderer *et al.*, 2006) have been grown. It is expected that this technique will play an important future role.

A frequent discussion in materials preparation concerns the relative importance of the various aspects. For instance, it is believed that the accuracy at which perfect stoichiometry can be achieved generally outweighs any efforts put into the purification of the starting elements. Empirically this is contrasted by the impressive list of unusual phenomena such as unconventional superconductivity that have been discovered in ultrapure compounds. Perhaps the most important challenge in materials preparation is the lack of methods for characterization. Generally speaking, high sample quality is proven by the combination of standard characterization (x-ray diffraction, microprobe, etc.) plus the physical properties themselves. This shows that despite all of the technical achievements the growth of high-quality single crystals continues to require great physical intuition, systematic work, and a fair bit of luck.

II. INTERPLAY OF ANTIFERROMAGNETISM AND SUPERCONDUCTIVITY

In this section we review the interplay of antiferromagnetism and *f*-electron superconductivity. Section II.A reviews systems where superconductivity emerges at the border of itinerant antiferromagnetism. In particular, properties of the series CeM_2X_2 and

$Ce_nM_mIn_{3n+2m}$ are addressed. Section II.B is concerned with superconductivity in antiferromagnetic compounds. This includes large-moment systems such as UPd_2Al_3 and UNi_2Al_3 as well as small-moment systems such as UPt_3 and URu_2Si_2 .

A. Border of antiferromagnetism

1. The series CeM_2X_2

The discovery of heavy-fermion superconductivity in $CeCu_2Si_2$ (Steglich *et al.*, 1979) was the first indication of unconventional superconductivity (Stewart *et al.*, 1984; Grewe and Steglich, 1991; Thalmeier *et al.*, 2005; Sparn *et al.*, 2006). $CeCu_2Si_2$ crystallizes in the tetragonal $ThCr_2Si_2$ crystal structure, as summarized in Table I. The heavy-fermion superconductivity in $CeCu_2Si_2$ generated much interest in the isostructural series of CeM_2X_2 compounds, where *M* is a transition metal ($M = Cu, Au, Rh, Pd, Ni$) and $X = Si$ or Ge . Because most members of this series exhibit antiferromagnetic order (Grier *et al.*, 1984; Thompson *et al.*, 1986) it represented a major breakthrough for the entire field when superconductivity was discovered in $CeCu_2Ge_2$, $CeRh_2Si_2$, and in particular $CePd_2Si_2$, as well as incipient superconductivity in $CeNi_2Ge_2$. For a summary see also Table I. Being a derivative of the $BaAl_4$ parent structure, the $ThCr_2Si_2$ structure is intimately related to the $BaNiSn_3$ and $CaBe_2Ge_2$ types of structures, as shown in Fig. 2. A surprise in recent years was the discovery of superconductivity in several Ce-based compounds with the non-centrosymmetric $BaNiSn_3$ structure because it was believed that triplet superconductivity cannot exist in crystal structures lacking inversion symmetry. For an account of this work see Sec. IV.A.2. Interestingly, no superconductivity has so far been found among the $CaBe_2Ge_2$ relatives of the $ThCr_2Si_2$ series, which is also noncentrosymmetric.

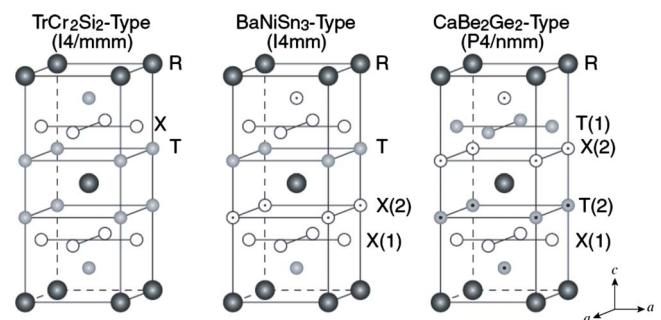


FIG. 2. (Color online) Variations in the tetragonal $BaAl_4$ crystal structure. The $ThCr_2Si_2$ structure is frequently found among CeM_2X_2 compounds reviewed in Sec. II.A.1. The $BaNiSn_3$ crystal structure, which lacks inversion symmetry, is typical of the $CeMT_3$ compounds reviewed in Sec. IV.A. Among *f*-electron systems with the noncentrosymmetric $CaBe_2Ge_2$ structure no compounds are known that exhibit superconductivity. From Kimura, Muro, and Aoki, 2007.

TABLE I. Key properties of superconductors in the series CeM_2X_2 (M : Cu, Pd, Rh, Ni; X : Si, Ge) and various miscellaneous Ce-based systems. Missing table entries may reflect more complex behavior discussed in the text. References are given in the text. Critical field values represent extrapolated $T=0$ values. (AF, antiferromagnet; SC, superconductor; and ISC, incipient superconductor.)

	CeCu ₂ Si ₂	CeCu ₂ Ge ₂	CePd ₂ Si ₂	CeRh ₂ Si ₂	CeNi ₂ Ge ₂	CeNiGe ₃	Ce ₂ Ni ₃ Ge ₅	CePd ₅ Al ₂
Structure	Tetragonal	Tetragonal	Tetragonal	Tetragonal	Tetragonal	Orthorh.	Orthorh.	Tetragonal
Type	ThCr ₂ Si ₂	SmNiGe ₃	U ₂ Co ₃ Si ₅	ZrNi ₂ Al ₅				
Space group	$I4/mmm$	$I4/mmm$	$I4/mmm$	$I4/mmm$	$I4/mmm$	$Cmmm$	$Ibam$	$I4/mmm$
a (Å)	4.102	4.186	4.223	4.092	4.150	21.808	9.814	4.156
b (Å)	9.930	10.299	9.897	10.181	9.842	4.135	11.844	4.156
c (Å)	9.930	10.299	9.897	10.181	9.842	4.168	5.963	14.883
c/a	2.420	2.460	2.343	2.488	2.372			
State	AF, SC	AF, SC	AF, SC	AF, SC	ISC	AF, SC	AF, SC	AF, SC
T_N (K)	0.8	4.15	10	36, 25		5.5	5.1, 4.5	3.9, 2.9
\vec{Q}	(0.22, 0.22, 0.53)	(0.28, 0.28, 0.53)	(0.5, 0.5, 0)	(0.5, 0.5, 0)	(0.5, 0.5, 0.5)			
μ_{ord} (μ_B)	0.1	1	0.62	1.42, 1.34		0.8	0.4	
γ (J/mol K ²)	1		0.062	0.027			0.09	0.056
T_s^{max} (K)	0.7, 2.5	0.64	0.4	0.42	0.3, 0.4	0.45	0.26	0.57
p_s^{max} (kbar)	0, 30	70	28	10	0, 18	70	36	108
$\Delta C / \gamma_n T_s$	1.4							
H_{c2}^{ab} (T)	0.45	2	0.7			1.55	0.7	0.25
$\frac{d}{dT} H_{c2}^{ab}$ (T/K)		-11	-12.7			-10.8		-1.04
H_{c2}^c (T)			1.3	0.28				
$\frac{d}{dT} H_{c2}^c$ (T/K)			-16	-1				
ξ_0^{ab} (Å)		90	300			100	210	
ξ_0^c (Å)			230	340				
Discovery of SC	1979	1993	1996	1996	1996	2004	2005	2007

a. CeCu₂Si₂ and CeCu₂Ge₂

The ground state properties of CeCu₂Si₂ are extremely sensitive to the precise Cu content, which may be controlled by an annealing procedure under Cu vapor (Assmus *et al.*, 1984). Samples with heavy-fermion superconductivity, antiferromagnetism, or a combination thereof may be obtained; they are referred to as S, A, or AS, respectively. For Cu-deficient samples the spin-density-wave (SDW) order is stabilized and the superconductivity is destroyed, while the SDW is destabilized and the superconductivity is stabilized for Cu excess. Since the changes in composition achieved under Cu annealing are less than a few percent, it is believed that the changes in properties originate mostly in changes in unit cell volume (Trovarelli *et al.*, 1997). This may be inferred also from doping with Ge which, being larger than Si, stabilizes the SDW, while hydrostatic pressure destabilizes the SDW and stabilizes the superconductivity (Krimmel and Loidl, 1997; Trovarelli *et al.*, 1997). In the following it is convenient to address S-type samples first.

Quite generally the normal state of CeCu₂Si₂ is characteristic of a heavy Fermi liquid with an extrapolated zero temperature Sommerfeld coefficient $C/T = \gamma = 1$ J/mol K² and an equally enhanced Pauli susceptibility. The heavy-fermion state develops in a crystal electric field ground state Kramers doublet and first and second excited doublets at 12.5 and 31 meV (Horn *et al.*, 1981). S-type samples of CeCu₂Si₂ display $T_s = 0.7$ K, accompanied by a distinct specific heat anomaly $\Delta C / \gamma T_s = 1.4$. These results established for the first time that heavy quasiparticles may undergo superconductive pairing. Under a magnetic field the superconductivity exhibits strong Pauli limiting with $H_{c2} \approx 0.45$ T (Rauchschwalbe *et al.*, 1982). The leading order temperature dependences of the specific heat $C(T)$, thermal expansion α (Lang *et al.*, 1991), and penetration depth λ (Gross *et al.*, 1988) vary as T^2 , which is characteristic of line nodes. NMR and nuclear quadrupole resonance (NQR) show the absence of a Hebel-Slichter peak and a power law dependence of the spin-lattice relaxation rate, also sug-

gesting line nodes (Ishida *et al.*, 1999; Kawasaki *et al.*, 2004).

The magnetic phase diagram of CeCu_2Si_2 for a magnetic field applied along the *a* axis in the basal plane is fairly complex (Bruls *et al.*, 1990 1994; Steglich *et al.*, 2001). Ultrasound and thermal expansion measurements suggested the presence of two spin-density-wave phases, referred to as A and B phases, respectively. A magnetic field first suppresses the superconductivity above H_{c2} , where the A phase is restored. The *B*-*T* boundary of the A phase is reminiscent of $H_{c2}(T)$ as if the A phase encompasses the superconductivity. Above a critical field $H_c \approx 6.4$ T a magnetic field suppresses the A phase and stabilizes the B phase. Little is known about the nature of the B phase.

Microscopic evidence for SDW order in CeCu_2Si_2 was absent for nearly 25 years. Progress was made only recently by systematic tracking the incommensurate spin-density-wave order of CeCu_2Ge_2 as a function of increasing Si content. It was found that the ordering wave vector changes little as a function of Si content, yielding a value of $\vec{Q} = (0.215, 0.215, 0.530)$ in AS samples of CeCu_2Si_2 (Stockert *et al.*, 2004). Neutron scattering studies identified an incommensurate spin-density wave in the A phase with a small ordered moment $\mu_{\text{ord}} \approx 0.1\mu_B$ per Ce site in CeCu_2Si_2 ; it evolves from the antiferromagnetic order in CeCu_2Ge_2 continuously with increasing Si content. The ordering wave vector thus agrees with the nesting wave vector found in Fermi surface calculations (Zwicknagl and Pulst, 1993). For the AS samples antiferromagnetism and superconductivity are mutually exclusive and separated by a first-order phase transition (Sparn *et al.*, 2006).

As a function of pressure, T_s in S-type CeCu_2Si_2 increases at around 2 GPa and enters a plateau of 2.25 K above 2.5 GPa, followed by a moderate decrease with a small shoulder around 7 GPa, as shown in Fig. 3 (Belarbi *et al.*, 1984; Thomas *et al.*, 1993). The unusual pressure dependence suggested that $T_s(p)$ may be explained in terms of two or more pairing interactions. The discovery of superconductivity in CeCu_2Ge_2 (Jaccard *et al.*, 1992) and CeRh_2Si_2 (Movshovich *et al.*, 1996), and in particular in CePd_2Si_2 (Mathur *et al.*, 1998), underscored the idea that superconductivity in CeCu_2Si_2 is somehow related to the magnetic properties. At the border of the A phase non-Fermi-liquid (NFL) properties of the normal metallic state were observed over a small temperature range that are characteristic of quantum critical spin fluctuations, where $\Delta\rho(T) \propto T^{3/2}$ and $C/T = \gamma = \gamma_0 - \alpha\sqrt{T}$ (Gegenwart *et al.*, 1998).

Under moderate doping with Ge, which introduces pair breaking defects, the superconducting phase disintegrates into two domes, as shown in Fig. 3 (Yuan *et al.*, 2003; Holmes *et al.*, 2004). Based on these studies two pairing interactions were proposed: antiferromagnetically mediated pairing in the vicinity of the SDW and pairing by charge-density fluctuations in the vicinity of a valence transition at high pressures. The latter consists of fluctuations that originate in a Ce^{3+} to Ce^{4+} change in

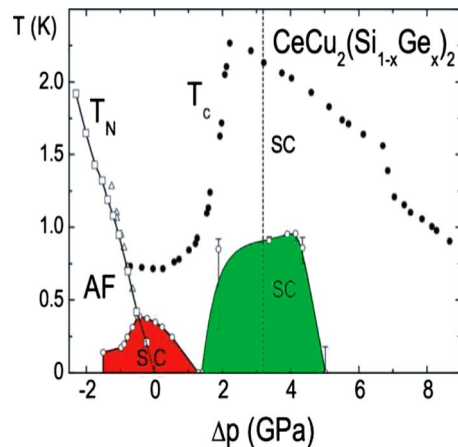


FIG. 3. (Color online) Temperature vs pressure phase diagram of $\text{CeCu}_2\text{Si}_{2-x}\text{Ge}_x$. The pressure dependence of the superconducting transition temperature, here denoted T_c , in S-type CeCu_2Si_2 exhibits a plateau between 20 and 70 kbar (black dots). Weak impurity scattering in moderately Ge-doped CeCu_2Si_2 decomposes the superconductivity into two domes, one at the border of antiferromagnetism and the other at a presumed valence transition. From Thalmeier *et al.*, 2005, representing a compilation of several studies described in the text.

valence, where the *4f* electron is delocalized in the high-pressure Ce^{4+} state. We address the question of charge-fluctuation-mediated pairing in Sec. IV.B.1.

The superconducting pairing symmetry has been reconsidered with knowledge of incommensurate SDW and band structure calculations based on the renormalized local density approximation (LDA) (Thalmeier *et al.*, 2005). A superconducting *d*-wave singlet state $d_{x^2-y^2}$ and the SDW order are treated here as two competing ordering phenomena. The model accounts for the change from the incommensurate SDW order in the A phase to superconductivity, where both order parameters have the Γ_3 symmetry imposed by the crystal electric fields.

Analogies of the thermopower in superconducting samples of CeCu_2Si_2 with CeCu_2Ge_2 motivated high-pressure experiments in CeCu_2Ge_2 (Jaccard *et al.*, 1992). At ambient pressure CeCu_2Ge_2 orders antiferromagnetically below $T_N = 4.15$ K into an incommensurate sinusoidally modulated structure with $\vec{Q} = (0.284, 0.284, 0.543) \pm 0.001$ and an ordered moment $\mu_{\text{ord}} = 0.74\mu_B$ (Knopp *et al.*, 1989; Krimmel *et al.*, 1997). The low-temperature properties develop in a crystal electric field environment of a ground state doublet and a first excited quartet at 19.1 meV. The metallic state of CeCu_2Ge_2 is moderately enhanced.

Under pressure, the Néel temperature of CeCu_2Ge_2 decreases and vanishes at $p_N \approx 70$ kbar (Jaccard *et al.*, 1992). Superconductivity appears above the critical pressure; $T_s \approx 0.64$ K is only weakly pressure dependent and extends over a wide range, and $H_{c2} \approx 2$ T with a large initial slope $dH_{c2}/dT = -11$ T/K. This suggests a coherence length of order $\xi = 90$ Å. The structural similarity and lack of pressure dependence of T_s suggest an inti-

mate similarity with CeCu_2Si_2 . In fact, evidence for a valence transition in CeCu_2Ge_2 at ~ 150 kbar, where T_s is largest, has been inferred from x-ray diffraction (Onodera *et al.*, 2002).

b. CePd_2Si_2 and CeNi_2Ge_2

The intense studies of the quasiparticle interactions in weakly ferromagnetic transition-metal compounds and selected *f*-electron systems mentioned above (Lonzarich, 1980, 1987, 1988) resulted in quantitative estimates of magnetically mediated superconductivity at the border of weak ferromagnetism. This motivated detailed high pressure studies in MnSi (Pfeleiderer *et al.*, 1993, 2004; Pfeleiderer, McMullan, *et al.*, 1997; Pfeleiderer, Julian, *et al.*, 2001) and related compounds. It also inspired studies of the suppression of antiferromagnetism under pressure of the isostructural and isoelectronic siblings CePd_2Si_2 and CeNi_2Ge_2 reviewed in the following.

At ambient pressure CePd_2Si_2 may be described as an intermediate-valence system. At high temperatures the resistivity varies weakly with temperature, followed by a rapid decrease below ~ 50 K and a sharp drop at the onset of antiferromagnetic order at $T_N \approx 10$ K. The antiferromagnetic order in CePd_2Si_2 consists of alternating ferromagnetic sheets with $\vec{Q}=(1/2, 1/2, 0)$ where the moments are oriented along $[110]$, i.e., they reside in the tetragonal basal plane (Grier *et al.*, 1984). Magnetism has been interpreted as local-moment-like, with a reduced ordered moment $\mu_{\text{ord}}=0.62\mu_B$ in the crystal field environment (van Dijk *et al.*, 2000). The CEF level scheme of the localized $\text{Ce}^{3+} 4f^1$ electrons has been determined from the susceptibility and inelastic neutron scattering as a sequence of three Kramers doublets: $\Gamma_7^{(1)}$ (0), Γ_6 (19 meV), and $\Gamma_7^{(2)}$ (24 meV). The metallic state may be described as a Fermi liquid with a moderately enhanced value of $\gamma=0.062$ J/mol K² (Steeman *et al.*, 1988).

Under pressure T_N in CePd_2Si_2 decreases and vanishes linearly at $p_c \approx 28$ kbar (Thompson *et al.*, 1986; Grosche *et al.*, 1996; Julian, Pfeleiderer, Grosche, *et al.*, 1996; Mathur *et al.*, 1998). Superconductivity has been observed in the immediate vicinity of p_c with a maximum of $T_s \approx 0.4$ K, as shown in Fig. 4. Observation of a wide superconducting dome in some experiments could be traced to pressure inhomogeneities (Raymond and Jaccard, 2000; Sheikin *et al.*, 2001). The gradual decrease in T_N with increasing pressure suggested that the antiferromagnetic order vanishes continuously at p_c . This has been confirmed more recently in neutron scattering experiments of the staggered magnetization (Kernavonis *et al.*, 2005). The expected abundance of quantum critical spin fluctuations near p_c is consistent with the temperature dependence of the electrical resistivity, which displays a power law dependence $\Delta\rho \sim T^{1.2}$ over a wider temperature range (Grosche *et al.*, 1996; Julian, Pfeleiderer, Grosche, *et al.*, 1996; Mathur *et al.*, 1998). In the context of these fluctuations it has been suggested

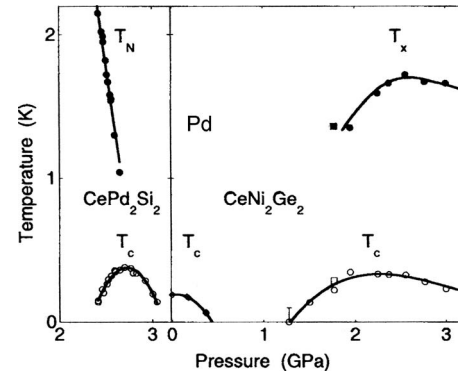


FIG. 4. Combined temperature vs pressure phase diagram of the isostructural isoelectronic pair of systems CePd_2Si_2 and CeNi_2Ge_2 , where superconductivity is observed at the border of antiferromagnetism and at low and high pressures, respectively. From Grosche *et al.*, 2000.

that the fluctuations in CePd_2Si_2 exhibit a reduced dimensionality.

Based on its vicinity to a quantum critical point, the superconducting pairing interaction was attributed to the exchange of antiferromagnetic spin fluctuations (Grosche *et al.*, 1996; Julian, Pfeleiderer, Grosche, *et al.*, 1996; Mathur *et al.*, 1998). Much evidence suggest unconventional pairing; a *d*-wave state appears to be the most promising candidate. The upper critical field and its initial variation are large and anisotropic: $H_{c2}^c=1.3$ T with $dH_{c2}^c/dT=-16$ T/K and $H_{c2}^{ab}=0.7$ T with $dH_{c2}^{ab}/dT=-12.7$ T/K (Sheikin *et al.*, 2001). These values suggest anisotropic Pauli limiting, where weak- or strong-coupling behavior cannot be distinguished unambiguously. The corresponding coherence lengths are quite short with $\xi^{ab}=300$ Å and $\xi^c=230$ Å.

The search for a compound in the CeM_2X_2 series with lattice parameters and electronic structure at ambient pressure that are akin to those of CePd_2Si_2 near p_c motivated further detailed studies of CeNi_2Ge_2 (publication of these studies was delayed for a long time and has been reviewed in Grosche *et al.* (2000)). The temperature versus pressure phase diagram of single-crystal CeNi_2Ge_2 as determined in resistivity measurements is shown on the right-hand side of Fig. 4. The phase diagram is dominated by a non-Fermi-liquid form of the resistivity at ambient pressure and indications of incipient superconductivity below $T_s \sim 0.3$ K. Further studies of the specific heat and susceptibility of polycrystalline samples suggest that CeNi_2Ge_2 at ambient pressure displays a genuine non-Fermi-liquid ground state (Gegenwart *et al.*, 1999). In particular, the specific heat shows a logarithmic divergence $C/T \sim \ln T_0/T$ and the susceptibility shows a square root divergence $\chi \sim \sqrt{T}$ for $T \rightarrow 0$.

Neutron scattering in CeNi_2Ge_2 established high-energy spin fluctuations with a characteristic energy of 4 meV at an incommensurate wave vector $\vec{q}=(0.23, 0.23, 0.5)$ (Fåk *et al.*, 2000). The wave vector is in good agreement with the ordering wave vector of the spin density wave in CeCu_2Si_2 and CeCu_2Ge_2 . The spin

fluctuations are quasi-two-dimensional, characteristic of a sine-modulated structure with the magnetic moments in the [110] plane. However, with decreasing temperature no critical slowing down of the high-energy spin fluctuations in CeNi₂Ge₂ is observed as may be expected for a quantum critical system.

Another surprise in CeNi₂Ge₂ was the observation of additional hints of superconductivity at high pressure (Grosche, Lister, *et al.*, 1997; Grosche, *et al.*, 2000). The origin of this superconductivity could not be related to a particular instability like a quantum phase transition; an anomaly of unknown origin in the normal state resistivity was denoted T_x . One possibility is a valence transition like the one considered in CeCu₂Si₂, but this has not been explored further. The evidence for superconductivity in CeNi₂Ge₂ is based purely on the resistivity, while no evidence for bulk superconductivity has been found in the samples studied to date.

c. CeRh₂Si₂

A pressure-induced transition from an antiferromagnetic ground state to superconductivity exists also in CeRh₂Si₂ (Movshovich *et al.*, 1996). Observation of superconductivity in this system is remarkable because it occurs at a fairly pronounced first-order quantum phase transition that may be related to the delocalization of the 4*f* electron. The properties of CeRh₂Si₂ have been reviewed in Settai, Takeuchi, *et al.* (2007).

At ambient pressure CeRh₂Si₂ orders antiferromagnetically below $T_{N1} \approx 36$ K (Thompson *et al.*, 1986). Neutron scattering establishes an ordering wave vector $\vec{Q}_1 = (1/2, 1/2, 0)$ with the moments aligned along [1, 0, 0] (Kawarazaki *et al.*, 2000). The single- \vec{Q} structure changes into a four- \vec{Q} structure below $T_{N2} \approx 24$ K described by two ordering wave vectors, $\vec{Q}_1 = (1/2, 1/2, 0)$ and $\vec{Q}_2 = (1/2, 1/2, 1/2)$. The ordered moment is quite large and differs slightly for the different Ce sites, namely, $1.42\mu_B$ at the corner site of the tetragonal structure and $1.34\mu_B$ at the body-centered Ce site. The size of the ordered moment is consistent with CEF-split localized 4*f*¹ state of the Ce atom, which when taken together with the entropy released at T_N , $\Delta S(T_N) \approx R \ln 2$, suggests a CEF Kramers doublet. As a function of magnetic field the antiferromagnetism is suppressed above ~ 26 T (Settai *et al.*, 1997). The metallic state is described by a weakly enhanced linear term in the specific heat $\gamma = 0.027$ J/mol K² (Graf *et al.*, 1997), and a quadratic temperature dependence of the resistivity (Grosche, Julian, *et al.*, 1997; Araki, Nakashima, *et al.*, 2002; Ohashi *et al.*, 2002).

As a function of pressure both T_{N1} and T_{N2} decrease and vanish at $p_{N1} = 10$ kbar and $p_{N2} = 6$ kbar, respectively (Kawarazaki *et al.*, 2000). A narrow dome of superconductivity emerges precisely at p_{N1} , where $T_s^{\max} \approx 0.42$ K (Movshovich *et al.*, 1996) with $H_{c2} = 0.28$ T and $dH_{c2}/dT = -1$ T/K for the *c* axis, corresponding to a coherence length of the order $\xi \approx 340$ Å.

Under pressure the ordered moment tracks T_{N1} , and both drop fairly abruptly at p_{N1} . The specific heat coefficient γ increases to 0.08 J/mol K² at p_{N1} and gradually decreases at higher pressures (Graf *et al.*, 1997), while the resistivity exhibits a T^2 resistivity at all pressures, the T^2 coefficient tracking the pressure dependence of γ consistently with the Kadowaki-Woods ratio (Grosche, Julian, *et al.*, 1997; Araki, Nakashima, *et al.*, 2002; Ohashi *et al.*, 2002). These features suggested a first-order transition at p_{N1} . Unambiguous evidence for a first-order suppression of antiferromagnetism was obtained in quantum oscillatory studies as a function of pressure (Araki *et al.*, 2001; Araki, Settai, *et al.*, 2002). More specifically, from the Fermi surface sheets observed it was concluded that the 4*f* electron changes discontinuously from a local to an itinerant state at p_{N1} . This scenario has received further support in recent studies of the thermal expansion under pressure (Villaume *et al.*, 2008).

2. The series Ce_{*n*}M_{*m*}In_{3*n*+2*m*}

The series Ce_{*n*}M_{*m*}In_{3*n*+2*m*} with *M* = Co, Ir, Rh displays heavy-fermion superconductivity with very high transition temperatures as compared to other Ce-based systems. The systems of interest are summarized in Table II. This suggests that a reduction from three to two dimensions is favorable to superconducting pairing. The superconductivity in these systems appears to be tied to the antiferromagnetic order, with similarities to the cuprates. The interplay of magnetism with superconductivity includes several tentative quantum critical points under pressure and magnetic field. There is finally strong evidence for the formation of a FFLO state in CeCoIn₅. Status reports on the series of Ce_{*n*}M_{*m*}In_{3*n*+2*m*} compounds have been given in Sarrao and Thompson (2007) and Settai, Takeuchi, *et al.* (2007).

For a more detailed review it is helpful to begin with the crystal structure of the series Ce_{*n*}M_{*m*}In_{3*n*+2*m*} as shown in Fig. 5. CeIn₃ crystallizes in the cubic Cu₃Au structure, space group *Pm3m*, with a lattice constant $a = 4.690$ Å. The tetragonal crystal structure of the series Ce_{*n*}M_{*m*}In_{3*n*+2*m*} may be derived from the cubic parent compound CeIn₃ in terms of *n*-fold layers of CeIn₃ separated by *m*-fold layers of MIn₂. For the single-layer compounds $n = m = 1$ (CeMIn₅), one layer of MIn₂ is added, while in the double-layer compounds $n = 2, m = 1$ (Ce₂MIn₈), a single layer of MIn₂ is added for every two layers of CeIn₃. Within this general scheme CeIn₃ may therefore be referred to as an ∞ -layer system ($n = \infty, m = 0$).

The low-temperature properties of Ce_{*n*}M_{*m*}In_{3*n*+2*m*} develop in a crystal electric field scheme that is intimately related for all members of the series. For CeIn₃ the CEFs split the $J = 5/2$ manifold into a Γ_7 ground state doublet and a Γ_8 quartet at around 12 eV (Benoit *et al.*, 1980; Groß *et al.*, 1980; Lawrence and Shapiro, 1980; Murani *et al.*, 1993; Christianson *et al.*, 2004). For the series CeMIn₅ the quartet is further split into two, Γ_7

TABLE II. Key properties of the series $Ce_nM_mIn_{3n+2m}$ and Pu- and Np-based heavy-fermion superconductors. Missing table entries may reflect more complex behavior discussed in the text. References are given in the text. Values of H_{c2} are extrapolated for $T \rightarrow 0$.

$Ce_nM_mIn_{3n+2m}$	CeIn ₃	CeCoIn ₅	CeRhIn ₅	CeIrIn ₅	Ce ₂ RhIn ₈	PuCoGa ₅	PuRhGa ₅	NpPd ₅ Al ₂
Structure	Cubic	Tetragonal	Tetragonal	Tetragonal	Tetragonal	Tetragonal	Tetragonal	Tetragonal
Space group	$Pm\bar{3}m$	$P4/mmm$	$P4/mmm$	$P4/mmm$	$P4/mmm$	$P4/mmm$	$P4/mmm$	$I4/mmm$
a (Å)	4.690	4.614	4.652	4.668	4.665(1)	4.2354	4.3012	4.148
c (Å)		7.552	7.542	7.515	12.244(5)	6.7939	6.8569	14.716
c/a	1	1.63676	1.62124	1.6099	2.624	1.604	1.594	3.547
B_0 (GPa)	67.0±3.0	78.2±1.8	78.4±2.0	87.6±2.0	71.4±1.1			
dB_0/dp	2.5±0.5	3.94±0.41	5.60±0.62	5.04±0.58	3.85±0.31			
κ_a (10 ⁻³ GPa ⁻¹)	4.98±0.13	4.35±0.08	3.96±0.08	3.44±0.06	4.20±0.04			
κ_c (10 ⁻³ GPa ⁻¹)	4.98±0.13	3.43±0.16	4.22±0.1	3.48±0.08	4.85±0.11			
CEF scheme	(Γ_7, Γ_8)	($\Gamma_7^1, \Gamma_7^2, \Gamma_6$)	($\Gamma_7^1, \Gamma_7^2, \Gamma_6$)	($\Gamma_7^1, \Gamma_7^2, \Gamma_6$)				
Δ_1, Δ_2 (meV)	12	8.6, 25	6.7, 29	6.9, 24				
State	AF, SC	SC	AF, SC	SC	AF, SC	SC	SC	SC
T_N (K)	10.2		3.8		2.8, 1.65			
\vec{Q}	($\frac{1}{2}, \frac{1}{2}, \frac{1}{2}$)		($\frac{1}{2}, \frac{1}{2}, 0.297$)		($\frac{1}{2}, \frac{1}{2}, 0$)			
μ_{ord} (μ_B)	0.48		0.37		0.55			
μ_{eff}^a (μ_B)						0.75	0.8	3.22
Θ_{CW}^a (K)								-42
μ_{eff}^c (μ_B)						0.75	0.8	3.06
Θ_{CW}^c (K)								-139
γ (J/mol K ²)	0.14		0.4	0.72	0.4	0.077	0.07	0.2
p_N (kbar)	25		17		~25			
T_s (K)	0.19(p_N)	2.3	2.12(p_N)	0.4	1.1	18.5	8.7	4.9
$\Delta C / \gamma_n T_s$		4.5	0.36	0.76		1.4	0.5	2.33
H_{c2}^{ab} (T)	0.45	11.6–11.9		1.0	5.4		27	3.7
$\frac{d}{dT} H_{c2}^{ab}$ (T/K)	-3.2	-24		-4.8	-9.2	-10	-3.5	-6.4
H_{c2}^c (T)	0.45	4.95	10.2	0.49			15	14.3
$\frac{d}{dT} H_{c2}^c / T$ (T/K)	-2.5	-8.2	-15	-2.54		-8	-2	-3.1
dT_s / dt (K/month)						-0.24	-0.39	
ξ_0^{ab} (Å)	300	82	57	260			35	
ξ_0^c (Å)		53		180	77		45	
$\kappa_{\text{GL},a}$ (Å)		108						
$\kappa_{\text{GL},c}$ (Å)		50						
κ_{GL} (Å)						32		28
Discovery of SC	1997	2001	2000	2001	2003	2002	2003	2007

and Γ_6 , Kramers doublets; the values of the first and second energy levels are given in Table II (Christianson *et al.*, 2004).

The series $Ce_nM_mIn_{3n+2m}$ exhibits metallic behavior with a fairly weak temperature dependence of the resistivity at high temperatures. The resistivity decreases monotonically with decreasing temperature, with a shoulder around 50 to 100 K, before decreasing drastically to a very low residual value of a few $\mu\Omega$ cm. The

normal state resistivity and magnetic anisotropy for the single- and double-layer series are weakly anisotropic by a factor of 2. The susceptibility displays a strong Curie-Weiss temperature dependence with the effective fluctuating moment for the easy axis corresponding to the free Ce^{3+} ion. The specific heat is characteristic of strong electronic correlations with a strongly enhanced electronic contribution. However, closer inspection shows that the temperature dependences of these electronic

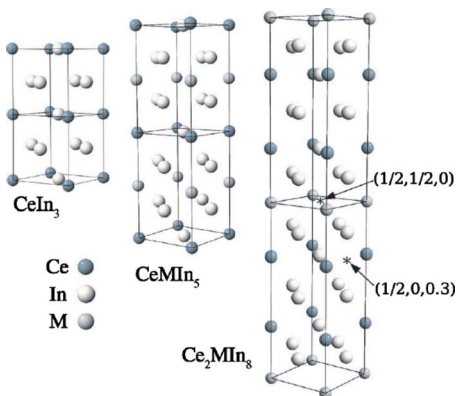


FIG. 5. (Color online) Depiction of the structural series $Ce_n M_m In_{3n+2m}$. The infinite-layer system $CeIn_3$ is shown on the left, the single-layer systems are shown in the middle, the double-layer systems, which are intermediate between the infinite- and the single-layer systems, are shown on the right. Also indicated are typical muon stopping sites in the double-layer system. From [Morris *et al.*, 2004](#).

contributions are more complex and typical of non-Fermi-liquid behavior, as discussed below.

a. $CeIn_3$

We begin with the cubic system $CeIn_3$, which displays the strikingly simple temperature versus pressure phase diagram shown in Fig. 6. Here the superconductivity forms a well-defined dome around an antiferromagnetic quantum critical point (QCP). This makes $CeIn_3$ an important point of reference for those systems in the series that are more two dimensions.

The superconducting properties of $CeIn_3$ are typical of a valence-fluctuating compound, i.e., by comparison

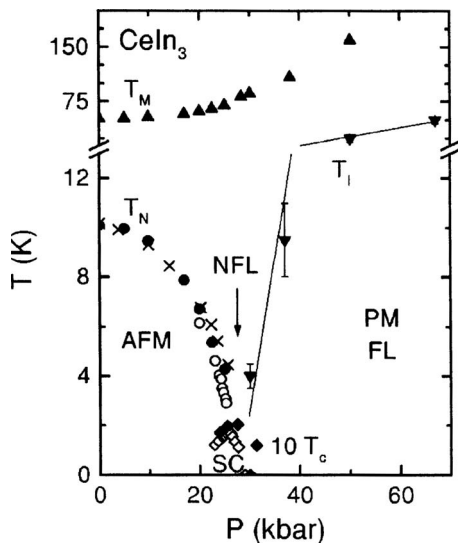


FIG. 6. Temperature vs pressure phase diagram of $CeIn_3$. T_M denotes the coherence maximum in the resistivity, T_N denotes the Néel temperature, T_c denotes the superconducting transition temperature, and T_1 denotes the upper boundary of the regime with Fermi-liquid resistivity. From [Knebel *et al.*, 2001](#).

to traditional heavy-fermion systems they are moderately enhanced with $\gamma=0.14$ J/mol K². The characteristic spin fluctuation temperature is fairly high, $T_{SF}=50$ – 100 K ([Lawrence, 1979](#); [Morin *et al.*, 1988](#)). At ambient pressure $CeIn_3$ orders antiferromagnetically below a Néel temperature $T_N=10.2$ K into a type-II state with ordering wave vector $\vec{Q}=(1/2, 1/2, 1/2)$, i.e., ferromagnetic planes of alternating direction stacked along the (111) cubic space diagonal ([Benoit *et al.*, 1980](#); [Lawrence and Shapiro, 1980](#)). The zero-temperature ordered moment $\mu_{ord}\approx 0.47\mu_B$ is reduced as compared to the value of $\sim 0.71\mu_B$, expected in the CEF ground state given by a Γ_7 doublet. It is also reduced as compared to the Curie-Weiss moment. This is typical of weak itinerant magnetism, where inelastic neutron scattering shows antiferromagnetic magnons as well as quasielastic and crystal field excitations ([Knafo *et al.*, 2003](#)).

Under hydrostatic pressure the Néel temperature in $CeIn_3$ decreases and vanishes continuously at $p_N\approx 25$ kbar ([Morin *et al.*, 1988](#)), consistent with a QCP (Fig. 6). The temperature dependence of the electrical resistivity changes from a quadratic temperature dependence at ambient pressure to $\Delta\rho\sim T^{1.5}$ in a narrow interval near p_N ([Walker *et al.*, 1997](#); [Knebel *et al.*, 2001](#)). This suggests scattering of the charge carriers by antiferromagnetic quantum critical fluctuations. In fact, $CeIn_3$ is one of the very few systems for which the pressure and magnetic field dependences of the resistivity are in good agreement with the predictions of an antiferromagnetic QCP ([Hertz, 1976](#); [Millis, 1993](#)). The existence of a QCP is not indicated by ¹¹⁵In NQR measurements, which show that the spin-lattice relaxation rate $1/T_1T\sim\text{const}$ near p_N as expected of a Fermi liquid ([Kawasaki *et al.*, 2001](#)). Quantum oscillatory studies through p_N further establish a reconstruction of the topology of the Fermi surface, interpreted as a localized to delocalized transition of the *4f* electrons ([Settai *et al.*, 2005](#)). As p_c is approached the cyclotron effective mass becomes strongly enhanced for at least one major Fermi surface sheet, reaching $m^*=60m_0$.

In pure samples of $CeIn_3$ with residual resistivities below $1\mu\Omega\text{ cm}$, the QCP is surrounded by a narrow dome of superconductivity, which exhibits a maximum $T_s\approx 0.22$ K ([Walker *et al.*, 1997](#)). A detailed study up to 100 kbar with a different set of samples and pressure cells showed that the phase diagram is rather robust and highly reproducible ([Knebel *et al.*, 2001](#)). Under a magnetic field T_s initially decreases with $dH_{c2}/dT=-3.2$ T/K, where $H_{c2}(T\rightarrow 0)=0.45$ T, both characteristic of heavy-fermion superconductivity ([Knebel *et al.*, 2001](#); [Onuki *et al.*, 2004](#)). The upper critical field may be accounted for in a strong-coupling framework in the clean limit, where the coherence length $\xi_0=300$ Å and the charge carrier mean free path $l=2000$ Å.

The location of the superconducting dome at the border of antiferromagnetic order, the evidence for quantum critical fluctuations in the resistivity, and the sensitivity of the superconductivity to sample purity ([Walker *et al.*, 1997](#); [Knebel *et al.*, 2001](#)), provide circumstantial

evidence of unconventional pairing. This question has been explored microscopically in NMR and NQR studies. The spin-lattice relaxation rate $1/T_1$ lacks a Hebel-Slichter peak, but the low value of T_s did not permit the temperature dependence below T_s to be determined (Kawasaki *et al.*, 2002). From a theoretical point of view it has been argued that the antiferromagnetic quantum critical spin fluctuations may provide a pairing interaction consistent with the size of T_s (Mathur *et al.*, 1998). A more detailed theoretical analysis suggested that the gap symmetry due to pairing by antiferromagnetic fluctuations near $\vec{Q}=(111)$ is either $d_{x^2-y^2}$ or $d_{3z^2-r^2}$ (Fukazawa and Yamada, 2003).

b. Introduction to $CeMIn_5$

We next turn to the single-layer systems in the series of $Ce_nM_mIn_{3n+2m}$ ($n=m=1$). Key properties are summarized in Table II, and references to the original publications may be found in the text. Much of the appeal of this series is based on the isovalent substitutions represented by the sequence $Co \rightarrow Rh \rightarrow Ir$. In this order the unit cell volume increases, while the c/a ratio of the lattice constants decreases.

Electronic structure calculations show that the Fermi surface in all three systems is highly two dimensional with several cylindrical sheets even though the electrical resistivity and magnetic susceptibility are not strongly anisotropic (see, e.g., Settai *et al.*, 2001). An important aspect for understanding the evolution of the physical properties within this series is that band structure calculations suggest that the transition-metal element affects the electronic properties only indirectly (Sarraf and Thompson, 2007). This may be related to the Ce atoms and the transition-metal atoms residing in different crystallographic planes, which may also explain why substitutional doping provides a comparatively controlled approach to tuning the ground state properties without metallurgical segregation and excessive effects of disorder (Pagliuso *et al.*, 2001; Zapf *et al.*, 2001; Pagliuso, Curro, *et al.*, 2002; Pagliuso, Moreno, *et al.*, 2002; Pagliuso, Movshovich, *et al.*, 2002).

The presentation proceeds as follows. We begin with the general phase diagrams of $CeCoIn_5$, $CeRhIn_5$, and $CeIrIn_5$ and discuss the tentative evidence for QCPs. This is followed by a discussion of the interplay of antiferromagnetism and superconductivity and the evidence for unconventional superconductivity. The section concludes with a discussion of possible analogies with the cuprates.

c. $CeCoIn_5$

$CeCoIn_5$ is a superconductor with a record high value among the Ce-based systems of $T_s=2.3$ K (Petrovic, Pagliuso, *et al.*, 2001). For the c axis $H_{c2}^c=4.95$ T and for the ab plane $H_{c2}^{ab}=11.6$ T. The anisotropy of H_{c2} may be accounted for by the effective mass model (Ikeda *et al.*, 2001; Petrovic, Pagliuso, *et al.*, 2001). Before reviewing the superconducting state of $CeCoIn_5$, it is helpful to

consider the normal state properties, which are in many ways anomalous. The electrical resistivity of $CeCoIn_5$ varies as $\rho(T)=\rho_0+a'T$ (Sidorov *et al.*, 2002) up to ~ 4 K above T_s . Taking into account CEF contributions, the normal state electronic specific heat varies as $C/T \propto -\ln T$, and the c -axis susceptibility diverges as $\chi \propto T^{-0.4}$, while the basal-plane susceptibility is essentially constant, $\chi^{-1} \propto a+bT^{0.1}$ (Kim, Alwood, *et al.*, 2001; Petrovic, Pagliuso, *et al.*, 2001). These normal state non-Fermi-liquid temperature dependences differ distinctly from those of a heavy Fermi-liquid state and suggest the vicinity to an antiferromagnetic quantum critical point.

In applied magnetic fields the normal state retains certain NFL characteristics regardless of field direction before Fermi liquid behavior is recovered well beyond H_{c2} (Bianchi, Movshovich, Vekhter, *et al.*, 2003; Paglione *et al.*, 2003; Malinowski *et al.*, 2005; Ronning *et al.*, 2005). This is surprising since the NFL characteristics due to a QCP are normally rapidly suppressed in a magnetic field. For instance, at H_{c2}^c the specific heat C/T diverges logarithmically, reaching $C/T=1.1$ J/mol K² at the lowest temperatures studied (Petrovic, Pagliuso, *et al.*, 2001), while Fermi-liquid behavior is observed only above 8 T. Likewise the dc susceptibility at H_{c2} diverges as $\chi(T)=\chi_0+C/(T^\alpha+a_0)$ with $\alpha = 0.8 - 1$ (Tayama *et al.*, 2002).

The electronic structure of $CeCoIn_5$ has been studied microscopically by angle-resolved photoemission spectroscopy (ARPES). The dispersion and peak width of the prominent quasi-two-dimensional Fermi surface sheet display an anomalous broadening near the Fermi level (Koitzsch *et al.*, 2008). Using resonant ARPES a flat f band is observed with a distinct temperature dependence. These observations are consistent with a two-level mixing model.

Direct microscopic evidence of a NFL normal state is supported by de Haas-van Alphen oscillations for a magnetic field along the c axis. Here strongly spin-dependent mass enhancements are observed in the immediate vicinity of H_{c2}^c , which are inconsistent with the Lifshitz-Kosevich expression and thus Fermi-liquid theory (McCollam *et al.*, 2005). This is supported by the spin-lattice relaxation rate T_1 in ¹¹⁵In nuclear quadrupole resonance, which displays a temperature dependence $1/T^4$ characteristic of antiferromagnetic spin fluctuations (Kohori *et al.*, 2001; Kawasaki *et al.*, 2003).

As discussed below, the electronic correlations at the heart of the NFL behavior are likely to be responsible for the superconductivity in $CeCoIn_5$. This raises the question of their origin and the possible nature and location of the QCP. The T^2 coefficient of the resistivity for H along the c axis diverges at an extrapolated field value below H_{c2} , suggesting a QCP within the superconducting regime, but the precise location has not been settled (Bianchi, Movshovich, *et al.*, 2003; Paglione *et al.*, 2003; Malinowski *et al.*, 2005). More recently, a dimensional crossover from three-dimensional to two-dimensional quantum criticality near H_{c2} was even inferred from the thermal expansion (Donath *et al.*, 2008).

Entirely unexplained is the observation of a giant Nernst effect in the normal state (Bel *et al.*, 2004; Izawa *et al.*, 2007). In fact, one scenario offered to explain the giant Nernst effect and scaling of the normal state resistivity as a function of field direction in the basal plane is the formation of a *d*-density wave (Hu *et al.*, 2006).

Further support for unconventional superconductivity with a *d*-wave gap has been observed in inelastic neutron scattering studies (Stock *et al.*, 2008). In the normal state slow commensurate fluctuations [$\hbar\Gamma = 0.3 \pm 0.15$ meV at $\vec{Q}_0=(1/2,1/2,1/2)$] with nearly isotropic spin correlations are observed. In the superconducting state a sharp spin resonance at $\hbar\omega = 0.60 \pm 0.03$ meV develops, with $\hbar\Gamma < 0.07$ meV. The spin resonance is indicative of strong coupling between *f*-electron magnetism and superconductivity. The similarity of this spin resonance with the properties of UPd₂Al₃ and the cuprates suggests that it may be understood in a common framework.

The specific heat anomaly of the superconducting transition is exceptionally large, $\Delta C/\gamma T_s=4.5$ when the value of γ at T_s is used. This would suggest an extreme case of strong-coupling superconductivity. However, $\Delta C/\gamma$ normally when is considered the extrapolated zero-temperature value of γ is used, which due to the NFL behavior here is ill defined. The initial variation in H_{c2} near T_s is large and characteristic of heavy fermion superconductivity, $dH_{c2}/dT=-11$ T/K and $dH_{c2}^{ab}/dT=-24$ T/K (Ikeda *et al.*, 2001). The short coherence lengths $\xi_a=82$ Å and $\xi_c=35$ Å and large penetration depth as inferred from microwave measurements, $\lambda(T \rightarrow 0)=1900$ Å (Ormeno *et al.*, 2002), along with the low Fermi energy and large charge carrier mean free paths of several 1000 Å, identify CeCoIn₅ as a type-II superconductor ($\kappa_a=108$ and $\kappa_c=50$) in the superclean limit (Kasahara *et al.*, 2005).

A large number of properties suggest an unconventional form of superconductivity in CeCoIn₅. For instance, the depression of T_s with rare-earth substitution correlates with the change in the mean free path (Paglionone *et al.*, 2007). The following experimental evidence suggests line nodes of a $d_{x^2-y^2}$ state: (i) the power law temperature dependence of the specific heat, $C \propto T^3$ (Movshovich *et al.*, 2001); (ii) the variation in the specific heat with fourfold symmetry for the magnetic field in the basal plane (Aoki *et al.*, 2004) (maxima along [110]); (iii) the power law dependence of the thermal conductivity, $\kappa \propto T^3$ (Movshovich *et al.*, 2001), (iv) the variation in the thermal conductivity with a fourfold symmetry for the magnetic field in the basal plane (maxima along [110]) (Izawa *et al.*, 2001); (v) the variation in H_{c2} of 1.2% with a fourfold symmetry in the basal plane (maxima along [100]) (Weickert *et al.*, 2006); and (vi) the differential conductance spectra as interpreted in the extended Blonder-Tinkham-Klapwijk model (Park *et al.*, 2008).

In contrast, a d_{xy} pairing symmetry has been inferred from the symmetry and the field and temperature dependences of the in-plane torque magnetization (Xiao *et al.*, 2008). Moreover, the magnetic field and temperature

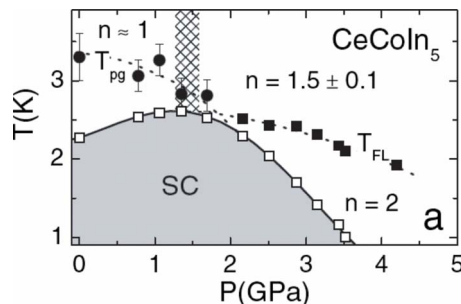


FIG. 7. (Color online) Temperature vs pressure phase diagram of CeCoIn₅. From the resistivity a “pseudogap” at T_{pg} is inferred that merges with the maximum in the onset of the SC. At high pressures the superconductivity condenses out of a Fermi liquid temperature dependence of the resistivity below T_{FL} . From Sidorov *et al.*, 2002.

dependences of the thermal conductivity were found to be inconsistent with the existence of unpaired electrons (Seyfarth *et al.*, 2008). The latter study points at multi-band superconductivity and a related complex multigap state.

Microscopic information on the pairing symmetry may be inferred from the Knight shift, which decreases for both field directions. This shows that the spin susceptibility decreases for all directions, consistent with even parity superconductivity (Kohori *et al.*, 2001). The NMR and NQR spin-lattice relaxation rate, show no Habel-Slichter peak and a power-law temperature dependence $1/T_1 \propto T^3$ (Kohori *et al.*, 2001) further suggesting a non-*s*-wave state.

Small-angle neutron scattering (SANS) shows a six-fold symmetry of the flux line lattice (FLL) at low fields and low temperatures. As a function of magnetic field the flux lattice symmetry undergoes a sequence of transitions from hexagonal to orthorhombic, to square, back to orthorhombic and finally to hexagonal symmetry near H_{c2} (Eskildsen *et al.*, 2003; DeBeer-Schmitt *et al.*, 2006; Bianchi *et al.*, 2008). Most remarkably, the form factor of the FLL as traced all the way to H_{c2} increases with increasing field, in stark contrast with the predictions of Abrikosov-Ginzburg-Landau theory (Bianchi *et al.*, 2008). This behavior has been attributed to a combination of Pauli paramagnetic effects around the vortex cores and the vicinity of the system to a quantum critical point. The temperature dependence of the penetration depth may be given by $\lambda_{\perp} \propto T^{1.5}$. This has been explained in terms of a temperature-dependent coherence length related to the vicinity to quantum criticality (Özcan *et al.*, 2003). Alternatively, the penetration depth has been given by $\lambda_{\perp} \propto aT + bT^2$ and $\lambda_{\parallel} \propto T$, where a crossover from weak- to strong-coupling superconductivity was proposed (Chia *et al.*, 2003).

The properties of CeCoIn₅ respond sensitively to hydrostatic pressure as shown in Fig. 7 (Nicklas *et al.*, 2001; Sparn *et al.*, 2002; Knebel *et al.*, 2004; Yashima *et al.*, 2004; Tayama *et al.*, 2005; Miclea *et al.*, 2006; Singh *et al.*, 2007). Up to 30 kbar, T_s traces out part of a dome; an initial increase is followed by a decrease for

$p > 16$ kbar. The specific heat anomaly $\Delta C/\gamma T_s$ decreases under pressure monotonically by nearly 80% up to 30 kbar (Sparn *et al.*, 2002; Knebel *et al.*, 2004). H_{c2} increases for the a - b plane while it decreases for the c axis from 4.95 to 2 T at 30 kbar (Shishido *et al.*, 2003), so that the anisotropy of H_{c2} increases from 2.34 at $p=0$ to 3.78 at 30 kbar (Tayama *et al.*, 2005).

Despite these rather drastic effects, ^{115}In NQR shows that the spin-lattice relaxation rate T_1 below T_s remains qualitatively unchanged, $T_1 \propto T^{-3}$, up to 20 kbar. This suggests that the nature of the superconductivity remains unchanged (Yashima *et al.*, 2004). An increase in the spin fluctuation temperature T_{SF} may be consistently inferred from (i) the decrease in the normal state value of γ , (ii) an increase in the coherence maximum in the resistivity from 50 to nearly 100 K at 15 kbar, and (iii) a change in the normal state spin-lattice relaxation rate. These properties suggest that pressure moves CeCoIn₅ away from quantum criticality.

Last, but not least, that CeCoIn₅ combines a unique set of properties: it shows strong Pauli limiting, the electronic structure is quasi-two-dimensional, and samples may be grown at ultrahigh purity. These are the preconditions for the formation of a FFLO phase. Indeed, striking evidence exists that CeCoIn₅ stabilizes the first example of such a state, as discussed in Sec. V.B.1.

d. CeRhIn₅In

The unit cell volume of CeRhIn₅ is larger than that of CeCoIn₅ and the c/a ratio is smaller, as shown in Table II. Taking into account the anisotropic compressibility for the a and c axes, the properties of CeRhIn₅ at high pressure may be expected to resemble those of CeCoIn₅. Considering the bulk modulus of CeIn₃, the CeIn₃ units may be viewed as experiencing an effective pressure of 14 kbar (Hegger *et al.*, 2000). The electronic properties of CeRhIn₅ emerge in a CEF Γ_7 ground state and Γ_7 and Γ_6 first and second excited states at 6 and 29.1 meV, respectively (Christianson *et al.*, 2004).

At ambient pressure CeRhIn₅ orders antiferromagnetically below $T_N=3.8$ K (Hegger *et al.*, 2000) with a temperature-independent antiferromagnetic ordering wave vector $\vec{Q}=(1/2, 1/2, 0.297)$. The ordered moment at 1.4 K of $\mu_{\text{ord}}=0.264(4)\mu_B$ is strongly reduced as compared to the moment expected in CEFs of $0.8\mu_B$ (Bao *et al.*, 2000, 2003). It spirals transversely along the c axis, while the nearest-neighbor moments on the tetragonal basal plane are aligned antiferromagnetically. Based on muon spin rotation (μSR) it has been suggested that a small ordered moment also exists at the Rh site (Schenck *et al.*, 2002). The antiferromagnetic transition as seen in neutron scattering and the bulk properties is second order, and the specific heat is characteristic of an anisotropic spin-density wave that gaps nearly 90% of the Fermi surface (Cornelius *et al.*, 2001). The entropy released at T_N corresponds to the small ordered moment (Hegger *et al.*, 2000).

The normal state specific heat of CeRhIn₅ is characteristic of a heavy-fermion state with $\gamma=0.42$ J/mol K² (Cornelius *et al.*, 2000). In contrast, the thermal expansion shows a non-Fermi-liquid divergence of α/T for [001] above T_N while the basal plane is well behaved with $\alpha/T \approx \text{const}$ (Takeuchi *et al.*, 2001). Moreover, while the susceptibility displays the Curie-Weiss behavior of nearly free Ce³⁺ moments at high temperatures, χ keeps increasing even at low temperatures below a shoulder around 30 K: $\chi_{ab}^{-1} \propto a + bT^{0.9}$ and $\chi_c^{-1} \propto a + T^{1.35}$ (Kim, Alwood, *et al.*, 2001). Similar anomalous behavior is also seen in the temperature dependence of the normal state electrical resistivity (Hegger *et al.*, 2000; Muramatsu *et al.*, 2001).

Microscopic evidence of an abundance of critical antiferromagnetic fluctuations up to $3T_N$ has been seen in inelastic neutron scattering (Bao, Aeppli, *et al.*, 2002) and the temperature dependence of the ^{115}In NQR spin-lattice relaxation (Mito *et al.*, 2001). The magnetic phase diagram of CeRhIn₅ as a function of an applied magnetic field has been studied up to 50 T for the [110] direction. A spin-flop transition is observed at 2 T and a metamagnetic transition (spin flip) around 45 T (for 3 K) (Cornelius *et al.*, 2001; Takeuchi *et al.*, 2001; Settai, Takeuchi, *et al.*, 2007). The c axis is the easy magnetic axis.

Under pressure the Néel temperature decreases. Superconductivity was first observed in CeRhIn₅ above 15 kbar, where an abrupt first-order change from antiferromagnetism to superconductivity was reported (Hegger *et al.*, 2000). Recent studies suggest that high-quality single crystals display superconductivity even in the antiferromagnetic state at ambient pressure below $T_s \approx 0.09$ – 0.11 K (Chen *et al.*, 2006; Paglione *et al.*, 2008). The bulk properties of the superconductivity at ambient pressure by comparison with other systems are characteristic of a state far from quantum criticality.

As a function of pressure T_s increases while T_N decreases until $T_N=T_s \approx 2.0$ K at $p_1 \sim 17.7$ kbar. The specific heat and susceptibility suggest a competitive phase coexistence of AFM and superconductivity for pressure below p_1 (Knebel *et al.*, 2006). Neutron scattering shows that the ordering wave vector and ordered moment initially change weakly (Majumdar *et al.*, 2002; Llobet *et al.*, 2004) and a second magnetic modulation emerges (Christianson *et al.*, 2005). For high pressures of 15 and 17 kbar the incommensurate propagation vector is $\vec{Q}_{\text{hp}}=(1/2, 1/2, 0.4)$, which differs from the ambient pressure propagation vector $\vec{Q}=(1/2, 1/2, 0.297)$ (Raymond, Knebel, *et al.*, 2008). A competitive coexistence of AF and superconductivity up to p_1 is supported by ^{115}In NQR (Mito *et al.*, 2003). Homogeneous volume superconductivity is observed above p_1 with a maximum value of $T_s \approx 2.1$ K around 20 kbar (Chen *et al.*, 2006; Knebel *et al.*, 2006).

Resistivity measurements in CeRhIn₅ extending up to 85 kbar indicate the presence of a second superconducting dome (Muramatsu *et al.*, 2001). This finding could not be confirmed, as reviewed by Knebel *et al.* (2008).

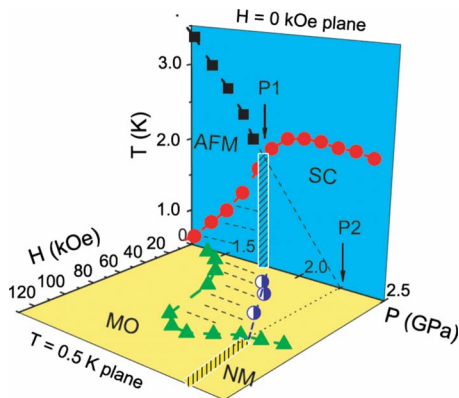


FIG. 8. (Color online) Temperature vs magnetic field and pressure phase diagram of CeRhIn₅ as reported by Park *et al.* (2006). Detailed studies of the specific heat suggest a well-defined line of quantum criticality, separating a regime where superconductivity and antiferromagnetism coexist with a regime of homogenous bulk superconductivity. From Park *et al.*, 2006 as shown in Sarrao and Thompson, 2007.

Electronic structure calculations suggest that the 4*f* electron is localized in CeRhIn₅ (Elgazzar *et al.*, 2004). The mass enhancement seen in the specific heat has therefore been attributed to spin fluctuations above frozen magnetic states, which become itinerant and add to the spectrum of fluctuations in CeCoIn₅. de Haas–van Alphen studies showed that the electronic structure of CeRhIn₅ is highly two dimensional (Cornelius *et al.*, 2000; Hall *et al.*, 2001). Under hydrostatic pressure a new branch emerges around 24 kbar, the extrapolated pressure where T_N vanishes. The similarity with CeCoIn₅ indeed suggests a delocalization of the 4*f* electron at this pressure (Shishido *et al.*, 2005).

The NFL normal state properties and immediate vicinity of the superconductivity to antiferromagnetism in CeRhIn₅ are circumstantial evidence suggesting unconventional pairing. The superconductivity is, nevertheless, rather unexplored. The most direct evidence for unconventional pairing may be the spin-lattice relaxation rate of ¹¹⁵In NQR in the superconducting state which does not show a Hebel-Slichter peak and varies as $1/T_1 \propto T^3$ (Mito *et al.*, 2001).

The structural similarity of CeRhIn₅ with CeCoIn₅ raises the question of an analogy in the superconducting phase diagram. In CeCoIn₅ the normal state properties hint at a quantum critical point that is masked by the superconducting dome. Under pressure, H_{c2} for $B \perp [001]$ initially tracks the increase in T_s and displays a maximum just above p_1 . Specific heat measurements under pressure and magnetic field in CeRhIn₅ reveal a phase boundary separating homogeneous volume superconductivity and a phase coexistence of antiferromagnetic order and superconductivity, as reported by Park *et al.* (2006) and shown in Fig. 8. In the magnetic field versus pressure plane the phase separation line increases from zero at p_1 and reaches H_{c2} at p_2 . The normal state properties in the B vs p plane are consistent with a

quantum critical point for $B \rightarrow 0$ and p_2 . Taken together with the de Haas–van Alphen studies, this provides evidence of a quantum critical point at p_2 that may be related to a delocalization transition of the 4*f* electrons.

e. CeIrIn₅

The heavy-fermion superconductor CeIrIn₅, has the largest unit cell volume and smallest c/a ratio in the CeMnIn₅ series, as shown in Table II. At ambient pressure the normal state properties are characteristic of strong electronic correlations that develop in crystal electric fields related to those of CeIn₃ (Christianson *et al.*, 2004). The specific heat exhibits a large enhancement with $\gamma = 0.72$ J/mol K² (Petrovic, Movshovich, *et al.*, 2001). The susceptibility exhibits a broad shoulder around 7 K (Takeuchi *et al.*, 2001), but continues to diverge slowly (Kim, Alwood, *et al.*, 2001). This and the resistivity, which varies as $\Delta\rho \propto T^n$ with $n \approx 1.3$, indicate non-Fermi-liquid characteristics of the normal state (Petrovic, Movshovich, *et al.*, 2001).

The bulk properties are consistent with the spin-lattice relaxation rate inferred from ¹¹⁵In NQR measurements, which suggests that CeIrIn₅ is an anisotropic incipient antiferromagnet (Kohori *et al.*, 2001; Zheng *et al.*, 2001). More detailed information on the normal state has been inferred from the Hall effect and the magnetoresistance, which also show non-Fermi-liquid behavior. Notably, there is a breakdown of Kohler's rule and the Hall angle varies as $\cot \Theta_H \propto T^2$ (Nair *et al.*, 2008; Nakajima *et al.*, 2008). When taken together, in the T vs B phase diagram the magnetotransport properties suggest a precursor regime of the normal metallic state that shares some similarities with the pseudogap regime in the cuprates (Nair *et al.*, 2008).

Various properties of CeIrIn₅ suggest two superconducting transitions. At $T_{s1} = 0.75$ K the resistivity vanishes and there are strong indications of an intrinsic form of filamentary superconductivity. At $T_{s2} = 0.4$ K superconductivity is observed in the specific heat (Petrovic, Movshovich, *et al.*, 2001) and in ¹¹⁵In NQR (Kawasaki *et al.*, 2005). Specific heat and In NQR under pressure show that T_{s2} increases to 0.8 K at a pressure of 16 kbar (Borth *et al.*, 2002; Kawasaki *et al.*, 2005). The increase in T_{s2} is consistent with the observed decrease in γ , which may be interpreted as an increase in the characteristic spin fluctuation temperature. H_{c2} is anisotropic; the resistivity and susceptibility show $H_{c2}^a = 6.8$ T, $H_{c2}^c = 3.5$ T and $H_{c2}^b = 1.0$ T, $H_{c2}^c = 0.49$ T for S1 and S2, respectively (Petrovic, Movshovich, *et al.*, 2001). The temperature dependence and anisotropy of H_{c2} of the incipient superconducting state and the bulk superconducting state track each other qualitatively (Petrovic, Movshovich, *et al.*, 2001), and the anisotropy may be accounted for by the anisotropic mass model (Haga *et al.*, 2001).

The specific heat, which varies as $C \propto T^3$ (Movshovich *et al.*, 2001), and the thermal conductivity for heat current along the a axis, which varies as $\kappa \propto T^2$ with a finite

residual $T=0$ value of $\kappa/T=0.46$ W/K² m, are consistent with an unconventional superconducting state and line nodes. This is supported microscopically by NMR and NQR, which shows (i) no Hebel-Slichter peak, (ii) a temperature dependence of the spin-lattice relaxation rate $1/T_1 \propto T^3$ at pressures up to 21 kbar, and (iii) a decrease in the Knight shift in the superconducting state with decreasing temperature for all field directions (Kohori *et al.*, 2001). However, the thermal conductivity with heat current along the *c* axis does not show a residual term at low temperatures (Shakeripour *et al.*, 2007), ruling out line nodes running along the *c* axis. Instead the formation of a hybrid gap structure with E_g symmetry has been proposed.

f. Ce_2RhIn_8

The properties of the double-layer compound Ce_2RhIn_8 , are intermediate between of $CeIn_3$ and of the single-layer compound $CeRhIn_5$ as might be expected from the larger fraction of $CeIn_3$ building blocks in the crystal structure. At ambient pressure Ce_2RhIn_8 develops antiferromagnetic order below a second-order phase transition at $T_{N1}=2.8$ K with an ordering wave vector $\vec{Q}=(1/2, 1/2, 0)$ and an ordered moment $\mu_{\text{ord}} \approx 0.55\mu_B/\text{Ce}$ (Bao *et al.*, 2001). The magnetic structure is more akin to that of $CeIn_3$, since the specific heat shows that only 8% of the Fermi surface is gapped in comparison to over 90% in $CeRhIn_5$ (Cornelius *et al.*, 2001). A second antiferromagnetic transition is observed in the resistivity at $T_{N2}=1.65$ K, which does not appear to be accompanied by an anomaly in the specific heat (Nicklas *et al.*, 2003). The magnetic phase diagram at ambient pressure is reminiscent of that of $CeRhIn_5$ (Cornelius *et al.*, 2001).

Hydrostatic pressure suppresses both T_{N1} and T_{N2} ; T_{N2} vanishes below 1 kbar and T_{N1} extrapolates to zero around $p_{N1} \approx 32$ kbar, suggesting a quantum critical point as in $CeRhIn_5$ (Nicklas *et al.*, 2003). The specific heat under pressure shows a broadening of the antiferromagnetic transition and a decrease in γ consistent with an increase in the spin fluctuation temperature (Lengyel *et al.*, 2004). A superconducting dome surrounds p_{N1} with a maximum $T_s=2.1$ K (Nicklas *et al.*, 2003). At 16.3 kbar $H_{c2}=5.36$ T and the initial temperature dependence $dH_{c2}/dT=-9.18$ T/K are large and comparable with values for other compounds in this series.

g. Substitutional doping in $Ce_nM_mIn_{3n+2m}$

Particularly appealing in the series $CeMIn_5$ is the relative metallurgical ease with which substitutional doping studies may be carried out. Three different aspects have been at the center of interest: (i) the sensitivity to doping of the *f* electron element, (ii) the stability of the ground state under replacement of the transition-metal element, and (iii) the sensitivity to disorder on the In site.

Substitutional doping of Ce in $CeMIn_5$ has been carried out with La, U, Pu, and Nd. In $CeCoIn_5$ La doping results in a two-fluid state, notably a combination of

single-impurity Kondo and dense Kondo lattice behavior (Nakatsuji *et al.*, 2002; Nakajima *et al.*, 2004). It is surprising that La doping does not yield additional complexities. Further, unconventional superconductivity in principle is very sensitive to disorder. However, the superconductivity is insensitive to La doping and vanishes only for $x \geq 0.15$. In the superconducting state the residual electronic thermal conductivity decreases while the residual electronic specific heat increases with *x*, i.e., the thermal conductivity does not track the electronic degrees of freedom that become available under doping. This has been taken as evidence of extreme multiband superconductivity in $CeCoIn_5$ (Tanatar *et al.*, 2005). Finally, Nd doping allows us to study the evolution from local-moment magnetism to heavy-fermion superconductivity (Hu *et al.*, 2008).

Across the series $Ce_mRh_nIn_{3n+2}$ ($n=0, 1$ and $m=1, 2$) increase in the La substitution for Ce leads to a suppression of T_N . For the tetragonal systems ($n=m=1, 2$) the critical concentration is $x_c \approx 0.4$ and for $CeIn_3$ $x_c \approx 0.65$ (Pagliuso, Curro, *et al.*, 2002). La doping of $CeRhIn_5$ leaves the antiferromagnetic wave vector essentially unchanged up to $x=0.1$ (Bao, Chritanson, *et al.*, 2002). Observation of the same x_c value for the tetragonal systems suggests, that antiferromagnetic order is essentially controlled by the $CeIn_3$ building blocks. The pressure dependence of La- and Sn-doped $CeRhIn_5$, notably $Ce_{0.9}La_{0.1}RhIn_5$ and $CeRhIn_{4.84}Sn_{0.16}$, shows that La doping shifts the phase diagram to higher pressures, while Sn doping shifts it to lower pressures (Ferreira *et al.*, 2008). This implies that the strength of the on-site Kondo coupling represents the dominant energy scale controlling the phase diagram of $CeRhIn_5$.

Several studies have explored the evolution of the series $CeMIn_5$ under the isovalent replacement of Co by Rh and Ir and of Rh by Ir. In the series $CeCo_{1-x}Rh_xIn_5$ and $CeRh_{1-x}Ir_xIn_5$ this allows the study of the evolution between superconductivity and antiferromagnetism, while the series $CeCo_{1-x}Ir_xIn_5$ allows the study of the evolution between two unconventional superconductors, as summarized in Fig. 9. In the series $CeCo_{1-x}Rh_xIn_5$ a coexistence of antiferromagnetism and superconductivity is observed for a large range of *x* (Zapf *et al.*, 2001). The total entropy released at the two transitions is thereby constant. This suggests that the two ordering phenomena are intimately related, representing two sides of the same coin. Further insights were gained on the nature of the linear temperature dependence of the resistivity (Paglione *et al.*, 2007). NQR studies of the normal state show that Rh doping boosts antiferromagnetic spin fluctuations (Kawasaki *et al.*, 2006). The antiferromagnetic structure of $CeRhIn_5$ changes from an incommensurate $\vec{Q}=(1/2, 1/2, 0.297)$ modulation to a modulated state with two wave vectors $\vec{Q}=(1/2, 1/2, 1/2)$ and $\vec{Q}=(1/2, 1/2, 0.42)$ at intermediate concentrations (Yokoyama *et al.*, 2008). Fluctuations with respect to these wave vectors may be relevant for the superconductivity at intermediate concentrations.

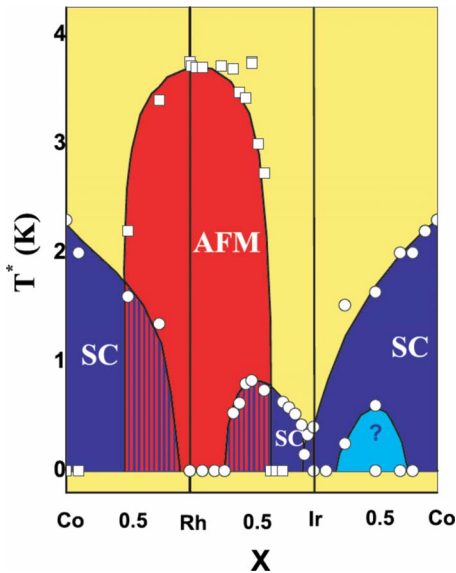


FIG. 9. (Color online) Compilation of the evolution of superconductivity and antiferromagnetic order in the series $CeMIn_5$, where $M=Co, Rh,$ and Ir . Note the continuous evolution of the superconducting transition temperature when going from Ir to Co despite the presence of disorder. This continuous evolution is interrupted by an antiferromagnetic dome in the series $Co \rightarrow Rh \rightarrow Ir$. From Pagliuso, Movshovich, *et al.*, 2002 as shown in Sarrao and Thompson, 2007.

Rh doping of $CeIrIn_5$ initially suppresses the filamentary transition at T_{s1} so that only the superconducting transition at T_{s2} remains. However, for higher Rh concentrations the bulk T_s increases until antiferromagnetism emerges for $x > 0.3$ (Bianchi *et al.*, 2001; Pagliuso *et al.*, 2001; Kawasaki *et al.*, 2006). Within the antiferromagnetic state superconductivity in coexistence with antiferromagnetism survives (Zheng *et al.*, 2004; Christianson *et al.*, 2005). Perhaps most importantly, the superconductivity is insensitive to the disorder associated with the doping. This suggests that the transition-metal element affects only indirectly those parts of the Fermi surface on which superconductivity is stabilized.

Finally, substitutional doping on the In site has provided some hints concerning the nature of the superconductivity. Extensive studies have been carried out in $CeCoIn_{5-x}Sn_x$, where the superconductivity vanishes rapidly for $x \geq 0.15$ (Bauer, Capan, *et al.*, 2005). Note that this represents a much smaller concentration than $x=0.15$ in La doping. Extended x-ray absorption fine structure (EXAFS) studies have established that the Sn atoms preferentially occupy the $In(1)$ site in the $CeIn_3$ planes (Daniel *et al.*, 2005), highlighting that the superconductivity is particularly sensitive to disorder in the $CeIn_3$ planes. Interestingly, the critical Sn concentration, when referred to the $CeIn_3$ planes, yields an average distance of the Sn atoms of the size of the superconducting coherence length. The suppression of superconductivity in $CeCoIn_{5-x}Sn_x$ may be compared with the suppression of antiferromagnetic order in $CeRhIn_{5-x}Sn_x$ at $x_c \approx 0.35$, where a quantum critical

point is generated (Bauer, Mixon, *et al.*, 2006). Assuming that the Sn atoms occupy the $In(1)$ site, as for $CeCoIn_{5-x}Sn_x$, this reveals that details of the electronic structure within the $CeIn_3$ planes control the stability of both antiferromagnetic order and superconductivity.

It is rather surprising that substitutional Cd doping of the In site induces a change from superconductivity to long-range antiferromagnetic order, and the phase diagram scales with the pressure-dependent phase diagram of $CeRhIn_5$ (Pham *et al.*, 2006). Electronically, Cd doping, in leading order, acts as the removal of electrons, which in turn compares with the effect of pressure on $CeRhIn_5$. However, NMR studies of the series of Cd -doped $CeCoIn_5$ establish a microscopic coexistence of the two forms of order, where the ordered moment of $0.7\mu_B$ is essentially unchanged and the magnetic order may be attributed to the local environment of the Cd dopant (Urbano *et al.*, 2007). Thus the magnetic order is not the result of a gradual modification of the Fermi surface but emerges in terms of droplets that coalesce at the onset of long-range antiferromagnetism.

Both the superconductivity and antiferromagnetism respond sensitively to nonmagnetic disorder within the $CeIn_3$ building blocks, while they are relatively insensitive to out-of-plane disorder. A possible explanation of this behavior is that it may be related to the warping of the Fermi surface, which is affected by local distortions created by the replacement of transition-metal elements. However, the detailed mechanisms that control the behavior in doping studies have not yet been identified.

h. Common features and analogies

We now discuss the more general features of the entire series of $Ce_nM_mIn_{3n+2m}$ compounds. We begin with material-specific aspects and conclude this section with a discussion of possible analogies with other layered superconductors, notably the cuprates.

A major theme across the literature on the $Ce_nM_mIn_{3n+2m}$ compounds is the tentative role of a quantum critical point in driving superconductivity. This is embodied and was first pointed out with respect to $CeIn_3$ (Walker *et al.*, 1997; Mathur *et al.*, 1998). A natural question concerns the mechanisms controlling T_s . For spin-fluctuation-mediated pairing it has been pointed out that a reduction in the effective dimension, notably magnetic and/or electronic anisotropy, favors superconductivity (Monthoux and Lonzarich, 2001, 2002). This is consistent with an empirical observation of T_s as a function of the c/a ratio, as reported by Bauer, Thompson, *et al.* (2004) and shown in Fig. 10.

Similarities of the series $Ce_nM_mIn_{3n+2m}$ with the cuprate superconductors have been taken as evidence that spin fluctuations are responsible for the pairing mechanism in the cuprates [see, e.g., Mathur *et al.* (1998)]. It is instructive to summarize these similarities in further detail. The consideration begins with the temperature versus pressure phase diagram, which shows a superconducting dome in the vicinity of antiferromagnetic order. At least in $CeIn_3$ a major qualitative difference is that a

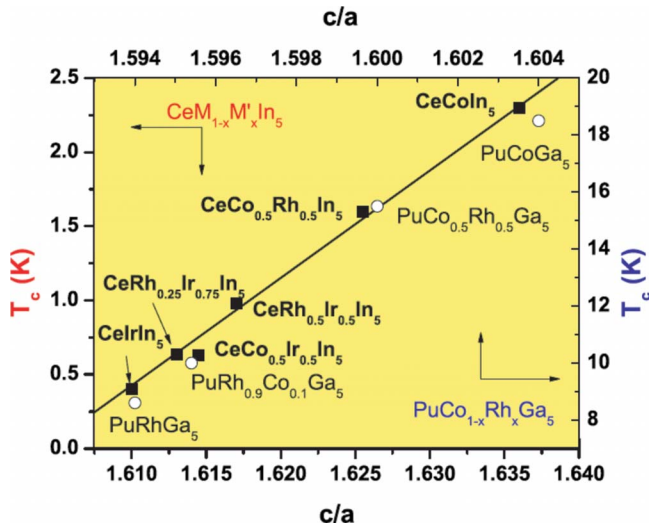


FIG. 10. (Color online) Evolution of the superconducting transition temperature as a function of c/a ratio for the lattice parameter in the series $CeMIn_5$ (left hand and bottom axis) and $PuMGa_5$ (top and right-hand axis). From Sarrao and Thompson, 2007.

proper antiferromagnetic transition vanishes at the putative QCP, while the equivalent feature in the cuprates is a pseudogap of unknown origin. Here the phase diagram of $CeCoIn_5$ is in better analogy with that of the cuprates although the temperature ranges of anomalous behavior in $CeCoIn_5$ are rather small.

Likewise, the analogy with the cuprates may also be seen in the sibling pair $CeCoIn_5$ and $CeRhIn_5$, where pressure induces superconductivity in $CeRhIn_5$ as well as in Ce_2RhIn_8 . The similarity of the phase diagrams is also loosely reflected in the doping studies when we keep in mind that the underlying microscopic processes, notably *s-f* hybridization in *f*-electron systems versus pure charge transfer in the cuprates, are radically different. Doping with Rh, driving $CeCoIn_5$ antiferromagnetic, is akin to hole doping in the cuprates. Likewise Cd doping may be understood as electron doping, stabilizing antiferromagnetic order. Moreover, the complex pressure, magnetic field, and temperature phase diagram in $CeRhIn_5$ yields another analogy in that magnetic field stabilizes a coexistence of superconductivity and antiferromagnetism (Park *et al.*, 2006). A related effect of magnetic field has also been found in certain cuprates (Lake *et al.*, 2002).

The analogy with the cuprates is not just based on qualitative features of the phase diagram but also on the bulk properties. As for the cuprates, the normal metallic state exhibits non-Fermi-liquid behavior. While the resistivity, susceptibility, and specific heat are not in good agreement, there is a similarity of the Hall effect and regarding the breakdown of Kohler's rule in the magnetoresistance in $CeCoIn_5$. In fact, a quadratic temperature dependence of the Hall angle and a breakdown of Kohler's rule have also been observed in $CeIrIn_5$, where they were interpreted as a precursor phase in the normal metallic state that shares similarities with the

pseudogap in the cuprates (Nair *et al.*, 2008). Moreover, just as for the cuprates a spin resonance at a frequency ω_0 has now been observed in the spectrum of slow antiferromagnetic fluctuations in $CeCoIn_5$, where the ratio of the resonance frequency to gap, $\hbar\omega_0/2\Delta_0 \approx 0.74$, is remarkably similar for $CeCoIn_5$, UPd_2Al_3 , and $Bi_2Sr_2CaCu_2O_{8+\delta}$ (Stock *et al.*, 2008).

It is at the same time also important to emphasize the differences between $Ce_nM_mIn_{3n+2m}$ and the cuprates. Quantum oscillatory studies of the electronic structure show a change in Fermi surface topology through the quantum critical point in $CeIn_3$ and $CeRhIn_5$ that appears to be related to a delocalization of the *f* electron. A stimulating question concerns whether an instability of the Fermi surface topology drives the superconductivity in the cuprates.

Finally, $CeIrIn_5$ has an even larger unit cell volume than $CeRhIn_5$, but there is no antiferromagnetic order nearby. The phase diagram shown in Fig. 9 may consequently be interpreted differently. Perhaps the entire series of $CeMIn_5$ is superconducting and T_s increases in a linear fashion from Co to Rh to Ir. However, a slight change in electronic structure of the Rh system changes the balance from a superconducting to an antiferromagnetic ground state. This does not rule out quantum critical fluctuations as key ingredients of the superconductivity though the origin of these fluctuations may differ from the conventional scenario of a simple quantum critical point.

3. Miscellaneous Ce systems

We next present several examples of compounds where evidence for superconductivity has been observed at the border of antiferromagnetic order. These compounds are each the first of a given crystal structure, being possibly the first member of a new class of *f*-electron superconductors. The properties of these miscellaneous Ce systems are summarized in Table I. The first two examples, $CeNiGe_3$ and $Ce_2Ni_3Ge_5$, are members of the ternary Ce-Ni-Ge series. The third system, $CePd_5Al_2$, is isostructural to $NpPd_5Al_2$ (cf. Sec. IV.B.2).

For completeness it is worthwhile to also mention $CeCu_5Au$, where antiferromagnetic order is suppressed around 40 kbar and a small drop of the resistivity is observed that may be related to superconductivity (Wilhelm *et al.*, 2001).

a. $CeNiGe_3$

We begin with the discovery of superconductivity in $CeNiGe_3$, which crystallizes in the orthorhombic $SmNiGe_3$ -type structure (space group $Cmmm$; see also Table I) (Nakajima *et al.*, 2004; Kotegawa *et al.*, 2006). At ambient pressure $CeNiGe_3$ orders antiferromagnetically below a Néel temperature $T_N=5.5$ K as determined from the resistivity and susceptibility. The paramagnetic susceptibility in polycrystals at high temperatures follows a Curie-Weiss dependence with $\mu_{eff}=2.54\mu_B$ as expected of Ce^{3+} . The antiferromagnetic transition is ac-

accompanied by a distinct anomaly, where the entropy released, $\Delta S = 0.65R \ln 2$, is characteristic of localized moments in a $4f$ crystal field doublet ground state. The magnetic structure has been explored by powder neutron diffraction, which revealed two transitions at T_{N1} and T_{N2} with ordering wave vectors $\vec{Q}_1 = (1, 0, 0)$ and $\vec{Q}_2 = (0, 0.409, 1/2)$, respectively, and an ordered moment of $\mu_{\text{ord}} = 0.8\mu_B$.

The electrical resistivity of polycrystalline CeNiGe₃ is dominated by a maximum around 100 K and a sharp drop at T_N , where no details of a second transition have been seen. The pressure dependence of the polycrystalline samples was investigated with two different pressure techniques: diamond anvil cells with NaCl (Nakajima *et al.*, 2004) and Daphne oil (Kotegawa *et al.*, 2006) as pressure transmitters. In the following we address only the results obtained with the latter setup which produces better homogeneity. As a function of pressure T_N initially rises to nearly 8 K at 40 kbar, followed by a fairly rapid decrease. T_N vanishes at $p_c \approx 70$ kbar, where the T^2 resistivity crosses over to a temperature dependence $\sim T^{1.5}$ in the range of 60–70 kbar. The residual resistivity ρ_0 increases and reaches a plateau above p_c .

For pressures in the range of 20–100 kbar, hints for superconductivity are observed in terms of a zero-resistance transition below 40 kbar and an incomplete resistive transition above 40 kbar, where T_s is as high as 0.45 K. The transition temperature exhibits two broad maxima separated by a shallow minimum near p_c . The ac susceptibility shows diamagnetic screening. H_{c2} increases under pressure from 0.015 to 1.55 T. Correspondingly, the coherence length decreases under pressure from 2000 to ~ 100 Å. The initial slope of H_{c2} near T_s increases and reaches $dH_{c2}/dT = -10.8$ T/K for the maximum $T_s \approx 0.45$ T. For low pressures orbital limiting is observed, while there is Pauli limiting for the highest values of T_s around 70 kbar.

b. Ce₂Ni₃Ge₅

Another system in the Ce-Ni-Ge series that attracts increasing interest is Ce₂Ni₃Ge₅ (Chevalier and Etourneau, 1999). This compound crystallizes in the U₂Co₃Si₅-type structure (space group *Ibam*; see also Table I). A discussion of structural similarities with CeNi₂Ge₂ may be found in Nakashima *et al.* (2005). The metallic state of Ce₂Ni₃Ge₅ is characteristic of a Kondo lattice system with $T_K \approx 5$ K, where a Curie-Weiss susceptibility of free Ce³⁺ moments is observed at high temperatures and antiferromagnetic order at low temperatures (Hossain *et al.*, 2000). The magnetization shows two transitions at $T_{N1} = 5.1$ K and $T_{N2} = 4.5$ K. The linear term in the specific heat is enhanced and the entropy released $\Delta S = 0.67R \ln 2$ at T_{N1} is characteristic of reduced moments. Powder neutron diffraction shows collinear antiferromagnetic order below T_{N1} with the magnetic moments aligned along the *a* axis and a small ordered moment of $\mu_{\text{ord}} = 0.4\mu_B$ at 1.4 K (Durivault *et al.*, 2002).

In comparison with Ce₂Ni₃Ge₅ the unit cell volume in the related compound Ce₂Ni₃Si₅ is 9.6% smaller. Ce₂Ni₃Si₅ exhibits properties of a nonmagnetic valence-fluctuating system (Mazumdar *et al.*, 1992). This suggests that hydrostatic pressure suppresses the antiferromagnetic order. Indeed T_{N1} in polycrystalline samples decreases under pressure and vanishes at $p_c = 36$ kbar, where a zero-resistance transition is observed at $T_s = 0.26$ K (Nakashima *et al.*, 2005) with $H_{c2} = 0.7$ T, corresponding to a coherence length $\xi = 210$ Å.

c. CePd₅Al₂

Another miscellaneous Ce-based superconductor is CePd₅Al₂ (Honda, Measson, *et al.*, 2008), which is isostructural to NpPd₅Al₂ reviewed in Sec. IV.B.2. At ambient pressure CePd₅Al₂ displays two antiferromagnetic transitions at $T_{N1} = 3.9$ K and $T_{N2} = 2.9$ K. The metallic state is moderately enhanced with $\gamma = 0.056$ J/mol K². The resistivity and susceptibility, as well as the magnetization, suggest crystal field levels at $\Delta_1 = 197$ K and $\Delta_2 = 224$ K. Under pressure T_{N1} and T_{N2} at first increase, although T_{N2} can be tracked only as high as ~ 30 kbar. T_{N1} displays a maximum around 50 kbar and appears to vanish around 90 kbar. The resistivity displays a superconducting transition in the pressure range of 80–120 kbar, with a maximum $T_s = 0.57$ K at 108 kbar.

B. Coexistence with antiferromagnetism

In a number of *f*-electron systems superconductivity emerges deep inside an antiferromagnetically ordered regime, i.e., $T_s \ll T_N$. These systems may be grouped into two classes, large- and small-moment systems. We first discuss the large-moment antiferromagnets UPd₂Al₃, UNi₂Al₃, and CePt₃Si. For these compounds the coexistence of antiferromagnetism and superconductivity appears to be homogeneous. The second class consists of antiferromagnets with small ordered moments, notably UPt₃ and URu₂Si₂. While the small moments in UPt₃ appear to be homogeneous, there is growing evidence for a small volume fraction of large ordered moments in URu₂Si₂.

1. Large-moment antiferromagnets

Superconductivity in the related pair of low-temperature antiferromagnets UPd₂Al₃ and UNi₂Al₃ was discovered in 1991 (Geibel, Schank, *et al.*, 1991; Geibel, Thies, *et al.*, 1991b). Both compounds crystallize in the hexagonal PrNi₂Al₃ structure (space group *P6/mmm*), as summarized in Table III. Large single crystals of UPd₂Al₃ may be grown, while the metallurgy of UNi₂Al₃ is more complex, i.e., there are fewer single-crystal studies for UNi₂Al₃. In turn the body of work on UPd₂Al₃ is much more complete. In the following we first review the present understanding of UPd₂Al₃ before turning to the properties of UNi₂Al₃. We address

TABLE III. Key properties of uranium-based heavy-fermion superconductors. Missing table entries may reflect more complex behavior discussed in the text. H_{c2} represents the extrapolated value for zero temperature. References are given in the text. (AF, antiferromagnet; FM, F, ferromagnetism; HO, hidden order; SC, superconductor).

U based	UBe ₁₃	UPt ₃	URu ₂ Si ₂	UPd ₂ Al ₃	UNi ₂ Al ₃	UGe ₂	URhGe	UCoGe	UIr
Structure	Cubic	Hexagonal	Tetragonal	Hexagonal	Hexagonal	Orthorh.	Orthorh.	Orthorh.	Monoclinic
Type	NaZn ₁₃		ThCr ₂ Si ₂	PrNi ₂ Al ₃	PrNi ₂ Al ₃				
Space group	$O_h^6 Fm\bar{3}c$	$P6_3/mmc$	$I4/mmm$	$P6/mmm$	$P6/mmm$	$Cmmm$	$Pnma$	$Pnma$	$P2_1$
<i>a</i> (Å)	10.248	5.764	4.128	4.189	5.207	3.997	6.875	6.845	5.62
<i>b</i> (Å)						15.039	4.331	4.206	10.59
<i>c</i> (Å)		4.899	9.592	5.382	4.018	4.087	7.507	7.222	5.60
State	SC	AF, SC	HO, SC	AF, SC	AF, SC	FM, SC	FM, SC	FM, SC	F1, F2, F3, SC
γ (J/mol K ²)		0.44	0.07	0.2	0.12	0.032	0.164	0.057	0.049
T_N, T_C (K)		5	17.5	14.2	4.6	52	9.5	3	46
Easy axis						<i>a</i>	<i>b, c</i>	<i>c</i>	[10 $\bar{1}$]
Hard axis						<i>b, c</i>	<i>a</i>	<i>a, b</i>	[010]
\vec{Q}		($\pm 1/2, 0, 1$)	(0,0,1)	(0,0,1/2)	(1/2 $\pm \delta, 0, 1/2$) $\delta=0.110\pm 0.003$				
μ_{ord} (μ_B)		0.01	0.03	0.85 \pm 0.03	0.24 \pm 0.10	1.48	0.42	0.07	0.5, 0.05, 0.1
μ_{eff} (μ_B)						2.7	1.8	1.7	
T_s (K)	0.95	0.530, 0.480	1.53	2.0	1.1	0.8	0.25 (S1) 0.4 (S2)	0.8	0.15 (in F3)
$\Delta C / \gamma_n T_s$	2.5	0.545, 0.272	0.93	1.48	0.4	0.2–0.3	0.45	1	
H_{c2}^{\parallel} (T)	14	2.1	3	3.9	0.9				
$\frac{d}{dT} H_{c2}^{\parallel}$ (T/K)	–45	–7.2 \pm 0.6	–5.3	–5.45	–1.14				
H_{c2}^{\perp} (T)		2.8	14	3.3	0.35				
$\frac{d}{dT} H_{c2}^{\perp}$ (T/K)		–4.4 \pm 0.3	–14.5	–4.6	–0.42				
H_{c2} (T)									0.0265
$\frac{d}{dT} H_{c2}$ (T/K)								–10.8	
$\xi_{\perp}, \xi_{\parallel}$ (Å)	50	~120	100, 25	85				150	1100
$\lambda_{\parallel}, \lambda_{\perp}$ (Å)	4000	4500, 7400	~7000	4500, 4800					
λ_{GL} (Å)							9100 (S1)		
κ	80	44	70	52	11				
Discovery of SC	1984	1984	1986	1991	1991	2000	2001	2007	2004

only briefly the coexistence of superconductivity and antiferromagnetism in CePt₃Si, which is reviewed in Sec. IV.A.1.

a. UPd₂Al₃

The electrical resistivity of UPd₂Al₃ decreases monotonically as a function of temperature below a broad

maximum around 85 K (Sato *et al.*, 1992). In single crystals the resistivity is weakly anisotropic by a factor of 2 with $\rho_c > \rho_{ab}$. The susceptibility exhibits a broad maximum around 35 K in the basal plane and an anisotropy of ~ 3.5 ($\chi_c < \chi_{ab}$) (Geibel, Thies, *et al.*, 1991). Above ~ 100 K a Curie-Weiss dependence is observed with a fluctuating moment μ_{eff} that changes from $3.2\mu_B/U$ to

$3.4\mu_B/U$ around 300 K (Grauel *et al.*, 1992). To account for the temperature dependence of the susceptibility the following crystal electric field scheme of a tetravalent uranium configuration has been proposed: a Γ_4 singlet ground state, a Γ_1 singlet first excited state at 33 K, two Γ_6 doublets at 102 K, two Γ_5 doublets at 152 K, a Γ_3 singlet at 562 K, and Γ_5 at 1006 K (Grauel *et al.*, 1992). Crystal field excitations at a temperature around 30 K have also been inferred from a dip in the elastic constants (Modler *et al.*, 1993).

A key characteristic of crystal electric fields in uranium compounds is that they hybridize strongly with the conduction electrons. This is also the case in UPd₂Al₃, where time-of-flight inelastic neutron scattering fails to detect well-defined crystal field excitations. Instead very broad spectra consisting of quasielastic Lorentzians plus additional inelastic scattering are observed (Krimmel *et al.*, 1996). The quasielastic scattering is thereby limited to an intrinsic width of 5 meV, consistent with the 50 K energy scale seen in the susceptibility and resistivity. When lattice contributions are subtracted by means of reference measurements in ThPd₂Al₃, the remaining inelastic scattering is consistent with the crystal field scheme given above.

UPd₂Al₃ develops strong electronic correlations at low temperatures with an enhanced linear temperature dependence of the specific heat in the paramagnetic state, $\gamma \sim 0.21$ J/mol K² (Geibel, Schank, *et al.*, 1991). Antiferromagnetic order is observed below $T_N = 14$ K (Geibel, Thies, *et al.*, 1991). The magnetic entropy released at T_N is a substantial fraction of the local Zeeman entropy, $S_m = 0.65R \ln 2$. The resistivity displays a change in slope at T_N (Caspar *et al.*, 1993). There is no evidence suggesting the formation of a density wave, such as the small maximum in the resistivity near T_0 in URu₂Si₂. In the ordered state the linear temperature dependence of the specific heat is also enhanced, $\gamma \sim 0.15$ J/mol K² (Geibel, Schank, *et al.*, 1991).

Early single-crystal studies suggested that the magnetic moments in UPd₂Al₃ orient in the basal plane of the hexagonal crystal structure, i.e., UPd₂Al₃ has an easy magnetic plane (Sato *et al.*, 1992). In zero magnetic field neutron scattering shows commensurate antiferromagnetic order with a wave vector $\vec{Q} = (0, 0, 1/2)$ and an ordered moment $\mu_{\text{ord}} = 0.85\mu_B/U$ (Krimmel *et al.*, 1993). This corresponds to ferromagnetic planes stacked antiferromagnetically along the *c* axis. The ordered moment in UPd₂Al₃ displays a mean-field temperature dependence that corresponds essentially to the form of an $S = 1/2$ Brillouin function. However, the moment is systematically larger than $S = 1/2$, consistent with a tetravalent uranium state.

The onset of antiferromagnetic order in UPd₂Al₃ may be seen in a large number of properties; Examples are (i) the thermal expansion, which shows a large sensitivity to uniaxial stress (Link *et al.*, 1995); (ii) the longitudinal and transverse elastic constants (Lüthi *et al.*, 1993; Modler *et al.*, 1993); (iii) a kink in the ²⁷Al spin-lattice relaxation rate and a gradual increase in the ²⁷Al NMR linewidth

(Kyogaku *et al.*, 1993); (iv) the emergence of a gap in tunneling spectroscopy (Aarts *et al.*, 1994); and (v) an increase in the thermal conductivity (Hiroi *et al.*, 1997).

The magnetic phase diagram of UPd₂Al₃, which yields key information about the nature of the magnetic and superconducting orders, has been studied in detail. For magnetic fields applied in the basal plane three transitions may be distinguished at $H_1 = 0.6$ T, $H_2 = 4.2$ T, and $H_m = 18$ T (de Visser *et al.*, 1992; Sugiyama *et al.*, 1993, 1994; Oda *et al.*, 1994). In contrast, for the *c* axis no field-induced transition can be observed up to 50 T, the highest field studied. At H_1 the ordered state changes from commensurate antiferromagnetism to a canted state (Grauel *et al.*, 1992; Kita *et al.*, 1994). The metamagnetic transition at H_m has attracted much interest. At H_m the magnetization increases from $\sim 0.5\mu_B/U$ to $\sim 1.5\mu_B/U$ (de Visser *et al.*, 1992). Below 4.2 K the transition becomes hysteretic (Sakon *et al.*, 2001). The magnetoresistance displays a peak at H_m for H and $i \parallel \langle 100 \rangle$, while there is a discontinuous step in the magnetoresistance for $H \parallel \langle 010 \rangle$ and $i \parallel \langle 001 \rangle$ (de Visser *et al.*, 1993).

The critical field H_m increases when the field direction is tilted toward the *c* axis. It exceeds 50 T, the highest field measured, for an angle larger than 60° (Oda *et al.*, 1994; Sugiyama *et al.*, 1994). The angular dependence is consistent with *XY* type of order. Torque magnetization measurements show that the basal plane anisotropy persists up to 60 K (Süllow *et al.*, 1996). The metamagnetic transition field changes only weakly as a function of temperature, terminating in a tricritical point around 12 K (Kim, Sator, and Stewart, 2001). For temperatures well above the tricritical point a crossover survives at H_m , reminiscent of the metamagnetic transition (Oda *et al.*, 1999). When taken together, the latter properties suggest that crystal electric fields and the electronic structure at the Fermi level play an important role in controlling the metamagnetic transition, possibly related to a change of *f* localization.

Superconductivity in UPd₂Al₃ is observed below $T_s = 2$ K. Even though T_s is among the highest of all heavy-fermion systems, it is nearly one order of magnitude smaller than T_N . This distinguishes UPd₂Al₃ and UNi₂Al₃ from the systems reviewed above. The superconducting transition is accompanied by a distinct anomaly in the specific heat, with $\Delta C / \gamma T_s \approx 1.48$. Below T_s the specific heat varies as $C(T) = \gamma T + AT^3$, suggesting the presence of line nodes (Caspar *et al.*, 1993). Also consistent with line nodes is the cubic temperature dependence of the thermal expansion, $\alpha \propto T^3$ (Modler *et al.*, 1993). The ratio of the thermal conductivity to the temperature κ/T shows a finite contribution for $T \rightarrow 0$ of the order of 10% of the normal state value (Chiao *et al.*, 1997). Near T_s a crossover is observed rather than a sharp kink, followed by a dependence $\kappa/T \propto T$, providing further evidence for line nodes (Hiroi *et al.*, 1997). In a magnetic field κ/T increases, a kink appears at $T_s(H)$, and the temperature dependence changes slightly. Recently angle-resolved magnetothermal transport measurements showed the absence of an orientation depen-

dence in the basal plane, while a twofold symmetry exists in the plane perpendicular to the basal plane (Watanabe, Izawa, *et al.*, 2004). From this it was concluded that the gap has a single line node orthogonal to the c axis, while the gap is isotropic in the basal plane and may be given as $\tilde{\Delta}(\vec{k}) = \Delta_0 \cos(k_z c)$.

The upper critical fields $H_{c2}^a = 3.3$ T and $H_{c2}^c = 3.9$ T and the initial slopes $\partial H_{c2}^a / \partial T|_{T_s} \approx -4.6$ T/K and $\partial H_{c2}^c / \partial T|_{T_s} \approx -5.45$ T/K are isotropic (Ishiguro *et al.*, 1995; Sato *et al.*, 1996). They correspond to a coherence length $\xi_{GL} \approx 85$ Å with the penetration depths $\lambda_{\perp}(0) = 4800 \pm 500$ Å and $\lambda_{\parallel}(0) = 4500 \pm 500$ Å (with respect to the c axis) inferred from magnetization and μ -SR measurements (Geibel, Schank, *et al.*, 1991; Feyerherm *et al.*, 1994). This establishes UPd₂Al₃ as strong type-II superconductor with $\kappa_{GL} \approx 52$. The anisotropy of H_{c2} for $T \rightarrow 0$ may be accounted for by an anisotropic mass model (Sato *et al.*, 1997a). It is instructive to compare the observed field values with the conventional weak-coupling orbital and paramagnetic limiting fields, $H_{p0} = 3.7$ T, $H_a^* = 6.4$ T and $H_c^* = 7.6$ T. Thus the upper critical fields are smaller than for orbital limiting and close to the paramagnetic limit.

The charge carrier mean free path inferred from the residual resistivity or the Dingle temperature in quantum oscillatory studies shows large values of the order of 10^3 Å. UPd₂Al₃ hence exhibits type-II superconductivity in the clean limit which that is dominated by paramagnetic limiting. This motivated interpretation of an anomalous dip in the ac susceptibility and magnetization near H_{c2} in terms of a FFLO state (Gloos *et al.*, 1993). The formation of a FFLO state has been questioned on theoretical grounds (Norman, 1993). However, further studies suggested that the anomalous dip exists at all temperatures below T_s in contrast to the finite temperature range predicted theoretically. Thus the anomalous behavior near H_{c2} is more characteristic of the peak effect (Haga *et al.*, 1996). For a further discussion of FFLO states see Sec. V.B.1.

To gain insight into the interplay of superconductivity and antiferromagnetism it is instructive to consider the nature of the $5f$ electrons. The U-U spacings in UPd₂Al₃ and UNi₂Al₃, given by $d_{U-U} = 4.186$ and 4.018 Å, respectively, are well above the Hill limit of 3.4 Å. This implies that any itinerancy of the f electrons must be related to a hybridization with s and d electrons. The larger spacing in UPd₂Al₃ is thereby consistent with the evidence of stronger localization of the $5f$ electrons. Several properties of UPd₂Al₃ are characteristic of local uranium moments. For instance, the susceptibility at high temperatures shows a Curie-Weiss dependence with a fluctuating moment $\mu_{\text{eff}} = 3.2 \mu_B / U$. Polarized neutron scattering of the magnetic form factors in an applied field of 4.6 T shows the lack of magnetic polarization at the Pd site, i.e., the magnetic polarization is well localized at the uranium site (Paolasini *et al.*, 1993). However, it was not possible to infer unambiguously from the magnetic form factor whether uranium is tet-

ravalent. The observed ratio of the orbital to the spin moment, $R = \mu_L / \mu_S \approx -2.01$, is closer to the value for U³⁺ ($R = -2.56$) than for U⁴⁺ ($R = -3.29$). Uranium $5f$ x-ray circular dichroism is characteristic of strong interactions between the $5f$ states and their environment (Yaouanc *et al.*, 1998).

The evidence for local-moment magnetism is in contrast to results of optical conductivity and quantum oscillatory studies of the Fermi surface, which show strongly renormalized quasiparticle conduction bands (Terashima *et al.*, 1997; Inada *et al.*, 1999). In the optical conductivity, Drude behavior is observed with ultraslow relaxation rates (Scheffler *et al.*, 2005). At the metamagnetic transition H_m a reconstruction of the Fermi surface topology is observed without substantial variation in the renormalization. This may be related to a magnetic-field-induced transition from an antiferromagnetic to a ferromagnetic exchange splitting, but does not appear to be driven by a localization of the f electrons.

Experimentally several properties of UPd₂Al₃ suggest a dual state, where some of the $5f$ electrons are localized and the others are itinerant, i.e., a combination of both characteristics may be seen in the same physical quantity. This was first noticed in measurements of the specific heat under pressure up to 10.8 kbar, where amongst other things the size of the anomaly at the antiferromagnetic transition is strongly suppressed, while at the superconducting transition it is not (Caspary *et al.*, 1993). The magnetic properties are also anisotropic as opposed to the superconducting properties which are isotropic (Feyerherm *et al.*, 1994; Ishiguro *et al.*, 1995; Sato *et al.*, 1996). Neutron scattering (Krimmel *et al.*, 1993) NMR and NQR studies (Kohori *et al.*, 1995) further showed that the antiferromagnetic order survives essentially unchanged in the superconducting state. This suggests that the two forms of order may be carried by different subsystems. Finally, the spectrum of excitations exhibits different contributions. Resonant $5d-5f$ photoemission showed a sharp peak near E_F and a broad hump at a binding energy of ~ 1 eV characteristic of the features expected of itinerant and localized $5f$ electrons, respectively (Ejima *et al.*, 1994; Takahashi *et al.*, 1995). Photoemission established that the electronic properties change as a function of temperature from itinerant to localized (Sato, 1999; Fujimoto, 2007). Inelastic neutron scattering showed a weakly dispersive mode at an energy of ~ 1.5 meV that softens at T_N , consistent with early studies (Petersen *et al.*, 1994) and a quasielastic signal at the antiferromagnetic ordering wave vector (Sato *et al.*, 1997b). UPd₂Al₃-Pb tunnel junctions showed a superconducting gap around 0.235 meV and antiferromagnetic spin-wave mode around 1.5 meV, consistent with the neutron scattering studies (Jourdan *et al.*, 1999).

At first sight the dispersive and quasielastic excitations in UPd₂Al₃ seen in neutron scattering may appear to be disconnected. However, polarized neutron scattering showed that the dispersive mode and the quasielastic signal are both transversely polarized. This suggests a common origin (Bernhoeft *et al.*, 1998). As part of this

study it was further shown that the spectrum of antiferromagnetic spin fluctuations in the framework of conventional paramagnon theory (Lonzarich and Taillefer, 1985; Moriya, 1985) is quantitatively consistent with T_N and the enhancement of the normal state specific heat. As the temperature decreases below T_s the quasielastic spectrum changes and a steep maximum emerges at very small ω . The maximum is also referred to as the resonance mode. When the maximum is plotted as a function of temperature, good agreement with the temperature dependence of a BCS gap is found, with $2\Delta = 3.86k_B T_s$ (Metoki *et al.*, 1998; Bernhoeft *et al.*, 1999). Under magnetic field the resonance vanishes at H_{c2} (Blackburn, Hiess, Bernhoeft, Lander, *et al.*, 2006). In a spin-echo neutron scattering study the vanishing of spectral weight in the superconducting state was investigated at μeV resolution (Blackburn, Hiess, Bernhoeft, Rheinstädter, *et al.* 2006). The experiments establish that the intensity vanishes completely, placing a strong constraint on the pairing symmetries.

Self-consistent LDA band structure calculations treating the *5f* states in UPd_2Al_3 as being itinerant reproduce the ordered magnetic moment, magnetocrystalline anisotropy, and de Haas–van Alphen spectra (Sandratskii *et al.*, 1994). These studies also showed that the antiferromagnetic and ferromagnetic ground states are nearly degenerate, consistent with the metamagnetic transition at $H_m = 18$ T. In these calculations the two largest Fermi surface sheets have markedly different *5f* contributions, one is almost purely *5f* and the other yields 30% *5f* character (Knöpfle *et al.*, 1996). These differences may provide a tentative explanation for the dual behavior.

In recent years a controversy has developed concerning the interplay of antiferromagnetic order and superconductivity in UPd_2Al_3 . In the traditional view of heavy-fermion systems the *f*-electron orbitals are screened by a singlet coupling with the conduction electrons and then condense into a heavy Fermi liquid at low temperatures. In this scenario the *f* electrons are itinerant and the superconductivity is due to an abundance of soft magnetic fluctuations. The effects of spin-orbit coupling may then be treated by a two-component susceptibility (Bernhoeft and Lonzarich, 1995; Bernhoeft *et al.*, 1998). Here observation that the correlation length associated with the resonance peak matches the superconducting coherence length provided an interpretation of the resonance peak as a key feature of the Copper pairs themselves. The main objection against the traditional scenario is its lack of material-specific aspects.

In an alternative scenario it has been proposed that only one of the three *5f* uranium electrons is itinerant, whereas the other two are localized (Sato *et al.*, 2001; Zwicky *et al.*, 2002). The microscopic underpinning of this so-called duality model are strong intra-atomic correlations that are subject to Hund's rules and weak anisotropic hopping (Efremov *et al.*, 2004). In the duality model the exchange interaction between the itinerant and localized-electron subsystems drives the supercon-

ductivity in the form of a magnetic exciton. The main objection against the duality model and a pairing mediated by crystal field excitations is that the crystal field levels cannot be distinguished experimentally. The model nevertheless proves to be quite powerful. In a first analysis an A_{1g} order parameter symmetry was predicted (Miyake and Sato, 2001). Further implications have been worked out in a strong-coupling approach and were found to be compatible with experiment (McHale *et al.*, 2004). The theoretical analysis established that the emergence of unconventional superconductivity results in a resonance peak in the spectrum of magnetic excitations, consistent with neutron scattering (Chang *et al.*, 2007).

We conclude this section with a review of the properties of UPd_2Al_3 at high pressure. The electrical resistivity under pressure shows that T_N decreases from 14 to about 8 K at a pressure of 65 kbar, while the normal state maximum in the resistivity increases (Link *et al.*, 1995). At low pressures elastic neutron scattering shows an initial increase of μ_{ord} , followed by a decrease above 5 kbar with a rate $d\mu_{\text{ord}}/dp = -0.16\mu_B/\text{kbar}$. This is tracked by T_N which decreases at a rate $dT_N/dp \approx -0.05$ K/kbar at high pressures (Honma *et al.*, 1999). Up to 11 kbar the lattice constants decrease at a rate $c_0^{-1}dc/dp = 7.5 \times 10^{-4} \text{kbar}^{-1}$ and $a_0^{-1}da/dp = 4.728 \times 10^{-4} \text{kbar}^{-1}$.

High-pressure x-ray diffraction in UPd_2Al_3 and UNi_2Al_3 up to 400 kbar shows that both compounds have initially the same bulk modulus $B_0 = 159(6)$ GPa (Krimmel *et al.*, 2000). In UPd_2Al_3 these studies further revealed a structural phase transition at $p_c = 250$ kbar from a high-symmetry hexagonal to a low-symmetry orthorhombic state with space group $Pmmm$. Up to 230 kbar the c/a ratio remains essentially constant. In the high-pressure phase the compressibility is a factor of 2 larger. The structure above p_c belongs to space group $Pmmm$, which is a subgroup of $Cmmm$, which in turn is a nonhexagonal nonisomorphic subgroup of $P6/mmm$. The shortest metal-metal spacing in UPd_2Al_3 is the U-Pd distance, which reaches 1.51 Å at p_c . Interestingly, this corresponds to the sum of ionic radii of U^{4+} and Pd^{4+} , suggesting a U^{4+} valence-fluctuating state below p_c and U^{4+} to U^{5+} transition at p_c , with the ionic radius of U^{5+} reduced by 15%. A combination of resonant inelastic x-ray scattering with first-principles structure calculations is consistent with a delocalization from $\text{U}^{4+\delta}$ to $\text{U}^{4+\delta}$ (Rueff *et al.*, 2007). Finally, the extrapolated pressure where the superconductivity in UPd_2Al_3 vanishes, corresponds to the critical pressure of the structural transition (Link *et al.*, 1995). While this may be completely fortuitous, it might alternatively identify the tetravalent U configuration as a precondition for superconductivity.

b. UNi_2Al_3

The magnetism and superconductivity in UNi_2Al_3 are much more typical of itinerant *5f* electrons than those of UPd_2Al_3 . The antiferromagnetic order is an incommen-

surate spin-density wave, and the superconductivity is a candidate for spin-triplet pairing. Further, at the antiferromagnetic transition at $T_N=4.6$ K the anomalies in the physical properties, such as the specific heat, are fairly weak. The corresponding magnetic entropy released at T_N is small, $S_m=0.12R \ln 2$ (Tateiwa *et al.*, 1998). Likewise the resistivity shows only a faint feature at T_N (Dalichaouch *et al.*, 1992). As compared with UPd₂Al₃ the smaller U-U distance, $d_{U-U}=4.018$ Å in UNi₂Al₃, is also compatible with the more itinerant character of the 5*f* electrons. As mentioned above, because the U-U distance in both compounds is above the Hill limit (3.4 Å), the itineracy must be due to hybridization with other electrons.

The normal state susceptibility of UNi₂Al₃ displays a broad maximum at $T^* \sim 100$ K, characteristic of a dominant energy scale, but the coherence temperature may be as high as 300 K (Sato *et al.*, 1996). The normal state properties of UNi₂Al₃ at low temperatures show the presence of strong electronic correlations. This is best seen in the specific heat, which shows an enhanced Sommerfeld coefficient $\gamma=0.12$ J/mol K² and an enhanced T^2 resistivity (Geibel, Schank, *et al.*, 1991).

Selected microscopic probes nevertheless suggest a certain degree of 5*f* localization. Photoemission exhibits a combination of a sharp peak near E_F , a smaller feature around 0.6 eV and a broad hump at 2 eV (Yang *et al.*, 1996). The features near E_F and at 0.6 eV have been attributed to itinerant and localized 5*f* electrons, respectively, while the hump at 2 eV is related to the Ni 3*d* states. The photoemission studies compare with polarized neutron scattering and circular dichroism measurements, which show a nearly spherical magnetization distribution at the uranium sites of the order of 86% in both UPd₂Al₃ and UNi₂Al₃. In UPd₂Al₃ the remaining 14% is due to diffuse background, while in UNi₂Al₃ the remaining 14% can be attributed to the Ni site (7%) and diffuse background (7%) (Kernavanois *et al.*, 2000). The 5*f* orbital contribution observed in circular dichroism is consistent with that inferred from the polarized neutron scattering study. Finally, a local character of the 5*f* electrons has also been inferred from μ SR measurements (Amato *et al.*, 2000; Schenck *et al.*, 2000). A peculiarity of the μ SR studies in UNi₂Al₃ is the extended muon stopping sites, where the muon may tunnel along a ring of six *m* sites that surrounds the *b* site at (0,0, 1/2).

The bulk magnetic anisotropy of UNi₂Al₃ is comparable to that of UPd₂Al₃ and of the order of 3–5 depending on the temperature (Sato *et al.*, 1996; Süllow *et al.*, 1997). The proposed crystal electric field scheme to account for the susceptibility is the same as for UPd₂Al₃, but with larger values. Specifically, a Γ_4 singlet ground state is followed by a Γ_1 first excited singlet at 100 K, two Γ_6 doublets at 340 K, two Γ_5 doublets at 450 K, one Γ_3 singlet at 1300 K, and a Γ_5 doublet at 1800 K (Süllow *et al.*, 1997). It is interesting to note that the ratio of ordered moment to T_N in both compounds is consistent with the crystal field scheme. As for UPd₂Al₃ the experi-

mental evidence hence also supports a tetravalent uranium configuration.

Neutron scattering experiments in UNi₂Al₃ at first failed to detect the antiferromagnetic order (Krimmel *et al.*, 1992), while μ SR and NMR showed numerous features hinting at incommensurate antiferromagnetism with a small ordered moment (Amato *et al.*, 1992; Kyogaku *et al.*, 1993). Moreover, ²⁷Al NMR shows an enhancement of the spin-lattice relaxation rate near T_N characteristic of an abundance of spin fluctuations (Kyogaku *et al.*, 1993). Single-crystal elastic neutron scattering eventually revealed a second-order phase transition of incommensurate antiferromagnetic order at $T_N=4.6$ K with a wave vector $\vec{Q}=(1/2 \pm \delta, 0, 1/2)$, where $\delta = 0.110 \pm 0.003$, and a magnetic correlation length $\xi_m \approx 400$ Å are typical of heavy-fermion systems. The ordered moment $\mu_{\text{ord}}=(0.24 \pm 0.10)\mu_B$ is indeed small (Schröder *et al.*, 1994; Lussier *et al.*, 1997) with a critical exponent $\beta=0.34 \pm 0.03$, characteristic of three-dimensional order. The latter feature in particular contrasts with the small-moment antiferromagnetism in UPt₃ and URu₂Si₂. Spherical neutron polarimetry established that the magnetic structure may indeed be viewed as a spin-density wave, where the moments point in the \vec{a}^* direction and the amplitude is modulated (Hiess *et al.*, 2001). The antiferromagnetic planes are stacked along the *c* axis. The magnetic phase diagram of UNi₂Al₃ as inferred from the bulk properties is fairly isotropic (Süllow *et al.*, 1997). An exception is the crystallographic *b* axis, where an additional transition has been taken as evidence of an incommensurate to commensurate phase transition, i.e., magnetic field allows the commensurability to be tuned. Altogether, the magnetic order in UNi₂Al₃ differs considerably from that in UPd₂Al₃.

UNi₂Al₃ is superconducting below a temperature $T_s=1.06$ K. In polycrystalline samples the specific heat anomaly is distinct but small, with $\Delta C/\gamma T_s \approx 0.4$. Magnetization measurements of $H_{c1}^a \approx 0.002$ T and $H_{c2}^a \approx 0.52$ T imply type-II superconductivity with a Ginzburg-Landau $\kappa \approx 11$ (Sato *et al.*, 1996). In contrast to UPd₂Al₃, which shows a fairly isotropic H_{c2} and initial slope near T_s and paramagnetic limiting, UNi₂Al₃ displays marked anisotropies where $H_{c2}^c \approx 0.9$ T, $dH_{c2}^c/dT=-1.14$ T/K and $H_{c2}^a \approx 0.35$ T, $dH_{c2}^a/dT=-0.42$ T/K, respectively (Sato *et al.*, 1996). As for UPd₂Al₃ these values may be compared with the expected paramagnetic limit $H_{p0}=0.18$ T and orbital limits $H_{c2}^{*a}=0.79$ T and $H_{c2}^{*c}=0.29$ T. Thus H_{c2} exhibits orbital limiting, $H_{c2} \approx H_{c2}^*$ and $H_{c2} < H_{p0}$, in stark contrast to UPd₂Al₃. At first sight this comparison suggests pure orbital limiting consistent with triplet pairing (Ishida *et al.*, 2002). However, it may also be reconciled with the coexistence of superconductivity and antiferromagnetic order (Sato *et al.*, 1996). In any case, the superconductivity shows numerous hints of unconventional pairing. For instance, NMR measurements show the absence of a Hebel-Slichter peak at T_s (Kyogaku *et al.*, 1993) and the decrease in $1/T_1$ in the superconducting state is consis-

tent with line nodes (Tou *et al.*, 1997). The Knight shift, moreover, remains unchanged in the superconducting state, as is characteristic of spin-triplet pairing (Ishida *et al.*, 2002). This contrasts with the behavior observed in UPd₂Al₃, where the decrease in the Knight shift indicates spin-singlet pairing. Spin-triplet pairing in bulk samples of UNi₂Al₃ is also in contrast with preliminary studies of thin epitaxial films of UNi₂Al₃. These studies suggest that T_s depends on the current direction, and H_{c2} implies spin-singlet pairing (Jourdan *et al.*, 2004).

Early μ SR measurements suggested a genuine coexistence of superconductivity and antiferromagnetism (Amato *et al.*, 1992). Moreover, elastic neutron scattering shows an effective increase in the ordered magnetic moment in the superconducting state (Lussier *et al.*, 1997). Inelastic neutron scattering shows quasielastic scattering around $\vec{Q}=(0.39,0,0.5)$ similar to what is observed in UPd₂Al₃ but with a reduced intensity of about 10%. However, there is neither a buildup of additional intensity nor a gap developing, nor a gapped spin-wave excitation (Aso *et al.*, 2000). Further studies established quasielastic scattering along $(H,0,n/2)$, where n is an odd integer, and the width is ~ 6 meV. This scattering shifts with increasing temperature from an incommensurate to a commensurate position (Gaulin *et al.*, 2002).

As for UPd₂Al₃ only a small pressure dependence of T_N and T_s is observed in UNi₂Al₃, given by $dT_N/dp \approx -0.12$ K/kbar and $dT_s/dp = -0.024 \pm 0.003$ K/kbar (Wassermann and Springford 1994). In fact, substitutional doping of Ni by Pd appears to act mainly like pressure. Likewise the bulk modulus determined by x-ray diffraction up to 385 kbar is similar and given by $B_0=150(5)$ GPa without evidence for a structural phase transition similar to UPd₂Al₃ (Krimmel *et al.*, 2000). In UNi₂Al₃ the pressure where a U-Pd spacing is reached that is equivalent to that in UPd₂Al₃ at p_c may be extrapolated as 725 kbar.

In summary, neither UPd₂Al₃ nor UNi₂Al₃ seems to be located in the immediate vicinity of a zero-temperature instability, that may be reached with hydrostatic pressure. This may provide an important hint that crystal electric fields indeed actually present a key ingredient for the occurrence of superconductivity in both compounds.

c. CePt₃Si

The discovery of heavy-fermion superconductivity in the antiferromagnetic state of CePt₃Si has attracted much interest, not because it coexists with antiferromagnetic order but because the crystal structure of CePt₃Si lacks inversion symmetry (Bauer, Hilscher, *et al.*, 2004). The low-temperature properties of this compound are characterized by the onset of commensurate antiferromagnetic order at $T_N=2.2$ K with an ordering wave vector $\vec{Q}=(0,0,1/2)$. Even though band structure calculations show dominant effects of the Rashba spin-orbit coupling on the electronic structure (Samokhin, 2004; Samokhin *et al.*, 2004), chiral components or a canting of the magnetic order have so far not been observed.

The value of $T_s=0.75$ K first reported for CePt₃Si is fairly high. In contrast, more recent work suggests a lower $T_s=0.45$ K in combination with sharper magnetic and superconducting transitions (Takeuchi *et al.*, 2007). Due to the lack of inversion symmetry CePt₃Si may be viewed as the first representative of a new class of heavy-fermion superconductors. Further members of this class discovered so far are CeRhSi₃, CeIrSi₃, and CeCoGe₃. The properties of the noncentrosymmetric superconductors including CePt₃Si are reviewed in Sec. IV.A.

2. Small moment antiferromagnets

a. UPt₃

The heavy-fermion compound UPt₃ exhibits two forms of order at low temperatures. At $T_N \approx 5$ K UPt₃ orders antiferromagnetically. This is followed by a superconducting transition at $T_s=0.54$ K. Because UPt₃ so far is the only intermetallic compound, that unambiguously displays multiple superconducting phases with different order parameter symmetries, it has been studied in great detail. In the following we review key features of the magnetic order and superconductivity to put them in context with the antiferromagnetic compounds addressed so far. Evidence for multiple superconducting phases is addressed in Sec. V. For an extensive review of the properties of UPt₃ see Joynt and Taillefer (2002).

UPt₃ crystallizes in a hexagonal structure, space group $P6_3/mmc$, point group D_{6h} . The lattice parameters are $a=5.764$ Å and $\tilde{c}=4.899$ Å, where \tilde{c} is the distance between neighboring planes. It is convenient to define the b axis perpendicular to the a axis (and thus parallel to the a^* axis). The nearest U-U distance $d_{U-U}=4.132$ Å is quite large. The compressibilities have been inferred from measurements of the sound velocity. They are given by $\kappa_a=-a^{-1}da/dp=0.164$ Mbar⁻¹, $\kappa_c=-c^{-1}dc/dp=0.151$ Mbar⁻¹, and for the volume $\kappa_V=2\kappa_a+\kappa_c=0.479$ Mbar⁻¹ (de Visser *et al.*, 1987). Several transmission electron microscopy studies have reported a possible incommensurate structural modulation. However, it is now generally believed that this modulation results from ion milling and is not present in bulk samples (Ellman *et al.*, 1995, 1997).

The normal state of UPt₃ at low temperatures is well described as a heavy Fermi liquid. The normal state specific heat in UPt₃ up to 1.5 K is linear in temperature with $C/T \approx 0.44 \pm 0.02$ J/K² mol and a weak cubic term $T^3 \ln(T/T^*)$ as discussed by de Visser *et al.* (1987). At higher temperatures an additional T^3 contribution emerges consistent with a Debye temperature $\Theta_D \approx 210$ K. For $H > H_{c2}$ an unexplained additional strong upturn in C/T emerges below ~ 0.1 K (Brison *et al.*, 1994).

As a function of temperature the resistivity of UPt₃ decreases monotonically from the room temperature values $\rho_{ab} \approx 230$ $\mu\Omega$ cm and $\rho_c \approx 130$ $\mu\Omega$ cm (de Visser *et al.*, 1987; Kimura *et al.*, 1995). At low temperatures a quadratic temperature dependence of the

resistivity is observed $\rho(T) = \rho_0 - AT^2$, where $A_{ab} \approx 1.55 \pm 0.1 \mu\Omega \text{ cm K}^{-2}$ and $A_c \approx 0.55 \pm 0.05 \mu\Omega \text{ cm K}^{-2}$ [see, e.g., Lussier *et al.* (1994); Kimura *et al.* (1995); Suderow *et al.* (1997)]. At low temperatures the anisotropy of the resistivity is essentially temperature independent with $\rho_b/\rho_c \approx 2.6$. The anisotropy is attributed to differences of Fermi velocities. The charge carrier mean free path inferred from the residual resistivity and quantum oscillatory studies is of the order of 5000 Å. Under pressure the A coefficient of the resistivity decreases at a rate $d \ln A / dp \approx -40 \text{ Mbar}^{-1}$ (Willis *et al.*, 1985; Ponchet *et al.*, 1986). Comparison of the T^2 resistivity with the linear temperature dependence of the specific heat establishes consistency of the ratio γ/\sqrt{A} with other heavy-fermion systems (Kadowaki and Woods, 1986). The observation that UPt₃ forms a slightly anisotropic three-dimensional Fermi liquid with strong electronic correlations is underscored by the temperature dependence observed in thermal conductivity measurements (Lussier *et al.*, 1994; Suderow *et al.*, 1997).

The normal state magnetic properties of UPt₃ are strongly enhanced. The uniform susceptibility in the basal plane exhibits a strong Curie-Weiss dependence at high temperature and a broad maximum around 20 K (Frings *et al.*, 1983). The susceptibility is anisotropic with $\chi_c < \chi_{ab}$. The behavior seen in the uniform susceptibility is tracked in ¹⁹⁵Pt NMR (Tou *et al.*, 1996). Inelastic neutron scattering establishes a complex spectrum of antiferromagnetic fluctuations (Aeppli *et al.*, 1987, 1988). At moderate temperatures a fluctuation spectrum of large uranium moments ($\sim 2\mu_B$) is observed with a characteristic energy of 10 meV. Below ~ 20 K antiferromagnetic correlations develop at $\vec{Q} = (0, 0, 1)$ and a peak around 5 meV. These fluctuations correspond to correlations between adjacent nearest-neighbor uranium sites. When the temperature is decreased well below 20 K additional antiferromagnetic correlations develop around $\vec{Q} = (\pm 1/2, 0, 1)$ with a characteristic energy ~ 0.3 meV and an effective moment of $\sim 0.1\mu_B$. These fluctuations correspond to intersite correlations within each hexagonal plane. Finally, slow magnetic fluctuations with a dispersive relaxation rate exist at low temperatures (Bernhoeft and Lonzarich, 1995). Thus the excitation spectrum yields a duality of slow and fast excitations somewhat similar to that of UPd₂Al₃. In what way these fluctuations affect the unconventional superconductivity in UPt₃ is an open issue.

Finally, the magnetic properties of UPt₃ also include an elastic component of the magnetic correlations at $\vec{Q} = (\pm 1/2, 0, 1)$ with a small ordered moment around $(0.01 - 0.03)\mu_B/U$. The antiferromagnetic order was first noticed in μSR and later confirmed by neutron scattering (Aeppli *et al.*, 1988). The magnetic order is collinear and commensurate with short correlation lengths of ~ 300 Å. It appears to be insensitive to sample quality. Perhaps most remarkably the only experimental probes that are sensitive to the antiferromagnetic order are neutron scattering and μSR . Notably, the antiferromag-

netism is not seen in NMR (Tou *et al.*, 1996), specific heat (Fisher *et al.*, 1991), and magnetization measurements. It has therefore been suggested that the magnetic order is essentially dynamic in nature.

Microscopic evidence that UPt₃ forms a heavy-fermion ground state was obtained in quantum oscillatory studies (Taillefer *et al.*, 1987; Taillefer and Lonzarich, 1988). These studies revealed a wide range of mass enhancements up to 120 times the free-electron mass. Despite these strong mass enhancements the spectra were found to be in good agreement with results of density functional theory taking the 5*f* electrons to be itinerant [see Joynt and Taillefer (2002), and references therein]. Most of the frequencies, especially those corresponding to large portions of the Brillouin zone, could be identified satisfactorily. In summary the Fermi surface consists of six sheets of uniformly high effective masses. In fact, the Fermi velocities on the observed sheets are extremely slow, $\langle v_F \rangle_{bc} \approx 5000$ m/s, and do not differ by more than 15%. In contrast to the topology of the Fermi surface, density functional theory fails to account for these large mass renormalizations.

It has been proposed that the mass enhancement in UPt₃ is due to a duality of the 5*f* electrons like that discussed for UPd₂Al₃ and UNi₂Al₃ (Zwicknagl *et al.*, 2002). In this scenario one *f* electron is itinerant while the other two are localized. The mass enhancement in UPt₃ can be accounted for when a crystal field level scheme similar to that of UPd₂Al₃ is assumed, with a Γ_4 ground state and Γ_3 first excited state. A potential weakness of this assumption is that the crystal field levels hybridize so strongly with the conduction electrons that inelastic neutron scattering fails to detect them. The relationship of the duality model as applied to UPt₃ and the experimentally observed small ordered moments is thus also an unresolved issue. The recent analysis of quantum oscillatory studies of the Fermi surface is, finally, in better agreement with fully itinerant *f* electrons (McMullan *et al.*, 2008).

Measurements of the resistivity, specific heat, and ac susceptibility establish UPt₃ as a bulk superconductor (Stewart *et al.*, 1984). Early studies of the ultrasound attenuation in a magnetic field (Müller *et al.*, 1987; Qian *et al.*, 1987; Schenstrom *et al.*, 1989) and of H_{c2} (Taillefer and Lonzarich, 1988) suggested the possibility of two superconducting phase transitions. This was eventually confirmed in high-resolution specific heat measurements (Fisher *et al.*, 1989; Hasselbach *et al.*, 1989). Further studies established that there are three superconducting phases, denoted A, B and C. The antiferromagnetic order can be shown to introduce an additional symmetry breaking that stabilizes these phases. In summary, three pieces of evidence identify UPt₃ as an unconventional superconductor. First, several transport quantities display marked anisotropies, most notably the ultrasound velocity and the thermal conductivity. Second, there is evidence for phase transitions within the superconducting state as seen in the specific heat and ultrasound attenuation. Third, several properties show activated tem-

perature dependences instead of the exponential freezing out of excitations. The superconducting phases of UPt_3 will be described further in Sec. V.

b. URu_2Si_2

The body-centered-tetragonal uranium compound URu_2Si_2 , space group $I4/mmm$, crystallizes with lattice constants $a=4.128 \text{ \AA}$ and $c=9.592 \text{ \AA}$. At low temperatures it undergoes two phase transitions (Schlabitz *et al.*, 1984): a transition to a hitherto unknown form at $T_0 \approx 17.5 \text{ K}$ and a second transition at $T_s \approx 1.4 \text{ K}$ to unconventional superconductivity (Palstra *et al.*, 1985; Maple *et al.*, 1986; Schlabitz *et al.*, 1986). The entropy released at T_0 is given by $\Delta S \approx 0.2R \ln 2$. Despite intense experimental and theoretical efforts the ordering phenomenon accounting for this entropy reduction has still not been identified. The phase below T_0 in URu_2Si_2 has in turn become known as “hidden order” (HO). The hidden order exhibits many characteristics of an electronic condensation: (i) the specific heat is consistent with a BCS gap (Maple *et al.*, 1986), (ii) the resistivity at T_0 is strongly reminiscent of the density-wave system chromium (Fawcett, 1988), (iii) slight doping suppresses the resistivity anomaly rapidly (Kim *et al.*, 2004), and (iv) the magnetization at T_0 suggests the formation of a spin gap (Park *et al.*, 1997), while optical conductivity indicates a charge gap (Bonn *et al.*, 1988). Recent thermal conductivity measurements also point toward a gap formation (Sharma *et al.*, 2005). The Hall effect and magnetoresistance suggest near compensation of particle and hole carriers and a strong interplay between the stability of the hidden order under Rh doping and the degree of polarization of the Fermi liquid and the Fermi surface topology (Jo *et al.*, 2007; Oh *et al.*, 2007).

Neutron diffraction in URu_2Si_2 shows antiferromagnetic order below T_0 with a $[001]$ modulation of small moments, $(0.03 \pm 0.01) \mu_B/\text{U}$, and the spins aligned along the c axis (Broholm *et al.*, 1987). The magnetic order is three dimensional with strong Ising-type spin anisotropy. Within a local-moment scenario the antiferromagnetism does not account for ΔS . This contrasts with the antiferromagnetism with a large moment of $0.4 \mu_B/\text{U}$ and the same Ising anisotropy, which emerges under large hydrostatic pressure (Amitsuka *et al.*, 1999). A phase diagram is shown in Fig. 11 (Amitsuka *et al.*, 2007). NMR (Matsuda *et al.*, 2001, 2003) and μSR (Amitsuka *et al.*, 2003) measurements suggest that the small-moment antiferromagnetism at ambient pressure represents a small volume fraction of large-moment antiferromagnetism. T_0 increases as a function of pressure and dT_0/dp increases at $p^* \approx 14 \text{ kbar}$. In fact, the increase in dT_0/dp at p^* even persists under Re doping (Jeffries *et al.*, 2007). There is currently growing consensus, that the small antiferromagnetic moment is not an intrinsic property of the hidden order. However, a spin-density wave close to perfect nesting may exhibit the combination of a small moment with a large reduction of entropy (Chandra *et al.*, 2003; Mineev and Zhitomirsky, 2005).

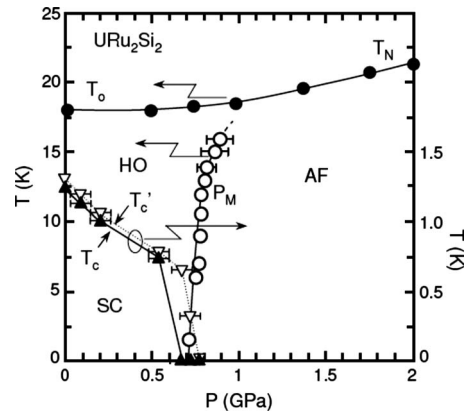


FIG. 11. Temperature vs pressure phase diagram of URu_2Si_2 inferred from various experimental probes. The onset of the hidden order T_0 is weakly pressure dependent. The hidden order changes to large-moment Ising antiferromagnetism above 7 kbar without pronounced effect on the evolution of T_0/T_N . Superconductivity vanishes with the appearance of the antiferromagnetism. HO, hidden order; AF, large moment antiferromagnet; and SC, superconductivity. From Amitsuka *et al.*, 2007.

The hidden order in URu_2Si_2 is bounded by more conventional behavior at high excitation energies, high pressure, and high magnetic fields. Inelastic neutron scattering shows a gap $\Delta(T \rightarrow 0) \approx 1.8 \text{ meV}$ in the excitation spectrum on top of the anisotropy gap (Broholm *et al.*, 1991). At low energies and temperatures, dispersive crystal field singlet excitations at the antiferromagnetic ordering wave vector are observed. These propagating excitations merge above 35 meV or for $T > T_0$ into a continuum of quasielastic antiferromagnetic spin fluctuations, as normally observed in heavy-fermion systems. The excitations exhibit the Ising anisotropy up to the highest energies investigated experimentally. A rough integration of the fluctuation spectra suggests that the size of the fluctuating moments would be consistent with ΔS , provided that these moments were involved in the ordering process (Broholm *et al.*, 1991; Wiebe *et al.*, 2007). Under large applied magnetic fields parallel to the c axis the antiferromagnetic moment and T_0 decrease, and T_0 collapses to zero at $B_m = 38 \text{ T}$ (Mason *et al.*, 1995; Santini *et al.*, 2000; Bourdarot *et al.*, 2003, 2005). At B_m a cascade of metamagnetic transitions is observed, in which a large uniform magnetization is recovered (Harrison *et al.*, 2003; Kim, Harrison, *et al.*, 2003). Up to B_m the entropy reduction at T_0 stays approximately constant (Kim, Hall, *et al.*, 2003), while the gap Δ , as seen in neutron scattering, increases at least up to 17 T (Bourdarot *et al.*, 2003). For a recent review see, e.g., Harrison *et al.* (2004).

The antiferromagnetic order in URu_2Si_2 is stabilized under uniaxial stress along certain crystallographic directions and under hydrostatic pressure. NMR (Matsuda *et al.*, 2001) μSR (Amitsuka *et al.*, 2003), and neutron scattering (Amitsuka *et al.*, 1999) measurements suggest that the AF volume fraction increases and reaches 100% above $p_c \sim 14 \text{ kbar}$. An analogous increase in the AF

signal is also seen in neutron scattering under uniaxial stress of a few kilobars along the [100] and [110] directions (Yokoyama *et al.*, 2002, 2005) but not under uniaxial stress along the *c* axis [001]. Inelastic neutron scattering under pressure shows that the dispersive crystal field singlet excitations at low energies vanish at high pressures (Amitsuka *et al.*, 2000), consistent with them being a property of the HO volume fraction.

Measurements of the Fermi surface represent a major challenge. For instance, de Haas–van Alphen (dHvA) studies under hydrostatic pressure (Nakashima *et al.*, 2003) do not resolve abrupt changes in the dHvA frequencies and cyclotron masses at p_c . This contrasts with the naive expectation of a distinct phase separation at p_c . In these studies the most important observation is a considerable increase in the cyclotron mass with increasing pressure. New insights may be achieved with ultrapure samples, which have recently become available (Kasahara *et al.*, 2007; Matsuda *et al.*, 2008).

A large number of microscopic scenarios have been proposed to explain the hidden order. These include various versions of spin- and charge-density-wave orders (Maki *et al.*, 2002; Mineev and Zhitomirsky, 2005), forms of crystal electric field polar order (Santini and Amoratti, 1994; Ohkawa and Shimizu, 1999; Kiss and Fazekas 2005), unconventional density waves (Ikeda and Ohashi, 1998) and orbital antiferromagnetism (Chandra *et al.*, 2002) Pomeranchuk instabilities (Varma and Zhu, 2006) or nematic electronic phases (Barzykin and Gorkov, 1993), and combinations of local with itinerant magnetism (Okuno and Miyake, 1998) and dynamical forms of order (Fåk *et al.*, 1999; Bernhoeft *et al.*, 2003). None of the models was able to satisfactorily explain the available experimental data; some models are purely phenomenological yet lack material-specific predictions that can be readily verified by experiment, while others focus only on selected microscopic features. This leaves considerable space for fresh theoretical input.

The nature of the superconductivity in the hidden order of URu₂Si₂ is still comparatively little explored. T_s depends sensitively on sample quality. It is as high as $T_s=1.53$ K in the purest samples, which have residual resistivities as low as several $\mu\Omega$ cm and charge carrier mean free paths $l\sim 1000$ Å as inferred from quantum oscillations (Brison *et al.*, 1995). In the specific heat the onset of superconductivity is accompanied by a pronounced anomaly, $\Delta C/\gamma T_s\approx 0.8-0.93$ (Fisher *et al.*, 1990; Brison *et al.*, 1994). However, this value is reduced by comparison to the weak-coupling BCS value of 1.43. Between T_s and $0.2T_s$ the specific heat varies as $C\propto T^2$ akin to that seen in UPt₃. This is consistent with line nodes of either an $E_u(1,1)$ or a B_g state (Hasselbach *et al.*, 1993). Line nodes and unconventional superconductivity have also been inferred from ²⁹Si NMR and ¹⁰¹Ru NQR, where $1/T_1$ is found to show no coherence peak and decreases as $1/T_1\propto T^3$ below T_s , while the Knight shift is unchanged (Kohori *et al.*, 1996; Matsuda *et al.*, 1996). However, it has been pointed out that the specific heat data are equally well explained in terms of *s*-wave pair-

ing in the presence of antiferromagnetism, where nodes are generated by the magnetic order (Brison *et al.*, 1994)

Further information about the possible location and nature of the nodal structure has been inferred from the angular field dependence of the specific heat, where the absence of an angular dependence in the tetragonal basal plane and marked anisotropy between *a* and *c* axes suggests that the gap nodes are rather localized near the *c* axis (Sakakibara *et al.*, 2007). An anisotropic gap has also been inferred from point contact spectroscopy, consistent with *d*-wave pairing (Hasselbach *et al.*, 1992; De Wilde *et al.*, 1994; Naidyuk *et al.*, 1996). If the experimental evidence for nodes is indeed due to the antiferromagnetism as suggested above, this requires that the small antiferromagnetic moments are an intrinsic property of the hidden order, or that the hidden order interacts with the superconductivity in the same way that antiferromagnetism would do.

A different scenario of the superconductivity has recently been proposed based on the electrical and thermal transport properties in ultrapure URu₂Si₂ (Kasahara *et al.*, 2007; Matsuda *et al.*, 2008). Here the Hall effect and magnetoresistance suggest multiband superconductivity in a compensated electronic environment. Most remarkably, in the low-temperature limit the thermal conductivity divided by temperature κ/T displays a rapid increase at low fields followed by a plateau up to some intermediate field $H_s<0.2H_{c2}$. Above H_s the dependence evolves differently for fields parallel and perpendicular to the *c* axis, but κ/T drops abruptly just below H_{c2} , characteristic of H_{c2} being first order (the first-order behavior occurs below ~ 0.5 K. Based on their observations Kasahara *et al.* (2007) suggested a two-component order parameter, with two distinct gaps: line nodes perpendicular to the *c* axis on a spherical light-hole band and point nodes along the *c* axis on the elliptical heavy-electron band. This scenario, notably the first-order behavior, and point nodes, is consistent with the magnetic field dependence of the specific heat in the superconducting state (Yano *et al.*, 2008). Interestingly, the thermal conductivity in the same ultrapure samples also suggests a melting transition of the flux line lattice and the formation of a coherent quasiparticle Bloch state (Okazaki *et al.*, 2008).

The lower critical field of the superconductivity in URu₂Si₂ of $H_{c1}(T\rightarrow 0)\approx 3.3\times 10^{-3}$ T is essentially isotropic and displays a weak temperature dependence (Wüchner *et al.*, 1993). H_{c2} is in contrast strongly anisotropic with $H_{c2}^a=14$ T and $H_{c2}^c=3$ T. This implies strong type-II behavior and short coherence lengths $\xi_a\approx 100$ Å and $\xi_c\approx 25$ Å. The anisotropy of H_{c2} may be accounted for reasonably well by an anisotropic mass model (Brison *et al.*, 1994). For the *c* axis, H_{c2} can be explained by Pauli limiting, while it can be described by a combination of Pauli and orbital limiting for the *a* axis with strongly anisotropic Pauli limiting between the *a* and *c* axes (Brison *et al.*, 1995).

An additional weak increase in H_{c2} for the *c* axis at low temperatures that exceeds Pauli limiting has been

considered as tentative evidence for a FFLO phase. Also unusual is the temperature dependence of the anisotropy H_{c2}^a/H_{c2}^c , which initially increases below T_s and becomes constant below $\sim 0.6T_s$. In fact, the Ginzburg-Landau parameter inferred from the magnetization exhibits a gradual decrease well below T_s , somewhat slower than the behavior anticipated from H_{c2} but consistent with paramagnetic limiting (Tenya *et al.*, 2000). Finally, a small positive curvature in the temperature dependence of H_{c2} near T_s has been considered as possible evidence of a multicomponent order parameter that couples to an antiferromagnetic moment (Kwok *et al.*, 1990; Thalmeier and Lüthi, 1991). Altogether, it is presently accepted that URu₂Si₂ does not display multiple superconducting phases in terms of real- or momentum-space modulations (cf. Secs. V.A.2.f and V.B.1).

The thermal expansion displays pronounced anomalies at T_s with $\Delta\alpha_a = -0.68 \times 10^{-6} \text{ K}^{-1}$ and $\Delta\alpha_c = 0.47 \times 10^{-6} \text{ K}^{-1}$ (van Dijk *et al.*, 1995). Thus, the superconductivity varies sensitively with uniaxial pressure, $dT_s/dp_a = -0.062 \text{ K/kbar}$ and $dT_s/dp_c = +0.043 \text{ K/kbar}$, consistent with experiment (Bakker *et al.*, 1991). The qualitative temperature dependence of H_{c2} for uniaxial pressure applied along the *a* axis remains therefore unchanged (Pfeleiderer, Bedin, *et al.*, 1997). For comprehensive information on the elastic constants, see Lüthi *et al.* (1995).

The interplay of hidden order, small-moment antiferromagnetism, and superconductivity in URu₂Si₂ is largely unresolved. Early neutron scattering studies suggested that the small antiferromagnetic moments either remain unchanged in the superconducting state (Broholm *et al.*, 1987; Mason *et al.*, 1990; Wei *et al.*, 1992) or may be decreasing by 1–2 % (Honma *et al.*, 1999). This is consistent with microscopic coexistence of hidden order and superconductivity. Under hydrostatic pressure T_s decreases and vanishes between 5 and 14 kbar (McElfresh *et al.*, 1987; Brison *et al.*, 1994; Jeffries *et al.*, 2007). The magnetization and specific heat thereby show that the superconducting volume fraction decreases or, alternatively, that the superconducting gap vanishes (Fisher *et al.*, 1990; Tenya *et al.*, 2005; Uemura *et al.*, 2005). Since the suppression of superconductivity is accompanied by an increase in volume fraction of large antiferromagnetic moments, the large-moment antiferromagnetism and superconductivity must represent competing forms of order. In contrast, the HO may even represent a precondition for the superconductivity in URu₂Si₂ to occur, which points at an unknown superconducting pairing interaction.

C. The puzzling properties of UBe₁₃

In the following we review the properties of UBe₁₃. Although the second system in which heavy-fermion superconductivity was identified, this compound remains one of the most puzzling materials among the systems known to date. For a long time UBe₁₃ seemed to be outside any of the patterns observed in the other sys-

tems. Recent work suggests possible vicinity to an antiferromagnetic quantum critical point under a magnetic field (Gegenwart *et al.*, 2004). It is not unlikely, however, that incipient antiferromagnetism is only part of the story.

UBe₁₃ crystallizes in the cubic NaZn₁₃ structure, space group O_h^6 or $Fm\bar{3}c$, with lattice constant $a = 10.248 \text{ \AA}$ (Pearson, 1958). There are 8 f.u. per unit cell, with two Be sites; the uranium atoms are surrounded by cages of 24 Be atoms (Goldman *et al.*, 1985). The U atoms form a simple-cubic sublattice, with a large U-U spacing $d'_{\text{U-U}} = 5.13 \text{ \AA}$, well above the Hill limit of 3.4 \AA , suggesting that any broadening of the uranium *f* states into bands is due to hybridization with the conduction bands and not the result of direct overlap of the *f* orbitals. By comparison with other heavy-fermion superconductors, the properties of UBe₁₃ are fairly insensitive to sample quality. In the normal metallic state of UBe₁₃ the specific heat exhibits a shallow maximum around 2 K, with a large linear term $C/T = \gamma \approx 1.1 \text{ J/mol K}^2$ (Ott *et al.*, 1983; Ott, Rudigier, Rice, *et al.*, 1984). The susceptibility displays a strong Curie-Weiss dependence with $\mu_{\text{eff}} \approx 3\mu_B$ and a Curie-Weiss temperature $\Theta \approx -70 \text{ K}$. The electrical resistivity increases with decreasing temperature and reaches a large value of order $240 \mu\Omega \text{ cm}$ before it decreases around 2 K and reaches a value of $130 \mu\Omega \text{ cm}$ at the onset of superconductivity. The extrapolated zero-temperature residual resistivity is $\rho_0 = 60 \mu\Omega \text{ cm}$ (Maple *et al.*, 1985).

Superconductivity was first observed in the resistivity of UBe₁₃ in 1975 (Bucher *et al.*, 1975)—four years prior to the discovery of superconductivity in CeCu₂Si₂. However, the zero-resistance transition at $T_s = 0.9 \text{ K}$ was erroneously attributed to a filamentary uranium segregation. The superconducting transition was eventually identified as the onset of heavy-fermion superconductivity in 1983 by means of specific heat measurements (Ott *et al.*, 1983). The specific heat anomaly is characteristic of strong-coupling superconductivity with $\Delta C/\gamma T_s \approx 2.5$. The initial variation in H_{c2} near T_s is exceptionally large, $dH_{c2}/dT = -45 \text{ T/K}$ (Maple *et al.*, 1985; Thomas *et al.*, 1996). In the zero-temperature limit $H_{c2}(T \rightarrow 0) = 14 \text{ T}$. H_{c2} exhibits strong Pauli limiting and as an additional feature a change in curvature at $T/T_s \sim 0.5 \text{ K}$. The unusual temperature dependence of H_{c2} has been attributed to a combination of very-strong-coupling superconductivity and the tendency to form a FFLO state (see also Sec. V.B.1). While the coupling constant $\lambda = 15$ in these calculations is suspiciously large and exceeds coupling constants in comparable systems by one order of magnitude, this scenario finds further support in the pressure dependence of λ , which tracks the mass enhancement inferred from $dH_{c2}/dT|_{T_s}$ and the specific heat (Glémot *et al.*, 1999).

Several properties suggest the presence of zeros of the superconducting gap. The power law dependence of the specific heat $C \sim T^3$ (Ott, Rudigier, Rice, *et al.*, 1984; Mayer *et al.*, 1986; Ott *et al.*, 1987) and penetration depth $\lambda \sim T^2$ (Einzel *et al.*, 1986; Gross *et al.*, 1986) suggests

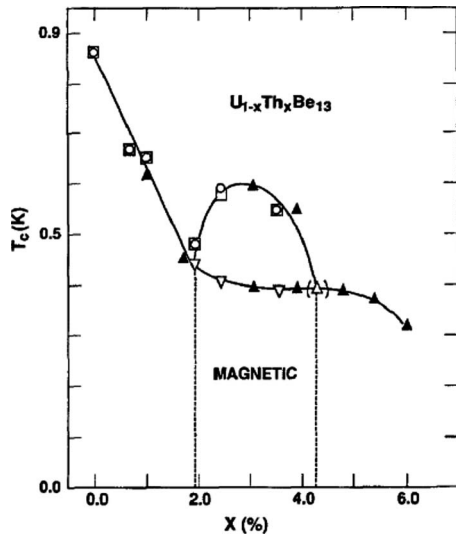


FIG. 12. Temperature vs Th concentration in $U_{1-x}Th_xBe_{13}$. The upper curve corresponds to the onset of superconductivity in the resistivity. In the range $2\% < x < 4\%$ a second transition is observed in the specific heat, which may be related to magnetic order and/or another superconducting phase. From Maple, 1995.

point nodes, whereas the NMR spin-lattice relaxation rate suggests line nodes (MacLaughlin *et al.*, 1987). This identifies UBe_{13} as an unconventional superconductor, a conjecture that is supported by the behavior under substitutional Th doping (Lambert *et al.*, 1986). $U_{1-x}Th_xBe_{13}$ displays a complex phase diagram as shown in Fig. 12 with multiple superconducting phases (Ott *et al.*, 1986). Thermal expansion and specific heat measurements identify a precursor of this effect in pure UBe_{13} (Kromer *et al.*, 1998, 2000). See Sec. V.A.2.g for a detailed discussion of this phase diagram.

The calculated electronic structure of UBe_{13} is relatively simple for itinerant *f* electrons (Norman *et al.*, 1987; Takegahara and Harima, 2000). The nature of the heavy-fermion state in UBe_{13} has nevertheless provided a major puzzle. By comparison to other heavy-fermion systems, the susceptibility and specific heat vary only weakly under a magnetic field. This is contrasted by a strong negative magnetoresistance (Rauchschalbe *et al.*, 1985; Remenyi *et al.*, 1986) providing tentative evidence that UBe_{13} is a low-density carrier system (Takegahara *et al.*, 1986; Norman *et al.*, 1987). Under hydrostatic pressure the normal metallic state assumes the more conventional form of a coherent Kondo lattice with a broad maximum at several 10 K and a decreasing resistivity at low temperatures (Aronson *et al.*, 1989; McElfresh *et al.*, 1990). The superconductivity is suppressed under pressure and T_s extrapolates to zero around 40 kbar. Interestingly, the residual resistivity decreases strongly around 40 kbar, suggesting that the scattering mechanism causing the residual resistivity may be involved in the superconducting pairing in UBe_{13} .

The first neutron scattering studies revealed a broad quasielastic Lorentzian spectrum of magnetic fluctua-

tions with a half-width of 13.2 meV (Goldman *et al.*, 1986). They failed to observe evidence for a narrow *f* resonance of antiferromagnetic correlations (Goldman *et al.*, 1986; Lander *et al.*, 1992). Recent studies, however, reveal short-range antiferromagnetic correlations below ~ 20 K for $\vec{Q}=(1/2, 1/2, 0)$ with a characteristic energy width of 1–2 meV (Coad *et al.*, 2000; Hiess *et al.*, 2002).

New studies of the normal metallic state as a function of magnetic field established non-Fermi-liquid behavior with $\rho \sim T^{3/2}$ and a related logarithmic divergence of the specific heat (Gegenwart *et al.*, 2004). For fields above H_{c2} a regime with T^2 resistivity emerges. This Fermi-liquid behavior has been linked with the suppression of a feature in the thermal expansion that has been interpreted as a freezing of three-dimensional antiferromagnetic fluctuations. When taken together with other results, this has motivated speculations on a field-tuned antiferromagnetic quantum critical point ~ 5 T in UBe_{13} , at least as a facet of the complex combination of properties of UBe_{13} .

III. INTERPLAY OF FERROMAGNETISM AND SUPERCONDUCTIVITY

Several *f*-electron ferromagnets have been found in recent years that exhibit superconductivity with $T_s \ll T_C$ (cf. Table III). These systems are in contrast with the reentrant superconductivity observed in $ErRh_4B_4$ and related compounds, where ferromagnetic order appears well below the superconducting transition temperature and both forms of order originate in separate microscopic subsystems. We begin this section with a review of systems that exhibit superconductivity in the ferromagnetic state, notably UGe_2 and $URhGe$. We next address superconductivity at the border of ferromagnetism in $UCoGe$ and UIr .

A. Superconducting ferromagnets

1. UGe_2

The superconducting ferromagnet UGe_2 crystallizes in the orthorhombic $ThGe_2$ crystal structure, space group $Cmmm$ (no. 65), with lattice constants $a = 3.997(3)$ Å, $b = 15.039(7)$ Å, and $c = 4.087(2)$ Å (Oikawa *et al.*, 1996; Boulet *et al.*, 1997). The crystal structure of UGe_2 is dominated by zigzag chains of U atoms along the *a* axis, with the U spacing $d_{U-U} = 3.85$ Å. As for UPd_2Al_3 and UNi_2Al_3 , the U-U distance is above the Hill limit and without hybridization with other electrons the *f* electrons would be localized. The U chains are stacked with Ge atoms at interstitial positions to form corrugated sheets. These sheets are separated by further Ge atoms along the *b* axis, giving the crystal structure a certain two-dimensional appearance perpendicular to the *b* axis. As discussed below the two-dimensional crystallographic appearance manifests itself in the electronic structure, which is dominated by a large cylindrical Fermi surface sheet along the *b* axis (Shick and Pickett, 2001; Shick *et al.*, 2004).

At ambient pressure UGe₂ develops ferromagnetic order below $T_C=52$ K with a zero-temperature ordered moment $\mu_s=1.48\mu_B/U$ aligned along the *a* axis. By comparison with the *a* axis, the *b* and *c* axes exhibit large magnetic anisotropy fields (~ 100 T for the *c* axis) (Onuki *et al.*, 1992). The magnetic anisotropy imposes a strong Ising character on the magnetic properties. In turn the temperature dependence of the ordered moment varies as $M(T)\propto(T-T_C)^\beta$ between $0.9T_C$ and T_C , with $\beta = 0.33$ close to the calculated value $\beta \approx 0.36$ of a three-dimensional Ising ferromagnet (Huxley *et al.*, 2001; Kernavonis *et al.*, 2001).

Neutron depolarization measurements down to 4.2 K establish that the magnetic moments are strictly aligned along the *a* axis, with a typical domain size in the *b-c* plane of the order $4.4 \mu\text{m}$ (Sakai *et al.*, 2005). This contrasts with earlier reports of macroscopic quantum tunneling of the magnetization below 1 K, where the inferred domain size was only $\sim 40 \text{ \AA}$ (Nishioka *et al.*, 2002; Lhotel *et al.*, 2003).

The susceptibility of the paramagnetic state is anisotropic, exhibiting a Curie-Weiss dependence for the *a* axis with a corresponding fluctuating moment of $\mu_{CW}=2.7\mu_B$, which exceeds the ordered moment considerably. Taken by itself, the reduced ordered moment as compared with the free uranium ion value is not proof of itinerant magnetism but may be reconciled with the presence of strongly hybridized crystal electric fields. We note that inelastic neutron scattering fails to detect distinct evidence for crystal electric fields, as common for uranium-based compounds. However, the reduction in the ordered moment as compared with the Curie-Weiss moment provides clear evidence of *5f* itineracy.

The degree of delocalization of the *5f* electrons has been explored by a variety of experimental techniques. Perhaps the most direct probe is a combination of quantum oscillatory studies with band structure calculations, showing dominant *f*-electron contributions at E_F (Shick and Pickett, 2001; Terashima *et al.*, 2001; Shick *et al.*, 2004). We discuss these studies below. Polarized neutron scattering shows that the magnetic order is strictly ferromagnetic without additional modulations (Kernavonis *et al.*, 2001). The magnetic form factor of the uranium atoms is equally well accounted for by a U^{3+} or U^{4+} configuration (Huxley *et al.*, 2001; Kernavonis *et al.*, 2001), since a magnetic field of 4.6 T does not induce any magnetic polarization at the Ge sites. However, the ratio of the orbital to spin moment R does not vary substantially as a function of temperature between the paramagnetic and ferromagnetic states. It is systematically the free-ion value, reduced below suggesting a delocalization of the *5f* electrons. The value of R for U^{3+} is in better agreement with results of circular dichroism measurements (Okane *et al.*, 2006) and LDA+*U* band structure calculations (Shick and Pickett, 2001), which support a trivalent uranium state.

Evidence for some delocalization of the *f* electrons in UGe₂ may also be seen in the specific heat and the spectrum of low-lying magnetic excitations. At the Curie

temperature the specific heat displays a pronounced anomaly, $\Delta C/T \approx 0.2 \text{ J/mol K}^2$. This compares with a moderately enhanced Sommerfeld contribution $C/T = \gamma = 0.032 \text{ J/mol K}^2$ at low temperatures (Huxley *et al.*, 2001). The strong uniaxial anisotropy causes a large anisotropy gap for spin-wave excitations. In turn inelastic neutron scattering near T_C only shows strongly enhanced spin fluctuations, which are characterized by a finite relaxation rate Γ_q for $q \rightarrow 0$ due to strong spin-orbit coupling (Huxley, Raymond, *et al.*, 2003). In a one-band approximation the finite relaxation at $q=0$ would imply that the magnetization is not conserved, which is not true in multiband systems. The Ising character of the spin fluctuations underscores that they are intermediate between local-moment and itinerant-electron fluctuations.

Itinerant ferromagnetism may finally be inferred from the fact that UGe₂ forms a very good metal. High-quality single crystals may be grown with residual resistivities well below $1 \mu\Omega \text{ cm}$. As a function of decreasing temperature, the resistivity decreases monotonically with a broad shoulder around 80 K. At the ferromagnetic transition the resistivity shows a pronounced decrease characteristic of the freezing out of an important scattering mechanism. As an additional feature the resistivity displays a downturn around $T_x \approx 25$ K, which is best seen in terms of a broad maximum in the derivative $d\rho/dT$ (Oomi *et al.*, 1995). Further evidence for anomalous behavior at T_x has been observed in terms of a minimum in the *a*-axis thermal expansion (Oomi *et al.*, 1993), a drastic decrease in thermal conductivity (Misiorek *et al.*, 2005), a pronounced minimum in the normal Hall effect (Tran *et al.*, 2004), and a broad hump in the specific heat (Huxley *et al.*, 2001). Finally, high-resolution photoemission shows the presence of a narrow peak in the density of states below E_F that suggests Stoner-like itinerant ferromagnetism (Ito *et al.*, 2002).

As explained below, the behavior at T_x is key to an understanding of the superconductivity in UGe₂. The available experimental evidence suggests that the density of states near T_x is increased, i.e., thermal fluctuations with respect to the Fermi level are sensitive to fine structure of the density of states such as local maxima or changes in slope. We now comment on two specific scenarios that have been proposed to account for the features at T_x .

The first scenario is inspired by the chainlike arrangement of the uranium atoms in UGe₂. The structural similarity with α -U, which develops a charge-density wave at low temperatures (Lander *et al.*, 1994), has motivated considerations that the anomaly at T_x may be related to a coupled spin and charge-density-wave instability (Watanabe and Miyake, 2002). Electronic structure calculations predict a dominant cylindrical Fermi surface sheet with strong nesting (Shick and Pickett, 2001). However, because the U-U spacing in UGe₂ is larger than for α -U, nesting is less important. Moreover, despite experimental efforts so far no direct microscopic evidence has been observed that would support a

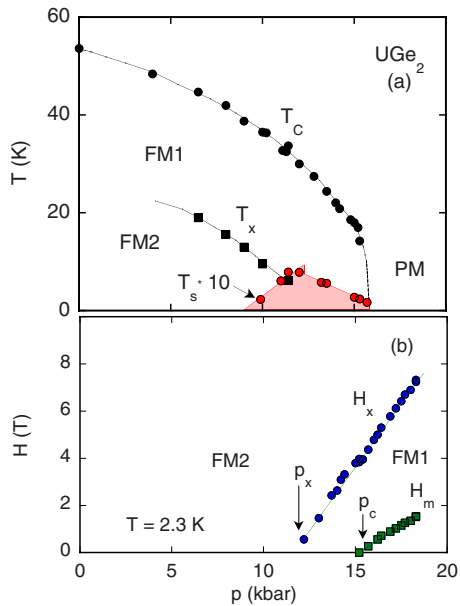


FIG. 13. (Color online) Ferromagnetism and superconductivity in UGe₂. (a) Pressure vs temperature phase diagram of UGe₂. Superconductivity is observed well within the ferromagnetic state in the vicinity of transition between a large-moment and a small-moment ferromagnet. (b) Magnetic field vs pressure phase diagram of UGe₂. The ferromagnetic transitions at p_x and at p_c are both first order as seen by first order metamagnetic transitions at H_x and H_m . From Pfeleiderer and Huxley, 2002.

density-wave instability (Huxley *et al.*, 2001; Huxley, Ressouche, *et al.*, 2003; Aso *et al.*, 2006). In fact, detailed inelastic neutron scattering studies of the phonons in UGe₂ show that the hump in the specific heat near T_x does not hint at soft phonons (Raymond *et al.*, 2006). This contrasts with the structural softness expected of an incipient charge-density wave.

The second scenario is also based on the LDA+*U* electronic structure calculations, which account for the ordered moment and the magnetocrystalline anisotropy (Shick and Pickett, 2001). In these calculations the ordered moment is identified as the sum of large opposing spin and orbital contributions. Closer inspection of the results shows the presence of two nearly degenerate solutions, which differ in terms of the orbital moment (Shick *et al.*, 2004). The upshot of these calculations is that the anomaly at T_x may be related to fluctuations between these two orbital states.

Under modest hydrostatic pressures UGe₂ exhibits a rich phase diagram, as shown in Fig. 13. The Curie temperature is suppressed monotonically and collapses continuously at $p_c=16$ kbar. ac susceptibility studies establish that the ferromagnetic transition changes from second to first order for pressures above ~ 12 kbar (Huxley *et al.*, 2000). A first-order transition at p_c is confirmed by the magnetization, which drops discontinuously at p_c (Pfeleiderer and Huxley, 2002). Note that the discontinuous change in the ordered moment is consistent with the continuous variation in T_C . Further evidence for a first-

order transition at p_c is provided by a discontinuous change in the spin-lattice relaxation rate $1/T_1T$ (Kotegawa *et al.*, 2005) and quantum oscillatory studies (Terashima *et al.*, 2001).

The broad anomaly at T_x is also suppressed under pressure and vanishes at $p_x=12$ kbar. This was first inferred from the derivative of the resistivity (Oomi *et al.*, 1995; Huxley *et al.*, 2001), but may also be seen in the thermal expansion (Ushida *et al.*, 2003) and the specific heat (Tateiwa *et al.*, 2004). In the magnetization a broad hump emerges near T_x , which turns into a sharp ferromagnetic phase transition near p_x with increasing pressure (Huxley *et al.*, 2001; Tateiwa, Hanazono, *et al.*, 2001; Pfeleiderer and Huxley, 2002). Below T_x the ferromagnetic moment increases. The low-temperature, large-moment phase is referred to as FM2, while the high-temperature low-moment phase is referred to as FM1 (cf. Fig. 13).

Neutron scattering of the magnetic order is comparatively straightforward. Due to the cancellation of nuclear scattering lengths certain Bragg peaks are purely magnetic. Comparison of selected Bragg peaks strongly suggests that both FM1 and FM2 are strictly ferromagnetic (Huxley, Ressouche, *et al.*, 2003). Moreover, neutron scattering at a pressure just below p_x shows that the intensity of the (100) Bragg spot scales with the square of the bulk magnetization. This shows that the FM2 state does not break up just below p_x .

Finally, within a finite pressure interval ranging from ~ 9 kbar to p_c the resistivity and ac susceptibility show a superconducting transition (Saxena *et al.*, 2000; Huxley *et al.*, 2001). As a function of pressure T_s increases below p_x and decreases above p_x with the possibility of a small discontinuity exactly at p_x (Huxley *et al.*, 2001; Nakashima *et al.*, 2005).

As a function of pressure the zero-temperature ferromagnetic moment drops discontinuously by $\sim 30\%$ at p_x , followed by a discontinuous drop at p_c (Pfeleiderer and Huxley, 2002). Application of a magnetic field along the *a* axis at pressures above p_x restores the full ordered moment at a characteristic transition field H_x , which emerges at p_x and increases rapidly under pressure [Fig. 13(b)]. For pressures above p_c the application of a magnetic field initially restores the ordered moment of the FM1 phase when the transition field H_m that emerges at p_c is crossed. This is followed by the recovery of the full moment at H_x . At low temperatures the transitions at H_x and H_m are both discontinuous (Pfeleiderer and Huxley, 2002). The lines of first-order transitions at $T=0$ at $H_x(p)$ and $H_m(p)$ are expected to end in a quantum critical point for very high fields. Likewise, as a function of increasing temperature at constant pressure the transition fields H_x and H_m terminate in critical end points. The importance of this finite-temperature criticality for the superconductivity is an open issue.

The Sommerfeld contribution γ to the specific heat is essentially unchanged at pressures well below p_x . Just below p_x the value of γ increases and settles at a nearly fourfold larger value $\gamma \approx 0.11$ J/mol K² above p_x

(Tateiwa, Kobayashi, *et al.*, 2001; Tateiwa *et al.*, 2004). Even though the pressure dependence of γ is sometimes described as a maximum at p_x , real data display rather the shape of a plateau characteristic of an increased linear specific heat term in the FM1 phase. This is supported by the temperature dependence of the resistivity, which shows a T^2 form everywhere. The T^2 coefficient A increases as a function of pressure from below to above p_x . For magnetic fields above H_x it varies as $A \propto 1/\sqrt{H-H_x}$ (Terashima *et al.*, 2006).

To explore the nature of the transitions at p_x and p_c , detailed quantum oscillatory studies have been carried out for magnetic fields parallel to the b axis (Settai *et al.*, 2001; Terashima *et al.*, 2001). These probe the predicted cylindrical Fermi surface sheets, without adding the complexities of the transitions at H_x and H_m (Shick and Pickett, 2001). In the FM2 phase starting from ambient pressure three fundamental frequencies are observed with $F_\alpha=6800\pm 30$ T, $F_\beta=7710\pm 10$ T, and $F_\gamma=9130\pm 30$ T. These frequencies exhibit considerable mass enhancements of $m_\alpha^*/m=23\pm 3$, $m_\beta^*/m=12\pm 1$, and $m_\gamma^*/m=17\pm 2$, which are weakly pressure dependent with $dF_\alpha/d\ln p=(3.9\pm 0.1)\times 10^{-3}$ kbar $^{-1}$, $dF_\beta/d\ln p=(-2.1\pm 0.1)\times 10^{-3}$ kbar $^{-1}$, and $dF_\gamma/d\ln p\approx(0\pm 0.1)\times 10^{-3}$ kbar $^{-1}$ (Terashima *et al.*, 2001). The mass enhancement is consistent with the specific heat values.

Between 11.4 and 15.4 kbar, the regime of the FM1 phase, the de Haas–van Alphen spectra change in the following manner: (i) the α and γ branches vanish, (ii) the β branch initially decreases followed by a steep rise with a substantial increase in the mass enhancement to 39.5 ± 5 and a reduction in signal size to just 2.5%, and (iii) a new δ branch emerges, which is similar to the β branch, where $F_\delta=4040\pm 40$ T, $m_\delta^*/m=22\pm 9$, and $dF_\delta/d\ln p=(15\pm 4)\times 10^{-3}$ kbar $^{-1}$.

It is interesting to note that no minority-spin counterpart to the β branch is observed; this is characteristic of a fully spin-polarized state. Under the assumption that the Fermi surface volume remains unchanged through p_x , it is not necessary to invoke a complete reconstruction of the Fermi surface to understand the data. When the β and α branches are assigned to extremal orbits of the majority-spin Fermi surface and the γ branch to a Fermi surface sheet with hole character, the δ branch may be understood as resulting from a shrinking and breaking up of the γ hole surface. Again, the mass enhancement is consistent with the specific heat results.

For the paramagnetic state above p_c the situation differs. Here the spectra consist of four new branches, which are not connected in any obvious manner with the spectra in the FM1 and FM2 phases. This suggests that the Fermi surface completely reconstructs at p_c . Because the change in the frequencies is abrupt, the reconstruction appears to be first order. Preliminary studies have also been carried out for a magnetic field along the a axis (Haga *et al.*, 2002; Terashima *et al.*, 2002). For fields above H_x in the FM2 phase the spectra and mass enhancements vary weakly with pressure. In contrast, little information could be obtained below H_x .

The very weak pressure dependence of the ordered moment in the FM1 and FM2 phases and the fact that the transition between FM1, FM2, and paramagnetism may be controlled by either pressure or magnetic field suggest an important role of maxima in the density of states (Huxley *et al.*, 2001; Pfeleiderer and Huxley, 2002; Sandeman *et al.*, 2003). However, several properties show that purely spin-based models or the delocalization of the $5f$ electrons would be too simple as an explanation. For instance, the derivative of the magnetization $\chi_{\parallel}=dM/dH$ measures the longitudinal susceptibility, i.e., the sensitivity to changes in amplitude of the ordered moment. A comparison of the pressure dependence of χ_{\parallel} for the a and c axes establishes that the anisotropy of the longitudinal susceptibility increases strongly under pressure, i.e., the magnetic response becomes more anisotropic instead of less (Pfeleiderer and Huxley, 2002; Huxley, Ressouche, *et al.*, 2003).

We further note that the transition at p_x is probably not controlled by a density-wave instability either. Neutron scattering of the crystal structure at high pressure shows that the U-U spacing at 14 kbar is reduced to $d_{U-U}\approx 3.5$ Å and the zigzag chain straightens (Huxley *et al.*, 2001). It is conceivable that the requirements for nesting would be much too sensitive to survive these fairly large structural changes up to p_x . Second, the observation of quantum oscillations on large Fermi surface sheets seems inconsistent with a charge-density-wave gap in the FM2 phase. Moreover, measurements of the uranium magnetic form factor show that it may still be accounted for by either a U^{3+} or a U^{4+} configuration, but the ratio of orbital to spin moment $R=\mu_L/\mu_S$ increases across p_x so that $R_{FM1}/R_{FM2}\approx 1.10\pm 0.05$ (Kuwahara *et al.*, 2002; Huxley, Ressouche, *et al.*, 2003). This is evidence against a delocalization of the $5f$ electrons since the orbital contribution should then decrease. It is interesting to note that the increase in R through p_x is consistent with the proposed degeneracy of orbital contributions in the FM1 and FM2 phases as calculated in the LDA+ U (Shick *et al.*, 2004). This suggests that the FM2 to FM1 transition at p_x and related properties may be driven by fluctuations between two different orbital moments.

Having reviewed the metallic and magnetic states extensively, we finally turn to the superconductivity in the ferromagnetic state of UGe_2 . The initial experiments suggested that the superconductivity in UGe_2 is extremely fragile. The critical current density, of order $j_c\approx 0.1$ A/cm 2 , is between one and two orders of magnitude smaller than for heavy-fermion systems such as UPt_3 and even three orders of magnitude smaller than for conventional superconductors (Huxley *et al.*, 2001). The reduced values of j_c may be reconciled with flux flow resistance, where the flux lattice forms spontaneously even at ambient field due to the internal field (the ordered moment corresponds to 0.19 T). The expected flux line spacing at this field is of the order 600–1000 Å (Huxley *et al.*, 2001). Further the susceptibility depends sensitively on the excitation amplitude, consistent with

very low j_c , and reaches full diamagnetic screening only for very small amplitudes (Saxena *et al.*, 2000). The diamagnetic shielding as seen in the ac susceptibility is largest at p_x . Note that this does not show the volume fraction of Meissner flux expulsion. Instead it may be the result of changes in sensitivity to the ac excitation amplitude. Interestingly, the diamagnetic screening and the pressure dependence of T_s do not reflect in a simple manner the difference of 30% of the ordered moment in the FM1 and FM2 phases.

Bulk superconductivity in UGe₂ was at first inferred from the magnetic field dependence of the flux flow resistance, which displays the characteristic convex increase up to H_{c2} (Huxley *et al.*, 2001). Less ambiguous information was provided by the specific heat, which was found to show a small yet distinct anomaly $\Delta C/\gamma T_s \approx 0.2-0.3$ (Tateiwa, Kobayashi, *et al.*, 2001). The spin-lattice relaxation rate in Ge NQR shows a change in slope at T_s . However, in contrast to the resistivity and susceptibility the specific heat suggests that bulk superconductivity exists only in a very narrow interval surrounding p_x (Tateiwa *et al.*, 2004). Such a narrow interval of bulk superconductivity at p_x is supported by $dH_{c2}/dT|_{T_s}$, which in the same narrow interval increases tenfold, exceeding $dH_{c2}/dT|_{T_s} < -20$ T/K (Nakashima *et al.*, 2005).

The superconductivity in UGe₂ is remarkable because T_s is always at least two orders of magnitude smaller than T_C . The superconductivity hence emerges in the presence of a strong ferromagnetic exchange splitting, estimated to be of the order of 70 meV. This suggests an unconventional form of superconductive pairing. For what is known about the Fermi surface, odd-parity equal-spin triplet pairing is thus the most promising candidate. This state is equivalent to the A1 phase of ³He.

As a first experimental hint of an unconventional state the superconductivity in UGe₂ is fairly sensitive to the sample purity, i.e., superconductivity vanishes when the charge carrier mean free path becomes shorter than the coherence length (Sheikin *et al.*, 2001). Triplet pairing was previously inferred from the mean free path dependence after doping with selected impurities in studies of UPt₃ (Dalichaouch *et al.*, 1995) and Sr₂RuO₄ (Mackenzie *et al.*, 1998). For UGe₂ the conclusion of triplet pairing has been questioned on the basis of superconductivity observed in polycrystalline UGe₂ samples with $\rho_0 \approx 3 \mu\Omega \text{ cm}$ (Bauer *et al.*, 2001). However, the purity dependence in polycrystals is still within the uncertainty with which the charge carrier mean free path can be inferred from ρ_0 . Interestingly the specific heat of the polycrystals shows only a faint superconducting anomaly and thus bulk superconductivity at 14.7 kbar. This may be caused by the presence of internal strains between the crystal grains (Vollmer *et al.*, 2002).

In single crystals the maximum specific heat anomaly $\Delta C/\gamma T_s \approx 0.2-0.3$ and the finite residual specific heat in the zero-temperature limit $\gamma_0/\gamma(T > T_s) \approx 0.3$ are characteristic of nodes in the superconducting gap, where the

linear T dependence of C/T more specifically suggests line nodes.

The strongest evidence supporting *p*-wave superconductivity thus far comes from comprehensive studies of H_{c2} (Sheikin *et al.*, 2001). Absolute values of H_{c2} vary strongly as a function of pressure and crystallographic direction, with typical values in the range of a few tesla. Below p_x the coherence lengths inferred from H_{c2} are fairly isotropic and of the order of 100 Å. In contrast, above p_x the coherence lengths display a marked anisotropy, e.g., for 15 kbar $\xi_a=210$ Å, $\xi_b=140$ Å, and $\xi_c=700$ Å.

It is helpful to address first two unusual features for the *a* axis, which are outside the more general pattern of behavior. At small magnetic fields H_{c2}^a displays negative curvature, which may be attributed to the internal fields associated with the ferromagnetic order. Second, for pressures just above p_x , pronounced reentrant behavior is observed in H_{c2} when the magnetic field crosses the transition at H_x (Huxley *et al.*, 2001). This reentrant behavior in H_{c2} may also provide a possible explanation for the pronounced extremum in dH_{c2}/dT (Nakashima *et al.*, 2005). Keeping these two aspects in mind, the more general features of H_{c2} may be summarized as follows: (i) H_{c2} exceeds conventional paramagnetic and orbital limiting for all field directions except very close to p_c , where the *a* and *b* axes show more conventional limiting; (ii) the anisotropy of H_{c2} in the vicinity of T_s may be described by the effective mass model; and (iii) the anisotropy seems to be related to the inverse of the magnetic anisotropy, i.e., H_{c2} for the *c* axis is always the largest.

A remarkable feature of the critical field for the *c* axis is the presence of positive curvature at temperatures as low as $0.1T_s$. The general form of H_{c2}^c is reminiscent of that observed in UBe₁₃. It may be accounted for in a strong-coupling scenario, where the coupling parameter λ decreases rapidly with increasing pressure: $\lambda=14, 7$, and 1.7 at $p=12, 13.2$, and 15 kbar, respectively. We note that for conventional electron-phonon-mediated superconductivity these high values of λ would imply an incipient lattice instability.

Neutron scattering shows that the ferromagnetic scattering intensity on (100) remains unchanged to within less than 1% when entering the superconducting state (Huxley *et al.*, 2001, 2005; Mineev, 2004; Aso *et al.*, 2005; Pfeleiderer *et al.*, 2005). These studies were probably not carried out sufficiently close to p_x to provide information in the narrow regime where bulk superconductivity is seen in the specific heat. When taken together, the available experimental evidence makes it highly unlikely, that the superconductivity is carried by small sections of the Fermi surface, where the exchange splitting vanishes.

The observation that the superconductivity in UGe₂ is confined to the ferromagnetic state has much theoretical interest. We conclude this section with a short list of the theoretical contributions UGe₂ has inspired. The microscopic coexistence of ferromagnetism and superconduc-

tivity has been addressed; see, e.g., Abrikosov (2001); Machida and Ohmi (2001); Spalek (2001); Suhl (2001); Sa (2002); Kirkpatrick and Belitz (2003). Possible order parameter symmetries of superconducting ferromagnets for given crystal structures and easy magnetization axes have been classified by Mineev (2002, 2004, 2005); Samokhin (2002); Samokhin and Walker (2002); Mineev and Champel (2004). For instance, it has been pointed out that ferromagnetic superconductors with triplet pairing and strong spin-orbit coupling are at least two-band superconductors. Without spin-orbit coupling it is generically expected that separate superconducting transitions take place for the majority and minority Fermi surface sheets (Belitz and Kirkpatrick, 2004; Kirkpatrick and Belitz, 2004). The upper critical field in these systems is determined by a novel type of orbital limiting, and the precise order parameter symmetry depends on the orientation of the ordered magnetic moment. The latter property, in principle, allows us to switch the superconducting order parameter through changes in orientation of the magnetization. The precise impact in this scenario of spin-orbit coupling, which of course is strong in *f* systems, awaits further clarification.

The absence of superconductivity above p_c has generated much fascination because it suggests ferromagnetism as a precondition for superconductivity. Experimentally the reconstruction of the Fermi surface topology supports a less generic explanation. It is interesting to note however, that a large number of mechanisms could be identified that promote superconductivity as confined to the ferromagnetic state. These include hidden quantum criticality, the enhancement of longitudinal (pair-forming) spin fluctuations in the ferromagnetic state, special features of the density of states, and the possible coupling of spin- and charge-density-wave order (Kirkpatrick *et al.*, 2001; Watanabe and Miyake, 2002; Karchev, 2003; Sandeman *et al.*, 2003). Several studies have considered the possible interplay of magnetic textures with superconductivity and spontaneous flux line lattices. We return to this issue in Sec. V.B.2.

2. URhGe

The series *UTX*, where *T* is a higher transition-metal element and *X*=Si or Ge, crystallizes in the orthorhombic TiNiSi crystal structure, space group *Pnma* (Sechovsky and Havella, 1998; Tran *et al.*, 1998). Even though the crystal structure of this series differs from that of UGe₂ it also shares certain similarities. In particular, as for UGe₂ the uranium atoms form zigzag chains. For URhGe the U-U spacing $d_{U-U} \approx 3.48$ Å compares well with the U spacing in UGe₂ at a pressure of 13 kbar. This has motivated detailed studies of high-quality crystals, which led to the discovery of superconductivity in the ferromagnetic state of URhGe (Aoki *et al.*, 2001). Further studies have revealed a metamagnetic transition within the ferromagnetic state, surrounded by superconductivity (Lévy *et al.*, 2005). For clarity we refer in the following to the superconductivity at ambient field

as S1 and to that around the metamagnetic transition as S2.

At ambient pressure URhGe displays a paramagnetic to ferromagnetic transition with a Curie temperature $T_C=9.6$ K and an ordered moment $\mu_{\text{ord}}=0.42\mu_B/U$ (Aoki *et al.*, 2001; Prokes *et al.*, 2002). Neutron scattering studies show that S1 superconducting samples are strictly ferromagnetic. This contrasts with earlier studies of polycrystalline samples which displayed a noncollinear magnetic structure (Tran *et al.*, 1998). Electronic structure calculations in the local spin density approximation (LSDA) (Shick, 2002) and linearized augmented plane wave (LAPW) and atomic sphere approximation (ASA) (Divis *et al.*, 2002) reproduce the ordered moment and magnetocrystalline anisotropy (LDA+*U* appears not to be necessary). These calculations also show the possibility of a canted antiferromagnetic state. In any case, as for UGe₂ the ordered moment is the result of strongly opposing spin and orbital contributions. In the following we discuss the properties of ferromagnetic URhGe only.

The ferromagnetic moment in URhGe is aligned with the crystallographic *c* axis (Huxley, Ressouche, *et al.*, 2003). In contrast to UGe₂, here the magnetic anisotropy field is large only for the *a* axis. As discussed below, a magnetic field $H_R=11.7$ T applied along the *b* axis rotates the ordered moment into the field direction. URhGe hence exhibits a quasideviant magnetic plane rather than the Ising anisotropy observed in UGe₂. The easy-axis susceptibility in URhGe follows a Curie-Weiss dependence above T_C with a fluctuating moment $\mu_{\text{eff}}=1.8\mu_B/U$ (Aoki *et al.*, 2001), while the *b*-axis susceptibility varies with temperature as expected of antiferromagnetic order at low temperatures (Huxley, Ressouche, *et al.*, 2003). This strongly suggests itinerant ferromagnetism with strongly delocalized 5*f* electrons.

The ferromagnetic transition shows a λ anomaly at T_C , where the magnetic entropy released at T_C is small $S_m=0.4R \ln 2$ (Hagmusa *et al.*, 2000). At low temperatures the specific heat follows a dependence $C \sim \gamma T + bT^2$, where $\gamma=0.164$ J/mol K². The λ anomaly is rapidly suppressed for magnetic fields applied parallel to the *c* and *b* axes, where γ in a field of 15 T decreases by $\sim 27\%$ and $\sim 19\%$, respectively. This underscores that URhGe has an easy magnetic plane.

High-quality polycrystalline and single crystal specimens of URhGe undergo a superconducting transition with $T_s \approx 0.25$ K (S1) (Aoki *et al.*, 2001). In polycrystalline samples $H_{c2}=0.71$ T corresponds to a Ginzburg-Landau coherence length $\xi_{\text{GL}} \approx 180$ Å. Measurements of the magnetization show the onset of weak flux expulsion consistent with a penetration length $\lambda_l=9100$ Å. The specific heat shows a clear anomaly at T_s characteristic of bulk superconductivity, where $\Delta C/\gamma T_s \approx 0.45$ is strongly reduced as compared with the weak-coupling BCS value. The superconductivity in URhGe is sensitive to the sample purity. With increasing residual resistivity T_s decreases, and vanishes for low sample quality, consistent with unconventional superconductivity.

H_{c2} of the S1 state is anisotropic, where the anisotropy compares with the inverse of the magnetic anisotropy, i.e., H_{c2} is largest for the *a* axis and smallest for the *c* axis (Hardy and Huxley, 2005). This suggests an intimate connection between superconductivity and ferromagnetism. For all directions $H_{c2}(T \rightarrow 0)$ exceeds paramagnetic limiting. As a function of sample quality it is found that $H_{c2}(T \rightarrow 0)$ varies proportionally to T_s^2 , showing the intrinsic nature of the large critical field values. The comparatively small anisotropy shows that large critical field values are not due to a reduced *g* factor or electronic anisotropies.

Because the superconductivity (S1 and S2) occurs in the ferromagnetic state, it is expected that the pairing dominantly occurs on the spin-majority Fermi surface akin to the odd-parity equal-spin *p*-wave pairing of the A1 phase of ^3He . This is consistent with the reduced specific heat anomaly as compared to the BCS value of $\Delta C/\gamma T_s = 1.43$ and residual zero-temperature specific heat $\gamma(T \rightarrow 0) = \gamma/2 (T > T_s)$ (Aoki *et al.*, 2001).

For the crystallographic point group of URhGe, a ferromagnetic moment parallel to the *c* axis and strong spin-orbit coupling, only two odd-parity states are possible (Hardy and Huxley, 2005). The temperature dependence of the ratios of the upper critical fields allows us to distinguish between these two states. The observed combination of 20% increase in H_{c2}^a/H_{c2}^b with decreasing temperature while $H_{c2}^a/H_{c2}^b = \text{const}$ strongly supports an odd-parity *p*-wave state with gap node parallel to the magnetic moments. Finally, the temperature dependence of H_{c2} is in good agreement with strong result of coupling calculations when the initial slope dH_{c2}/dT near T_s is taken from experiment.

It is interesting to note that the ratio of the Curie temperature to the maximal superconducting transition temperature in UGe₂ ($T_C/T_s \approx 30/0.8 = 37.5$) compares well with that in URhGe ($T_C/T_s \approx 9.6/0.25 = 38.4$). Together with the structural similarity of the uranium zigzag chains, this raises a question about further similarities, notably the pressure dependence. The thermal expansion of the ferromagnetic transition in URhGe shows positive anomalies for all three crystallographic axes: $\Delta\alpha^a = 3.4(1) \times 10^{-6} \text{ K}^{-1}$ so that $dT_C^a/dp = 0.052(3) \text{ K/kbar}$, $\Delta\alpha^b = 1.7(1) \times 10^{-6} \text{ K}^{-1}$ so that $dT_C^b/dp = 0.026(2) \text{ K/kbar}$, and $\Delta\alpha^c = 2.7(1) \times 10^{-6} \text{ K}^{-1}$ so that $dT_C^c/dp = 0.041(2) \text{ K/kbar}$. This yields a volume thermal expansion and a pressure dependence of T_C of $\Delta V^a = 7.8(2) \times 10^{-6} \text{ K}^{-1}$ and $dT_C/dp = +0.119(6) \text{ K/kbar}$, respectively (Sakarya *et al.*, 2003) i.e., T_C increases under pressure. This has been confirmed in experimental studies up to 140 kbar (Hardy *et al.*, 2005). In these studies T_s is found to be suppressed for pressures above ~ 30 kbar. Despite the increase in T_C under pressure the ordered moment decreases with $d\mu_{\text{ord}}/dp = -6.3 \times 10^{-3} \mu_B/\text{kbar}$ (Hardy *et al.*, 2004).

As depicted in Fig. 14 magnetic field applied parallel to the *b* axis may be used to tune the ferromagnetic transition (denoted as continuous transition line) toward

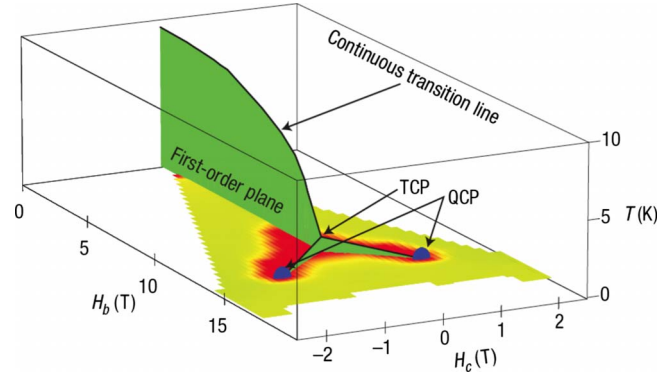


FIG. 14. (Color online) Temperature vs magnetic field phase diagram of URhGe for magnetic fields in the *b-c* plane. The critical end point of the reorientation transition of the magnetic order is surrounded by a dome of superconductivity (S2). From Lévy *et al.*, 2007.

zero. Close to the field value where T_C would vanish the dependence of T_C versus field bifurcates. Because the transition is continuous throughout, the bifurcation represents a tricritical point (TCP). Application of a magnetic field with suitably chosen components along the *b* axis and *c* axis allows us to further reduce the T_s until it vanishes at a field-tuned quantum critical point (QCP) for $\vec{H} = (0, H^b = \pm 12 \text{ T}, H^c = \pm 2 \text{ T})$. Neutron scattering and the torque magnetization establish that the transition is driven by a change in orientation of the ordered magnetic moment, where the moment in general is not parallel to the applied field. The bifurcation in $T_C(H)$ suggests that the excitation spectrum includes longitudinal fluctuations.

In the vicinity of the TCP and QCPs of URhGe, S2 superconductivity emerges (Lévy *et al.*, 2005). For a magic angle in the range of 30° – 55° , S2 even stabilizes for field components along the *c* axis. The maximum value of $T_s = 0.4 \text{ K}$ exceeds that observed at zero applied field. The wide range of orientations of the ordered moment under which superconductivity is seen shows that the superconductivity is not related to the Jaccarino-Peter effect (a cancellation of the internal field by the applied field). Instead, the phenomenology of the phase diagram suggests that the superconductivity is driven by the field-tuned quantum critical point. The possible connection of the superconductivity at ambient field with that at high field as different manifestations of this quantum critical point and the associated changes in the triplet pairing has been discussed by Mineev (2006).

Perhaps the most spectacular characteristic of the superconducting state is the upper critical field for the hard magnetic *a* axis. Here H_{c2} diverges and exceeds 28 T, the highest field studied (Lévy *et al.*, 2007). The anisotropy of the upper critical field may be accounted for in terms of an anisotropic mass model, where $H_{sc1} = (\Phi_0/2\pi\xi_c) \sqrt{\xi_a^2 \cos^2(\gamma) + \xi_b^2 \sin^2(\gamma)}$, with $H_{sc1a} = \Phi_0/(2\pi\xi_c\xi_b) = 2.53 \text{ T}$, $H_{sc1b} = \Phi_0/(2\pi\xi_c\xi_a) = 2.07 \text{ T}$, and $H_{sc1c} = \Phi_0/(2\pi\xi_b\xi_a) = 0.69 \text{ T}$. Further, assuming that the anisotropy of the critical fields that is observed at zero

applied field remains unchanged for the high-field superconductivity, a geometric average of the coherence length $\xi = \sqrt{\xi_a \xi_b \xi_c}$ can be inferred. Remarkably, the coherence length ξ as a function of applied magnetic field for the *b* axis diverges at H_R , where the magnetic field dependence of ξ of both superconducting phases falls on the same line. The coherence length thereby decreases from $\xi(H_b=0)=143 \text{ \AA}$ to $\xi(H_R) < 44 \text{ \AA}$. The common field dependence of the coherence length suggests that both superconducting phases have the same origin, notably the quantum critical point at high fields.

B. Border of ferromagnetism

Recently two superconducting ferromagnets have been discovered, UIr (Akazawa, Hidaka, Fujiwara, *et al.*, 2004; Akazawa, Hidaka, Kotegawa, *et al.*, 2004) and UCoGe (Huy *et al.*, 2007), in which the ordered moment of the ferromagnetic state is small as compared with the compounds introduced so far. The superconductivity in both compounds is observed at the border of ferromagnetism rather than deep inside the ferromagnetic state.

1. UCoGe

UCoGe is orthorhombic and isostructural to URhGe with lattice constants $a=6.645 \text{ \AA}$, $b=4.206 \text{ \AA}$, and $c=7.222 \text{ \AA}$. It was long thought that UCoGe is paramagnetic but polycrystalline samples were recently found to exhibit ferromagnetic order with a small ordered moment $\mu_{\text{ord}}=0.03\mu_B/\text{U}$ below $T_C=3 \text{ K}$. The ordered moment is much smaller than the fluctuating moment observed in the paramagnetic state, $\mu_{\text{eff}}=1.7\mu_B/\text{U}$. The specific heat shows a small anomaly at T_C , where the magnetic entropy released is small, $S_m=0.03R \ln 2$, and the normal state specific heat is moderately enhanced, $C/T=\gamma=0.057 \text{ J/mol K}^2$. The thermal expansion shows a volume contraction, with the idealized discontinuity in α estimated to be $\Delta\alpha=-1.1 \times 10^{-6} \text{ K}^{-1}$. Thus, according to the Ehrenfest relation, the Curie temperature would decrease under pressure at a rate $dT_C/dp=V_m T_C \Delta\alpha/\Delta C=-0.25 \text{ K/kbar}$ and is expected to vanish around 12 kbar ($V_m=3.13 \times 10^{-5} \text{ m}^3/\text{mol}$ is the molar volume).

Polycrystalline samples of UCoGe display superconductivity with $T_s \approx 0.8 \text{ K}$, i.e., T_s is much smaller than T_C . The superconducting transition is seen in the resistivity, ac susceptibility, specific heat and thermal expansion. In the ac susceptibility the diamagnetic screening is of the order of 60–70 %. In the specific heat the anomaly corresponds to $\Delta C/\gamma T_s \approx 1$, which is smaller than the weak-coupling BCS value. The thermal expansion displays a positive anomaly, with an idealized change in length at T_s of the order of $\Delta L/L \approx -1 \times 10^{-7}$. This implies that T_s increases under pressure at a rate $dT_s/dp \approx 0.048 \text{ K/kbar}$.

Experimentally it is found that T_C in polycrystals rapidly drops under pressure and appears to vanish between 8 and 20 kbar, while T_s is essentially unchanged consistent with the thermal expansion. The width of the

superconducting transition and additional features of the normal state resistivity, such as the residual resistivity and the temperature dependence, suggest a quantum critical point already at 7 kbar (Hassinger *et al.*, 2008). In any case, the superconductivity in UCoGe appears to survive in the nonferromagnetic state at high pressure. However, data available to date do not rule out survival of a ferromagnetic moment at high pressures. The pressure dependence is supplemented by the variation in the superconductivity and ferromagnetism as a function of Si substitution in polycrystals, $\text{UCoGe}_{1-x}\text{Si}_x$, which shows a simultaneous suppression of T_C and T_s at the same critical concentration $x_c \approx 0.12$ (de Nijs *et al.*, 2008).

The upper critical field of polycrystalline UCoGe varies near T_s as $dH_{c2}/dT \approx -5.2 \text{ T/K}$ for the sample with the largest T_s . This implies a fairly short coherence length $\xi \approx 150 \text{ \AA}$ as compared with the charge carrier mean free path $l=500 \text{ \AA}$ inferred from the residual resistivity $\rho_0=12 \mu\Omega \text{ cm}$. In other words, the samples are in the clean limit, a precondition for unconventional superconductivity. An unconventional superconducting state is also inferred from H_{c2} , which exceeds 1.2 T, the highest field measured, and is thus clearly larger than the Pauli limit.

NMR and NQR measurements in polycrystals also point at unconventional pairing (Ohta *et al.*, 2008). In the normal state the spin-lattice relaxation and the Knight shift are characteristic of ferromagnetic quantum critical fluctuations, where $T_C \approx 2.5 \text{ K}$ was observed. This underscores that the system is indeed at the border of ferromagnetism. However, in the superconducting state the spin-lattice relaxation rate appears to yield two contributions. These may be related to a superconducting and a normal volume fraction, which are either due to poor sample quality or the result of the spontaneous formation of flux lines due to the ferromagnetism.

Recently single crystals of UCoGe have become available with $T_C=2 \text{ K}$ and $T_s=0.6 \text{ K}$, which are also in the clean limit (Huy *et al.*, 2008). The ferromagnetic moment $m_s=0.07\mu_B$ is aligned with the *c* axis and the *a* and *b* axes are magnetically hard. Thus UCoGe is an easy-axis ferromagnet like UGe_2 , in contrast with the hard-axis ferromagnetism in URhGe. H_{c2} of single-crystal UCoGe shows a marked anisotropy between the *a*–*b* plane and the *c* axis, where B_{c2} for fields parallel to the *a* and *b* axes exceeds the Pauli limit with $B_{c2}^a \approx B_{c2}^b \approx 5 \text{ T} \gg B_{c2}^c \approx 0.6 \text{ T}$. The initial slope $dB_{c2}^{a,b}/dT \approx -8 \text{ T/K}$ is also large. This suggests an equal-spin pairing state with an axial symmetry of the gap function and with point nodes along the *c* axis. Moreover, an upward kink of B_{c2}^a may indicate multiband superconductivity.

2. UIr

The signatures of the superconductivity in UIr are still rather incomplete as the superconductivity exists at high pressures and very low temperatures. The crystal structure of UIr lacks inversion symmetry; the properties of UIr are presented in more detail in Sec. IV.A.3, which deals with noncentrosymmetric superconductors.

3. Note on d -electron ferromagnets

It is worthwhile to comment on two ferromagnetic d -electron systems in which superconductivity has been reported. High-purity samples of iron exhibit superconductivity above 140 kbar (Shimizu *et al.*, 2001; Jaccard *et al.*, 2002). It turns out that the superconductivity occurs in the hexagonally close-packed ϵ phase of iron, which is believed to represent an incipient antiferromagnet (Saxena and Littlewood, 2001; Mazin *et al.*, 2002). Nevertheless several hints, such as great sensitivity to sample purity and a non-Fermi-liquid temperature dependence of the resistivity near the highest value of T_s , suggest unconventional pairing.

The other system is the weak itinerant-electron magnet ZrZn_2 , where an incomplete resistivity transition has been reported (Pfeleiderer, Uhlarz, *et al.*, 2001). Here recent work suggests that the superconductivity is not intrinsic but due to the Zn depletion of spark-eroded sample surfaces (Yelland *et al.*, 2005).

IV. EMERGENT CLASSES OF SUPERCONDUCTORS

A growing number of intermetallic compounds exhibit unusual forms of superconductivity that do not fit into the general category of magnetism and superconductivity covered in Secs. II and III. These compounds promise to be representatives of new classes of superconductors. The following section reviews these emergent classes of f electron superconductors. We distinguish noncentrosymmetric systems, materials at the border to a valence transition, and systems at the border of polar order.

A. Noncentrosymmetric superconductors

In general the strong electronic correlations in heavy-fermion systems may be viewed as an abundance of magnetic fluctuations, which being pair breaking suppress conventional s -wave superconductivity. This is in contrast to spin-triplet pairing, which may occur as long as time-reversal and inversion symmetry are satisfied (Anderson, 1984). In turn it was long believed that pure spin-triplet heavy-fermion superconductivity cannot exist in noncentrosymmetric systems. However recently superconductivity was discovered in the antiferromagnets CePt_3Si (Bauer, Hilscher, *et al.*, 2004), CeRhSi_3 (Kimura *et al.*, 2005), CeIrSi_3 (Suginishi and Shimahara, 2006), and CeCoGe_3 (Settai, Okuda, *et al.*, 2007; Kawai, Muranaka, *et al.*, 2008). Perhaps most remarkably superconductivity has even been discovered at the border of ferromagnetism in the non-centrosymmetric compound UIr (Akazawa, Hidaka, Fujiwara, *et al.*, 2004; Akazawa, Hidaka, Kotegawa, *et al.*, 2004). In this section we review the current understanding of these compounds (see Table IV). Because their properties may be explained by a mixed s - plus p -wave pairing state they may be representatives of a new class of superconductors, outside the traditional scheme of classification.

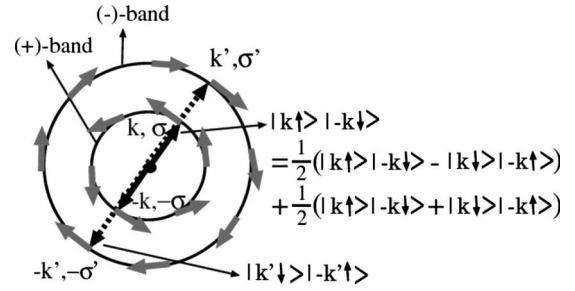


FIG. 15. Qualitative depiction of chiral exchange splitting of a spherical Fermi surface by Rashba spin-orbit interactions. Also shown are Cooper pairs that may form under such an exchange splitting, notably a mixed singlet with triplet state. From Fujimoto, 2007.

From a theoretical point of view noncentrosymmetric heavy-fermion superconductors are interesting because in these materials the Fermi surface exhibits a splitting due to antisymmetric spin-orbit coupling $\alpha(\vec{k} \times \nabla \phi) \cdot \sigma$. In two-dimensional electron gases a similar splitting is referred to as the Rashba effect and in bulk compounds as Dresselhaus effect (Dresselhaus, 1955; Rashba, 1960). As a reminder, spin-orbit coupling is a purely relativistic effect that is due to gradients of the electric potential $\vec{\nabla} \phi = \vec{E}$ transverse to the motion of the electrons. It can be shown that antisymmetric spin-orbit coupling leads to a splitting of the Fermi surface along $\vec{k}_F \times \vec{\nabla} \phi$. In magnetic materials the asymmetric spin-orbit coupling also generates a contribution to the exchange interaction that is akin to superexchange, where the role of the nonmagnetic atom is played by an empty orbital (Moriya, 1963). This superexchange is known as the Dzyaloshinsky-Moriya interaction.

In a simple-minded view the asymmetric spin-orbit coupling leads to a highly unusual chiral exchange splitting of the Fermi surface [see, e.g., Fujimoto (2007)]. A qualitative depiction is shown in Fig. 15, where $\vec{\nabla} \phi$ is along the z axis (the x and y axes are in the plane). The exchange splitting translates into dispersion curves that energetically favor a precessional motion of the electron spin with a particular handedness; the axis of the precession is denoted by the gray arrows in Fig. 15. For a Fermi surface with chiral exchange splitting a Cooper pair forming between electrons with momentum \vec{k} and spin \uparrow and momentum $-\vec{k}$ and \downarrow does not correspond to a spin-singlet state because $|\vec{k} \uparrow\rangle | -\vec{k} \downarrow\rangle$ and $|\vec{k} \downarrow\rangle | -\vec{k} \uparrow\rangle$ form on different Fermi surface sheets. Instead it has long been predicted (Edelstein, 1989; Gor'kov and Rashba, 2001) that superconductive pairing requires an admixture of a spin-singlet with a spin-triplet state.

The formation of parity-violating Cooper pairs in terms of the singlet-triplet mixing applies also in more general cases with more complicated forms of $\vec{\nabla} \phi$. To quantify the absence of inversion symmetry it is convenient to introduce a vector $\alpha \vec{g}_{\vec{k}}$, where α is the Rashba parameter and $\langle |\vec{g}_{\vec{k}}|^2 \rangle_0 = 1$ is the normalization condition in terms of the average over the Fermi surface. The vec-

TABLE IV. Key properties of noncentrosymmetric intermetallic superconductors. Missing table entries may reflect more complex behavior discussed in the text. H_{c2} represents the extrapolated value for zero temperature. References are given in the text.

	CePt ₃ Si	CeIrSi ₃	CeRhSi ₃	CeCoGe ₃
Structure	Tetrag.	Tetrag.	Tetrag.	Tetrag.
Space group	<i>P4mm</i>	<i>I4mm</i>	<i>I4mm</i>	<i>I4mm</i>
<i>a</i> (Å)	4.072(1)	4.252	4.244	
<i>c</i> (Å)	5.442(1)	9.715	9.813	
<i>c/a</i>	1.336	2.284	2.312	
CEFs	$\Gamma_6, \Gamma_7, \Gamma_6$ $\Gamma_7, \Gamma_6, \Gamma_7$	$\Gamma_7, \Gamma_6, \Gamma_7$	$\Gamma_7, \Gamma_6, \Gamma_7$	
Δ_1 (meV)	13 or 1.4	13.7	22.4	
Δ_2 (meV)	24	43	23.3	
State	AF, SC	AF, SC	AF, SC	AF, SC
T_N (K)	2.2	5.0	1.6	21, 12, 8
\vec{Q}	$(0, 0, \frac{1}{2})$		$(0.215, 0, \frac{1}{2})$	
μ_{ord} (μ_B)	0.2			
γ (J/mol K ²)	0.39 0.35 ^a	0.12	0.11	0.032
<i>A</i> ($\mu\Omega$ cm/K ²)		0.33	0.2	0.011
T_K (K)	7–11		50	
p_c (kbar)	8	25	20	55
$T_{s,\text{max}}$ (K)	~0.75 ~0.45 ^a	1.6(p_c)	0.72	0.69
$\Delta C / \gamma_n T_s$	~0.25			
H_{c2}^{ab} (T)	~3.6 ~2.3 ^a	9.5		
dH_{c2}^{ab}/dT	–8.5 –7.2 ^a	–13		
H_{c2}^c (T)	~4	>30	>30	~45
dH_{c2}^c/dT	–8.5	–20(p_N)	–23	–20
ξ_0^{ab} (Å)	~82			
ξ_0^c (Å)	~90	54	70	
Discovery of SC	2004	2006	2007	2008

^aSamples with much sharper antiferromagnetic and superconducting transitions.

tor $\vec{g}_{\vec{k}}$ may be determined by symmetry arguments. For the analysis of the allowed superconducting pairing symmetry $\vec{g}_{\vec{k}}$ is compared with $\vec{d}(\vec{k})$. For simple cases, such as CePt₃Si, the gap function Δ_{\pm} may then be expressed as $\Delta_{\pm}(\vec{k}) = (\psi \pm d|\vec{g}_{\vec{k}}|)$, where ψ corresponds to the wave function of the singlet condensate and $d|\vec{g}_{\vec{k}}|$ to the triplet state (Gor'kov and Rashba, 2001; Agterberg *et al.*, 2006).

The discovery of the noncentrosymmetric heavy-fermion superconductors reviewed in the following has revived the interest in noncentrosymmetric superconductors with weak or modest electronic correlations. For instance, the boride superconductor Li₂(Pd,Pt)₃B (Badica *et al.*, 2005) displays conventional BCS behavior

for Li₂Pd₃B (Togano *et al.*, 2004) and unconventional superconductivity for Li₂Pt₃B. Interestingly the evolution from conventional to unconventional superconductivity may be studied as a function of composition where superconductivity is observed for all compositions; i.e., the disorder introduced by the alloying does not affect the superconductivity.

The gap symmetry is explained as *s* wave with spin-singlet and spin-triplet admixtures (Yuan *et al.*, 2006). Another example is the pyrochlore oxide system CdRe₂O₇ (Hanawa *et al.*, 2001; Sakai *et al.*, 2001). For this system a structural phase transition leads to a loss of inversion symmetry at low temperatures, so that strong

spin-orbit coupling effects change the electronic structure (Hanawa *et al.*, 2002). Past examples from the literature are rare-earth sesquicarbides R_2C_{3-y} , where $R = \text{La}$ or Y . For instance Y_2C_{3-y} displays a high $T_s = 18$ K, but only weak spin-orbit coupling (Giorgi *et al.*, 1970; Krupta *et al.*, 1969; Amano *et al.*, 2004). On a more general note we also mention that amorphous superconductors have no center of inversion. However, they are characterized by a very low diffusivity and associated large Ginzburg-Landau parameter $\kappa \gg 1$, i.e., in contrast to the materials listed so far they are in the extreme dirty limit. Likewise thin superconducting films lack inversion symmetry and also fall into a different category.

1. CePt₃Si

The compound CePt₃Si was the first noncentrosymmetric compound in which heavy-fermion superconductivity was discovered (Bauer, Hilscher, *et al.*, 2004). Recent reviews may be found in Bauer, Bonalde, *et al.* (2005); Bauer, Hilscher, *et al.* (2005); Bauer *et al.* (2007); Settai, Takeuchi, *et al.* (2007). In the following we first introduce the structural and physical properties of the normal metallic state. We then proceed to present the magnetic properties. This sets the stage for the superconducting properties presented at the end of this section.

CePt₃Si crystallizes in the tetragonal CePt₃B-type structure with space group $P4mm$ (no. 99). The lattice constants are $a = 4.072(1)$ Å and $c = 5.442(1)$ Å. Perhaps the most important feature of the crystal structure is a lack of inversion symmetry, i.e., for the generating point group C_{4v} the mirror plane $z \rightarrow -z$ is missing. The crystal structure of CePt₃Si may be derived from the cubic AuCu₃-type crystal structure of CePt₃, which is isostructural to CeIn₃. In contrast to the series of $\text{Ce}_n\text{M}_m\text{In}_{3n+2m}$ compounds discussed above, which are related to CeIn₃ in terms of additional MIn_2 layers, the structure of CePt₃Si evolves from the AuCu₃ structure by filling a void with Si. It is interesting to note that the filling of a void in cage-like structures, like the skutterudites discussed in this review, plays a key role in their properties in terms of soft rattling modes. This does not seem to be the case for CePt₃Si. Rather, there is an important indirect role played by the Si atom in generating the lack of inversion symmetry and a considerable tetragonal distortion with $c/a = 1.336$.

Below $T_N = 2.2$ K CePt₃Si displays long-range antiferromagnetic order followed by the superconducting transition at T_s (Bauer, Hilscher, *et al.*, 2004). Recent studies suggest that samples exhibit either $T_s = 0.75$ or ≈ 0.45 K, the samples with lower T_s showing much sharper magnetic and superconducting transitions (Settai, Takeuchi, *et al.*, 2007; Takeuchi *et al.*, 2007). Neutron scattering in samples with $T_s = 0.75$ K revealed subtle metallurgical segregations and a broad distribution of lattice constant (Pfeleiderer *et al.*, 2008). Similar conclusions were drawn from the pressure dependence of T_N and T_s , i.e., the larger T_s seems related to a distribution of lattice constant (Aoki *et al.*, 2008). A systematic study of small

specimens that were all cut from the same polycrystalline ingot showed the same T_N for all pieces. However, samples displayed either $T_s = 0.45$ or 0.75 K (Motoyama, Maeda, *et al.*, 2008) characteristic of two different superconducting states. This may be consistent with the earlier observation of a superconducting double transition (Scheidt *et al.*, 2005). To date the majority of studies have been carried out in samples with the larger T_s .

The antiferromagnetism and superconductivity in CePt₃Si emerge from a normal state above T_N that is typical of *f*-electron heavy-fermion systems. The specific heat exhibits an enhanced Sommerfeld contribution $C/T = \gamma \sim 0.39$ J/mol K² as extrapolated from $T > T_N$. The resistivity varies quadratically just above T_N with $A = 2.23$ μΩ cm/K², where the samples exhibiting superconductivity have low residual resistivities ρ_0 of a few μΩ cm.

The low-temperature properties of CePt₃Si may be attributed to an interplay of three energy scales: Ruderman-Kittel-Katsuya-Yoshida interactions as the origin of the magnetic order, Kondo screening as the origin of strong correlations, and finally crystal electric fields. The Kondo temperature may be deduced in various different ways, with values in the range of 7–11 K (Bauer *et al.*, 2007). This uncertainty is rather typical for *f*-electron-systems. Nevertheless, T_N falls below T_K . The CEFs lift the $(2j+1=6)$ -fold-degenerate ground state of the $j=5/2$ total angular momentum of the Ce atom. However, the crystal electric field levels have not been identified conclusively.

Based on inelastic neutron scattering measurements it has been proposed that the CEF levels consist of three doublets (Bauer, Hilscher, *et al.*, 2005), where the Γ_7 first excited state and Γ_6 second excited state are separated from the Γ_6 ground state by 13 and 24 meV, respectively. The proposed CEF level scheme has been compared with the bulk properties, and the related La compound LaPt₃Si and substitutional doping with La have been considered additionally. Because LaPt₃Si is metallic with a Debye temperature $\Theta_D \approx 160$ K, the second excited CEF level cannot be identified quantitatively in the bulk properties.

It is also interesting to note that the ratio $A/\gamma^2 \approx 1.0 \times 10^{-3}$ m mol K²/J² is consistent with a small degeneracy of the ground state as lifted by the CEFs. This differs from another group of materials in the Kadowaki-Woods plot with large degeneracy and small CEF splitting, where $A/\gamma^2 \approx 0.4 \times 10^{-3}$ m mol K²/J² (Bauer, Bonalde, *et al.*, 2005). The CEF assignment given by Bauer *et al.* (2007) is in contrast to inelastic neutron scattering measurements providing evidence of CEF excitations at 1.4 and 24 meV (Metoki *et al.*, 2004). The associated CEF level scheme is a Γ_7 ground state and Γ_6 and Γ_7 first and second excited states, respectively, where the lower two doublets originate from a Γ_8 quartet in the cubic point symmetry. The CEF scheme with the low-lying Γ_6 was found to account for the magnetization as measured up to 50 T (Takeuchi *et al.*, 2005)

We return to a discussion of the high-field magnetization below.

The magnetic properties of CePt₃Si are dominated by a strong Curie-Weiss susceptibility at high temperatures with an effective fluctuating moment $\mu_{\text{eff}}=2.54\mu_B$ of the free Ce³⁺ ion and a Curie temperature $\Theta_p=-46$ K characteristic of antiferromagnetic exchange coupling of the moments. The Curie-Weiss susceptibility extends down to ~ 11 K, where a broad maximum in χ signals Kondo-type screening of the fluctuating moments. At $T_N=2.25$ K a λ anomaly in the specific heat shows the onset of long-range antiferromagnetic order. The size of the specific heat anomaly implies a release of entropy through T_N of $\Delta S \approx 0.22R \ln 2$, characteristic of small ordered moments. Under pulsed magnetic fields up to 50 T the magnetization increases almost linearly up to ~ 23 T for $H \parallel [100]$ and $[110]$. Above 23 T the magnetization levels off and settles around $0.8\mu_B/\text{Ce}$. This implies a rather small in-plane magnetic anisotropy.

Microscopic evidence for antiferromagnetic order below T_N has been obtained in neutron diffraction (Metoki *et al.*, 2004) and muon spin rotation (Amato *et al.*, 2005) experiments. Neutron diffraction is consistent with a magnetic ordering vector $\vec{Q}=(0,0,1/2)$ and small ordered moments $\mu \approx 0.2\mu_B$ at $T=1.8$ K. The antiferromagnetic order consists of ferromagnetic planes stacked along the *c* axis, where the ordered moments are oriented in plane. Unlike the slightly reduced moment expected of a degenerate Γ_8 CEF quartet, $\mu(\Gamma_8)=1.96\mu_B$, the ordered moment is strongly reduced. This may be due to the doublet ground state, but suggests also significant Kondo screening. μSR measurements show that the small ordered moments exist throughout the entire sample volume (Amato *et al.*, 2005).

Keeping in mind what is presently known about the antiferromagnetic order of CePt₃Si, it is interesting to consider the spin-orbit splitting of the Fermi surface due to the lack of inversion symmetry. Quantum oscillatory studies in CePt₃Si have shown a small number of branches (Hashimoto *et al.*, 2004). Cyclotron masses up to 20 times the bare electron mass have been observed, where masses of up to 65 times the bare electron mass are expected. While this is not a definitive identification, it nevertheless represents strong evidence for a fairly conventional heavy-fermion state. The lack of inversion symmetry generates a spin-orbit splitting consistent with the de Haas-van Alphen data in LaPt₃Si (Hashimoto *et al.*, 2004). In principle this splitting may generate chiral components of the magnetization.

The crystal structure and magnetic properties of CePt₃Si set a stage where no superconductivity is expected. Yet, superconductivity emerges in CePt₃Si well below T_N . A number of properties suggest unconventional superconductivity. For instance, under substitutional doping of Ce by La, superconductivity is suppressed in La_{*x*}Ce_{*1-x*}Pt₃Si for $x \geq 0.02$ (Young *et al.*, 2005). A high sensitivity to nonmagnetic impurities is considered a hallmark of unconventional pairing. However, removal of a magnetic atom from the structure may not

qualify as a nonmagnetic impurity but rather a magnetic defect.

Near T_s the upper critical field varies strongly as $dH_{c2}/dT|_{T_s}=-8.5$ T/K for samples with $T_s=0.75$ K (Bauer *et al.*, 2007) and as $dH_{c2}/dT|_{T_s}=-7.2$ T/K for samples with $T_s=0.45$ K (Takeuchi *et al.*, 2007). This is characteristic of heavy-fermion superconductivity and consistent with the mass enhancement inferred from the normal state specific heat. The upper critical field reaches $H_{c2} \sim 5$ T for the samples with the highest $T_s \approx 0.75$ K (Bauer *et al.*, 2007). The value of H_{c2} exceeds the Pauli-Clogston limit by a large margin, $H_{\text{PC}} \sim 1.1$ T, when conventional spin-orbit coupling is not taken into account. Most remarkably, H_{c2} does not display a sizable anisotropy, namely, $H_{c2}^c/H_{c2}^{ab} \approx 1.18$.

Calculations of the electronic structure of CePt₃Si show a large Rashba parameter $\alpha=100$ meV (Samokhin, 2004). This implies that spin-orbit splitting of the Fermi surface plays an important role in the superconductivity. An analysis of the Rashba splitting in CePt₃Si in terms of group theory for the space group $P4mm$ and generating point group C_{4v} suggests that $\vec{g}_{\vec{k}}=k_F^{-1}(k_y, -k_x, 0)$ (Frigeri, Agterberg, *et al.*, 2004). The most stable spin pairing state expected for $\vec{d}(\vec{k}) \parallel \vec{g}_{\vec{k}}$ then corresponds to a *p* state $\vec{d}(\vec{k})=\hat{x}k_y-\hat{y}k_x$. This state is characterized by point nodes. However, for mixing of this triplet state with a singlet state the experimental properties are expected to display the behavior of line nodes. Alternatively, a Balian-Werthamer state $\vec{d}(\vec{k})=\hat{x}k_x+\hat{y}k_y+\hat{z}k_z$ is possible, which would have no nodes. However, the Balian-Werthamer state is expected to be less stable (Frigeri, Agterberg, *et al.*, 2004). In fact, one may consider the $\hat{x}k_y-\hat{y}k_x$ *p* state as protected by the Rashba exchange splitting.

A key characteristic of the $\hat{x}k_y-\hat{y}k_x$ state for a magnetic field parallel to the *c* axis is the absence of paramagnetic limiting, while there would be considerable paramagnetic limiting for a magnetic field perpendicular to the *c* axis. To account for the nearly isotropic behavior of H_{c2} it has been suggested that the superconducting wave function develops a helical phase factor $\exp(i\vec{q} \cdot \vec{R})$ in applied magnetic fields (Kaur *et al.*, 2005; Agterberg *et al.*, 2006). It is also important, however, to take into account the interplay of antiferromagnetic order with the superconductivity, which accounts in part for the reduced anisotropy (Yanase and Sigrist, 2007).

The superconducting transition in samples with larger T_s is accompanied by a fairly broad anomaly in the specific heat, with $\Delta C/\gamma T_s \approx 0.25$. This value is strongly reduced as compared with the isotropic BCS value $\Delta C/\gamma T_s \approx 1.43$ (Bauer, Hilscher, *et al.*, 2004). It deviates in particular from strong-coupling behavior frequently observed in heavy-fermion superconductors. The reduced specific heat anomaly may be explained by a vanishing of the superconducting gap on parts of the Fermi surface, e.g., due to an unconventional Cooper pair symmetry. It also raises the question of how the antiferromagnetic order and superconductivity coexist micro-

scopically. In single-crystal samples with $T_s \approx 0.6$ K the specific heat varies as $C_e/T = \gamma_s + \beta_s T$ with $\gamma_s = 34.1$ mJ/mol K² and $\beta_s = 1290$ mJ/mol K³ below 0.3 K (Takeuchi *et al.*, 2007). Moreover, the specific heat displays a nonlinear magnetic field dependence $\gamma_s \propto \sqrt{H}$. When taken together these results suggest line nodes of the superconducting gap.

The presence of line nodes has also been inferred from measurements of the temperature and magnetic field dependence of the thermal conductivity $\kappa(T, H)$ in single crystals (Izawa *et al.*, 2005). The key results of this study are (i) a residual term in $\kappa(T, 0)$ for $T \rightarrow 0$ in quantitative agreement with the universal conductivity (Lee, 1993; Sun and Maki, 1995; Graf *et al.*, 1996), (ii) a linear temperature dependence $\kappa(T, 0) \propto T$ at low T , and (iii) a magnetic field dependence that exhibits one-parameter scaling of the form T/\sqrt{H} . This behavior is taken as evidence that the magnetic field dependence is due to a Doppler shift of the quasiparticles (Volovik effect) (Volovik, 1993; Kübert and Hirschfeld, 1998; Vekhter and Houghton, 1999; Hussey, 2002).

Measurements of the penetration depth $\lambda(T)$ represent the most direct probe of the superfluid density. They are not connected with any other preponderant interaction process, notably the long-range antiferromagnetic order. The experimental data in polycrystals and single crystals display a broad transition with a point of inflection around 0.5 K (Bonalde *et al.*, 2005, 2007). Below $\sim 0.165 T_s$ changes in the penetration depth are linear in temperature, characteristic of line nodes in the gap (Hayashi *et al.*, 2006b).

While the low-temperature specific heat, thermal conductivity, and penetration depth only shed light on the behavior well below T_s , NMR measurements of the spin-lattice relaxation rate $1/T_1$ and the Knight shift provide insights into the full temperature dependence (Yogi *et al.*, 2004, 2006). For the spin-lattice relaxation rate the behavior appears to be a mixture of differing contributions. Near T_s a Hebel-Slichter peak is observed. The variation below T_s deviates from conventional exponential activation, but it does not fully settle into a power-law dependence either. The data have been interpreted in two different ways. In the first scenario the temperature dependence is attributed to a mixing of the singlet and triplet states (Hayashi *et al.*, 2006a). This accounts for the Hebel-Slichter peak and shows that the low-temperature data are essentially limited to the T^3 dependence expected of line nodes. In the second scenario the interplay of the antiferromagnetic order with the triplet contribution to the superconducting pairing symmetry is considered (Fujimoto, 2006). In particular it is pointed out that the signatures of line nodes may be found even in fully gapped triplet superconductors in the presence of suitably chosen magnetic order.

The NMR Knight shift as measured at a field of 2 T perpendicular and parallel to the field does not change when the superconducting state is reached (Yogi *et al.*, 2006). The Knight shift may be taken as a probe of the spin susceptibility χ . The experimental result is in con-

trast with the theoretical prediction for spin-singlet and spin-triplet states in the presence of asymmetric spin-orbit interactions (Frigeri, Agterberg, *et al.*, 2004b). For the spin-singlet state both χ_\perp and χ_\parallel are expected to decrease in the superconducting state with some anisotropy, the decrease becoming smaller with increasing α . For the spin-triplet state the susceptibility becomes independent of the size of the spin-orbit coupling. Here χ_\parallel shows no decrease, while χ_\perp shows a modest decrease. Thus the experimental absence of any decrease is taken as evidence for the dominant spin-triplet component, and the in-plane behavior awaits further clarification.

In a phase diagram that combines the effects of pressure and substitutional Ge doping and assumes a bulk modulus $B_0 = 1000$ kbar (Yasuda *et al.*, 2004; Nicklas *et al.*, 2005; Tateiwa *et al.*, 2005; Bauer *et al.*, 2007; Takeuchi *et al.*, 2007) two features may be noticed. First, the antiferromagnetism vanishes for pressures in excess of $p_N \approx 6\text{--}8$ kbar. Second, the superconductivity decreases with decreasing volume and thus increasing pressure and vanishes around $p_s \approx 15$ kbar. Interestingly, the superconducting transition broadens considerably in the range between p_N and p_s in samples with higher T_s (Nicklas *et al.*, 2005); note that the crystal structure of $\text{CePt}_3\text{Si}_{1-x}\text{Ge}_x$ is not stable for $x > 0.06$. An unresolved issue concerns the pressure dependence of samples with the lower T_s . In samples with larger T_s the dc susceptibility is rapidly suppressed (Motoyama, Yamaguchi, *et al.*, 2008). This might be the result of the large distribution of lattice constants in these samples as mentioned above.

The phase diagram suggests the vicinity of a quantum critical point. This is underscored by tentative evidence for critical fluctuations in the specific heat and inelastic neutron scattering of pure CePt_3Si at ambient pressure. Above T_N electronic contributions to the specific heat decrease as $\Delta C/T \sim \ln(T)$. Preliminary inelastic neutron scattering measurements suggest that there is Q -independent quasielastic scattering at high temperatures typical of conventional heavy-fermion systems. At low temperatures, however, short range correlations are observed for $Q^{-1} \approx 0.8$ Å at energy transfers of a few meV that may be related to the NFL behavior.

In the light of the possible Rashba splitting of the Fermi surface, the nature of the excitations that mediate the superconductivity is an open issue. In the studies of CePd_2Si_2 and CeIn_3 the circumstantial evidence suggests that quantum critical spin fluctuations may be key ingredients. However, due to the lack of inversion symmetry these may include complex spin textures, e.g. (Röbler *et al.*, 2006).

It is finally interesting to note that several LaMX_3 compounds are superconducting. In particular, LaRh_3Si , LaIr_3Si , and LaPd_3Si show superconductivity with T_s of 1.9, 2.7, and 2.6 K, respectively (Muro, 2000). However, for LaRh_3Si the upper critical field is low $H_{c2} = 0.03$ T.

2. $CeMX_3$

Following the discovery of superconductivity in the antiferromagnetic state of the noncentrosymmetric heavy-fermion system $CePt_3Si$, superconductivity was also discovered in the noncentrosymmetric systems $CeRhSi_3$ (Kimura *et al.*, 2005), $CeIrSi_3$ (Suginishi and Shimahara, 2006), and $CeCoGe_3$ (Settai, Okuda, *et al.*, 2007; Kawai, Muranaka, *et al.*, 2008). These compounds belong to the class of isostructural $CeMX_3$ systems where $M=Co, Ru, Pd, Os, Ir, Pt, Fe,$ and Rh and $X=Si$ and Ge . The $BaNiSn_3$ crystal structure, space group $I4mm$ (no. 107), of the $CeMX_3$ series derives from the body-centered-tetragonal $BaAl_4$ crystal structure, space group $I4/mmm$. We note that $BaAl_4$ is also the parent structure of the body-centered $ThCr_2Si_2$ systems of the heavy-fermion superconductors $CeCu_2Si_2$, $CeCu_2Ge_2$, $CePd_2Si_2$, $CeRh_2Si_2$, and URu_2Si_2 (cf. Fig. 2). It is moreover the parent structure of the series of $CaBe_2Ge_2$ body-centered-tetragonal ternary systems, none of which have so far been found to be superconducting. As shown in Fig. 2 the $BaSnNi_3$ structure is composed of a sequence of planes along the c axis, $R-M-X(1)-X(2)-R-M-X(1)-X(2)-R$, where $X(1)$ and $X(2)$ denote different lattice positions of the X atom. Thus the structure lacks inversion symmetry along the c axis. The generating point group C_{4v} is identical to that of $CePt_3Si$.

For a review of the properties of the series CMX_3 see Kawai *et al.* (2008b). This review includes considerations of the crystal electric fields, which play a prominent role in the ground state properties. Among the systems studied, $CeCoGe_3$ has the highest antiferromagnetic ordering temperature. Interestingly, those compounds with low values of T_N have the a axis as easy magnetic axis, while in $CeCoGe_3$ the c axis is magnetically soft. It is interesting to note that the antiferromagnetic transition temperatures, their pressure dependence, and the Sommerfeld coefficient of the specific heat as a function of decreasing unit cell volume are consistent with a Doniach phase diagram (Fig. 16). To date superconductivity near a magnetic quantum phase transition has been observed in those systems that are on the right-hand border of the phase diagram.

In passing we note that the system $CeNiGe_3$, which also displays superconductivity when antiferromagnetism is suppressed at high pressure (Nakajima *et al.*, 2004; Kotegawa *et al.*, 2006), crystallizes in a centrosymmetric orthorhombic structure (see Sec. II.A.3).

a. $CeRhSi_3$

The first system in this class for which superconductivity was observed is $CeRhSi_3$. For a recent review see Kimura, Muro, *et al.* (2007b). The lattice constants are $a=4.244 \text{ \AA}$ and $c=9.813 \text{ \AA}$ and the single crystals studied had very low residual resistivities of a few tenths of a $\mu\Omega \text{ cm}$. At ambient pressure $CeRhSi_3$ orders antiferromagnetically below $T_N=1.6 \text{ K}$. The antiferromagnetic order is anisotropic, where the basal plane a axis

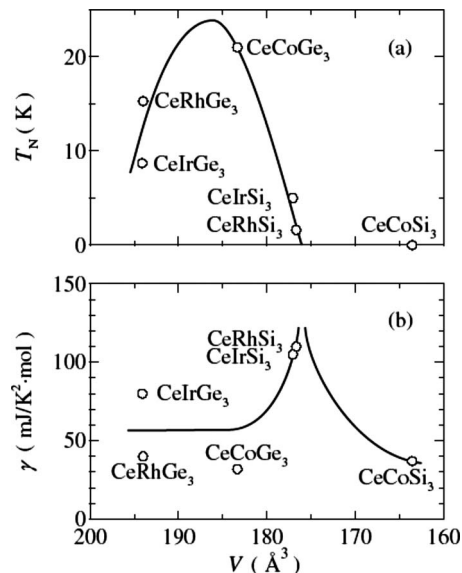


FIG. 16. Key properties in the series $CeMX_3$ ($M=Rh, Ir, Co$; $X=Si, Ge$). (a) Néel temperature T_N vs unit cell volume V in the series $CeMX_3$ ($M=Rh, Ir, Co$; $X=Si, Ge$). (b) Sommerfeld coefficient γ of the specific heat vs unit cell volume V in the series $CeMX_3$. From Kawai, Muranaka, *et al.*, 2008.

is the easy axis. Neutron scattering shows that the antiferromagnetic order is incommensurate with $\vec{Q}=(\pm 0.215, 0, 0.5)$ (Aso *et al.*, 2007). The magnetic field dependence of the magnetization suggests an anisotropy of about 2. Only a small magnetization is seen up to 8 T. At high temperatures an isotropic Curie-Weiss susceptibility is observed with a fluctuating moment $\mu_{\text{eff}}=2.65\mu_B$ as expected of the full Ce^{3+} moment.

The specific heat may be interpreted in terms of a Schottky anomaly around 100 K and Kondo temperature of order $T_K \approx 50 \text{ K}$. The Kondo screening is affected by the CEF level scheme, where inelastic neutron scattering results have been interpreted in terms of three doublets with a Γ_6 ground state and Γ_7 and Γ_6 first and second excited states at 260 and 270 K, respectively (Muro *et al.*, 2007). The low-temperature specific heat above T_N exhibits a strongly enhanced Sommerfeld contribution $\gamma=0.110 \text{ J/mol K}^2$. This suggests that a heavy-fermion state forms despite a large Kondo temperature, in which incommensurate antiferromagnetism is stabilized at very low temperatures. The Fermi surface has been investigated by means of quantum oscillations (Kimura *et al.*, 2001; Kimura, Muro, *et al.*, 2007) and compared to $LaRhSi_3$. Substantial differences are interpreted as evidence for an itinerant-*f*-electron and spin-density-wave type of antiferromagnetism. Moreover, several branches show a small splitting with similar angular dependences. This is seen as evidence for Rashba splitting.

The pressure dependence of T_N in $CeRhSi_3$ is unique. Up to 9 kbar T_N increases moderately before decreasing again gradually up to 20 kbar. For pressure above 2 kbar (Kimura *et al.*, 2005; Kimura, Muro, *et al.*, 2007) superconductivity emerges in the antiferromagnetic state, and

T_s increases up to 30 kbar, the highest pressure measured. The superconducting dome is exceptionally wide. The ac susceptibility shows superconducting screening with additional features that require further clarification. Together with the zero-resistance state the susceptibility is a strong indication of superconductivity. However, it does not establish spontaneous Meissner flux expulsion and thus volume superconductivity. The initial slope of H_{c2} is strongly enhanced and becomes anomalously large around 26 kbar with $dH_{c2}/dT|_{T_s} = -23$ T/K. This suggests that H_{c2} is exceptionally large and may even exceed 30 T (Kimura, Ito, *et al.*, 2007).

b. CeIrSi₃

The compound CeIrSi₃ is isostructural to CeRhSi₃ with lattice constants $a = 4.252$ Å and $c = 9.715$ Å (Muro *et al.*, 1998). The ambient pressure properties of CeIrSi₃ are characteristic of a heavy-fermion system with an enhanced Sommerfeld contribution to the normal state specific heat $\gamma = 0.12$ J/mol K² and antiferromagnetic order below $T_N = 5.0$ K. The CEF levels have been inferred from magnetization data, where the ground state is a Γ_6 doublet and the first and second excited states are Γ_7 and Γ_6 doublets at 149 and 462 K, respectively (Okuda *et al.*, 2007). The magnetization is anisotropic by a factor of about 2, where the a axis is the easy axis. Quantum oscillatory studies of LaIr₃Si show that the Fermi surface is similar to that of LaCoGe₃, characteristic of a compensated metal where branches with an exchange splitting of 1000 K exhibit angular dependences that track each other rather closely. This suggests the presence of Rashba splitting due to the lack of inversion symmetry.

The antiferromagnetism in CeIrSi₃ vanishes for pressures in excess of $p_N = 22.5$ kbar (Suginishi and Shimahara, 2006; Tateiwa *et al.*, 2007) and a superconducting dome emerges, with $T_s^{\max} = 1.65$ K for pressure in excess of p_N , as shown in Fig. 17. H_{c2} exhibits a strong temperature dependence near T_s . For the basal plane $dH_{c2}^{\text{ab}}/dp = -13$ T/K at p_N with $H_{c2}^{\text{ab}}(T \rightarrow 0) = 9.5$ T. For the c axis $dH_{c2}^c/dp = -20$ T/K and H_{c2}^c reaches 18 T just below 1 K, suggesting an extremely large value in excess of 30 T (Settai *et al.*, 2008). This is strikingly similar to results for CeRhSi₃. Recent specific heat and ac susceptibility measurements up to 35 kbar show distinct specific heat anomalies for both the antiferromagnetic and superconducting transitions, i.e., they may be well tracked as a function of pressure using an ac method, but quantitative information is not available (Tateiwa *et al.*, 2007). Above p_N the specific heat anomaly is particularly pronounced and suggests strong-coupling superconductivity. NMR studies show the absence of a coherence peak in the spin-lattice relaxation rate and a cubic temperature dependence characteristic of line nodes (Mukuda *et al.*, 2008). The normal state spin-lattice relaxation rate is thereby characteristic of an abundance of antiferromagnetic spin fluctuations, which are likely to be implicated in the superconducting pairing.

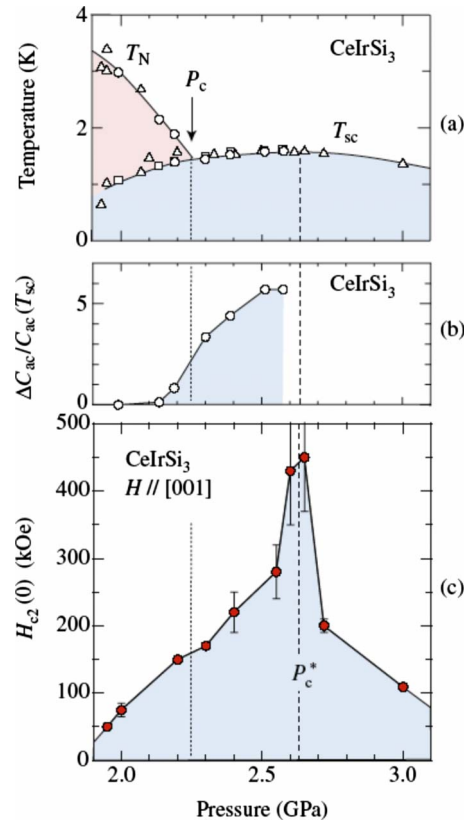


FIG. 17. (Color online) Magnetism and superconductivity in CeIrSi₃. (a) Temperature vs pressure phase diagram of CeIrSi₃. At the border of antiferromagnetic order a wide superconducting dome emerges. Note that the pressure axis begins at 19 kbar. (b) Superconducting specific heat anomaly as a function of pressure. (c) Extrapolated zero-temperature upper critical field. From Settai *et al.*, 2008.

Rather remarkable is the behavior observed under substitutional doping in CeIr_{1-x}Co_xSi₃ (Okuda *et al.*, 2007). Replacement of Ir with Co represents to leading order a reduction in unit cell volume equivalent to the application of pressure. For $x = 0.2$ and 0.35 the Néel temperature is reduced and superconductivity is observed. Metallurgical tests suggest that the compound for $x = 0.35$ is not single phase but has a dominant contribution of the $x = 0.2$ phase. In any case the result suggests that the superconductivity is not particularly sensitive to disorder.

c. CeCoGe₃

Among the CeMX₃ compounds CeCoGe₃ has the highest magnetic ordering temperature $T_{N1} = 21$ K, followed by two more transitions at $T_{N2} = 12$ K and $T_{N3} = 8$ K (Settai, Okuda, *et al.*, 2007; Kuwai, Muronatka, *et al.*, 2008). The metallic state is well described as a moderately enhanced Fermi liquid with a Sommerfeld coefficient of the specific heat $\gamma = 0.032$ J/mol K² and a coefficient of the quadratic temperature dependence of the resistivity $A = 0.11$ μΩ cm/K². The easy magnetic axis is the c axis, as opposed to other members of the CeMX₃ series, where the a axis is the easy axis. Under pressure

T_{N1} decreases and vanishes around 55 kbar, where the rate of suppression drops around 30 kbar. Superconductivity is observed in the range of 54–75 kbar with $T_s = 0.69$ K at a pressure around 65 kbar. For this pressure the value of H_{c2} along the *c* axis, as extrapolated from the very large increase near T_s , given by $dH_{c2} = -20$ K/T, is exceptionally large and may reach 45 T.

The Fermi surface of the series LaTGe_3 ($T = \text{Fe, Co, Rh, Ir}$) has been reported by Kawai, Muranaka, *et al.* (2008). All systems exhibit strong Rashba spin-orbit splitting. It will be interesting to see how the characteristics of these superconductors relate to those of the Ce systems. For instance, the La compounds may display the singlet state superconductivity with which the triplet state pairing gets admixed in the Ce systems.

We finally note that superconductivity has also been reported in CeCoSi_3 at 0.5 K (Haen *et al.*, 1985). This observation could not be confirmed down to 50 mK in a subsequent study (Eom *et al.*, 1998).

3. UIr

Superconductivity in noncentrosymmetric heavy-fermion systems also exists at the border of ferromagnetism in UIr (Akazawa, Hidaka, Fujiwara, *et al.*, 2004; Akazawa, Hidaka, Katagawa, *et al.*, 2004). The structure of UIr is monoclinic of PbBi type (space group $P2_1$) and lacks inversion symmetry (Dommann and Hullinger, 1988). Four different uranium sites may be distinguished. In the paramagnetic state the susceptibility follows a Curie-Weiss dependence with an effective moment $\mu_{\text{eff}} = 2.4\mu_B/U$. Below a Curie temperature $T_{C1} = 46$ K Ising ferromagnetism develops with a reduced ordered moment of $0.5\mu_B/U$, characteristic of itinerant electron magnetism. The easy axis is $[10\bar{1}]$. The properties of UIr are summarized in Table III.

A recent review of the temperature–pressure–magnetic field phase diagram of UIr may be found in Kobayashi *et al.* (2007). Several samples of varying quality have been studied so far, where an indenter pressure cell was used. This pressure technique leaves room for uncertainties regarding the possible role of nonhydrostatic conditions. As shown in Fig. 18, the resistivity, ac susceptibility, and magnetization establish that three magnetic phases may be distinguished under pressure. Data were collected for the $[10\bar{1}]$ easy axis and $[010]$ hard axis. The nature of the magnetic states has not been identified by means of microscopic probes yet. Based on the available bulk data the phases are referred to as ferromagnetic states.

Under pressure the FM1 state vanishes for pressure in excess of $p_{c1} = 17$ kbar. The transition at T_{c1} may be readily seen in the resistivity, ac susceptibility, and magnetization. The ordered moment decreases gradually between $0.5\mu_B/U$ and $0.27\mu_B/U$ before dropping discontinuously at p_{c1} . In the limit $T \rightarrow 0$ the FM2 phase exists between p_{c1} and $p_{c2} = 21$ kbar. As a function of temperature the FM2 transition may be seen in the ac susceptibility but not in the resistivity. The ordered moment in

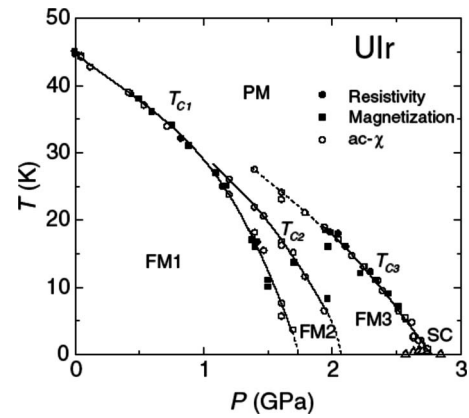


FIG. 18. Temperature vs pressure phase diagram of UIr. Three ferromagnetic phases have been identified. Superconductivity is only observed at the border of the FM3 phase with very low superconducting transition temperatures. From Kobayashi *et al.*, 2007.

the FM2 state is strongly reduced and not larger than $0.05\mu_B/U$. The FM3 phase exists in the limit $T \rightarrow 0$ for pressures up to $p_{c3} = 27.5$ kbar. The ordered moment in the FM3 phase vanishes continuously at p_{c3} ; the behavior between p_{c1} and p_{c3} is complex with the possibility of a metamagnetic transition from the FM2 to the FM3 phase. The magnetic ordering temperature of the FM3 phase at T_{c3} may be seen in the resistivity and ac susceptibility. As a rather peculiar feature of the FM3 phase $T_{c3}(p)$ is not directly connected with either $T_{c1}(p)$ or $T_{c2}(p)$ but begins in the middle of the paramagnetic regime, as shown in Fig. 18. Based on symmetry considerations there must be another transition line along which the symmetry breaking takes place.

Superconductivity is observed in the FM3 phase of UIr for pressures in the range $26 \text{ kbar} < p < p_{c3}$ (Akazawa, Hidaka, Fujiwara, *et al.*, 2004; Akazawa, Hidaka, Katagawa, *et al.*, 2004), reaching $T_s = 0.15$ K where $H_{c2} = 0.0258$ T is quite low. Superconductivity has been seen in the resistivity and ac susceptibility, i.e., bulk superconductivity has not been established yet. No superconductivity is observed in the paramagnetic regime above p_{c3} . Superconductivity is also observed only for samples with fairly high residual resistivity ratios (>170). Observation of superconductivity in the ferromagnetic state and for high-purity samples suggests unconventional pairing. A possible Ir-based impurity phase has been ruled out on the basis of the pressure dependence of T_s of Ir, which does not match or track the behavior observed experimentally.

We finally return to the nature of the FM1, FM2, and FM3 phases. The FM1 phase appears to be a straightforward Ising ferromagnet. In contrast, the dominant feature of the FM2 phase is a 25-fold increase in the residual resistivity for the magnetically hard $[010]$ axis (Hori *et al.*, 2006) and a strongly reduced spontaneous moment. Moreover, quantum oscillations vanish outside the FM1 phase (Shishido *et al.*, 2006). This led to the speculation of a multilayerlike phase separation along

the [010] axis. It is presently not clear whether this structure is related to a structural modification, so far not supported by high-pressure x-ray diffraction. The easy and hard axes of the magnetization are unchanged in the FM3 phase, which supports the superconductivity at low temperatures (Kobayashi *et al.*, 2007). The FM3 phase again appears to be a straightforward Ising ferromagnet with a strongly reduced ordered moment. It has been argued that there is no additional modulation in the FM3 state because the easy and hard axes are unchanged. Finally, it appears unlikely that the crystal structure has recovered the centrosymmetric symmetry under pressure because this would require major rearrangements of the atomic positions. The ordered magnetic moment in the FM3 phase ($\sim 0.05\mu_B/U$) corresponds to a fairly small internal field, also consistent with conventional superconductivity. The coherence length of $\xi = 1100 \text{ \AA}$ as inferred from H_{c2} is also comparable to the charge carrier mean free path of $l = 1240 \text{ \AA}$. The role of the different U sites has not been addressed at all. Taken together, the interplay of magnetism and superconductivity in UIr possesses a large number of experimental and theoretical challenges for the future.

B. Superconductivity near electron localization

The degree of itineracy of the *f* electrons in intermetallic compounds provides a major source of scientific debate. The transition from an itinerant to a localized state creates variations in the charge density that also drive strong correlations in the spin density. Interestingly, heavy-fermion superconductivity is found in materials at the border of such a localization transition. This suggests that the nature of the superconductive interactions is related to charge density fluctuations as a new route to superconductivity. The interplay of these fluctuations with spin fluctuations and further degrees of freedom is an open issue.

1. Border of valence transitions

It has been suggested that the superconductivity maximum in CeCu₂Si₂ at high pressures is related to a Ce³⁺ to Ce⁴⁺ valence transition (cf. Fig. 3), where the 4*f* electron is delocalized in the high-pressure Ce⁴⁺ state (Yuan *et al.*, 2003; Holmes *et al.*, 2004). This type of QPT transition is non-symmetry-breaking in the spirit of itinerant-electron metamagnetism. The suggestion was inspired by the analogy of the temperature versus pressure phase diagrams of CeCu₂Ge₂ and CeCu₂Si₂. In CeCu₂Ge₂ x-ray diffraction suggests a valence transition at a pressure $p_{c2} \approx 15 \text{ GPa}$ (Onodera *et al.*, 2002). However, there is no microscopic evidence for a valence transition in CeCu₂Si_{2-x}Ge_x except for faint features seen in the L_{III} x-ray absorption (Roehler *et al.*, 1988) and changes in the metallic state, notably the electrical resistivity.

Studies of the magnetic phase diagram under pressure establish that the T^2 coefficient of the resistivity

qualitatively tracks dH_{c2}/dT up to $\sim 4.5 \text{ GPa}$ but drops to a value about two orders of magnitude smaller above $\sim 4.5 \text{ GPa}$ (Vargoz *et al.*, 1998). Further studies established that the T^2 coefficient of the resistivity drops abruptly when the characteristic temperature scale T_1^{max} , which varies under pressure or Ge doping, reaches a value of $\sim 70 \text{ K}$ (Holmes *et al.*, 2004). Under the same conditions a fivefold enhancement of the residual resistivity is observed and a tiny maximum in the specific heat coefficient.

It is conceivable that the superconductivity in CeCu₂Si₂ at high pressure develops with a rather different pairing symmetry. A microscopic pairing mechanism has been proposed in which the pairing is dominantly mediated by the exchange of charge fluctuations between the conduction bands and the *f* site (Onishi and Miyake, 2004). In the limit of a spherical Fermi surface and weak coupling this model predicts a *d*-wave superconducting state, where the value of T_c scales with the slope of the continuous valence transition as a function of the *f*-level energy.

2. Plutonium- and neptunium-based systems

Another surprise in recent years has been the discovery of heavy-fermion superconductivity in the actinide compounds PuCoGa₅ (Sarrao *et al.*, 2002), PuRhGa₅ (Wastin *et al.*, 2003), and NpPd₅Al₂ (Aoki, Haga, *et al.*, 2007). The properties of these systems are summarized in Table II. Status reports for PuCoGa₅ and PuRhGa₅ have been given by Thompson, Ekimov, *et al.* (2006); Thompson, Nicklas, *et al.* (2006); Park *et al.* (2006); Haga *et al.* (2007); Sarrao and Thompson (2007). The striking features about the superconductivity in PuCoGa₅, PuRhGa₅, and NpPd₅Al₂ are values of T_s of 18.5, 8.7, and 4.9 K, respectively, which are the highest for any *f*-electron system. It seems natural to assume that the key ingredients responsible for the high transition temperatures in these systems are related to the special electronic properties of the 5*f* electrons in the elements.

First, plutonium is delicately placed at the border between a large and a small Wigner-Seitz radius characteristic of the transition between delocalized and localized *f* electrons. Second, because Coulomb screening is stronger for 4*f* than 5*f* electrons, the typical bandwidth of 5*f* systems is intermediate between those of 3*d* and 4*f* systems. Moreover, the effects of spin-orbit coupling in 5*f* systems vary quite strongly along the series and change from weak for U to very strong for Pu, A, and Cm (Moore and van der Laan, 2009). Qualitatively this suggests that 5*f* superconductors are intermediate between the traditional 4*f* heavy-fermion superconductors and 3*d* high- T_c superconductors. This conjecture is strongly supported by the experimentally observed properties, especially when T_s is plotted versus a temperature characteristic of the electronic correlations, T_0 (cf. the bandwidth).

a. PuCoGa₅ and PuRhGa₅

Both PuCoGa₅ and PuRhGa₅ crystallize in the tetragonal HoCoGa₅ structure, space group $P4/mmm$ (Sarraf *et al.*, 2002; Wastin *et al.*, 2003). The structure is identical to that of the series of Ce_{*n*}M_{*m*}In_{3*n*+2*m*} compounds reviewed in Sec. II.A.2 and derives from the cubic HoGa₃ in terms of *M*Ga₂ layers stacked sequentially along the [100] axis [for further information see Wastin *et al.* (2003)]. The normal state of both PuCoGa₅ and PuRhGa₅ is characterized by a Curie-Weiss susceptibility with an effective fluctuating moment $\mu_{\text{eff}} \sim 0.75\mu_B/\text{Pu}$. The effective moment is close to that of the 5*f*⁵ (Pu³⁺) configuration of 0.84 μ_B . In PuCoGa₅ the Curie-Weiss temperature, $\Theta = -2$ K, is remarkably low (Sarraf *et al.*, 2002). Above ~ 100 K the effective moment in PuRhGa₅ assumes the free-ion value (Haga *et al.*, 2007). The susceptibility exhibits Curie-Weiss behavior throughout the normal state. The temperature dependence of the electrical resistivity is anomalous, showing a power-law dependence proportional to T^n with $n \sim 1.35$ instead of the conventional quadratic temperature dependence of an enhanced Fermi liquid. In both systems the specific heat is well described as that of a heavy-Fermi-liquid state plus lattice term $C(T) = \gamma T + \beta T^3$, where $\gamma = 0.077$ and 0.07 J/mol K² for PuCoGa₅ and PuRhGa₅, respectively. The value for β corresponds to a Debye temperature $\Theta_D \sim 240$ K for PuCoGa₅ and PuRhGa₅.

Below $T_s = 18.5$ K PuCoGa₅ exhibits superconductivity. The initial change in the upper critical field near T_s in polycrystals is unusually large, $dH_{c2}/dT = -5.9$ T/K. This implies $H_{c2} = 74$ T (Werthamer *et al.*, 1966), which exceeds the estimated Pauli limit ($H_P = 34$ T) by a factor of 2. The estimated value of H_{c2} corresponds to a Ginzburg-Landau coherence length $\xi_{GL} \approx 21$ Å. The heat capacity confirms bulk superconductivity, where the size of the anomaly, $\Delta C/\gamma T_s = 1.4$, is consistent with conventional BCS superconductivity. Further specific heat studies in single crystals confirm these conjectures and show a quadratic temperature dependence, consistent with an axial gap symmetry with line nodes (Javorský *et al.*, 2007). This study also establishes the possibility of a FFLO state in PuCoGa₅, where a large Maki parameter α is inferred. The magnetization is characteristic of strong type-II superconductivity.

It has been noted that the anisotropy of the superconductivity in PuCoGa₅ and PuRhGa₅ in an applied magnetic field qualitatively matches that of the antiferromagnetism in NpCoGa₅ and NpRhGa₅ in an applied magnetic field (Colineau *et al.*, 2006; Wastin *et al.*, 2006). This supports the notion that the magnetic interactions arise on the same grounds as the superconductivity. However, using polarized neutron scattering, orbital and spin contributions to the Curie-Weiss susceptibility have been discriminated (Hiess *et al.*, 2008). While the microscopic magnetization in NpCoGa₅ agrees with the bulk susceptibility, there is a large discrepancy in PuCoGa₅. In fact, the polarized neutron scattering data imply that orbital contributions to the fluctuating moment are

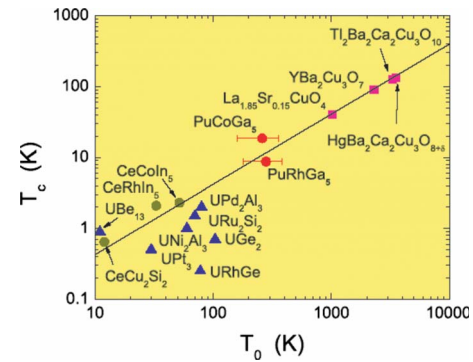


FIG. 19. (Color online) Comparison of superconducting transition temperature with the characteristic spin fluctuation temperature. The latter is essentially a bandwidth and may be insensitive to the precise microscopic nature of the correlations. From Curro *et al.*, 2005 as shown in Sarraf and Thompson, 2007.

dominant. In turn this suggests that the superconductivity is not straightforwardly due to the more traditional versions of spin-fluctuation-mediated pairing.

Microscopic evidence for unconventional superconductivity has been inferred from measurements of the ^{69,71}Ga and ⁵⁹Co Knight shift K_s and nuclear spin-lattice relaxation rate T_1 in PuCoGa₅ (Curro *et al.*, 2005; Sakai *et al.*, 2006) and PuRhGa₅ (Sakai *et al.*, 2005; Bang *et al.*, 2006). The Knight shift provides information about the orbital susceptibility χ_o , which is essentially constant, and the spin susceptibility χ_s , which decreases in the superconducting state. This clearly identifies PuCoGa₅ and PuRhGa₅ as spin-singlet *d*-wave superconductors. The spin-lattice relaxation rate in both systems drops abruptly when entering the superconducting state without evidence of a Hebel-Slichter peak. Below T_s the relaxation rate initially varies as $T_1^{-1} \propto T^3$ and settles into a dependence $T_1^{-1} \propto T$ at the lowest temperatures presumably due to impurity scattering.

The spin-lattice relaxation in PuCoGa₅ and PuRhGa₅ differs markedly from that in conventional electron-phonon-mediated superconductors, such as Al or MgB₂, corresponding to the predictions of antiferromagnetically mediated superconductive pairing, and scales with the behavior observed in CeCoIn₅ and YBa₂Cu₃O₇. Thus the observed form of T_1 suggests common microscopic features of the superconductivity for materials with vastly different values of T_s which, however, are all strong contenders for antiferromagnetic pairing. In fact, when T_s is plotted versus spin fluctuation temperature, which measures the effective bandwidth, PuCoGa₅ and PuRhGa₅ are found to be intermediate between the class of 4*f* heavy-fermion superconductors and the 3*d* high- T_c cuprates, as shown in Fig. 19. Interestingly, the temperature dependence of T_1 in the normal state of PuRhGa₅ deviates from that observed in PuCoGa₅, CeCoIn₅, and YBa₂Cu₃O₇. This has been interpreted as a pseudogap consistent with the canonical phase dia-

gram of a superconducting dome surrounding a quantum phase transition.

The strong radioactivity of Pu imposes several experimental constraints. Self-heating generates a considerable heat load that does not allow experiments to be performed at very low temperatures. A typical value is $\sim 0.45 \mu\text{W}/\text{mg}$ for PuRhGa₅. More important is the structural damage incurred by the radioactive decay of ²³⁹Pu, which results in a uranium nucleus and a high-energy alpha particle. The uranium nucleus is displaced by a mean distance of 120 Å and creates on average 2300 Frenkel pairs of vacancies and displaced interstitials distributed over a range of 75 Å (Wolfer, 2000).

Several studies have addressed the effects of self-irradiation (Jutier *et al.*, 2005, 2006; Ohishi *et al.*, 2006, 2007), which may be seen as a unique opportunity to study the evolution of a superconducting state as a function of increasing defect concentration. Experimentally it is observed that T_s decreases in both compounds under self-irradiation, where $\Delta T_s/\Delta t \sim -0.39 \text{ K}/\text{month}$ for PuRhGa₅ and $\Delta T_s/\Delta t \sim -0.24 \text{ K}/\text{month}$ for PuCoGa₅ (Jutier *et al.*, 2005). For doped samples with PuCo_{0.1}Rh_{0.9}Ga₅ and PuCo_{0.5}Rh_{0.5}Ga₅ the rates of decrease are intermediate (Jutier *et al.*, 2006). H_{c2} and the critical current density show more complex behavior. The initial variation in H_{c2} near T_s increases in 553 days for PuCoGa₅ from $dH_{c2}/dT = -5.5 \text{ T}/\text{K}$ to $dH_{c2}/dT = -13 \text{ T}/\text{K}$, while it decreases strongly for PuRhGa₅ from $dH_{c2}/dT = -3.4 \text{ T}/\text{K}$ to $dH_{c2}/dT = -0.8 \text{ T}/\text{K}$. The same trends are reflected in the critical currents. These studies suggest that self-irradiation generates point defects, where defects of the size of the coherence length are known to represent effective pinning centers (Campbell and Evetts, 1972).

The nature of the damage caused by self-irradiation has been studied microscopically by μSR (Ohishi *et al.*, 2006, 2007). The μSR linewidths are found to narrow dramatically with increasing self-irradiation. This is seen as the result of an abundance of pinning centers that trap flux lines thereby reducing the internal field distribution. The absolute value of the penetration depth as inferred from the μSR data strongly depends on the defect concentration. Yet the low-temperature variation $\lambda \propto T$ consistently shows *d*-wave behavior for the pristine and irradiated samples. Overall, the results suggest that the superconducting state is rather robust against the damages incurred by self-irradiation.

Finally, when the consequences of self-irradiation were monitored over a period of four years, the degradation of the superconductivity actually deviates from a strictly linear behavior (Jutier *et al.*, 2008). This deviation has been explained in the framework of the Eliashberg theory of a “dirty” *d*-wave superconductor, consistent with the NMR measurements. They pointed out that a phononic mechanism reproduces the experimental data, leaving open the role of the spin and orbital fluctuations.

We now turn to the possible nature of the superconductivity in PuCoGa₅ and PuRhGa₅. The Curie-Weiss

dependence may be taken as evidence of localized 5*f* electrons. Yet PuIn₃ shows a similar strong Curie-Weiss susceptibility, but quantum oscillatory studies establish that the 5*f* electrons are in an itinerant state. An itinerant *f*-electron state in PuCoGa₅ and PuRhGa₅ is also supported by the temperature dependence of the resistivity. This is supported further by band structure calculations for PuCoGa₅ in the local density approximation which suggest that the origin of the high value of T_s indeed lies in the 5*f* electrons (Maehira *et al.*, 2003; Opahle and Openeer, 2003; Szajek and Morkowski, 2003).

Comparison of the resistivity of the series *ACoGa*₅ (*A*=U, Np, Pu, and Am) also establishes that the resistivities for the systems CeCoIn₅, PuCoGa₅, and UCoGa₅ scale with each other characteristic of a single spin fluctuation energy. Moreover, the physical properties of the *ACoGa*₅ systems suggest that PuCoGa₅ resides near an itinerant to localized crossover of the 5*f* electrons that occur near Pu in the actinide series (Moore and van der Laan, 2009). The peculiar emergence of the superconductivity out of a metallic state with strong Curie-Weiss susceptibility has inspired theoretical considerations concerning the symplectic symmetry of the spin in PuCoGa₅ and NpCoGa₅ and how a coupling of local spins with the conduction electrons may promote superconductivity (Flint *et al.*, 2008).

The specific heat of PuCoGa₅ suggests a Debye temperature $\Theta_D = 240 \text{ K}$, which using the McMillan equation with a Coulomb pseudopotential $\mu^* = 0.1$ and weak electron-phonon couplings $\lambda = 0.5$ and 1 suggests $T_s \approx 2.5$ and $\sim 14 \text{ K}$, respectively (Thompson *et al.*, 2004). Thus conventional electron-phonon-mediated pairing cannot be ruled out. However, it is difficult to reconcile these results with the large fluctuating magnetic moments seen in the normal state susceptibility. Moreover, because the temperature dependence of the resistivity is best explained in terms of scattering by antiferromagnetic spin fluctuations, it has been concluded that superconductivity in PuCoGa₅ is unconventional. In fact, taking into account the presence of defects as measured by the residual resistivity $\rho_0 = 20 \mu\Omega \text{ cm}$ transition temperatures as high as $\sim 40 \text{ K}$ may be expected (Bang *et al.*, 2004).

The lattice dynamics of PuCoGa₅ was studied experimentally by room temperature inelastic x-ray scattering (Raymond *et al.*, 2006) and compared to first-principles calculations using the generalized gradient approximation (GGA) in density functional theory (Piekarz *et al.*, 2005). Excellent quantitative agreement was obtained when the on-site Coulomb repulsion was taken into account with $U = 3 \text{ eV}$ (GGA+*U*) and Hund’s rule exchange. The estimated averaged electron-phonon constant is calculated to be $\lambda = 0.7$ (Piekarz *et al.*, 2005). In the Allen-Dynes or equivalently McMillan formalism this value of λ , when taken together with the Debye temperature and a pseudo-Coulomb interaction μ^* below 0.1, implies T_s to be in the range of 7–14 K. In other words electron-phonon coupling alone cannot be re-

sponsible for the superconductivity in PuCoGa₅. However, the detailed understanding of electron-phonon interactions in PuCoGa₅ and CeCoIn₅ requires one to also resolve why UCoGa₅ is not superconducting even though the phonon spectra are similar.

The dual nature of the 5*f* electrons was inferred from a photoemission study of PuCoGa₅ (Joyce *et al.*, 2003), where good agreement with a so-called mixed-level calculation (MLL) in density functional theory was observed. In this calculation one *f* electron is in an itinerant state and four *f* electrons are localized 1.2 eV below E_F . The data are in stark contrast with the predictions of purely itinerant *f* electrons in the GGA. The conclusion of the MLL calculation has been questioned by a first-principles calculation of the ground state (Söderlind, 2004). It transpires that the photoemission spectra can be accounted for by fully itinerant *f* electrons when the spin and orbital degrees of freedom are allowed to be correlated.

Using relativistic linear augmented plane waves, the Fermi surface was found to be dominated by several large cylindrical *f* electron sheets in fair agreement with the Fermi surface of CeMIn₅ (Maehira *et al.*, 2003). In particular, the bandwidth of the 5*f* electrons is intermediate to typical 3*d* and 4*f* systems. While the calculated Fermi surface of PuCoGa₅ and CeMIn₅ ($M = \text{Co, Ir, Rh}$) is similar it differs from the calculated Fermi surface of the pair of actinide systems UCoGa₅ and NpCoGa₅, which consists of several small sheets plus a single large sheet for the case of NpCoGa₅.

The similarities of the Fermi surface in PuCoGa₅ and CeMIn₅ can be explained in terms of a tight-binding calculation taking into account *j-j* coupling (Hotta and Ueda, 2003; Maehira *et al.*, 2003). The analogy may be traced to the pseudospin representation of the *j-j* coupling, where one electron exists in the $j=5/2$ sextet for Ce³⁺, while there is one hole for the five electrons of Pu³⁺ in the sextet. Thus Pu³⁺ may be viewed as the hole analog of the one electron state of Ce³⁺. The increased value of T_s may then be attributed to the increased width of the 5*f* bands, where an additional role for the orbital structure of the Pu systems is likely.

The role of the transition-metal element in controlling the nature of the ground state in PuCoGa₅ and related compounds has been explored experimentally by substitutional replacement of Pu by U and Np and of Co by Fe, Rh, and Ni (Boulet *et al.*, 2005). Superconductivity is most dramatically suppressed for U and Np substitutions, while isoelectronic substitution is the least destructive. These results are theoretically underpinned by density functional theory calculations in the full-potential linear-muffin-tin-orbital approximation, where the transition-metal element does not contribute directly to the density of states at the Fermi level (Oppeneer *et al.*, 2006). Rather, the transition-metal effectively hole- or electron-dopes the Pu atom.

Ab initio total energy calculations in the local spin density approximation suggest antiferromagnetic ground states for PuCoGa₅ and PuRhGa₅ (Opahle *et al.*, 2004).

When we take into consideration that LSDA calculations do not treat correlation effects properly, these results suggest that PuCoGa₅ and PuRhGa₅ are at least close to antiferromagnetic order. The effects of Coulomb correlations have been addressed in a study using the relativistic LSDA+*U* (Shick *et al.*, 2005). This study unexpectedly shows a considerable reconstruction of the LSDA results suggesting *j-j*-like coupling for the Pu 5*f* manifold, similar to what is observed for pure Pu metal. The dynamical mean field theory, finally, suggests an important role of van Hove singularities in the \vec{k} -resolved spectral density that may provide strong enhancements of the magnetic susceptibility leading to *d*-wave superconductivity (Pourovskii *et al.*, 2006).

The analogy of Pu*M*Ga₅ and Ce*M*Ga₅ has been explored experimentally in several studies. Besides the evidence for an important role of critical antiferromagnetic fluctuations and the general considerations based on the calculated band structure given above, there is striking similarity concerning the dependence of T_s on the ratio c/a of the lattice parameters, as shown in Fig. 10 (Bauer, Thompson, *et al.*, 2004). This trend is consistent with trends predicted for magnetically mediated pairing (Monthoux and Lonzarich, 2001, 2002). However, the experimental investigation of the lattice parameters under high pressure establishes that for none of the Pu*M*Ga₅ and Ce*M*Ga₅ systems the value of T_s scales with c/a . This suggests that there are other important aspects besides the c/a ratio (Normile *et al.*, 2005). On another note it has been suggested that the normalized pressure dependence of the superconductivity is consistent with a dome, which may be qualitatively viewed in a common phase diagram (Park *et al.*, 2006).

b. NpPd₅Al₂

We next turn to the question of further actinide superconductors that are based on neither uranium nor plutonium. An important element in this respect is neptunium, which is adjacent to plutonium. The Wigner-Seitz radius thereby suggests that the *f* electrons in Np are in an itinerant state. Examination of spectroscopic and physical properties shows that the 5*f* states of Np are beginning to show the effects of delocalization, however, the metal is still fairly delocalized (Moore and van der Laan, 2009).

Recently heavy-fermion superconductivity has also been discovered in NpPd₅Al₂ (Aoki, Haga, *et al.*, 2007; Griveau *et al.*, 2008). This represents the first Np-based superconducting system. It is interesting to compare the properties of this system with the Pu-based heavy-fermion superconductors. The crystal structure of NpPd₅Al₂ is ZrNi₂Al₅ type body-centered tetragonal, space group $I4/mmm$, with atomic positions Np (0,0,0), Pd(1) (1, 1/2, 0.1467), Pd(2) (0,0, 1/2), and Al (0,0,0.255). The lattice constants establish a particularly anisotropic material, $c=14.716$ Å and $a=4.148$ Å. Electronic structure calculations suggest itinerant 5*f* electrons (Yamagami *et al.*, 2008).

The normal state is characterized by a Fermi-liquid specific heat with $\gamma=0.2$ J/mol K². In contrast, the magnetic susceptibility is temperature independent for the *c* axis, but diverges until superconductivity sets in. This and the linear temperature dependence of the electrical resistivity for the *a* axis clearly signal NFL properties.

The normal state susceptibility shows a Curie-Weiss temperature dependence with fluctuating moments $\mu_{\text{eff}}^{ab}=3.22\mu_B/\text{Np}$ and $\mu_{\text{eff}}^c=3.06\mu_B/\text{Np}$ for the *a-b* plane and *c* axis, respectively, that is intermediate between the free Np 5f⁸ free-ion value of 3.62/Np and the Np 5f⁴ configuration with 2.68/Np. The Curie-Weiss susceptibility extends down to the onset of superconductivity at $T_s=4.9$ K. The tetragonal *c* axis is magnetically hard. The electrical resistivity is characteristic of a good metal and decreases monotonically from its room temperature value of ~ 65 $\mu\Omega$ cm down to T_s . Just above T_s the resistivity is linear in temperature, characteristic of charge carrier scattering by critical fluctuations consistent with the Curie-Weiss susceptibility. The extrapolated residual resistivity is $\rho_0 \approx 5$ $\mu\Omega$ cm. Despite the evidence for strongly temperature dependent fluctuations in the normal state specific heat shows the behavior of a Fermi liquid with an enhanced $\gamma=0.2$ J/mol K².

The superconducting transition is accompanied by a pronounced λ anomaly in the specific heat, where $\Delta C/\gamma T_s=2.33$. This is characteristic of strong-coupling superconductivity. The temperature dependence of the specific heat in the superconducting state is highly unconventional, following initially a T^2 dependence that settles into a T^3 dependence below ~ 1.8 K. The T^3 dependence of the low-temperature specific heat is consistent with point nodes in the superconducting gap. In combination with the antiferromagnetic fluctuations inferred from the normal state susceptibility this suggests a *d*-wave state with point nodes.

The initial slopes of H_{c2} near T_s are anomalously large with $dH_{c2}^{ab}/dT=-6.4$ T/K and $dH_{c2}^c/dT=-31$ T/K, as for the Pu-based superconductors. However, H_{c2} is highly anisotropic and in comparison to the Pu-based systems reduced, where $H_{c2}^{ab}(T \rightarrow 0)=3.7$ T and $H_{c2}^c(T \rightarrow 0)=14.3$ T. This suggests considerable paramagnetic limiting of H_{c2} . The dc magnetization shows that the lower critical field $H_{c1}=0.008$ T, coherence length $\xi=94$ Å, penetration depth $\lambda=2600$ Å, and Ginzburg-Landau parameter $\kappa=28$. For the *c* axis the magnetization suggests first-order behavior at low temperatures, akin CeCoIn₅ (for the *a* axis H_{c2} is too large). This implies also the possibility for a FFLO state.

²⁷Al NMR in single-crystal NpPd₅Al₂ (Chudo *et al.*, 2008) shows a broadening of the NMR spectra when the superconducting state is entered, consistent with a flux line lattice. Further, there is no coherence peak and the spin-lattice relaxation rate $1/T_1$ shows a cubic temperature dependence. Both the spin-lattice relaxation rate and the Knight shift point at line nodes and strong coupling *d*-wave superconductivity.

Changes in the temperature dependence of the resistivity under magnetic field suggest the vicinity to a quan-

tum critical point; the T^2 coefficient decreases as if it is singular at H_{c2} . Interestingly pressure suppresses T_s above 57 kbar, reminiscent of a superconducting dome (Aoki *et al.*, 2007). This is also consistent with a vicinity to quantum criticality.

As for the Pu-based superconductors it is not clear where the entropy of the magnetic fluctuations is dumped in the superconducting state. Based on the striking similarity of the Pu and Np superconductors it is interesting to speculate on the possible implications of the paramagnetic limiting as the only difference. Since Pu is closer to the localization of the *f* electron, this may suggest an important role of charge fluctuations (Schlottmann, 1989). In fact, similar considerations as for the vicinity of a valence instability discussed above may also apply here, and charge density fluctuations may promote the superconductive pairing (Onishi and Miyake, 2000; Monthoux and Lonzarich, 2004).

C. Border of polar order

For systems where the quasiparticle dressing cloud is dominated by excitations of the crystal electric fields an interesting question concerns whether the quasiparticle interactions also include attractive components that may stabilize superconductivity. A scenario of this kind has been proposed for UPd₂Al₃, as discussed in Sec. II.B.1.a. However, for UPd₂Al₃ the superconductivity coexists with large-moment antiferromagnetism where $T_s \ll T_N$. In turn the interplay of the crystal field excitations with the antiferromagnetic order is of considerable complexity and essentially not accessible directly experimentally due to the strong hybridization of the 5*f* electrons with the conduction electrons.

In comparison to U-based compounds, Pr-based compounds generally show distinct crystal electric field excitations. The quasiparticle dressing clouds in the Fermi liquid regime in pure Pr were, for instance, identified as being excitonic (Lonzarich, 1988). In recent years heavy-fermion superconductivity has been discovered in PrOs₄Sb₁₂ and related compounds (cf. Table V). There is now growing consensus that the superconductivity in PrOs₄Sb₁₂ may be mediated by the exchange of quadrupolar fluctuations. In the following we first review the properties of PrOs₄Sb₁₂. For more detailed reviews see Maple, 2005; Aoki, Tayama, *et al.*, 2007; Hassinger *et al.*, 2008; Maple *et al.*, 2008). The section concludes with a discussion on PrRu₄P₁₂, in which superconductivity emerges, when an insulating state is suppressed at 110 kbar.

1. PrOs₄Sb₁₂

PrOs₄Sb₁₂ belongs to the rare-earth-filled skutterudites, a class of systems with an exceptionally rich spectrum of vastly different ground states. Examples include insulating and metallic behaviors, long range magnetic and polar order, and conventional and unconventional superconductivities (Sales, 2003; Aoki *et al.*, 2005; Maple, 2005; Sato *et al.*, 2007; Maple *et al.*, 2008).

TABLE V. Key properties of Pr-based heavy-fermion superconductors and siblings exhibiting conventional superconductivity. Missing table entries may reflect more complex behavior discussed in the text. References are given in the text.

	PrOs ₄ Sb ₁₂	PrRu ₄ Sb ₁₂	PrRu ₄ P ₁₂
Structure	Cubic	Cubic	Cubic
Space group	$Im\bar{3}$	$Im\bar{3}$	$Im\bar{3}$
a (Å)	9.302		
Δ_{CEF} (meV)	7	64	
State	SC, AFQ	SC	IN, SC
T_c (K)	1.3 (at 9 T)		62
\vec{Q}	(0, 0, 1)		
μ_{ord} (μ_B)	0.085		
γ (J/mol K ²)	0.5	0.059	
T_s (K)	1.85	1.3	1.8 ($p > 110$ kbar)
$\Delta C / \gamma_n T_s$	> 5		
H_{c2} (T)	2.3	0.2	2
dH_{c2}/dT (T/K)	-1.9		
ξ_0 (Å)	120	400	
λ_0 (Å)	3440	3650	
κ_{GL} (Å)	28	9	
Discovery of SC	2002	2005	2004

The large variety of electronic behaviors may be traced to the unusual crystal structure, which for the case of PrOs₄Sb₁₂ consists of a stiff icosahedron Sb cage typical of binary skutterudites, filled with a loosely bound Pr ion. The Pr ion is presumably in an off-center position (Goto *et al.*, 2004). The space group of the crystal structure is $Im\bar{3}$; the local point symmetry of the rare-earth ion is tetrahedral $T_h(m\bar{3})$, which does not include a four-fold rotation axis. Consequently, the crystal electric fields split the $J=4$ multiplet of the Pr³⁺ ions into a Γ_1 singlet, a non-Kramers nonmagnetic doublet Γ_3 and two triplets $\Gamma_4^{1,2}$ (Takeuchi *et al.*, 2001). As for all rare-earth-filled skutterudites the Pr ion exhibits “rattling” modes, leading to almost dispersionless low-energy phonons as seen in Raman scattering (Ogita *et al.*, 2008). In neutron scattering the rattling modes result in large Debye-Waller factors and in Raman scattering a second order phonon peak has been observed (Goto *et al.*, 2004; Kaneko *et al.*, 2006). Even though the Pr ion is only loosely bound, the *p-f* hybridization is expected to be large because of the cage of Sb atoms surrounding it.

The resistivity of PrOs₄Sb₁₂ decreases monotonically with temperature and displays a roll-off around 10 K followed by a superconducting transition at $T_s=1.85$ K (Bauer *et al.*, 2002). The susceptibility displays a broad maximum around 3 K and the specific heat exhibits a pronounced Schottky anomaly. The features in the resistivity, susceptibility, and specific heat are due to ther-

mally populated CEF-split Pr³⁺ energy levels. Two differing crystal field schemes were initially proposed, a Γ_1 singlet ground state and Γ_4 triplet first excited state (Aoki *et al.*, 2002) and vice versa (Maple *et al.*, 2002; Vollmer *et al.*, 2003). Inelastic neutron scattering (Goremychkin *et al.*, 2004) and detailed measurements of the magnetic field dependence (Aoki *et al.*, 2002) have settled this issue and it is now accepted (Bauer, Ho, *et al.*, 2006) that the ground state is a Γ_1 singlet, followed by a Γ_4 triplet first excited state.

Quantum oscillatory studies show Fermi surface sheets consistent with localized 4*f* electrons (Sugawara *et al.*, 2002, 2008). In comparison with other systems in this series the Fermi surface lacks nesting and compares well with that of LaOs₄Sb₁₂. The similarity of the Fermi surface topology is underscored by Hall effect and thermopower measurements, which are similar for both compounds (Sugawara *et al.*, 2005).

It was immediately recognized that PrOs₄Sb₁₂ represents the first example of a Pr-based heavy-fermion superconductor (Bauer *et al.*, 2002). Although the low-temperature specific heat is dominated by a Schottky anomaly around 2 K, it is possible to infer a strongly enhanced linear term in the normal state specific heat $C/T \approx 0.2-0.75$ J/mol K² [for a comprehensive discussion of the analysis of $C(T)$ see Grube *et al.* (2006), and references therein]. A related large anomaly is observed in the specific heat at the superconducting transition, $\Delta C/T_s \approx 0.5$ J/mol K², which depending on the strength of the coupling also points to a large value of γ . Finally, $H_{c2} \sim 2.2$ T is close to the orbital limit $H_{c2}^{\text{orb}} = 2.4$ T, inferred from the experimentally observed variation $dH_{c2}/dT \approx -1.9$ T/K near T_s . The large value of dH_{c2}/dT also supports heavy-fermion superconductivity.

An increasing number of experimental data suggest that the superconductivity in PrOs₄Sb₁₂ is unconventional. μ SR shows that the superconductivity is accompanied by time-reversal symmetry breaking (Aoki *et al.*, 2003). The penetration depth measurements show a temperature dependence of the penetration depth $\lambda \propto T^2$ and superfluid density $\rho_s \propto T^2$ down to $0.3T_s$ (Chia *et al.*, 2003). The zero-temperature penetration depth $\lambda = 3440$ Å is comparatively short. The data for λ and ρ_s are consistent with point nodes of strong-coupling superconductivity with $\Delta(0)/k_B T_s = 2.6$. This is contrasted by Sb NMR of the spin-lattice relaxation rate, which lacks a coherence peak and shows a temperature dependence consistent with an isotropic energy gap of a very-strong-coupling state (Kotegawa *et al.*, 2003). A well-developed superconducting gap, which is nearly isotropic, is also observed in tunneling spectroscopy (Suderow *et al.*, 2004). Small angle neutron scattering in PrOs₄Sb₁₂ has revealed an asymmetry of the flux line lattice that suggests a *p*-wave superconducting state (Huxley, Measson, *et al.*, 2004).

The case for unconventional superconductivity in PrOs₄Sb₁₂ is underscored by the observation of conventional superconductivity in the Pr-filled skutterudites PrRu₄Sb₁₂ (Frederick *et al.*, 2005) and PrRu₄As₁₂

($T_s=2.4$ K) (Shirotani *et al.*, 1997), as well as the La-filled skutterudites $\text{LaRu}_4\text{As}_{12}$ ($T_s=10.4$ K), $\text{LaFe}_4\text{P}_{12}$ ($T_s=4.1$ K), $\text{LaRu}_4\text{P}_{12}$ ($T_s=7.2$ K), $\text{LaRu}_4\text{Sb}_{12}$ ($T_s=3.4$ K), and $\text{LaOs}_4\text{Sb}_{12}$ ($T_s=.74$ K) (Maple *et al.*, 2002; Sato *et al.*, 2003; Miyake *et al.*, 2004). Remarkably, upon doping $\text{PrOs}_4\text{Sb}_{12}$ with La on the Pr site and Ru on the Os site the heavy-fermion superconductivity gradually turns into conventional superconductivity. This suggests that a certain stability of the heavy-fermion superconductivity against defects exists.

A controversial question in $\text{PrOs}_4\text{Sb}_{12}$ concerns whether the superconductivity consists of multiple superconducting phases and/or is multiband superconductivity. The specific heat and thermal expansion display a double superconducting transition (Aoki *et al.*, 2002; Bauer *et al.*, 2002; Vollmer *et al.*, 2003; Measson *et al.*, 2004; Oeschler *et al.*, 2004; Rotundu *et al.*, 2004). The similarity of the observed behavior across a large number of different samples seems to suggest that the behavior is intrinsic. However, recent studies of a very high-quality single crystal show only a single transition (Seyfarth *et al.*, 2006; Méasson *et al.*, 2008). A detailed study of samples with a double transition in the specific heat using micro-Hall probe and magneto-optical imaging reveal considerable inhomogeneities that question the bulk nature of the double transition (Kasahara *et al.*, 2008). The double transition is also reflected in the susceptibility (Frederick *et al.*, 2004; Measson *et al.*, 2004, 2008; Cichorek *et al.*, 2005; Grube *et al.*, 2006) and resistivity (Measson *et al.*, 2004), which points at an extrinsic origin. Multiband superconductivity has been suggested on the basis of thermal conductivity measurements, which readily return to the normal state behavior in small magnetic fields (Seyfarth *et al.*, 2005, 2006). Further, H_{c2} shows positive curvature near T_s (Measson *et al.*, 2004). Multiband superconductivity has also been inferred from Sb NQR studies (Yogi *et al.*, 2008), which supports a fully gapped large Fermi surface that drives strong-coupling superconductivity accompanied by a small Fermi surface with line nodes.

Additional transitions to further superconducting states have been inferred from magnetothermal transport (Izawa *et al.*, 2003), the low field magnetization (Cichorek *et al.*, 2005), and Andreev reflections (Turel *et al.*, 2008). As for the magnetothermal transport, a change in symmetry is observed at fairly high fields ~ 1 T, while the magnetization shows a pronounced enhancement of the lower critical field and critical current density below ~ 0.5 K. The transitions in the magnetothermal transport and magnetization are unrelated. Both await further clarification in terms of other experimental quantities.

Inelastic neutron scattering suggests that quadrupolar fluctuations are involved in the superconducting pairing (Kuwahara *et al.*, 2005; Raymond, Kuwahara, *et al.*, 2008). A clear dispersion is found for the transition Γ_1 to $\Gamma_4^{(2)}$ for $\vec{Q}=(\zeta, 0, 0)$ in zero magnetic field. Both the excitation energy and scattering intensity exhibit a minimum at $\vec{q}=(1, 0, 0)$, the ordering wave vector of the field-

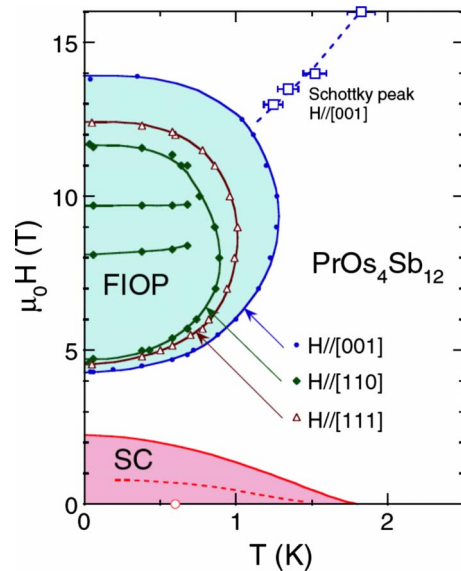


FIG. 20. (Color online) Magnetic field vs temperature phase diagram of $\text{PrOs}_4\text{Sb}_{12}$. In high magnetic field an ordered state is stabilized that is driven by the level crossing of the crystal electric fields under magnetic field. From Aoki, Haga, *et al.*, 2007.

induced antiferroquadrupolar order described below. The excitations hence are quadrupolar and not magnetic. When the superconducting state is entered, the excitation energy and its width decrease, signaling an interplay that may be due to either a freezing out of the damping by particle-hole excitations or an indication that the quadrupolar excitations are directly involved in the pairing. In particular, for low temperatures and magnetic fields the energy of this excitation compares with the superconducting gap. This suggests that superconducting pairing may be mediated by this excitation.

We finally turn to the remarkable vicinity of long-range polar order and superconductivity in $\text{PrOs}_4\text{Sb}_{12}$. A pronounced phase transition emerges above ~ 4 T that reaches 1.3 K at 9 T followed by a decrease and suppression above 13 T, as summarized in Fig. 20 (Aoki *et al.*, 2002; Tayama *et al.*, 2003; Vollmer *et al.*, 2003; Oeschler *et al.*, 2004; Rotundu *et al.*, 2004; Sugawara *et al.*, 2005). The large entropy released at this phase transition shows that the $4f$ electrons are involved in the ordering process. Neutron diffraction reveals a small antiferromagnetic modulation in the high-field phase (Kohgi *et al.*, 2003; Kaneko *et al.*, 2007). For field $\vec{H}\parallel[0, 0, 1]$ and $\vec{H}\parallel[1, 1, 0]$ the superlattice has wave vector $\vec{q}=(1, 0, 0)$, where the corresponding ordered moment of $\mu_{\text{ord}}=0.025\mu_B/\text{Pr}$ represents only a few percent of the uniform magnetization.

It is possible to show that this modulation results from Γ_5 -type antiferroquadrupolar interactions (Shiina, 2004; Shiina and Aoki, 2004). Within this scenario the anisotropy of the field induced ordered phase is due to the tetrahedral point symmetry T_h of the Pr ion. The antiferroquadrupolar order is driven by the Zeeman splitting and the crossing of the lower triplet with the singlet

level at 9 T. It is interesting to note that the ordering wave vector corresponds to the nesting wave vector in $\text{PrRu}_4\text{P}_{12}$ (Lee *et al.*, 2001; Hao *et al.*, 2004) and $\text{PrFe}_4\text{P}_{12}$ (Iwasa *et al.*, 2002), which display anomalous ordering transitions.

2. $\text{PrRu}_4\text{P}_{12}$

The Pr filled skutterudite compound $\text{PrRu}_4\text{P}_{12}$ exhibits a metal insulator transition at $T_{\text{MI}}=62$ K, which defies an explanation in terms of magnetic or charge ordering (Sekine *et al.*, 1997). Under hydrostatic pressure T_{MI} varies only weakly, but additional anomalies emerge below T_{MI} that suggest further ordering transitions. Above 110 kbar $\text{PrRu}_4\text{P}_{12}$ turns metallic with a superconductivity below $T_s \sim 1.8$ K (Miyake *et al.*, 2004). The upper critical field of this superconducting state is rather high $H_{c2} \approx 2$ T. Whether or not the superconductivity is unconventional awaits further clarification, where the similarity of T_s and H_{c2} with $\text{PrOs}_4\text{Sb}_{12}$ is interesting to note.

V. MULTIPLE PHASES

A. Order parameter transitions

Many of the superconducting phases of intermetallic compounds reviewed here are candidates for unconventional superconductivity with complex superconducting order parameters. They may in turn display various symmetry-broken superconducting phases. In the following we summarize the evidence for such multiple superconducting phases. At present the only stoichiometric superconductor, where multiple superconducting phases are observed beyond doubts, is the archetypical heavy-fermion system UPt_3 , which will be addressed first. This is followed by short summaries on further candidates for such phases, where prominent examples are $\text{PrOs}_4\text{Sb}_{12}$ and $\text{U}_{1-x}\text{Th}_x\text{Be}_{13}$.

1. Superconducting phases of UPt_3

The normal state properties of UPt_3 have been introduced in Sec. II.B.2.a. At low temperature UPt_3 displays a peculiar form of commensurate antiferromagnetic order below $T_N=5$ K with small magnetic moments, which appears to be related to a highly dynamic magnetic ground state. The antiferromagnetic order is observed only in neutron scattering and the metallic state shares the properties of a strongly renormalized Fermi liquid. In this heavy-fermion ground state superconductivity appears below $T_s=0.54$ K. While heavy-fermion superconductivity in its own right would already be quite remarkable, it is the observation of three superconducting phases that has attracted tremendous scientific interest. In the following we review the superconducting phase diagram in UPt_3 . A detailed account may be found in Joynt and Taillefer (2002).

The first indication for multiple superconducting phases was observed in the ultrasound attenuation in applied magnetic fields and in H_{c2} . The bulk property

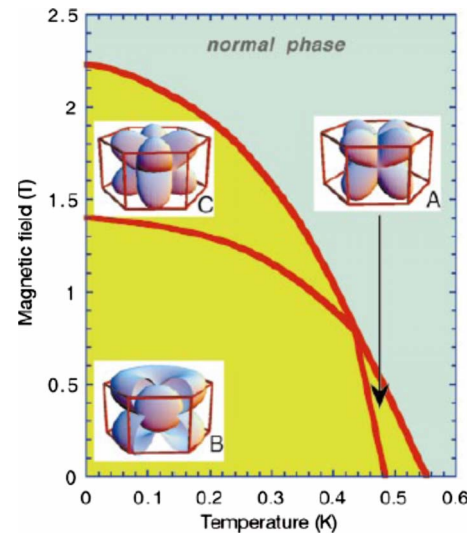


FIG. 21. (Color online) Superconducting phases of UPt_3 as a function of magnetic field. The insets show the nodal structures of the E_{1u} representations proposed on the basis of small angle neutron scattering of the flux line lattice. From Huxley *et al.*, 2000.

that exhibits the most distinct evidence of multiple superconducting phases is the specific heat, where two transitions are seen. The transition temperatures are $T_s^+=0.530$ K and $T_s^-=0.480$ K (Fisher *et al.*, 1989). Thus the splitting is of the order $\sim 10\%$ of T_s and rather small. With respect to the linear term of the normal state specific heat $\gamma_n=0.44$ J/mol K², the anomalies at T_s are given by $\Delta C^+/\gamma T_s^+=0.545$ and $\Delta C^-/\gamma T_s^-=0.272$. The ratio of the height of the upper to the lower anomalies is hence about 2:1. Even though the specific heat anomalies are substantial, they are small by comparison to the BCS value. This indicates nodes in the superconducting gap. Another signature of nodes in the gap is a linear decrease in C/T below T_s down to 0.1 K, below which a pronounced upturn is observed (Brison *et al.*, 1994).

An applied magnetic field has been found to reduce T_s^+ and T_s^- at different initial rates without significant broadening for field parallel and perpendicular to the c axis, as shown in Fig. 21 (Hasselbach *et al.*, 1989, 1990). The transition merges at a tetracritical point (H^*, T_H^*), where for $H \parallel \hat{c}$, $H^*=0.4$ T, $T_H^*=T_s^+-0.1$ K. For $H \perp \hat{c}$, $H^*=0.8$ T, $T_H^*=T_s^+-0.15$ K. Tetracriticality has been confirmed by ultrasound attenuation (Adenwalla *et al.*, 1990; Bruls *et al.*, 1990), dilatometry (van Dijk *et al.*, 1993), and the magnetocaloric effect (Bogenberger *et al.*, 1993). The general consensus has become that UPt_3 exhibits three superconducting phases referred to as A, B and C. Phases A and B support a Meissner and a Shubnikov phase below and above H_{c1} . As a function of temperature H_{c1} shows a sudden increase in slope at T_s^- (Vincent *et al.*, 1991). Qualitatively the three-component phase diagram contrasts an extrinsic origin, where the phase transition lines may be expected to have similar field dependences.

In general H_{c2} in UPt_3 exceeds Pauli limiting. The anisotropy of $H_{c2}^{\parallel\hat{c}}$ and $H_{c2}^{\perp\hat{c}}$ changes at around 0.2 K with $H_{c2}^{\parallel} < H_{c2}^{\perp}$ at low temperatures and $H_{c2}^{\parallel} > H_{c2}^{\perp}$ near T_s (Shivaram *et al.*, 1986). The presence of the three superconducting phases requires one to distinguish coherence lengths and penetration depths according to these phases. On the one hand, the zero-temperature value of H_{c2} is characteristic of the C phase, where $H_{c2}^{\parallel}(T \rightarrow 0) = 2.1$ T and $H_{c2}^{\perp}(T \rightarrow 0) = 2.8$ T. The anisotropy of H_{c2} may be accounted for by an anisotropic mass enhancement. The coherence length inferred from H_{c2} then is $\xi \approx 120$ Å. On the other hand, the initial slope of H_{c2} with temperature near T_s^+ is characteristic of the A phase, where $dH_{c2}^{\parallel}/dT|_{T_s^+} = -7.2 \pm 0.6$ T/K and $dH_{c2}^{\perp}/dT|_{T_s^+} = -4.4 \pm 0.3$ T/K. When this anisotropy is accounted for in terms of the effective mass enhancement, it is possible to obtain an estimate of the Ginzburg-Landau parameter $\kappa_{\text{GL}} = 44$. In other words UPt_3 is a strong type-II superconductor. Some simple estimates arrive at values of the penetration depth of the order $\lambda_{\parallel}(T \rightarrow 0) = 4500$ Å and $\lambda_{\perp}(T \rightarrow 0) = 7400$ Å, consistent with the short coherence length estimated for the C phase. It can finally be shown that weak-coupling theory yields the same value of κ_{GL} . This implies that UPt_3 is still fairly well described in a weak-coupling approximation.

The effect of hydrostatic pressure on the superconducting transitions and the antiferromagnetic order strongly suggests that the antiferromagnetic order is instrumental for the symmetry breaking between the different superconducting phases. In the specific heat the two superconducting transitions are found to decrease at different rates, eventually merging into a single transition above ~ 3 kbar (Trappmann *et al.*, 1991). At the same time neutron scattering establishes that the ordered moment decreases under pressure and vanishes above ~ 3 kbar, while T_N is essentially not affected by pressure (Hayden *et al.*, 1992).

Numerous other experimental probes suggest unconventional pairing and provide important hints as to the precise nature of the gap symmetry. For instance, in a recent small angle neutron scattering study the magnetic field dependence of the flux line lattice has been established. The upshot of this study is that the three superconducting phases belong to the E_{2u} symmetry (Huxley *et al.*, 2000) [see also Champel and Mineev (2001) for theoretical considerations on the flux line lattice]. For an extended review and critical discussion of the various theoretical scenarios see Joynt and Taillefer (2002). Despite the large body of studies the search for the correct order parameter symmetry has not been entirely conclusive so far.

2. Further candidates

Nearly all of the systems covered in this review in one way or the other may be candidates for multiple superconducting phases. The nature of these phases may be quite different, representing either different order pa-

rameter symmetries or real-space modulations with different ordered states. In the following we draw attention to candidates that await further clarification.

a. CeCu_2Si_2

As reviewed in Secs. II.A.1 and IV.B.1 recent high-pressure studies in pure and Ge-doped CeCu_2Si_2 reveal the presence of two superconducting domes (Fig. 3). At low pressures this material is a candidate for magnetically mediated pairing driven by the vicinity to an antiferromagnetic quantum critical point. At high pressures a second dome emerges and it has been argued that this superconducting phase is related to fluctuations in the charge density of a valence transition (Yuan *et al.*, 2003; Holmes *et al.*, 2004).

b. CeNi_2Ge_2

At ambient pressure CeNi_2Ge_2 displays an incipient form of superconductivity. It has been argued that the ambient pressure behavior is reminiscent of CePd_2Si_2 in the vicinity of the critical pressure. Under pressure the signatures of superconductivity vanish. At high pressures an additional superconducting transition emerges, as shown in Fig. 4 (Grosche, Lister, *et al.*, 1997). In principle this second superconducting dome may hint at an additional superconducting phase but little is known about this state.

c. CeIrIn_5

Pure single crystals of CeIrIn_5 display a difference of the temperature of a zero-resistance transition, $T_{s1} = 0.75$ K, and the bulk superconducting transition in the specific heat, $T_{s2} = 0.4$ K. It is tempting to attribute the resistive transition to sample inhomogeneities. However, if the two transitions are intrinsic, it may signal the presence of two superconducting instabilities, where the first transition corresponds to incipient superconductivity.

d. UPd_2Al_3

In UPd_2Al_3 single crystals grown with an Al-rich starting composition showed particularly sharp superconducting transitions at T_s in the resistivity (Sakon *et al.*, 1993). This suggested an improved sample quality. Remarkably the specific heat, the thermal expansion, and the elastic constants in these samples revealed an additional anomaly around 0.6 K well below T_s (Matsui *et al.*, 1994; Sakon *et al.*, 1994; Sato *et al.*, 1994). The nature of this transition has so far not been settled; either it signals an additional superconducting transition akin the double transition observed in UPt_3 or it corresponds to another ordering transition. For the first case, it is conceivable that the antiferromagnetic order of UPd_2Al_3 represents the symmetry-breaking field. In the latter case, it is possible that the emerging order leads to an additional symmetry breaking of the superconducting order that may stabilize additional superconducting phases.

e. URu_2Si_2

Early studies on the specific heat of the superconducting transition in URu_2Si_2 showed features reminiscent of the double transition in UPt_3 (Hasselbach *et al.*, 1991). Detailed studies in high-quality single crystals did not confirm the first findings. Keeping in mind that the small-moment antiferromagnetism in UPt_3 represents the symmetry-breaking field, which stabilizes the different superconducting phases, it seems plausible that the same might occur in URu_2Si_2 . However, the antiferromagnetism in URu_2Si_2 seems to be related to an impurity phase. Moreover, under pressure the superconductivity vanishes when large-moment antiferromagnetism appears. The observed change in curvature in H_{c2} of URu_2Si_2 has motivated considerations of the possible formation of a FFLO state. However, as discussed below URu_2Si_2 does not develop a FFLO state. In turn it is currently accepted that URu_2Si_2 does not support additional superconducting phases.

f. UBe_{13}

Doping UBe_{13} with Th results in the phase diagram shown in Fig. 12 (Ott *et al.*, 1986). For $x_1=0.02 < x < x_2=0.042$ two successive transitions at $T_{s1} > T_{s2}$ are observed in the specific heat. The onset of superconductivity is thereby at T_{s1} . The pressure dependence of Th-doped samples also suggest the existence of two superconducting phases (Lambert *et al.*, 1986), where an investigation of the lower critical field suggests that T_{s2} indeed marks the onset of another superconducting phase (Rauchschalbe *et al.*, 1987). A group theoretical analysis of these properties has been reported by Luk'yanchuk and Mineev (1989) and Makhlin and Mineev (1992). However, it still seems unsettled whether the lower transition at T_{s2} indeed represents another superconducting transition (Kumar and Wölfle, 1987; Sigrist and Rice, 1989; Martisovits *et al.*, 2000) or the onset of a defect-induced form of magnetic order as suggested by μ SR (Heffner *et al.*, 1986).

g. UGe_2

Pressure and magnetic field studies suggest that the superconductivity in UGe_2 is driven by the first order transition between the FM1 and FM2 ferromagnetic phases (Fig. 13). The superconductivity hence exists in the presence of two different forms of ferromagnetic order. Theoretical considerations have shown that the order parameter symmetry in ferromagnetic superconductors depends on the orientation of the ferromagnetic moment. Experimental evidence that tentatively supports different superconducting phases in the FM1 and FM2 states may be seen in the discontinuity of T_s at p_x and the reentrance of H_{c2} for pressures just above p_x and field applied along the crystallographic *a* axis. However, as discussed in Sec. III.A.1, the magnetic anisotropy of UGe_2 remains unchanged under pressure. It therefore appears unlikely that the superconducting

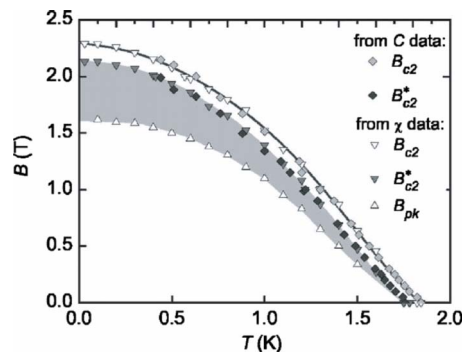


FIG. 22. (Color online) Superconducting phase diagram of $PrOs_4Sb_{12}$. From Grube *et al.*, 2006.

phases in the FM1 and FM2 states are fundamentally different. Further studies will have to clarify this issue.

h. $URhGe$

One of the most unusual phase diagrams among all *f*-electron superconductors is observed in $URhGe$. As a function of magnetic field superconductivity is at first suppressed but reappears at high magnetic fields when the ordered moment is forced to rotate from the *c* axis to the *b* axis. The phase diagram yields up to three different superconducting phases: the zero field state, the high-field state below H_R , where the moment is almost rotated into the *b* axis, and finally above H_R , where the moment is essentially aligned with the *b* axis. As for UGe_2 the allowed order parameter symmetries have been worked out for the orthorhombic crystal structure.

i. $CePt_3Si$ and $CeMX_3$

The pressure versus temperature phase diagram of the four noncentrosymmetric heavy-fermion superconductors is dominated by a decrease in the Néel temperature. The transition line crosses the superconducting dome in the middle, so that the phase diagram is comprised of a regime where $T_N > T_s$ and a regime where T_N has vanished. These two regimes are in principle candidates for differences in the order parameter.

j. $PrOs_4Sb_{12}$

The superconducting state of $PrOs_4Sb_{12}$ exhibits several features that have been interpreted as tentative evidence for multiple superconducting phases. The specific heat of $PrOs_4Sb_{12}$ displays two superconducting transitions (Vollmer *et al.*, 2003, 2004; Measson *et al.*, 2004), where doping by Ru and La stabilizes the upper transition while mechanical thinning stabilizes the lower transition. However, the origin of the double transition is a controversial issue, where recent studies suggest that it may of extrinsic origin (Seyfarth *et al.*, 2006; Kasahara *et al.*, 2008; Méasson *et al.*, 2008) (for details see Sec. IV.C). As shown in Fig. 22 tentative transition lines in the susceptibility and a variety of other quantities may be traced to zero temperature. Studies of the thermal conductivity (Izawa *et al.*, 2003) also suggest multiple super-

conducting phases, but with a different phase diagram that is not matched by any other property. Finally, high-precision measurements of the magnetization suggest the possible existence of yet another transition line at very low fields (Cichorek *et al.*, 2005). A comprehensive discussion along with detailed measurements of the specific heat and ac susceptibility has been given by Grube *et al.* (2006).

B. Textures

An important fundamental and technological question in condensed matter systems concerns weak interactions, which cause the formation of intermediate- and long-scale textures. The f -electron superconductors reviewed here exhibit several forms of electronic order and thus possess different types of characteristic rigidities. As far as the superconducting state is concerned these are the coherence length and penetration depth, while the magnetic state is characterized by the spin-wave stiffness, spin-orbit coupling, CEF pinning potential, and dipolar interactions. As a first example the competition of exchange splitting with superconducting pairing is addressed. This competition may result in real-space modulations of the superconductivity and spin polarization as reviewed in Sec. V.B.1. The possible interplay of ferromagnetic domain structures and superconductivity is addressed in Sec. V.B.2.

1. Fulde-Ferrell-Larkin-Ovchinnikov states

The novel forms of superconductivity of interest here are characterized by real-space modulations and anisotropies of the superconducting gap function that are caused by a loss of symmetries beyond those of the underlying crystal structure. In turn the phase rigidity of the superconducting condensate in these superconductors yields changes in sign in momentum space. An entirely different class of novel superconducting states was predicted by Fulde, Ferrel, Larkin, and Ovchinnikov (FFLO) (Fulde and Ferrell, 1964; Larkin and Ovchinnikov, 1965). As opposed to changes in momentum space in the FFLO state the order parameter changes sign in real space. In its original version the FFLO state considered superconductivity in the presence of a strong uniform exchange field. The Cooper pairs thereby form between Zeeman-split parts of the Fermi surface, so that pairing with a finite momentum \vec{q} is stabilized, where $(\vec{k}\uparrow, -\vec{k}+\vec{q}\downarrow)$. In the following we review the current status of FFLO states in the f -electron superconductors addressed here. Detailed reviews may be found, in Buzdin *et al.* (1997), Casalbuoni and Nardulli (2004), Matsuda and Shimahara (2007); for recent theory see Houzet and Mineev (2006, 2007).

Despite intense efforts, only a small number of candidate materials could be identified that may support an FFLO state, notably heavy-fermion superconductors and quasi-two-dimensional organic superconductors for fields parallel to the layers (Gruenberg and Gunther, 1966; Gloos *et al.*, 1993; Yin and Maki, 1993; Burkhardt

and Rainer, 1994; Shimahara, 1994; Oupuis, 1995; Tachiki *et al.*, 1996; Buzdin and Kachkachi, 1997). This may be traced back to the rather severe conditions under which the FFLO state is expected to form. As a first precondition, pair breaking in applied magnetic fields must be dominated by paramagnetic limiting and not orbital limiting (Gruenberg and Gunther, 1966). Second, impurities are detrimental to the FFLO state, making high-purity samples a key requirement (Aslamazov, 1969; Takada and Izuyama, 1969). Third, large anisotropies of the Fermi surface are favorable to the FFLO state.

FFLO considered the effects of a uniform exchange field on s -wave superconductors. In the presence of pure orbital limiting the superconducting transition is second order at all magnetic fields and the superconductivity is unchanged by the exchange field. In contrast, in the presence of pure Pauli limiting the superconducting transition changes in finite fields from second to first order for temperatures below $T^\dagger=0.56T_s$ (Saint-James *et al.*, 1969; Ketterson and Song, 1999). Below T^\dagger an inhomogeneous form of superconductivity stabilizes, in which the Cooper pairs support a finite momentum $(\vec{k}\uparrow, -\vec{k}+\vec{q}\downarrow)$.

In the bulk properties the signature of the FFLO state is an increase in H_{c2} below T^\dagger , which may be accompanied by a change in curvature. The size of this increase depends sensitively on the anisotropy of the Fermi surface ranging from 7% of the Pauli limit for three dimensions (Fulde and Ferrell, 1964; Larkin and Ovchinnikov, 1965; Saint-James *et al.*, 1969; Takada and Izuyama, 1969), over 42% for two dimensions (Aoi *et al.*, 1974; Bulaevskii, 1974; Burkhardt and Rainer, 1994; Shimahara, 1994) to a divergence for one dimension (Machida and Nakanishi, 1984; Suzumura and Ishino, 1983). Microscopically the FFLO state consists in spatial modulations of the superconductivity in real space, for which the order parameter may be given in general as $\Delta(\vec{r}) = \sum_{m=1}^M \Delta_m \exp(i\vec{q}_m \cdot \vec{r})$ (Fulde and Ferrell, 1964; Larkin and Ovchinnikov, 1965; Shimahara, 1998; Bowers and Rajagopal, 2002; Mora and Combescot, 2004; Combescot and Tonini, 2005; Mora and Combescot, 2005; Wang *et al.*, 2006). The superposition of degenerate components then yields a rich variety of symmetries of the real-space modulations, such as hexagonal, square, triangular, and one-dimensional modulations.

It has long been appreciated that the stringent requirements for an FFLO state may be satisfied in superconductors with short coherence length because the orbital limiting field diverges as $H_{c2}^{\text{orb}} \propto 1/\xi^2$ so that Pauli limiting may dominate. Prime examples are the heavy-fermion superconductors reviewed here. The situation for an FFLO state then involves (i) a finite admixture of orbital limiting, (ii) the coexistence of antiferromagnetic ferromagnetic order, and (iii) anisotropic (unconventional) order parameter symmetries. The exploration of these issues has stimulated many theoretical studies (Gruenberg and Gunther, 1966; Buzdin and Brison, 1996a, 1996b; Shimahara *et al.*, 1996; Tachiki *et al.*, 1996;

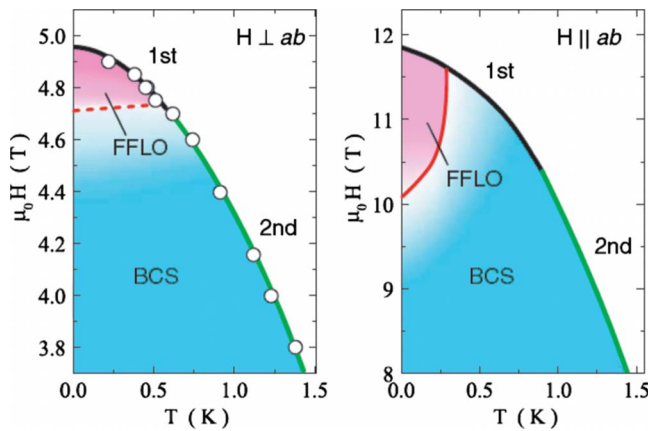


FIG. 23. (Color online) Superconducting phase diagram of CeCoIn₅. In the low-temperature limit a body of evidence suggests the formation of a FFLO state (shading). From Matsuda and Shimahara, 2007.

Shimahara and Rainer, 1997; Klein *et al.*, 2000; Adachi and Ikeda, 2003; Yang and MacDonald, 2004; Houzet and Mineev, 2006; Suginishi and Shimahara, 2006). For a recent review of these studies see Matsuda and Shimahara, 2007.

The question on whether FFLO states exist in heavy-fermion superconductors has been explored in a number of systems. For instance, the ac susceptibility, magnetization, ultrasound velocity, and thermal expansion near H_{c2} in CeRu₂ and UPd₂Al₃ exhibit the characteristics of a peak effect (Gegenwart *et al.*, 1996; Haga *et al.*, 1996; Steglich *et al.*, 1996; Tachiki *et al.*, 1996; Takahashi *et al.*, 1996). It is now broadly accepted that these features do not yield microscopic characteristics related to a FFLO state, but instead may be due to subtle forms of defect related pinning. Further candidates for a FFLO state are URu₂Si₂ and UBe₁₃, which display additional contributions in H_{c2} (Brison *et al.*, 1995; Buzdin and Brison, 1996a, 1996b; Glémot *et al.*, 1999). For URu₂Si₂ this contribution is seen for the c axis and rather small. In contrast UBe₁₃ displays a change in curvature in $H_{c2}(T)$. It has been shown that these features are consistent with a vicinity to the FFLO formation, but the FFLO state does not form. Possible explanations include the sample purity, which is very good but does not reach the exceptionally clean limit required. Candidates for a FFLO state that have recently been identified in specific heat studies under magnetic field are PuCoGa₅, PuRhGa₅ (Javorský *et al.*, 2007), and NpPd₅Al₂ (Aoki, Hagar, *et al.*, 2007).

Perhaps the best candidate of an FFLO state known to date has been identified in CeCoIn₅ (Fig. 23). Several features in the superconducting phase diagram have been observed uniquely in CeCoIn₅. The specific heat (Bianchi, Movshovich, Capan, *et al.*, 2003; Radovan *et al.*, 2003), magnetization (Gratens *et al.*, 2006), magnetostriction (Correa *et al.*, 2007), thermal conductivity (Capan *et al.*, 2004), penetration depth (Martin *et al.*, 2005), ultrasound velocity (Watanabe, Kasahara, *et al.*, 2004), and NMR Knight shift (Kakuyanagi *et al.*, 2005; Kuma-

gai *et al.*, 2006; Mitrović *et al.*, 2006) show that the transition at H_{c2} is first order for $T < 0.3T_s$ and $T < 0.4T_s$ for fields parallel and perpendicular to the c axis, respectively. This is the behavior expected for paramagnetic limiting of H_{c2} , where the samples studied were readily in the ultrapure limit, i.e., the coherence length is only a small fraction of the charge carrier mean free path. It is thereby helpful to note that the orbital limit $H_{c2,ab}^{\text{orb}} = 38.6$ T and $H_{c2,c}^{\text{orb}} = 11.7$ T inferred from the initial slope of H_{c2} near T_s substantially exceeds the experimentally observed values of H_{c2} . The corresponding values of the Maki parameter near 5 exceed the threshold of 1.8 by a large margin, above which a FFLO state may be expected.

Specific heat and torque magnetization first identified a second-order phase transition line in the superconducting state that branches off from $H_{c2}(T)$ at a temperature well below that of the change from second to first order and decreases with decreasing temperature (see Fig. 23) (Bianchi *et al.*, 2002; Miclea *et al.*, 2006). The presence of this line was confirmed in subsequent measurements of the penetration depth (Martin *et al.*, 2005), thermal conductivity (Capan *et al.*, 2004), ultrasound velocity (Watanabe, Kasahara, *et al.*, 2004), magnetization (Gratens *et al.*, 2006), magnetostriction (Correa *et al.*, 2007), and NMR (Kakuyanagi *et al.*, 2005; Mitrović *et al.*, 2006). The resulting phase pocket is a strong contender for a FFLO state.

The size of the novel phase pocket is anisotropic and considerably smaller in a field perpendicular to the a - b plane. The transition field is weakly temperature dependent for field direction perpendicular to the a - b plane and strongly field dependent for field direction parallel to the a - b plane. The anisotropy suggests that the FFLO state is more stable for field parallel to the a - b plane. This may be related to the two-dimensional character of the Fermi surface and the anisotropy of the spin fluctuation spectra, where the latter appear to be involved in the pairing interactions as discussed in Sec. II.A.2.

Key characteristics observed for the novel phase pocket may be summarized as follows. The penetration depth in the a - b plane increases, consistent with a decrease in the superfluid density (Martin *et al.*, 2005). The thermal conductivity, providing a directional probe of the quasiparticle spectrum, is highly anisotropic. For heat current parallel to the applied field the thermal conductivity is enhanced, while it has not been possible to clarify changes in the thermal conductivity for heat current transverse to the applied field. As this behavior is somewhat counterintuitive, it has been proposed that the interplay of vortex lattice, spatial order parameter modulation, and nodal gap structure results in an effective increase in vortex cores in the nodal plane (Capan *et al.*, 2004).

The flux line lattice in CeCoIn₅ has been studied by the ultrasound velocity (Watanabe, Kasahara, *et al.*, 2004; Ikeda, 2006), which provides information on the pinning of the vortex cores by defects. Notably it is possible to extract information on the c_{44} dispersive flux line

tilt mode. A careful analysis of the decrease observed in c_{44} implies a decrease in the superconducting volume fraction. Small angle neutron scattering studies did not meet the scattering condition necessary to probe the FFLO state (Bianchi *et al.*, 2008). Microscopic information on the FFLO regime is also provided by NMR spectra of the In(1) and In(2) sites in the CeIn₃ and CoIn₂ layers, respectively (Singleton *et al.*, 2001; Kakuyanagi *et al.*, 2005; Kumagai *et al.*, 2006; Mitrović *et al.*, 2006; Young *et al.*, 2007). In the FFLO regime a key feature for both field directions is the appearance of a second resonance line in the superconducting state, where the lines are close to the values of the normal and superconducting states. It is currently unresolved if the NMR spectra for field parallel to the *a-b* plane also reveal antiferromagnetic components of the vortex cores (Singleton *et al.*, 2001; Kakuyanagi *et al.*, 2005; Miclea *et al.*, 2006; Young *et al.*, 2007). Moreover, Cd doping of CeCoIn₅ leads to a rapid suppression of the first-order behavior of H_{c2} , but Hg doping only smears out the phase pocket without change in characteristic temperatures (Tokiwa *et al.*, 2008). These studies support a non-magnetic origin of the phase pocket as in the original FFLO proposal.

2. Magnetic domains versus flux lines

An issue that has not yet been explored experimentally in bulk compounds concerns the interplay of the length scales, characteristic of superconductivity with those characteristic of competing or coexisting forms of order. For superconducting ferromagnets several papers have explored this question from a theoretical point of view; see, e.g., Sonin and Felner (1998); Sonin (2002); Buzdin and Mel'nikov (2003).

VI. PERSPECTIVES

Even though the first example of a heavy-fermion superconductor, CeCu₂Si₂, was discovered nearly 30 years ago, an impressive series of new systems with surprising combinations of properties has come to light only recently. This has resulted in two developments. First, many systems are different and we are only beginning to distinguish new classes of systems that are outside the general patterns recognized earlier. Second, the more general experimental ingredients controlling unconventional superconductivity are finally becoming apparent. In the following we summarize these new developments.

Dominant interactions that control the properties of *f*-electron compounds may be summarized as follows: (i) the degree of *f*-electron localization, (ii) crystal electric fields, (iii) spin and orbital degrees of freedom and their coupling, and (iv) electron-phonon interactions. Among the large variety of *f*-electron superconductors that have been discovered in recent years, there are candidates where any one of the first three interaction channels appears to dominate the pairing interactions. For instance most members of the series CeM₂X₂ and Ce_nM_mIn_{3n+2m} are candidates for antiferromagnetically mediated pair-

ing. The U compounds UGe₂, URhGe, and UCoGe are candidates for ferromagnetically mediated pairing. Systems such as PrOs₄Sb₁₂ are candidates for pairing by quadrupolar fluctuations, while CeCu₂Si₂ at high pressure or the Pu-based superconductors are candidates for valence fluctuations of the *f* electrons and thus electron density. For instance, DMFT calculations reveal the fluctuating valence of Pu between 4, 5, and 6, ending in an average *f*-occupancy of 5.2. Despite their great microscopic differences all these systems may be combined in a single graph shown in Fig. 19, where the superconducting transition temperature (denoted here as T_c) is compared to logarithmic scales with characteristic temperature scale T_0 of the correlations (Sarrao and Thompson, 2007). Note that because T_0 represents essentially an effective bandwidth, this does not capture just spin-fluctuation-mediated pairing.

Regarding the bulk properties of the *f*-electron superconductors reviewed here a host of characteristics suggests unconventional superconductivity with a complex nodal structure of the superconducting gap. A particularly remarkable property concerns the large upper critical field. In the immediate vicinity of a quantum critical point these upper critical fields become additionally enhanced. Examples include URhGe, CeRhSi₃, and CeIrSi₃. It will be interesting to learn more about the mechanism underlying this exceptional enhancement.

A common theme for many of the systems covered in this review is the vicinity of the superconductivity to inherent Fermi surface instabilities. In the bulk properties this may be seen in the observed deviations from Fermi liquid behavior. As a rather remarkable microscopic piece of information quantum oscillatory studies under pressure reveal changes in the Fermi surface topology precisely where the superconductivity is most pronounced. Examples include CeRh₂Si₂, CeIn₃, CeRhIn₅, and UGe₂. This contrasts with the traditional ansatz of treating superconductivity as a property of stable Fermi liquids. It may therefore be highly instructive to investigate both theoretically and experimentally scenarios of superconductivity in the vicinity of Fermi surface reconstructions. For the case of the high- T_c cuprates this question has been explored extensively in a variety of scenarios, such as Pomeranchuk instabilities, preformed pairs, orbital currents, and stripes. In this context it is interesting to consider whether the recent discovery of electron pockets with the Fermi surface in a hole-doped cuprate actually hits on yet another analogy of the superconducting phases of *f*-electron compounds (Pfeleiderer and Hackl, 2007).

Many compounds discovered so far exhibit superconductivity in the vicinity of zero temperature instabilities. Examples are the systems such as CeM₂X₂, Ce_nM_mIn_{3n+2m}, UGe₂, URhGe, UCoGe, UIr, CePt₃Si, and CeMX₃. It has been noted that moderate anisotropies of the electronic and crystal structure promote the occurrence of superconductivity, while full inversion symmetry of the crystal structure does not seem to be a precondition. These studies suggest as a requirement for

superconductive pairing the need to balance stronger interactions that would otherwise lead to other forms of order such as magnetism. Although this is an important theme, one should also keep in mind that the recent discoveries were made by following this approach experimentally to start with. It is then interesting to note that a number of compounds are also quite insensitive to pressure. Examples are CeCu₂Ge₂ above p_c , UPd₂Al₃, UNi₂Al₃, and UBe₁₃. This implies either that we do not have an appropriate control parameter to change the particular balance in these compounds or that unconventional forms of superconductivity exist, which are much more robust and do not require the vicinity to a zero-temperature instability.

Experimentally the types of *f*-electron superconductors observed so far enforce the question of why heavy-fermion superconductivity has only been observed in systems containing Ce, Pr, U, Pu, and Np. There is *a priori* no reason why compounds based on other *f*-electron elements should not also exhibit unconventional forms of superconductivity. Clearly, as concerns the electronic properties of these compounds the understanding must be far from complete.

Last but not least, the importance of high sample quality cannot be emphasized enough. It is not just that the unconventional superconductivity tends to be extraordinarily sensitive to defects. Well-characterized high-quality single crystals are also essential to unravel the precise nature of the superconductivity alongside any other electronic properties in these compounds. Once high quality samples are available, controlled experimental techniques to systematically screen the evolution of these materials as a function of a nonthermal-control parameter have become the outstanding tool.

We conclude with the remark that it is generally very difficult to unambiguously assign the possible pairing interactions to a single interaction channel in a number of the *f*-electron compounds. For example, in UPd₂Al₃ both an antiferromagnetically mediated and an excitonic pairing mechanism have been proposed. This underscores quite generally the need for a description based on a coupling of two or more correlated subsystems. From a purely esthetic point of view, complex coupled systems tend to appear less beautiful because they are generally over parametrized and less tractable. However, the very need to consider these complexities also emphasizes the potential for new and entirely unexpected phenomena, many of which are yet to be discovered.

Note added in proof. Recently several more *f*-electron superconductors have been discovered. Amongst these are Eu (Debessai *et al.*, 2009), Ce₂PdIn₈ (Kaczorowski *et al.*, 2009), and beta-YbAlB₄ (Nakatsuji *et al.*, 2009).

ACKNOWLEDGMENTS

I wish to thank P. Böni, R. Hackl, and M. Sigrist for carefully reading the manuscript. Comments by Y. Aoki, I. Eremin, S. Fujimoto, A. D. Huxley, M. Janoschek, T. Kobayashi, J. Linder, K. Machida, V. P. Mineev, S. Mühl-

bauer, K. Moore, M. Norman, P. Sacramento, F. Steglich, J. D. Thompson, and Y. J. Uemura are gratefully acknowledged.

REFERENCES

- Aarts, J., A. P. Volodin, A. A. Menovsky, G. J. Nieuwenhuys, and J. A. Mydosh, 1994, *Europhys. Lett.* **26**, 203.
- Abrikosov, A. A., 1952, *Dokl. Akad. Nauk SSSR* **86**, 489.
- Abrikosov, A. A., 2001, *J. Phys.: Condens. Matter* **13**, L943.
- Abrikosov, A. A., and L. P. Gor'kov, 1961, *Sov. Phys. JETP* **12**, 1243.
- Adachi, H., and R. Ikeda, 2003, *Phys. Rev. B* **68**, 184510.
- Adenwalla, S., S. W. Lin, Q. Z. Ran, Z. Zhao, J. B. Ketterson, J. A. Sauls, L. Taillefer, D. G. Hinks, M. Levy, and B. K. Sarma, 1990, *Phys. Rev. Lett.* **65**, 2298.
- Aeppli, G., E. Bucher, C. Broholm, J. K. Kjems, J. Baumann, and J. Hufnagl, 1988, *Phys. Rev. Lett.* **60**, 615.
- Aeppli, G., E. Bucher, A. I. Goldman, D. Shirane, C. Broholm, and J. K. Kjems, 1987, *J. Magn. Magn. Mater.* **76-77**, 385.
- Agterberg, D. F., P. A. Frigeri, R. P. Kaur, A. Koga, and M. Sigrist, 2006, *Physica B* **378-380**, 351.
- Akazawa, T., H. Hidaka, T. Fujiwara, T. C. Kobayashi, E. Yamamoto, Y. Haga, R. Settai, and Y. Onuki, 2004, *J. Phys.: Condens. Matter* **16**, L29.
- Akazawa, T., H. Hidaka, H. Kotegawa, T. C. Kobayashi, T. Fujiwara, E. Yamamoto, Y. Haga, R. Settai, and Y. Onuki, 2004, *J. Phys. Soc. Jpn.* **73**, 3129.
- Allen, P., and R. C. Dynes, 1975, *Phys. Rev. B* **12**, 905.
- Amano, G., S. Akutagawa, T. Muranaka, Y. Zenitani, and J. Akimitsu, 2004, *J. Phys. Soc. Jpn.* **73**, 530.
- Amato, A., D., Andreica, F. N. Gygax, M. Pinkpank, N. K. Sato, A. Schenck, and G. Solt, 2000, *Physica B* **289-290**, 447.
- Amato, A., E. Bauer, and C. Baines, 2005, *Phys. Rev. B* **71**, 092501.
- Amato, A., C. Geibel, F. Gygax, R. Heffner, E. Knetsch, D. Maclaughlin, C. Schank, A. Schenck, F. Steglich, and M. Weber, 1992, *Z. Phys. B: Condens. Matter* **86**, 159.
- Amitsuka, H., K. Matsuda, I. Kawasaki, K. Tenya, M. Yokoyama, C. Sekine, N. Tateiwa, T. C. Kobayashi, S. Kawarazaki, and H. Yoshizawa, 2007, *J. Magn. Magn. Mater.* **310**, 214.
- Amitsuka, H., M. Sato, N. Metoki, M. Yokoyama, K. Kuwahara, T. S. Sakakibara, H. Morimoto, S. Kawarazaki, Y. Miyako, and J. A. Mydosh, 1999, *Phys. Rev. Lett.* **83**, 5114.
- Amitsuka, H., K. Tenya, M. Yokoyama, A. Schenck, D. Andreica, F. N. Gygax, A. Amato, Y. Miyako, Y. K. Huang, and J. A. Mydosh, 2003, *Physica B* **326**, 418.
- Amitsuka, H., *et al.*, 2000, *J. Phys. Soc. Jpn. (Suppl. A)* **69**, 5.
- Anderson, P. W., 1959, *J. Phys. Chem. Solids* **11**, 26.
- Anderson, P. W., 1984, *Phys. Rev. B* **30**, 4000.
- Andrei, N., 1982, *Phys. Lett.* **87A**, 299.
- Andres, K., J. E. Graebner, and H. R. Ott, 1975, *Phys. Rev. Lett.* **35**, 1779.
- Aoi, K., W. Dieterich, and P. Fulde, 1974, *Z. Phys.* **267**, 223.
- Aoki, D., Y. Haga, T. D. Matsumo, N. Tateiwa, S. Ikeda, Y. Homma, H. Sakai, Y. Shiokawa, E. Yamamoto, A. Nakamura, R. Settai, and Y. Onuki, 2007, *J. Phys. Soc. Jpn.* **76**, 063701.
- Aoki, D., A. Huxley, E. Ressouche, D. Braithwaite, J. Flouquet, J.-P. Brison, E. Lhotel, and C. Paulsen, 2001, *Nature (London)* **413**, 613.

- Aoki, H., T. Sakakibara, H. Shishido, R. Settai, Y. Onuki, P. Miranovic, and K. Machida, 2004, *J. Phys.: Condens. Matter* **16**, L13.
- Aoki, Y., T. Namiki, S. Ohsaki, S. R. Saha, H. Sugawara, and H. Sato, 2002, *J. Phys. Soc. Jpn.* **71**, 2098.
- Aoki, Y., H. Sugawara, H. Harima, and H. Sato, 2005, *J. Phys. Soc. Jpn.* **74**, 209.
- Aoki, Y., A. Sumiyama, G. Motoyama, Y. Oda, T. Yasuda, R. Settai, and Y. Onuki, 2008, *J. Phys. Soc. Jpn.* **76**, 114708.
- Aoki, Y., T. Tayama, T. Sakakibara, K. Kuwahara, K. Iwasa, M. Kohgi, W. Higemoto, D. E. MacLaughlin, H. Sugawara, and H. Sato, 2007, *J. Phys. Soc. Jpn.* **76**, 051006.
- Aoki, Y., A. Tsuchiya, T. Kanayama, S. R. Saha, H. Sugawara, H. Sato, W. M. Higemoto, A. Koda, K. Ohishi, K. Nishiyama, and R. Kadono, 2003, *Phys. Rev. Lett.* **91**, 067003.
- Araki, S., M. Nakashima, R. Settai, T. C. Kobayashi, and Y. Onuki, 2002, *J. Phys.: Condens. Matter* **14**, L377.
- Araki, S., R. Settai, T. C. Kobayashi, H. Harima, and Y. Onuki, 2001, *Phys. Rev. B* **64**, 224417.
- Araki, S., R. Settai, M. Nakashima, H. Shishido, S. Ikeda, H. Nakawaki, Y. Haga, N. Tateiwa, T. C. Kobayashi, H. Harima, H. Yamagami, Y. Aoki, T. Namiki, H. Sato, and Y. Onuki, 2002, *J. Phys. Chem. Solids* **63**, 1133.
- Aronson, M. C., J. D. Thompson, J. L. Smith, Z. Fisk, and M. W. McElfresh, 1989, *Phys. Rev. Lett.* **63**, 2311.
- Aslamazov, L. G., 1969, *Sov. Phys. JETP* **28**, 773.
- Aso, N., H. Miyano, H. Yoshizawa, N. Kimura, T. Komatsubara, and H. Aoki, 2007, *J. Magn. Magn. Mater.* **310**, 602.
- Aso, N., H. Nakane, G. Motoyama, N. K. Sato, Y. Uwatoko, T. Takeuchi, Y. Homma, Y. Shiokawa, and K. Hirota, 2005, *Physica B* **359-360**, 1051.
- Aso, N., K. Ohwada, T. Watanuki, A. Machida, A. Ohmura, T. Inami, Y. Homma, Y. Shiokawa, K. Hirota, and N. K. Sato, 2006, *J. Phys. Soc. Jpn.* **75S**, 88.
- Aso, N., B. Roessli, N. Bernhoeft, R. Calemczuk, N. K. Sato, Y. Endoh, T. Komatsubara, A. Hiess, G. H. Lander, and H. Kadowaki, 2000, *Phys. Rev. B* **61**, 11867.
- Assmus, W., M. Herrmann, U. Rauchschalbe, S. Riegel, W. Lieke, H. Spille, S. Horn, G. Weber, F. Steglich, and G. Cordier, 1984, *Phys. Rev. Lett.* **52**, 469.
- Badica, P., T. Kondo, and K. Togano, 2005, *J. Phys. Soc. Jpn.* **74**, 1014.
- Bakker, K., A. de Visser, E. Brück, A. A. Menovsky, and J. J. M. Franse, 1991, *J. Magn. Magn. Mater.* **108**, 63.
- Bang, Y., A. V. Balatsky, F. Wastin, and J. D. Thompson, 2004, *Phys. Rev. B* **70**, 104512.
- Bang, Y., M. J. Graf, N. J. Curro, and A. V. Balatsky, 2006, *Phys. Rev. B* **74**, 054514.
- Bao, W., G. Aeppli, J. W. Lynn, P. G. Pagliuso, J. L. Sarrao, M. F. Hundley, J. D. Thompson, and Z. Fisk, 2002, *Phys. Rev. B* **65**, 100505.
- Bao, W., A. Chritianson, P. Pagliuso, J. Sarrao, J. Thompson, A. H. Lacerda, and J. W. Lynn, 2002, *Physica B* **312-313**, 120.
- Bao, W., P. G. Pagliuso, J. L. Sarrao, J. D. Thompson, Z. Fisk, and J. W. Lynn, 2001, *Phys. Rev. B* **64**, 020401.
- Bao, W., P. G. Pagliuso, J. L. Sarrao, J. D. Thompson, Z. Fisk, J. W. Lynn, and R. W. Erwin, 2000, *Phys. Rev. B* **62**, R14621.
- Bao, W., P. G. Pagliuso, J. L. Sarrao, J. D. Thompson, Z. Fisk, J. W. Lynn, and R. W. Erwin, 2003, *Phys. Rev. B* **67**, 099903.
- Bardeen, J., L. N. Cooper, and J. R. Schrieffer, 1957, *Phys. Rev.* **108**, 1175.
- Barzykin, V., and L. P. Gorkov, 1993, *Phys. Rev. Lett.* **70**, 2479.
- Bauer, E., I. Bonalde, and M. Sigrist, 2005, *Fiz. Nizk. Temp.* **31**, 984.
- Bauer, E., G. Hilscher, H. Michor, C. Paul, E.-W. Scheidt, A. Griбанov, Y. Seropegin, H. Noel, M. Sigrist, and P. Rogl, 2004, *Phys. Rev. Lett.* **92**, 027003.
- Bauer, E., G. Hilscher, H. Michor, M. Sieberer, E. Scheidt, A. Griбанov, Y. Seropegin, P. Rogl, A. Amato, W. Y. Song, J.-G. Park, D. T. Adroja, M. Nicklas, G. Sparn, M. Yogi, and Y. Kitaoka, 2005, *Physica B* **359-361**, 360.
- Bauer, E., H. Kaldarar, A. Prokofiev, E. Royanian, A. Amato, J. Sereni, W. Brämer-Escamilla, and I. Bonalde, 2007, *J. Phys. Soc. Jpn.* **76**, 051009.
- Bauer, E., D. Mixon, F. Ronning, N. Hur, R. Movshovich, J. Thompson, J. Sarrao, M. Hundley, P. Tobash, and S. Bobev, 2006, *Physica B* **378-380**, 142.
- Bauer, E. D., C. Capan, F. Ronning, R. Movshovich, J. D. Thompson, and J. L. Sarrao, 2005, *Phys. Rev. Lett.* **94**, 047001.
- Bauer, E. D., R. P. Dickey, V. S. Zapf, and M. B. Maple, 2001, *J. Phys.: Condens. Matter* **13**, L759.
- Bauer, E. D., N. A. Frederick, P. C. Ho, V. S. Zapf, and M. B. Maple, 2002, *Phys. Rev. B* **65**, 100506(R).
- Bauer, E. D., P.-C. Ho, M. B. Maple, T. Schauerer, D. L. Cox, and F. B. Anders, 2006, *Phys. Rev. B* **73**, 094511.
- Bauer, E. D., J. D. Thompson, J. L. Sarrao, L. A. Morales, F. Wastin, J. Rebizant, J. C. Griveau, P. Javorsky, P. Boulet, E. Colineau, G. H. Lander, and G. R. Stewart, 2004, *Phys. Rev. Lett.* **93**, 147005.
- Bel, R., K. Behnia, Y. Nakajima, K. Izawa, Y. Matsuda, H. Shishido, R. Settai, and Y. Onuki, 2004, *Phys. Rev. Lett.* **92**, 217002.
- Belitz, D., and T. R. Kirkpatrick, 2004, *Phys. Rev. B* **69**, 184502.
- Belitz, D., T. R. Kirkpatrick, and T. Vojta, 2005, *Rev. Mod. Phys.* **77**, 579.
- Bellarbi, B., A. Benoit, D. Jaccard, J. M. Mignot, and H. F. Braun, 1984, *Phys. Rev. B* **30**, 1182.
- Benoit, A., J. X. Boucherle, P. Convert, J. Flouquet, J. Palleau, and J. Schweitzer, 1980, *Solid State Commun.* **34**, 293.
- Berk, N. F., and J. R. Schrieffer, 1966, *Phys. Rev. Lett.* **17**, 433.
- Bernhoeft, N., B. Roessli, N. Sato, N. Aso, A. Hiess, G. H. Lander, Y. Endoh, and T. Komatsubara, 1999, *Physica B* **259-261**, 614.
- Bernhoeft, N., N. Sato, B. Roessli, N. Aso, A. Hiess, G. H. Lander, Y. Endoh, and T. Komatsubara, 1998, *Phys. Rev. Lett.* **81**, 4244.
- Bernhoeft, N. R., G. H. Lander, M. J. Longfield, S. Langridge, D. Mannix, E. Lidstrom, E. Colineau, A. Hiess, C. Vettier, F. Wastin, J. Rebizant, and P. Lejay, 2003, *Acta Phys. Pol. B* **34**, 1367.
- Bernhoeft, N. R., and G. G. Lonzarich, 1995, *J. Phys.: Condens. Matter* **7**, 7325.
- Bianchi, A., R. Movshovich, C. Capan, P. G. Pagliuso, and J. L. Sarrao, 2003, *Phys. Rev. Lett.* **91**, 187004.
- Bianchi, A., R. Movshovich, M. Jaime, J. D. Thompson, P. G. Pagliuso, and J. L. Sarrao, 2001, *Phys. Rev. B* **64**, 220504.
- Bianchi, A., R. Movshovich, N. Oeschler, P. Gegenwart, F. Steglich, J. D. Thompson, P. G. Pagliuso, and J. L. Sarrao, 2002, *Phys. Rev. Lett.* **89**, 137002.
- Bianchi, A., R. Movshovich, I. Vekhter, P. G. Pagliuso, and J. L. Sarrao, 2003, *Phys. Rev. Lett.* **91**, 257001.
- Bianchi, A. D. *et al.*, 2008, *Science* **319**, 177.
- Blackburn, E., A. Hiess, N. Bernhoeft, and G. H. Lander, 2006, *Phys. Rev. B* **74**, 024406.

- Blackburn, E., A. Hiess, N. Bernhoeft, M. C. Rheinstädter, W. Häußler, and G. H. Lander, 2006, *Phys. Rev. Lett.* **97**, 057002.
- Bogenberger, B., H. v. Löhneysen, T. Trappmann, and L. Taillefer, 1993, *Physica B* **186-188**, 248.
- Bonalde, I., W. Brämer-Escamilla, and E. Bauer, 2005, *Phys. Rev. Lett.* **94**, 207002.
- Bonalde, I., W. Brämer-Escamilla, C. Rojas, Y. Haga, E. Bauer, T. Yasuda, and Y. Onuki, 2007, *Physica C* **460**, 659.
- Bonn, D. A., J. D. Garrett, and T. Timusk, 1988, *Phys. Rev. Lett.* **61**, 1305.
- Borth, R., E. Lengyl, P. Pagliuso, J. Sarrao, G. Sparn, F. Steglich, and J. Thompson, 2002, *Physica B* **312-313**, 136.
- Boulet, P., E. Colineau, F. Wastin, J. Rebizant, P. Javorský, G. H. Lander, and J. D. Thompson, 2005, *Phys. Rev. B* **72**, 104508.
- Boulet, P., A. Daoudi, M. Potel, H. Noël, G. M. Gross, G. André, and F. Bourée, 1997, *J. Alloys Compd.* **247**, 104.
- Bourdarot, F., A. Bombardi, P. Burlet, M. Enderle, J. Flouquet, P. Lejay, N. Kernavanois, V. P. Mineev, L. Paolasini, M. E. Zhitomirsky, and B. Fåk, 2005, *Physica B* **359-361**, 986.
- Bourdarot, F., B. Fåk, K. Habicht, and K. Prokes, 2003, *Phys. Rev. Lett.* **90**, 067203.
- Bowers, J. A., and K. Rajagopal, 2002, *Phys. Rev. D* **66**, 065002.
- Brison, J.-P., N. Keller, A. Verniere, P. Lejay, L. Schmidt, A. Buzdin, J. Flouquet, S. R. Julian, and G. G. Lonzarich, 1995, *Physica C* **250**, 128.
- Brison, J.-P., *et al.*, 1994, *Physica B* **199-200**, 70.
- Broholm, C., J. K. Kjems, W. J. L. Buyers, P. Matthews, T. T. M. Palstra, A. A. Menovsky, and J. A. Mydosh, 1987, *Phys. Rev. Lett.* **58**, 1467.
- Broholm, C., H. Lin, P. T. Matthews, T. E. Mason, W. J. L. Buyers, M. F. Collins, A. A. Menovsky, J. A. Mydosh, and J. K. Kjems, 1991, *Phys. Rev. B* **43**, 12809.
- Bruls, G., D. Weber, B. Wolf, P. Thalmeier, B. Lüthi, A. Visser, and A. Menovsky, 1990, *Phys. Rev. Lett.* **65**, 2294.
- Bruls, G., B. Wolf, D. Finsterbusch, P. Thalmeier, I. Kouroudis, W. Sun, W. Assmus, B. Lüthi, M. Lang, K. Gloos, F. Steglich, and R. Modler, 1994, *Phys. Rev. Lett.* **72**, 1754.
- Bucher, E., J. P. Maita, and A. S. Cooper, 1972, *Phys. Rev. B* **6**, 2709.
- Bucher, E., J. P. Maita, G. W. Hull, R. C. Fulton, and A. S. Cooper, 1975, *Phys. Rev. B* **11**, 440.
- Budko, S., and P. C. Canfield, 2006, *C. R. Phys.* **7**, 56.
- Bulaevskii, L. N., 1974, *Sov. Phys. JETP* **38**, 634.
- Bulaevskii, L. N., A. I. Buzdin, M. L. Kubic, and S. V. Panjukov, 1985, *Adv. Phys.* **34**, 175.
- Burkhardt, H., and D. Rainer, 1994, *Ann. Phys.* **3**, 181.
- Buschow, K. H. J., 1979, *Rep. Prog. Phys.* **42**, 1373.
- Buschow, K. H. J., and H. J. van Daal, 1970, *Solid State Commun.* **8**, 363.
- Buzdin, A. I., and J.-P. Brison, 1996a, *Phys. Lett. A* **218**, 359.
- Buzdin, A. I., and J.-P. Brison, 1996b, *Europhys. Lett.* **35**, 707.
- Buzdin, A. I., and H. Kachkachi, 1997, *Phys. Lett. A* **225**, 341.
- Buzdin, A. I., and A. S. Mel'nikov, 2003, *Phys. Rev. B* **67**, 020503.
- Buzdin, J. P. B. A., L. Glemont, F. Thomas, and J. Flouquet, 1997, *Physica B* **230-232**, 406.
- Campbell, A. M., and J. E. Evetts, 1972, *Adv. Phys.* **21**, 199.
- Capan, C., A. Bianchi, F. Ronning, A. Lacerda, J. D. Thompson, M. F. Hundley, P. G. Pagliuso, J. L. Sarrao, and R. Movshovich, 2004, *Phys. Rev. B* **70**, 180502.
- Casalbuoni, R., and G. Nardulli, 2004, *Rev. Mod. Phys.* **76**, 263.
- Caspary, R., P. Hellmann, M. Keller, G. Sparn, C. Wassilew, R. Köhler, C. Geibel, C. Schank, F. Steglich, and N. E. Phillips, 1993, *Phys. Rev. Lett.* **71**, 2146.
- Champel, T., and V. P. Mineev, 2001, *Phys. Rev. Lett.* **86**, 4903.
- Chandra, P., P. Coleman, J. A. Mydosh, and V. Tripathi, 2002, *Nature (London)* **417**, 831.
- Chandra, P., P. Coleman, J. A. Mydosh, and V. Tripathi, 2003, *J. Phys.: Condens. Matter* **15**, S1965.
- Chandrasekhar, B. S., 1962, *Appl. Phys. Lett.* **1**, 7.
- Chang, J., I. Eremin, P. Thalmeier, and P. Fulde, 2007, *Phys. Rev. B* **75**, 024503.
- Chen, G. F., K. Matsubayashi, S. Ban, K. Deguchi, and N. K. Sato, 2006, *Phys. Rev. Lett.* **97**, 017005.
- Chevalier, B., and J. Etourneau, 1999, *J. Magn. Magn. Mater.* **196-197**, 880.
- Chia, E. E. M., M. B. Salamon, H. Sugawara, and H. Sato, 2003, *Phys. Rev. Lett.* **91**, 247003.
- Chiao, M., B. Lussier, B. Ellman, and L. Taillefer, 1997, *Physica B* **230-232**, 370.
- Christianson, A. D., E. D. Bauer, J. M. Lawrence, P. S. Riseborough, N. O. Moreno, P. G. Pagliuso, J. L. Sarrao, J. D. Thompson, E. A. Goremychkin, F. R. Trouw, M. P. Hehlen, and R. J. McQueeney, 2004, *Phys. Rev. B* **70**, 134505.
- Christianson, A. D., *et al.*, 2005, *Phys. Rev. Lett.* **95**, 217002.
- Chudo, H., H. Sakai, Y. Tokunaga, S. Kambe, D. Aoki, Y. Homma, Y. Shiokawa, Y. Haga, S. Ikeda, T. D. Matsuda, Y. Onuki, and H. Yasuoka, 2008, *J. Phys. Soc. Jpn.* **77**, 083702.
- Cichorek, T., A. C. Mota, F. Steglich, N. A. Frederick, W. M. Yuhasz, and M. B. Maple, 2005, *Phys. Rev. Lett.* **94**, 107002.
- Clogston, A. M., 1962, *Phys. Rev. Lett.* **9**, 266.
- Coad, S., A. Hiess, D. F. McMorrow, G. H. Lander, G. Aeppli, Z. Fisk, G. R. Stewart, S. M. Hayden, and H. A. Mook, 2000, *Physica B* **276**, 764.
- Colineau, E., F. Wastin, P. Javorsky, and J. Rebizant, 2006, *Physica B* **378-380**, 1015.
- Combescot, R., and G. Tonini, 2005, *Phys. Rev. B* **72**, 094513.
- Cordes, H. G., K. Fischer, and F. Pobell, 1981, *Physica B & C* **107**, 531.
- Cornelius, A. L., A. J. Arko, J. L. Sarrao, M. F. Hundley, and Z. Fisk, 2000, *Phys. Rev. B* **62**, 14181.
- Cornelius, A. L., P. G. Pagliuso, M. F. Hundley, and J. L. Sarrao, 2001, *Phys. Rev. B* **64**, 144411.
- Correa, V. F., T. P. Murphy, C. Martin, K. M. Purcell, E. C. Palm, G. M. Schmiedeshoff, J. C. Cooley, and S. W. Tozer, 2007, *Phys. Rev. Lett.* **98**, 087001.
- Curro, N. J., T. Caldwell, E. D. Bauer, L. A. Morales, M. J. Graf, Y. Bang, A. V. Balatsky, J. D. Thompson, and J. J. L. Sarrao, 2005, *Nature (London)* **434**, 622.
- Dalichaouch, Y., M. C. de Andrade, D. A. Gajewski, R. Chau, P. Visani, and M. B. Maple, 1995, *Phys. Rev. Lett.* **75**, 3938.
- Dalichaouch, Y., M. C. de Andrade, and M. B. Maple, 1992, *Phys. Rev. B* **46**, 8671.
- Daniel, M., E. D. Bauer, S.-W. Han, C. H. Booth, A. L. Cornelius, P. G. Pagliuso, and J. L. Sarrao, 2005, *Phys. Rev. Lett.* **95**, 016406.
- Debessai, M., T. Matsuoka, J. J. Hamlin, J. S. Schilling, and K. Shimizu, 2009, *Phys. Rev. Lett.* **102**, 197002.
- DeBeer-Schmitt, L., C. D. Dewhurst, B. W. Hoogenboom, C. Petrovic, and M. R. Eskildsen, 2006, *Phys. Rev. Lett.* **97**, 127001.
- de Gennes, P. G., 1989, *Superconductivity of Metals and Alloys* (Addison-Wesley, Reading MA), reprint of 1966 edition.
- de Nijs, D. E., N. T. Huy, and A. de Visser, 2008, *Phys. Rev. B*

- 77, 140506.
- De Visser, A., K. Bakker, L. T. Tai, A. A. Menovsky, S. Mentink, G. Nieuwenhuys, and J. Mydosh, 1993, *Physica B* **186-188**, 291.
- de Visser, A., A. Menovsky, and J. J. M. Franse, 1987, *Physica B & C* **147**, 81.
- de Visser, A., H. Nakotte, L. Tai, A. A. Menovsky, S. Mentink, G. Nieuwenhuys, and J. A. Mydosh, 1992, *Physica B* **179**, 84.
- De Wilde, Y., J. Heil, A. G. M. Jansen, P. Wyder, R. Deltour, W. Assmus, A. Menovsky, W. Sun, and L. Taillefer, 1994, *Phys. Rev. Lett.* **72**, 2278.
- Divis, M., L. M. Sandratskii, M. Richter, P. Mohn, and P. Novak, 2002, *J. Alloys Compd.* **337**, 48.
- Dommann, E., and F. Hullinger, 1988, *Solid State Commun.* **65**, 1093.
- Donath, J. G., F. Steglich, E. D. Bauer, J. L. Sarrao, and P. Gegenwart, 2008, *Phys. Rev. Lett.* **100**, 136401.
- Dresselhaus, G., 1955, *Phys. Rev.* **100**, 580.
- Dungate, D. G., 1990, Ph.D. thesis, University of Cambridge, Cambridge.
- Dupuis, N., 1995, *Phys. Rev. B* **51**, 9074.
- Durivault, L., F. Bourée, B. Chevalier, G. André, and J. Etourneau, 2002, *J. Magn. Magn. Mater.* **246**, 366.
- Edelstein, V. M., 1989, *Sov. Phys. JETP* **68**, 1244.
- Efremov, D. V., N. Hasselmann, E. Runge, P. Fulde, and G. Zwirknagl, 2004, *Phys. Rev. B* **69**, 115114.
- Einzel, D., P. J. Hirschfeld, F. Gross, B. S. Chandrasekhar, K. Andres, H. R. Ott, J. Beuers, Z. Fisk, and J. L. Smith, 1986, *Phys. Rev. Lett.* **56**, 2513.
- Ejima, T., S. Suzuki, S. Sato, N. Sato, S. i. Fujimori, M. Yamada, K. Sato, T. Komatsubara, T. Kasuya, Y. Tezuka, S. Shin, and T. Ishi, 1994, *J. Phys. Soc. Jpn.* **63**, 2428.
- Elgazzar, S., I. Opahle, R. Hayn, and P. M. Oppeneer, 2004, *Phys. Rev. B* **69**, 214510.
- Eliashberg, G. M., 1960, *Sov. Phys. JETP* **11**, 696.
- Ellman, B., M. Sutton, B. Lussier, R. Brünig, L. Taillefer, and S. M. Hayden, 1997, unpublished.
- Ellman, B., A. Zaluska, and L. Taillefer, 1995, *Physica B* **205**, 346.
- Eom, D., M. Ishikawa, J. Kitagawa, and N. Takeda, 1998, *J. Phys. Soc. Jpn.* **67**, 2495.
- Eskildsen, M. R., C. D. Dewhurst, B. W. Hoogenboom, C. Petrovic, and P. C. Canfield, 2003, *Phys. Rev. Lett.* **90**, 187001.
- Fåk, B., B. Farago, and N. H. van Dijk, 1999, *Physica B* **259-261**, 644.
- Fåk, B., J. Flouquet, G. Lapertot, T. Fukuhara, and H. Kawakami, 2000, *J. Phys.: Condens. Matter* **12**, 5423.
- Fawcett, E., 1988, *Rev. Mod. Phys.* **60**, 209.
- Fay, D., and J. Appel, 1977, *Phys. Rev. B* **16**, 2325.
- Fay, D., and J. Appel, 1980, *Phys. Rev. B* **22**, 3173.
- Felsch, W., and K. Winzer, 1973, *Solid State Commun.* **13**, 569.
- Ferreira, L. M., *et al.*, 2008, *Phys. Rev. Lett.* **101**, 017005.
- Fertig, W. A., D. C. Johnston, L. E. DeLong, R. W. McCallum, M. B. Maple, and B. T. Matthias, 1977, *Phys. Rev. Lett.* **38**, 987.
- Feyerherm, R., A. Amato, F. N. Gyax, A. Schenck, C. Geibel, F. Steglich, N. Sato, and T. Komatsubara, 1994, *Phys. Rev. Lett.* **73**, 1849.
- Fischer, Ø., 1990, *Ferromagnetic Materials*, Topics in Current Physics Vol. 5 (Elsevier, New York).
- Fischer, Ø., and M. B. Maple 1982, Eds., *Superconductivity in Ternary Compounds I*, Topics in Current Physics Vol. 32 (Springer-Verlag, Berlin).
- Fisher, R. A., S. Kim, B. F. Woodfield, N. E. Phillips, L. Taillefer, K. Hasselbach, J. Flouquet, A. L. Giorgi, and J. L. Smith, 1989, *Phys. Rev. Lett.* **62**, 1411.
- Fisher, R. A., S. Kim, Y. Wu, N. E. Phillips, M. W. McElfresh, M. S. Torikachvili, and M. B. Maple, 1990, *Physica B* **163**, 419.
- Fisher, R. A., B. F. Woodfield, S. Kim, N. E. Phillips, L. Taillefer, A. L. Giorgi, and J. L. Smith, 1991, *Solid State Commun.* **80**, 263.
- Flint, R., M. Dzero, and P. Coleman, 2008, *Nat. Phys.* **4**, 643.
- Flouquet, J., 2005, *Prog. Low Temp. Phys.* **15**, 139.
- Flouquet, J., G. Knebel, D. Braithwaite, D. Aoki, J. Brison, F. Hardy, A. Huxley, S. Raymond, B. Salce, and I. Sheikin, 2006, *C. R. Phys.* **7**, 22.
- Fort, D., 1987, *J. Less-Common Met.* **134**, 45.
- Frazer, B. H., *et al.*, 2001, *Eur. Phys. J. B* **19**, 177.
- Frederick, N. A., T. D. Do, P.-C. Ho, N. P. Butch, V. S. Zapf, and M. B. Maple, 2004, *Phys. Rev. B* **69**, 024523.
- Frederick, N. A., T. A. Sayles, and M. B. Maple, 2005, *Phys. Rev. B* **71**, 064508.
- Frigeri, P. A., D. F. Agterberg, A. Koga, and M. Sgrist, 2004, *Phys. Rev. Lett.* **92**, 097001.
- Frigeri, P. A., D. F. Agterberg, and M. Sgrist, 2004, *Mem. Sci. Rev. Metall.* **6**, 115.
- Frings, P. H., J. J. M. F. F. R. de Boer, and A. Menovsky, 1983, *J. Magn. Magn. Mater.* **31-34**, 240.
- Fujimoto, S., 2006, *J. Phys. Soc. Jpn.* **75**, 083704.
- Fujimoto, S., 2007, *J. Phys. Soc. Jpn.* **76**, 034712.
- Fukazawa, H., and K. Yamada, 2003, *J. Phys. Soc. Jpn.* **72**, 2449.
- Fulde, P., and R. Ferrell, 1964, *Phys. Rev.* **135**, A550.
- Gaulin, B. D., M. Mao, C. R. Wiebe, Y. Qiu, S. M. Shapiro, C. Broholm, S.-H. Lee, and J. D. Garrett, 2002, *Phys. Rev. B* **66**, 174520.
- Gegenwart, P., M. Deppe, M. Koppen, F. Kromer, M. Lang, R. Modler, M. Weiden, C. Geibel, F. Steglich, T. Fukase, and N. Toyota, 1996, *Ann. Phys.* **5**, 307.
- Gegenwart, P., F. Kromer, M. Lang, G. Sparn, C. Geibel, and F. Steglich, 1999, *Phys. Rev. Lett.* **82**, 1293.
- Gegenwart, P., C. Langhammer, C. Geibel, R. Helfrich, M. Lang, G. Sparn, F. Steglich, R. Horn, L. Donnevert, A. Link, and W. Assmus, 1998, *Phys. Rev. Lett.* **81**, 1501.
- Gegenwart, P., C. Langhammer, R. H. N. O. M. L. J. S. Kim, G. R. Stewart, and F. Steglich, 2004, *Physica C* **408-410**, 157.
- Geibel, C., C. Schank, S. Thies, H. Kitazawa, C. D. Bredl, A. Bohm, M. Rau, A. Grauel, R. Caspary, R. Helfrich, U. Ahlheim, G. Weber, and F. Steglich, 1991, *Z. Phys. B: Condens. Matter* **84**, 1.
- Geibel, C., S. Thies, D. Kazorowski, A. Mehner, A. Grauel, B. Seidel, U. Ahlheim, R. Helfrich, K. Petersen, C. D. Bredl, and F. Steglich, 1991, *Z. Phys. B: Condens. Matter* **83**, 305.
- Ginzburg, V. L., 1957, *Sov. Phys. JETP* **4**, 153.
- Giorgi, A., E. G. Szkalrz, M. Krupta, and N. H. Krikoria, 1969, *J. Less-Common Met.* **17**, 121.
- Glémot, L., J. P. Brison, J. Flouquet, A. I. Buzdin, I. Sheikin, D. Jaccard, C. Thessieu, and F. Thomas, 1999, *Phys. Rev. Lett.* **82**, 169.
- Gloos, K., R. Modler, H. Schimanski, C. D. Bredl, C. Geibel, F. Steglich, A. I. Buzdin, N. Sato, and T. Komatsubara, 1993, *Phys. Rev. Lett.* **70**, 501.
- Goldman, A. I., S. M. Shapiro, D. E. Cox, J. L. Smith, and Z. Fisk, 1985, *Phys. Rev. B* **32**, 6042.
- Goldman, A. I., S. M. Shapiro, G. Shirane, J. L. Smith, and Z. Fisk, 1986, *Phys. Rev. B* **33**, 1627.

- Goremychkin, E. A., R. Osborn, E. D. Bauer, M. B. Maple, N. A. Frederick, W. M. Yuhasz, F. M. Woodward, and J. W. Lynn, 2004, *Phys. Rev. Lett.* **93**, 157003.
- Gor'kov, L. P., and E. I. Rashba, 2001, *Phys. Rev. Lett.* **87**, 037004.
- Goto, T., Y. Nemoto, K. Sakai, T. Yamaguchi, M. Akatsu, T. Yanagisawa, H. Hazama, K. Onuki, H. Sugawara, and H. Sato, 2004, *Phys. Rev. B* **69**, 180511.
- Graf, M. J., S.-K. Yip, J. A. Sauls, and D. Rainer, 1996, *Phys. Rev. B* **53**, 15147.
- Graf, T., J. D. Thompson, M. F. Hundley, R. Movshovich, Z. Fisk, D. Mandrus, R. A. Fisher, and N. E. Phillips, 1997, *Phys. Rev. Lett.* **78**, 3769.
- Gratens, X., L. M. Ferreira, Y. Kopelevich, N. F. Oliveira, Jr., P. G. Pagliuso, R. Movshovich, R. R. Urbano, J. L. Sarrao, and J. D. Thompson, 2006, e-print arXiv:cond-mat/0608722.
- Grauel, A., A. Böhm, H. Fischer, C. Geibel, R. Köhler, R. Modler, C. Schank, F. Steglich, G. Weber, T. Komatsubara, and N. Sato, 1992, *Phys. Rev. B* **46**, 5818.
- Grewe, N., and F. Steglich, 1991, *Heavy Fermions*, Handbook of the Physics and Chemistry of Rare Earths Vol. 14 (North-Holland, Amsterdam), Chap. 97.
- Grier, B. H., J. M. Lawrence, V. Murgai, and R. D. Parks, 1984, *Phys. Rev. B* **29**, 2664.
- Griveau, J.-C., K. Gofryk, and J. Rebizant, 2008, *Phys. Rev. B* **77**, 212502.
- Grosche, F. M., P. Argarwa, S. R. Julian, N. J. Wilson, R. K. W. Haselwimmer, S. J. S. Lister, N. D. Mathur, F. V. Carter, S. S. Saxena, and G. G. Lonzarich, 2000, *J. Phys.: Condens. Matter* **12**, L533.
- Grosche, F. M., S. R. Julian, N. D. Mathur, F. V. Carter, and G. G. Lonzarich, 1997, *Physica B* **237-238**, 197.
- Grosche, F. M., S. R. Julian, N. D. Mathur, and G. G. Lonzarich, 1996, *Physica B* **223-224**, 50.
- Grosche, F. M., S. J. S. Lister, F. Carter, S. S. Saxena, R. K. W. Haselwimmer, N. D. Mathur, S. R. Julian, and G. G. Lonzarich, 1997, *Physica B* **239**, 62.
- Gross, F., B. Chandrasekhar, K. Andres, U. Rauchschwalbe, E. Bucher, and B. Lüthi, 1988, *Physica C* **153-155**, 439.
- Gross, F., B. S. Chandrasekhar, D. Einzel, K. Andres, P. K. Hirschfeld, H. R. Ott, J. Beurs, Z. Fisk, and J. L. Smith, 1986, *Z. Phys. B: Condens. Matter* **64**, 175.
- Groß, W., K. Knorr, A. P. Murani, and K. H. J. Buschow, 1980, *Z. Phys. B* **37**, 123.
- Grube, K., S. Drobnik, C. Pfeleiderer, H. v. Löhneysen, E. D. Bauer, and M. B. Maple, 2006, *Phys. Rev. B* **73**, 104503.
- Gruenberg, L. W., and L. Gunther, 1966, *Phys. Rev. Lett.* **16**, 996.
- Haen, P., P. Lejay, B. Chevalier, B. Lloret, J. Etourneau, and P. Hagenmuller, 1985, *Mater. Res. Bull.* **19**, 115.
- Haga, Y., T. Honma, E. Yamamoto, H. Ohkuni, Y. Onuki, M. Ito, and N. Kimura, 1998, *Jpn. J. Appl. Phys., Part 1* **37**, 3604.
- Haga, Y., Y. Inada, H. Harima, K. Oikawa, M. Murakawa, H. Nakawaki, Y. Tokiwa, D. Aoki, H. Shishido, S. Ikeda, N. Watanabe, and Y. Onuki, 2001, *Phys. Rev. B* **63**, 060503.
- Haga, Y., M. Nakashima, R. Settai, S. Ikeda, T. Okubo, S. Araki, T. Kobayashi, N. Tateiwa, and Y. Onuki, 2002, *J. Phys.: Condens. Matter* **14**, L125.
- Haga, Y., H. Sakai, and S. Kambe, 2007, *J. Phys. Soc. Jpn.* **76**, 051012.
- Haga, Y., E. Yamamoto, Y. Inada, D. Aoki, K. Tenya, M. Ikeda, T. Sakakibara, and Y. Onuki, 1996, *J. Phys. Soc. Jpn.* **65**, 3646.
- Hagmusa, I. H., K. Prokes, Y. Echizen, T. Takabatake, T. Fujita, J. C. P. Klaasse, E. Brück, V. Sechovsky, and F. R. de Boer, 2000, *Physica B* **281-282**, 223.
- Hall, D., *et al.*, 2001, *Phys. Rev. B* **64**, 064506.
- Hanawa, M., Y. Muraoka, T. Tayama, T. Sakakibara, J. Yamaura, and Z. Hiroi, 2001, *Phys. Rev. Lett.* **87**, 187001.
- Hanawa, M., J. Yamaura, Y. Muraoka, F. Sakai, and Z. Hiroi, 2002, *J. Phys. Chem. Solids* **63**, 1027.
- Hao, L., K. Iwasa, K. Kuwahara, M. Kohgi, H. Sugawara, Y. Aoki, H. Sato, C. Sekine, C. H. Lee, and H. Harima, 2004, *J. Magn. Magn. Mater.* **272-276**, E271.
- Hardy, F., and A. D. Huxley, 2005, *Phys. Rev. Lett.* **94**, 247006.
- Hardy, F., A. D. Huxley, J. Flouquet, B. Salce, G. Knebel, D. Braithwaite, D. Aoki, M. Uhlarz, and C. Pfeleiderer, 2005, *Physica B* **359-361**, 1111.
- Hardy, F., M. Uhlarz, A. D. Huxley, and C. Pfeleiderer, 2004, unpublished.
- Harrison, N., M. Jaime, and J. A. Mydosh, 2003, *Phys. Rev. Lett.* **90**, 096402.
- Harrison, N., K. H. Kim, M. Jaime, and J. A. Mydosh, 2004, *Physica B* **346-347**, 92.
- Hashimoto, S., T. Yasuda, T. Kubo, H. Shishido, T. Ueda, R. Settai, T. D. Matsuda, Y. Haga, H. Harima, and Y. Onuki, 2004, *J. Phys.: Condens. Matter* **16**, L287.
- Hasselbach, K., J. R. Kirtley, and J. Flouquet, 1993, *Phys. Rev. B* **47**, 509.
- Hasselbach, K., J. R. Kirtley, and P. Lejay, 1992, *Phys. Rev. B* **46**, 5826.
- Hasselbach, K., P. Lejay, and J. Flouquet, 1991, *Phys. Lett. A* **156**, 313.
- Hasselbach, K., L. Taillefer, and J. Flouquet, 1989, *Phys. Rev. Lett.* **63**, 93.
- Hasselbach, K., L. Taillefer, and J. Flouquet, 1990, *Physica B* **165-166**, 357.
- Hassinger, E., D. Aoki, and J. Flouquet, 2008, *J. Phys. Soc. Jpn.* **77**, 073703.
- Hayashi, N., K. Wakabayashi, P. A. Frigeri, and M. Sigrist, 2006a, *Phys. Rev. B* **73**, 092508.
- Hayashi, N., K. Wakabayashi, P. A. Frigeri, and M. Sigrist, 2006b, *Phys. Rev. B* **73**, 024504.
- Hayden, S. M., L. Taillefer, C. Vettier, and J. Flouquet, 1992, *Phys. Rev. B* **46**, 8675.
- Heffner, R. H., D. W. Cooke, Z. Fisk, R. L. Hutson, M. E. Schillaci, J. L. Smith, J. O. Willis, D. E. MacLaughlin, C. Boekema, R. L. Lichti, A. B. Denison, and J. Oostens, 1986, *Phys. Rev. Lett.* **57**, 1255.
- Hegger, H., C. Petrovic, E. G. Moshopoulou, M. F. Hundley, J. L. Sarrao, Z. Fisk, and J. D. Thompson, 2000, *Phys. Rev. Lett.* **84**, 4986.
- Hein, R. A., R. L. Falge, B. T. Matthias, and C. Corenzwit, 1959, *Phys. Rev. Lett.* **2**, 500.
- Herring, C., 1958, *Physica (Amsterdam)* **24**, S184.
- Hertz, J. A., 1976, *Phys. Rev. B* **14**, 1165.
- Hewson, A. C., 1993, *The Kondo Problem to Heavy Fermions* (Cambridge University Press, Cambridge).
- Hiess, A., P. J. Brown, E. Lelièvre-Berna, B. Roessli, N. Bernhoeft, G. H. Lander, N. Aso, and N. K. Sato, 2001, *Phys. Rev. B* **64**, 134413.
- Hiess, A., R. H. Heffner, J. E. Sonier, G. H. Lander, J. L. Smith, and J. C. Cooley, 2002, *Phys. Rev. B* **66**, 064531.
- Hiess, A., A. Stunault, E. Colineau, J. Rebizant, F. Wastin, R. Caciuffo, and G. H. Lander, 2008, *Phys. Rev. Lett.* **100**, 076403.

- Hiroi, M., M. Sera, N. Kobayashi, Y. Haga, E. Yamamoto, and Y. Onuki, 1997, *J. Phys. Soc. Jpn.* **66**, 1595.
- Holmes, A. T., D. Jaccard, and K. Miyake, 2004, *Phys. Rev. B* **69**, 024508.
- Honda, F., M.-A. Measson, Y. Nakano, N. Yoshitani, E. Yamamoto, Y. Haga, T. Takeuchi, H. Yamagami, K. Shimizu, R. Settai, and Y. Onuki, 2008, *J. Phys. Soc. Jpn.* **77**, 043701.
- Honma, T., Y. Haga, E. Yamamoto, N. Metoki, Y. Koike, H. Ohkuni, N. Suzuki, and Y. Onuki, 1999, *J. Phys. Soc. Jpn.* **68**, 338.
- Hori, A., H. Hidaka, H. Kotegawa, T. Kobayashi, T. Akazawa, S. Ikeda, E. Yamamoto, Y. Haga, R. Settai, and Y. Onuki, 2006, *J. Phys. Soc. Jpn.* **75**, 82.
- Horn, S., E. Holland-Moritz, M. Loewenhaupt, F. Steglich, H. Scheuer, A. Benoit, and J. Flouquet, 1981, *Phys. Rev. B* **23**, 3171.
- Hossain, Z., S. Hamashima, K. Umeo, T. Takabatake, C. Geibel, and F. Steglich, 2000, *Phys. Rev. B* **62**, 8950.
- Hotta, T., and K. Ueda, 2003, *Phys. Rev. B* **67**, 104518.
- Houzert, M., and V. P. Mineev, 2006, *Phys. Rev. B* **74**, 144522.
- Houzert, M., and V. P. Mineev, 2007, *Phys. Rev. B* **76**, 224508.
- Hu, R., Y. Lee, J. Hudis, V. F. Mitrovic, and C. Petrovic, 2008, *Phys. Rev. B* **77**, 165129.
- Hu, T., H. Xiao, T. A. Sayles, M. B. Maple, K. Maki, B. Dóra, and C. C. Almasan, 2006, *Phys. Rev. B* **73**, 134509.
- Hussey, N. E., 2002, *Adv. Phys.* **51**, 1685.
- Huxley, A., P. Rodiere, D. M. Paul, N. van Dijk, R. Cubitt, and J. Flouquet, 2000, *Nature (London)* **406**, 160.
- Huxley, A. D., M. A. Measson, K. Izawa, C. D. Dewhurst, R. Cubitt, B. Grenier, H. Sugawara, J. Flouquet, Y. Matsuda, and H. Sato, 2004, *Phys. Rev. Lett.* **93**, 187005.
- Huxley, A. D., V. Mineev, B. Grenier, E. Ressouche, D. Aoki, J. P. Brison, and J. Flouquet, 2004, *Physica C* **403**, 9.
- Huxley, A. D., S. Raymond, and E. Ressouche, 2003, *Phys. Rev. Lett.* **91**, 207201.
- Huxley, A. D., E. Ressouche, B. Grenier, D. Aoki, J. Flouquet, and C. Pfeleiderer, 2003, *J. Phys.: Condens. Matter* **15**, S1945.
- Huxley, A. D., I. Sheikin, E. Ressouche, N. Kernavanois, D. Braithwaite, R. Calemczuk, and J. J. Flouquet, 2001, *Phys. Rev. B* **63**, 144519.
- Huy, N., A. Gasparini, J. Klaase, A. de Visser, S. Sakarya, and N. van Dijk, 2007, e-print arXiv:0704.2116.
- Huy, N. T., D. E. de Nijs, Y. K. Huang, and A. de Visser, 2008, *Phys. Rev. Lett.* **100**, 077002.
- Ikeda, H., and Y. Ohashi, 1998, *Phys. Rev. Lett.* **81**, 3723.
- Ikeda, R., 2006, e-print arXiv:cond-mat/0610796.
- Ikeda, S., H. Shishido, M. Nakashima, R. Settai, D. Aoki, Y. Haga, H. Harima, Y. Aoki, T. Namiki, H. Sato, and Y. Onuki, 2001, *J. Phys. Soc. Jpn.* **70**, 2248.
- Inada, Y., H. Yamagami, Y. Haga, K. Sakurai, Y. Tokiwa, T. Honma, E. Yamamoto, Y. Onuki, and T. Yanagisawa, 1999, *J. Phys. Soc. Jpn.* **68**, 3643.
- Ishida, K., Y. Kawasaki, K. Tabuchi, K. Kashima, Y. Kitaoka, K. Asayama, C. Geibel, and F. Steglich, 1999, *Phys. Rev. Lett.* **82**, 5353.
- Ishida, K., D. Ozaki, T. Kamatsuka, H. Tou, M. Kyogaku, Y. Kitaoka, N. Tateiwa, N. K. Sato, N. Aso, C. Geibel, and F. Steglich, 2002, *Phys. Rev. Lett.* **89**, 037002.
- Ishiguro, A., A. Sawada, Y. Inada, J. Kimura, M. Suzuki, N. Sato, and T. Komatsubara, 1995, *J. Phys. Soc. Jpn.* **64**, 378.
- Ishikawa, I., and O. Fischer, 1977, *Solid State Commun.* **23**, 37.
- Ito, T., H. Kumigashira, S. Souma, T. Takahashi, Y. Haga, and Y. Onuki, 2002, *J. Phys. Soc. Jpn.* **71**, 265.
- Iwasa, K., Y. Watanabe, K. Kuwahara, M. Kohgi, H. Sugawara, T. D. Matsuda, Y. Aoki, and H. Sato, 2002, *Physica B* **312-313**, 834.
- Izawa, K., K. Behnia, Y. Matsuda, H. Shishido, R. Settai, Y. Onuki, and J. Flouquet, 2007, *Phys. Rev. Lett.* **99**, 147005.
- Izawa, K., Y. Kasahara, Y. Matsuda, K. Behnia, T. Yasuda, R. Settai, and Y. Onuki, 2005, *Phys. Rev. Lett.* **94**, 197002.
- Izawa, K., Y. Nakajima, J. Goryo, Y. Matsuda, S. Osaki, H. Sugawara, H. Sato, P. Thalmeier, and K. Maki, 2003, *Phys. Rev. Lett.* **90**, 117001.
- Izawa, K., H. Yamaguchi, Y. Matsuda, H. Shishido, R. Settai, and Y. Onuki, 2001, *Phys. Rev. Lett.* **87**, 057002.
- Jaccard, D., K. Behnia, and J. Sierro, 1992, *Phys. Lett. A* **163**, 475.
- Jaccard, D., A. T. Holmes, G. Behr, Y. Inada, and Y. Onuki, 2002, *Phys. Lett. A* **299**, 282.
- Jaccarino, V., and M. Peter, 1962, *Phys. Rev. Lett.* **9**, 290.
- Javorský, P., E. Colineau, F. Wastin, F. Jutier, J.-C. Griveau, P. Boulet, R. Jardin, and J. Rebizant, 2007, *Phys. Rev. B* **75**, 184501.
- Jeffries, J. R., N. P. Butch, B. T. Yukich, and M. B. Maple, 2007, *Phys. Rev. Lett.* **99**, 217207.
- Jo, Y. J., L. Balicas, C. Capan, K. Behnia, P. Lejay, J. Flouquet, J. A. Mydosh, and P. Schlottmann, 2007, *Phys. Rev. Lett.* **98**, 166404.
- Jourdan, M., M. Huth, and H. Adrian, 1999, *Nature (London)* **398**, 47.
- Jourdan, M., A. Zakharov, M. Foerster, and H. Adrian, 2004, *Phys. Rev. Lett.* **93**, 097001.
- Joyce, J. J., J. M. Wills, T. Durakiewicz, M. T. Butterfield, E. Guzewicz, J. L. Sarrao, L. A. Morales, A. J. Arko, and O. Eriksson, 2003, *Phys. Rev. Lett.* **91**, 176401.
- Joynt, R., and L. Taillefer, 2002, *Rev. Mod. Phys.* **74**, 235.
- Julian, S. R., C. Pfeleiderer, F. M. Grosche, N. D. Mathur, G. J. McMullan, A. J. Diver, I. R. Walker, and G. G. Lonzarich, 1996, *J. Phys.: Condens. Matter* **8**, 9675.
- Jutier, F., J. C. Griveau, E. Colineau, J. Rebizant, P. Boulet, and F. Wastin, 2005, *Physica B* **359-361**, 1078.
- Jutier, F., J. Griveau, E. Colineau, F. Wastin, J. Rebizant, P. Boulet, and E. Simon, 2006, *J. Phys. Soc. Jpn.* **75**, 47.
- Jutier, F., G. A. Ummarino, J.-C. Griveau, F. Wastin, E. Colineau, J. Rebizant, N. Magnani, and R. Caciuffo, 2008, *Phys. Rev. B* **77**, 024521.
- Kaczorowski, D., A. P. Pikul, D. Gnida, and V. H. Tran, 2009, *Phys. Rev. Lett.* **103**, 027003.
- Kadowaki, K., and S. B. Woods, 1986, *Solid State Commun.* **58**, 507.
- Kakuyanagi, K., M. Saitoh, K. Kumagai, S. Takashima, M. No-hara, H. Takagi, and Y. Matsuda, 2005, *Phys. Rev. Lett.* **94**, 047602.
- Kaneko, K., N. Metoki, T. D. Matsuda, and M. Kohgi, 2006, *J. Phys. Soc. Jpn.* **75**, 034701.
- Kaneko, K., N. Metoki, R. Shiina, T. D. Matsuda, M. Kohgi, K. Kuwahara, and N. Bernhoeft, 2007, *Phys. Rev. B* **75**, 094408.
- Karchev, N., 2003, *Phys. Rev. B* **67**, 054416.
- Kasahara, S., K. Hirata, H. Takeya, T. Tamegai, H. Sugawara, D. Kikuchi, and H. Sato, 2008, *J. Phys. Soc. Jpn.* **77**, 327.
- Kasahara, Y., T. Iwasawa, H. Shishido, T. Shibauchi, K. Behnia, Y. Haga, T. D. Matsuda, Y. Onuki, M. Sigrist, and Y. Matsuda, 2007, *Phys. Rev. Lett.* **99**, 116402.
- Kasahara, Y., Y. Nakajima, K. Izawa, Y. Matsuda, K. Behnia, H. Shishido, R. Settai, and Y. Onuki, 2005, *Phys. Rev. B* **72**, 214515.

- Kaur, R. P., D. F. Agterberg, and M. Sigrist, 2005, *Phys. Rev. Lett.* **94**, 137002.
- Kawai, T., H. Muranaka, T. Endo, N. D. Dong, Y. Doi, S. Ikeda, T. D. Matsuda, Y. Haga, H. Harima, R. Settai, and Y. Onuki, 2008, *J. Phys. Soc. Jpn.* **77**, 064717.
- Kawai, T., H. Muranaka, M.-A. Measson, T. Shimoda, Y. Doi, T. D. Matsuda, Y. Haga, G. Knebel, G. Lapertot, D. Aoki, J. Flouquet, T. Takeuchi, R. Settai, and Y. Onuki, 2008, *J. Phys. Soc. Jpn.* **77**, 064716.
- Kawarazaki, S., M. Sato, Y. Miyako, N. Chigusa, K. Watanabe, N. Metoki, Y. Koike, and M. Nishi, 2000, *Phys. Rev. B* **61**, 4167.
- Kawasaki, S., T. Mito, Y. Kawasaki, G.-q. Zheng, Y. Kitaoka, H. Shishido, S. Araki, R. Settai, and Y. Onuki, 2002, *Phys. Rev. B* **66**, 054521.
- Kawasaki, S., T. Mito, G.-q. Zheng, C. Thessieu, Y. Kawasaki, K. Ishida, Y. Kitaoka, T. Muramatsu, T. C. Kobayashi, D. Aoki, S. Araki, Y. Haga, R. Settai, and Y. Onuki, 2001, *Phys. Rev. B* **65**, 020504.
- Kawasaki, S., M. Yashima, Y. Mugino, H. Mukuda, Y. Kitaoka, H. Shishido, and Y. Onuki, 2006, *Phys. Rev. Lett.* **96**, 147001.
- Kawasaki, S., G. qing Zheng, H. Kan, Y. Kitaoka, H. Shishido, and Y. Onuki, 2005, *Phys. Rev. Lett.* **94**, 037007.
- Kawasaki, Y., K. Ishida, S. Kawasaki, T. Mito, G. q. Zheng, Y. Kitaoka, C. Geibel, and F. Steglich, 2004, *J. Phys. Soc. Jpn.* **73**, 194.
- Kawasaki, Y., S. Kawasaki, M. Yashima, T. Mito, G. q. Zheng, Y. Kitaoka, H. Shishido, R. Settai, Y. Haga, and Y. Onuki, 2003, *J. Phys. Soc. Jpn.* **72**, 2308.
- Kernavonnois, N., B. Grenier, A. Huxley, E. Ressouche, J. P. Sanchez, and J. Flouquet, 2001, *Phys. Rev. B* **64**, 174509.
- Kernavonnois, N., J.-X. Boucherle, P. D. de Réotier, F. Givord, E. Lelievre-Barna, E. Ressouche, A. Rogalev, J. Sanchez, N. Sato, and A. Yaouanc, 2000, *J. Phys.: Condens. Matter* **12**, 7857.
- Kernavonnois, N., S. Raymond, E. Ressouche, B. Grenier, J. Flouquet, and P. Lejay, 2005, *Phys. Rev. B* **71**, 064404.
- Ketterson, J. B., and S. N. Song, 1999, *Superconductivity* (Cambridge University Press, Cambridge).
- Kim, J. S., J. Alwood, G. R. Stewart, J. L. Sarrao, and J. D. Thompson, 2001, *Phys. Rev. B* **64**, 134524.
- Kim, J. S., D. Hall, P. Kumar, and G. R. Stewart, 2003, *Phys. Rev. B* **67**, 014404.
- Kim, J. S., N. K. Sato, and G. R. Stewart, 2001, *J. Low Temp. Phys.* **124**, 527.
- Kim, K. H., N. Harrison, H. Amitsuka, G. A. Jorge, M. Jaime, and J. A. Mydosh, 2004, *Phys. Rev. Lett.* **93**, 206402.
- Kim, K. H., N. Harrison, M. Jaime, G. S. Boebinger, and J. A. Mydosh, 2003, *Phys. Rev. Lett.* **91**, 256401.
- Kimura, N., K. Ito, H. Aoki, S. Uji, and T. Terashima, 2007, *Phys. Rev. Lett.* **98**, 197001.
- Kimura, N., K. Ito, K. Saitoh, Y. Umeda, H. Aoki, and T. Terashima, 2005, *Phys. Rev. Lett.* **95**, 247004.
- Kimura, N., Y. Muro, and H. Aoki, 2007, *J. Phys. Soc. Jpn.* **76**, 051010.
- Kimura, N., R. Settai, Y. Onuki, H. Toshima, E. Yamamoto, K. Mezawa, H. Aoki, and H. Harima, 1995, *J. Phys. Soc. Jpn.* **64**, 3881.
- Kimura, N., Y. Umeda, T. Asai, T. Terashima, and H. Aoki, 2001, *Physica B* **294-295**, 280.
- Kirkpatrick, T. R., and D. Belitz, 2003, *Phys. Rev. B* **67**, 024515.
- Kirkpatrick, T. R., and D. Belitz, 2004, *Phys. Rev. Lett.* **92**, 037001.
- Kirkpatrick, T. R., D. Belitz, T. Vojta, and R. Narayanan, 2001, *Phys. Rev. Lett.* **87**, 127003.
- Kiss, A., and P. Fazekas, 2005, *Phys. Rev. B* **71**, 054415.
- Kita, H., A. Dönni, Y. Endoh, K. Kakurai, N. Sato, and T. Komatsubara, 1994, *J. Phys. Soc. Jpn.* **63**, 726.
- Klamut, P. W., B. Dabrowski, S. Kolesnik, M. Maxwell, and J. Mais, 2001, *Phys. Rev. B* **63**, 224512.
- Klein, U., D. Rainer, and H. Shimahara, 2000, *J. Low Temp. Phys.* **118**, 91.
- Knafo, W., S. Raymond, B. Fåk, G. Lapertot, P. C. Canfield, and J. Flouquet, 2003, *J. Phys.: Condens. Matter* **15**, 3741.
- Knebel, G., D. Aoki, D. Braithwaite, B. Salce, and J. Flouquet, 2006, *Phys. Rev. B* **74**, 020501.
- Knebel, G., D. Aoki, J.-P. Brison, and J. Flouquet, 2008, *J. Phys. Soc. Jpn.* **77**, 114704.
- Knebel, G., D. Braithwaite, P. C. Canfield, G. Lapertot, and J. Flouquet, 2001, *Phys. Rev. B* **65**, 024425.
- Knebel, G., M.-A. Méasson, B. Salce, D. Aoki, D. Braithwaite, J. P. Brison, and J. Flouquet, 2004, *J. Phys.: Condens. Matter* **16**, 8905.
- Knöpfle, K., A. Mavromaras, L. M. Sandratskii, and J. Kübler, 1996, *J. Phys.: Condens. Matter* **8**, 901.
- Knopp, G., A. Loidl, K. Knorr, L. Pawlak, M. Duczmal, R. Caspary, U. Gottwick, H. Spille, F. Steglich, and A. P. Murani, 1989, *Z. Phys. B: Condens. Matter* **77**, 95.
- Kobayashi, T., A. Hori, S. Fukushima, H. Hidaka, H. Kotegawa, T. Akezawa, K. Takeda, Y. Ohishi, and E. Yamamoto, 2007, *J. Phys. Soc. Jpn.* **76**, 051007.
- Kohgi, M., K. Iwasa, M. Nakajima, N. Metoki, S. Araki, N. Bernhoeft, J.-M. Mignot, A. Gukasov, H. Sato, Y. Aoki, and H. Sugawara, 2003, *J. Phys. Soc. Jpn.* **72**, 1002.
- Kohori, Y., K. Matsuda, and T. Kohara, 1995, *Solid State Commun.* **95**, 121.
- Kohori, Y., K. Matsuda, and T. Kohara, 1996, *J. Phys. Soc. Jpn.* **65**, 1083.
- Kohori, Y., Y. Yamato, Y. Iwamoto, T. Kohara, E. D. Bauer, M. B. Maple, and J. L. Sarrao, 2001, *Phys. Rev. B* **64**, 134526.
- Koitzsch, A., S. V. Borisenko, D. Inosov, J. Geck, V. B. Zaboltnyy, H. Shiozawa, M. Knupfer, J. Fink, B. Büchner, E. D. Bauer, J. L. Sarrao, and R. Follath, 2008, *Phys. Rev. B* **77**, 155128.
- Kotegawa, H., A. Harada, S. Kawasaki, Y. Kawasaki, Y. Kitaoka, Y. Haga, E. Yamamoto, Y. Onuki, K. M. Itoh, E. E. Haller, and H. Harima, 2005, *J. Phys. Soc. Jpn.* **74**, 705.
- Kotegawa, H., K. Takeda, T. Miyoshi, S. Fukushima, H. Hidaka, T. C. Kobayashi, T. Akazawa, Y. Ohishi, M. Nakashima, A. Thamizhavel, R. Settai, and Y. Onuki, 2006, *J. Phys. Soc. Jpn.* **75**, 044713.
- Kotegawa, H., M. Yogi, Y. Imamura, Y. Kawasaki, G. Q. Zheng, Y. Kitaoka, S. Ohsaki, H. Sugawara, and Y. A. H. Sato, 2003, *Phys. Rev. Lett.* **90**, 027001.
- Krimmel, A., P. Fischer, B. Roessli, H. Maletta, C. Geibel, C. Schank, A. Grauel, A. Loidl, and F. Steglich, 1992, *Z. Phys. B: Condens. Matter* **86**, 161.
- Krimmel, A., and A. Loidl, 1997, *Physica B* **234-236**, 877.
- Krimmel, A., A. Loidl, R. Eccleston, C. Geibel, and F. Steglich, 1996, *J. Phys.: Condens. Matter* **8**, 1677.
- Krimmel, A., A. Loidl, P. Fischer, B. Roessli, A. Dönni, H. Kita, N. Sato, Y. Endoh, T. Komatsubara, C. Geibel, and F. Steglich, 1993, *Solid State Commun.* **87**, 829.
- Krimmel, A., A. Loidl, K. Knorr, B. Buschinger, C. Geibel, C. Wassilew, and M. Hanfland, 2000, *J. Phys.: Condens. Matter*

- 12**, 8801.
- Krimmel, A., A. Loidl, H. Schober, and P. C. Canfield, 1997, *Phys. Rev. B* **55**, 6416.
- Kromer, F., R. Helfrich, M. Lang, F. Steglich, C. Langhammer, A. Bach, T. Michels, J. S. Kim, and G. R. Stewart, 1998, *Phys. Rev. Lett.* **81**, 4476.
- Kromer, F., M. Lang, N. Oeschler, P. Hinze, C. Langhammer, F. Steglich, J. S. Kim, and G. R. Stewart, 2000, *Phys. Rev. B* **62**, 12477.
- Krupka, M. C., A. L. Giorgi, N. H. Krikorian, and E. G. Szklarz, 1969, *J. Less-Common Met.* **17**, 91.
- Kübert, C., and P. J. Hirschfeld, 1998, *Phys. Rev. Lett.* **80**, 4963.
- Kumagai, K., M. Saitoh, T. Oyaizu, Y. Furukawa, S. Takashima, M. Nohara, H. Takagi, and Y. Matsuda, 2006, *Phys. Rev. Lett.* **97**, 227002.
- Kumar, P., and P. Wölffe, 1987, *Phys. Rev. Lett.* **59**, 1954.
- Kuwahara, K., K. Iwasa, M. Kohgi, K. Kaneko, N. Metoki, S. Raymond, M.-A. Méasson, J. Flouquet, H. Sugawara, Y. Aoki, and H. Sato, 2005, *Phys. Rev. Lett.* **95**, 107003.
- Kuwahara, K., H. Sagayama, K. Iwasa, M. Kohgi, Y. Haga, Y. Onuki, K. Kakurai, M. Nishi, K. Nakajima, N. Aso, and Y. Uwatoko, 2002, *Physica B* **312-313**, 106.
- Kwok, W. K., L. E. DeLong, G. W. Crabtree, D. G. Hinks, and R. Joynt, 1990, *Phys. Rev. B* **41**, 11649.
- Kyogaku, M., Y. Kitaoka, K. Asayama, C. Geibel, C. Schank, and F. Steglich, 1993, *J. Phys. Soc. Jpn.* **62**, 4016.
- Lake, B., *et al.*, 2002, *Nature (London)* **415**, 299.
- Lambert, S. E., Y. Dalichaouch, M. B. Maple, J. L. Smith, and Z. Fisk, 1986, *Phys. Rev. Lett.* **57**, 1619.
- Lander, G. H., E. S. Fischer, and S. D. Bader, 1994, *Adv. Phys.* **43**, 1.
- Lander, G. H., S. M. Shapiro, C. Vettier, and A. J. Dianoux, 1992, *Phys. Rev. B* **46**, 5387.
- Lang, M., R. Modler, U. Ahlheim, R. Helfrich, P. Reinder, F. Steglich, W. Assmus, W. Sun, G. Bruls, D. Weber, and B. Lüthi, 1991, *Phys. Scr., T* **T39**, 135.
- Larkin, A. I., and Y. N. Ovchinnikov, 1965, *Sov. Phys. JETP* **20**, 762.
- Laver, M., E. M. Forgan, S. P. Brown, D. Charalambous, D. Fort, C. Powell, S. Ramos, R. J. Lycett, D. K. Christen, J. Kohlbrechter, C. D. Dewhurst, and R. Cubitt, 2006, *Phys. Rev. Lett.* **96**, 167002.
- Lawrence, J., 1979, *Phys. Rev. B* **20**, 3770.
- Lawrence, J. M., and S. M. Shapiro, 1980, *Phys. Rev. B* **22**, 4379.
- Layzer, A., and D. Fay, 1971, *Int. J. Magn.* **1**, 135.
- Lee, C. H., M. Matsuhata, A. Yamamoto, T. Ohta, H. Takazawa, K. Ueno, C. Sekine, I. Shirota, and T. Hirayama, 2001, *J. Phys.: Condens. Matter* **13**, L45.
- Lee, P. A., 1993, *Phys. Rev. Lett.* **71**, 1887.
- Leggett, A. J., 1975, *Rev. Mod. Phys.* **47**, 331.
- Lengyel, E., J. Sarrao, G. Sparn, F. Steglich, and J. Thompson, 2004, *J. Magn. Magn. Mater.* **272-276**, 52.
- Lévy, F., I. Sheikin, B. Grenier, and A. D. Huxley, 2005, *Science* **309**, 1343.
- Lévy, F., I. Sheikin, and A. Huxley, 2007, *Nat. Phys.* **3**, 460.
- Lhotel, E., C. Paulsen, and A. D. Huxley, 2003, *Phys. Rev. Lett.* **91**, 209701.
- Link, P., D. Jaccard, C. Geibel, C. Wassilew, and F. Steglich, 1995, *J. Phys.: Condens. Matter* **7**, 373.
- Llobet, A., J. S. Gardner, E. G. Moshopoulou, J.-M. Mignot, M. Nicklas, W. Bao, N. O. Moreno, P. G. Pagliuso, I. N. Goncharenko, J. L. Sarrao, and J. D. Thompson, 2004, *Phys. Rev. B* **69**, 024403.
- Lonzarich, G. G., 1980, *Fermi Surface Studies of Ground State and Magnetic Excitations in Itinerant Electron Ferromagnets* (Cambridge University Press, Cambridge), pp. 224-277.
- Lonzarich, G. G., 1987, *J. Magn. Magn. Mater.* **70**, 445.
- Lonzarich, G. G., 1988, *J. Magn. Magn. Mater.* **76-77**, 1.
- Lonzarich, G. G., 1997, *The Magnetic Electron* (Cambridge University Press, Cambridge).
- Lonzarich, G. G., and L. Taillefer, 1985, *J. Phys. C* **18**, 4339.
- Luk'yanchuk, I. A., and V. P. Mineev, 1989, *Sov. Phys. JETP* **68**, 402.
- Lussier, B., B. Ellman, and L. Taillefer, 1994, *Phys. Rev. Lett.* **73**, 3294.
- Lussier, J. G., M. Mao, A. Schröder, J. D. Garrett, B. D. Gaulin, S. M. Shapiro, and W. J. L. Buyers, 1997, *Phys. Rev. B* **56**, 11749.
- Lüthi, B., B. Wolf, D. Finsterbusch, and G. Bruls, 1995, *Physica B* **204**, 228.
- Lüthi, B., B. Wolf, P. Thalmeier, M. Günther, W. Sixl, and G. Bruls, 1993, *Phys. Lett. A* **175**, 237.
- Machida, K., and H. Nakanishi, 1984, *Phys. Rev. B* **30**, 122.
- Machida, K., and T. Ohmi, 2001, *Phys. Rev. Lett.* **86**, 850.
- Mackenzie, A. P., R. K. W. Haselwimmer, A. W. Tyler, G. G. Lonzarich, Y. Mori, S. Nishizaki, and Y. Maeno, 1998, *Phys. Rev. Lett.* **80**, 161.
- MacLaughlin, D. E., M. D. Lan, C. Tien, J. M. Moore, G. C. W. H. R. Ott, Z. Fisk, and J. L. Smith, 1987, *J. Magn. Magn. Mater.* **63-64**, 455.
- McMillan, W. L., 1968, *Phys. Rev.* **167**, 331.
- Maehira, T., T. Hotta, K. Ueda, and A. Hasegawa, 2003, *J. Phys. Soc. Jpn.* **72**, 854.
- Majumdar, S., G. Balakrishnan, M. R. Lees, D. M. Paul, and G. J. McIntyre, 2002, *Phys. Rev. B* **66**, 212502.
- Makhlin, Y., and V. P. Mineev, 1992, *J. Low Temp. Phys.* **86**, 49.
- Maki, K., B. Dora, B. Korin-Hamzic, M. Basletic, A. Virostek, and M. V. Kartsovnik, 2002, *J. Phys. IV* **12**, 49.
- Malinowski, A., M. F. Hundley, C. Capan, F. Ronning, R. Movshovich, N. O. Moreno, J. L. Sarrao, and J. D. Thompson, 2005, *Phys. Rev. B* **72**, 184506.
- Maple, M. B., 1969, Ph.D. thesis, University of California in San Diego.
- Maple, M. B., 1970, *Solid State Commun.* **8**, 1915.
- Maple, M. B., 1976, *Appl. Phys.* **9**, 179.
- Maple, M. B., 1995, *Physica B* **215**, 110.
- Maple, M. B., 2005, *J. Phys. Soc. Jpn.* **74**, 222.
- Maple, M. B., J. W. Chen, Y. Dalichaouch, T. Kohara, C. Rossel, M. S. Torikachvili, M. W. McElfresh, and J. D. Thompson, 1986, *Phys. Rev. Lett.* **56**, 185.
- Maple, M. B., J. W. Chen, S. E. Lambert, Z. Fisk, J. L. Smith, H. R. Ott, J. S. Brooks, and M. J. Naughton, 1985, *Phys. Rev. Lett.* **54**, 477.
- Maple, M. B., W. Fertig, A. Mota, L. DeLong, D. Wohlleben, and R. Fitzgerald, 1972, *Solid State Commun.* **11**, 829.
- Maple, M. B., and Ø. Fischer, 1982, Eds., *Superconductivity in Ternary Compounds II*, Topics in Current Physics Vol. 34 (Springer-Verlag, Berlin).
- Maple, M. B., and Z. Fisk, 1968, Proceedings of the 11th International Conference on Low Temperature Physics, San Andrews (unpublished), p. 1288.
- Maple, M. B., Z. Henkie, R. Baumbach, T. Sayles, N. Butch, P.-C. Ho, T. Yanagisawa, W. Yuhasz, R. Wawryk, T. Cichorek, and A. Peitraszko, 2008, *J. Phys. Soc. Jpn.* **77**, 7.
- Maple, M. B., P.-C. Ho, V. S. Zapf, N. A. Frederick, E. D.

- Bauer, W. M., Yuhasz, F. M., Woodward, and J. W. Lynn, 2002, *J. Phys. Soc. Jpn. Suppl.* **71**, 23.
- Martin, C., C. C. Agosta, S. W. Tozer, H. A. Radovan, E. C. Palm, T. P. Murphy, and J. L. Sarrao, 2005, *Phys. Rev. B* **71**, 020503.
- Martisovits, V., G. Zaránd, and D. L. Cox, 2000, *Phys. Rev. Lett.* **84**, 5872.
- Mason, T. E., W. J. L. Buyers, T. Petersen, A. A. Menovsky, and J. D. Garrett, 1995, *J. Phys.: Condens. Matter* **7**, 5089.
- Mason, T. E., B. D. Gaulin, J. D. Garrett, Z. Tun, W. J. L. Buyers, and E. D. Isaacs, 1990, *Phys. Rev. Lett.* **65**, 3189.
- Mathur, N. D., F. M. Grosche, S. R. Julian, I. R. Walker, D. M. Freye, R. K. W. Haselwimmer, and G. G. Lonzarich, 1998, *Nature (London)* **394**, 39.
- Matsuda, K., Y. Kohori, and T. Kohara, 1996, *J. Phys. Soc. Jpn.* **65**, 679.
- Matsuda, K., Y. Kohori, T. Kohara, H. Amitsuka, K. Kuwahara, and T. Matsumoto, 2003, *J. Phys.: Condens. Matter* **15**, 2363.
- Matsuda, K., Y. Kohori, T. Kohara, K. Kuwahara, and H. Amitsuka, 2001, *Phys. Rev. Lett.* **87**, 087203.
- Matsuda, T. D., D. Aoki, S. Ikeda, E. Yamamoto, Y. Haga, H. Ohkuni, R. Settai, and Y. Onuki, 2008, *J. Phys. Soc. Jpn.* **77**, 362.
- Matsuda, Y., and H. Shimahara, 2007, *J. Phys. Soc. Jpn.* **76**, 051005.
- Matsui, H., T. Goto, N. Sato, and T. Komatsubara, 1994, *Physica B* **119-200**, 140.
- Matthias, B. T., H. Suhl, and E. Corenzwit, 1958a, *Phys. Rev. Lett.* **1**, 449.
- Matthias, B. T., H. Suhl, and E. Corenzwit, 1958b, *Phys. Rev. Lett.* **1**, 92.
- Mayer, H. M., U. Rauchschwalbe, C. D. Bredl, F. Steglich, H. Rietschel, H. Schmidt, H. Wühl, and J. Beuers, 1986, *Phys. Rev. B* **33**, 3168.
- Mazin, I. I., D. A. Papaconstantopoulos, and M. J. Mehl, 2002, *Phys. Rev. B* **65**, 100511.
- Mazumdar, C., and R. Nagarajan, 2005, *Curr. Sci.* **88**, 83.
- Mazumdar, C., R. Nagarajan, S. K. Dhar, L. C. Gupta, R. Vijayaraghavan, and B. D. Padalia, 1992, *Phys. Rev. B* **46**, 9009.
- McCollam, A., R. Daou, S. R. Julian, C. Bergemann, J. Flouquet, and D. Aoki, 2005, *Physica B* **359-361**, 1.
- McDonough, J., and A. D. Huxley, 1995, *Rev. Sci. Instrum.* **66**, 1105.
- McElfresh, M. W., M. B. Maple, J. O. Willis, Z. Fisk, J. L. Smith, and J. D. Thompson, 1990, *Phys. Rev. B* **42**, 6062.
- McElfresh, M. W., J. D. Thompson, J. O. Willis, M. B. Maple, T. Kohara, and M. S. Torikachvili, 1987, *Phys. Rev. B* **35**, 43.
- McHale, P., P. Fulde, and P. Thalmeier, 2004, *Phys. Rev. B* **70**, 014513.
- McMullan, G. J., P. M. C. Rourke, M. R. Norman, A. D. Huxley, N. Doiron-Leyraud, J. Flouquet, G. G. Lonzarich, A. McCollam, and S. R. Julian, 2008, *New J. Phys.* **10**, 053029.
- Measson, M. A., D. Braithwaite, J. Flouquet, G. Seyfarth, J. P. Brison, E. Lhotel, C. Paulsen, H. Sugawara, and H. Sato, 2004, *Phys. Rev. B* **70**, 064516.
- Méasson, M.-A., D. Braithwaite, G. Lapertot, J.-P. Brison, J. Flouquet, P. Bordet, H. Sugawara, and P. C. Canfield, 2008, *Phys. Rev. B* **77**, 134517.
- Meissner, W., and R. Ochsenfeld, 1933, *Naturwiss.* **21**, 787.
- Metoki, N., Y. Haga, Y. Koike, and Y. Onuki, 1998, *Phys. Rev. Lett.* **80**, 5417.
- Metoki, N., K. Kaneko, T. D. Matsuda, A. Galatanu, T. Takeuchi, S. Hashimoto, T. Ueda, R. Settai, Y. Onuki, and N. Bernhoeft, 2004, *J. Phys.: Condens. Matter* **16**, L207.
- Miclea, C. F., M. Nicklas, D. Parker, K. Maki, J. L. Sarrao, J. D. Thompson, G. Sparn, and F. Steglich, 2006, *Phys. Rev. Lett.* **96**, 117001.
- Mihalik, M., F. E. Kayzel, T. Yoshida, K. Kuwahara, H. Amitsuka, T. Sakakibara, A. A. Menovsky, J. A. Mydosh, and J. J. M. Franse, 1997, *Physica B* **230-232**, 364.
- Millis, A. J., 1993, *Phys. Rev. B* **48**, 7183.
- Mineev, V., 2006, *C. R. Phys.* **7**, 35.
- Mineev, V. P., 2002, *Phys. Rev. B* **66**, 134504.
- Mineev, V. P., 2004, *Int. J. Mod. Phys. B* **18**, 2963.
- Mineev, V. P., 2005, *Phys. Rev. B* **71**, 012509.
- Mineev, V. P., and T. Champel, 2004, *Phys. Rev. B* **69**, 144521.
- Mineev, V. P., and K. V. Samokhin, 1999, *Introduction to Unconventional Superconductivity* (Gordon and Breach, Amsterdam).
- Mineev, V. P., and M. E. Zhitomirsky, 2005, *Phys. Rev. B* **72**, 014432.
- Misorek, H., J. Mucha, R. Troc, and B. Coqblin, 2005, *J. Phys.: Condens. Matter* **17**, 679.
- Mito, T., S. Kawasaki, Y. Kawasaki, G. q. Zheng, Y. Kitaoka, D. Aoki, Y. Haga, and Y. Onuki, 2003, *Phys. Rev. Lett.* **90**, 077004.
- Mito, T., S. Kawasaki, G.-q. Zheng, Y. Kawasaki, K. Ishida, Y. Kitaoka, D. Aoki, Y. Haga, and Y. Onuki, 2001, *Phys. Rev. B* **63**, 220507.
- Mitrović, V. F., M. Horvatić, C. Berthier, G. Knebel, G. Lapertot, and J. Flouquet, 2006, *Phys. Rev. Lett.* **97**, 117002.
- Miyake, A., K. Shimizu, C. Sekine, K. Kihou, and I. Shirovani, 2004, *J. Phys. Soc. Jpn.* **73**, 2370.
- Miyake, K., and N. K. Sato, 2001, *Phys. Rev. B* **63**, 052508.
- Modler, R., K. Gloos, H. Schimanski, C. Geibel, M. Günther, G. Bruls, B. Lüthi, T. Komatsubara, N. Sato, C. Schank, and F. Steglich, 1993, *Physica B* **186-188**, 294.
- Moncton, D. E., D. B. McWhan, J. Eckert, G. Shirane, and W. Thomlinson, 1977, *Phys. Rev. Lett.* **39**, 1164.
- Monthoux, P., and G. G. Lonzarich, 2001, *Phys. Rev. B* **63**, 054529.
- Monthoux, P., and G. G. Lonzarich, 2002, *Phys. Rev. B* **66**, 224504.
- Monthoux, P., and G. G. Lonzarich, 2004, *Phys. Rev. B* **69**, 064517.
- Monthoux, P., D. Pines, and G. G. Lonzarich, 2007, *Nature (London)* **450**, 1177.
- Moore, K. T., and G. van der Laan, 2009, *Rev. Mod. Phys.* **81**, 235.
- Mora, C., and R. Combescot, 2004, *Europhys. Lett.* **66**, 833.
- Mora, C., and R. Combescot, 2005, *Phys. Rev. B* **71**, 214504.
- Morel, P., and P. W. Anderson, 1962, *Phys. Rev.* **125**, 1263.
- Morin, P., C. Vettier, J. Flouquet, M. Konczykowski, Y. Lassailly, J.-M. Mignot, and U. Welp, 1988, *J. Low Temp. Phys.* **70**, 377.
- Moriya, T., 1963, *Weak Ferromagnetism*, Magnetism Vol. 1 (Academic, New York), Chap. 3.
- Moriya, T., 1985, *Spin Fluctuations in Itinerant Electron Magnetism*, Solid-State Sciences Vol. 56 (Springer, Berlin).
- Morris, G. D., R. H. Heffner, N. O. Moreno, P. G. Pagliuso, J. L. Sarrao, S. R. Dunsiger, G. J. Nieuwenhuys, D. E. MacLaughlin, and O. O. Bernal, 2004, *Phys. Rev. B* **69**, 214415.
- Motoyama, G., K. Maeda, and Y. Oda, 2008, *J. Phys. Soc. Jpn.* **77**, 044710.

- Motoyama, G., Y. Yamaguchi, K. Maeda, A. Sumiyama, and Y. Oda, 2008, *J. Phys. Soc. Jpn.* **77**, 075004.
- Movshovich, R., T. Graf, J. D. Thompson, J. L. Smith, and Z. Fisk, 1996, *Phys. Rev. B* **53**, 8241.
- Movshovich, R., M. Jaime, J. D. Thompson, C. Petrovic, Z. Fisk, P. G. Pagliuso, and J. L. Sarrao, 2001, *Phys. Rev. Lett.* **86**, 5152.
- Mühlbauer, S., C. Pfeleiderer, T. Böni, M. Laver, E. M. Forgan, D. Fort, U. Keiderling, and G. Behr, 2009, *Phys. Rev. Lett.* **102**, 136408.
- Mukuda, H., T. Fuji, T. Ohara, A. Harada, M. Yashima, Y. Kitaoka, Y. Okuda, R. Settai, and Y. Onuki, 2008, *Phys. Rev. Lett.* **100**, 107003.
- Müller, V., Ch. Roth, D. Maurer, E. W. Scheidt, K. Lüders, E. Bucher, and H. E. Bömmel, 1987, *Phys. Rev. Lett.* **58**, 1224.
- Müller-Hartmann, E., and J. Zittartz, 1971, *Phys. Rev. Lett.* **26**, 428.
- Muramatsu, T., N. Tateiwa, T. C. Kobayashi, K. Shimizu, K. A. D. Aoki, H. Shishido, Y. Haga, and Y. Onuki, 2001, *J. Phys. Soc. Jpn.* **70**, 3362.
- Murani, A. P., A. D. Taylor, R. Osborn, and Z. A. Bowden, 1993, *Phys. Rev. B* **48**, 10606.
- Muro, Y., 2000, Ph.D. thesis, Tokyo University of Science, Tokyo
- Muro, Y., D. Eom, N. Takeda, and M. Ishikawa, 1998, *J. Phys. Soc. Jpn.* **67**, 3601.
- Muro, Y., M. Ishikawa, K. Hirota, Z. Hiroi, N. Takeda, N. Kimura, and H. Aoki, 2007, *J. Phys. Soc. Jpn.* **76**, 033706.
- Naidyuk, Y. G., H. v. Löhneysen, G. Goll, I. K. Yanson, and A. A. Menovsky, 1996, *Europhys. Lett.* **33**, 557.
- Nair, S., S. Wirth, M. Nicklas, J. L. Sarrao, J. D. Thompson, Z. Fisk, and F. Steglich, 2008, *Phys. Rev. Lett.* **100**, 137003.
- Nakajima, Y., K. Izawa, Y. Matsuda, S. Uji, T. Terashima, H. Shishido, R. Settai, Y. Onuki, and H. Kontani, 2004, *J. Phys. Soc. Jpn.* **73**, 5.
- Nakajima, Y., H. Shishido, H. Nakai, T. Shibauchi, M. Hedo, Y. Uwatoko, T. Matsumoto, R. Settai, Y. Onuki, H. Kontani, and Y. Matsuda, 2008, *Phys. Rev. B* **77**, 214504.
- Nakashima, M., H. Kohara, A. Thamizhavel, T. DMatsuda, Y. Haga, M. Hedo, Y. Uwatoko, R. Settai, and Y. Onuki, 2005, *J. Phys.: Condens. Matter* **17**, 4539.
- Nakashima, M., H. Ohkuni, Y. Inada, R. Settai, Y. Haga, E. Yamamoto, and Y. Onuki, 2003, *J. Phys.: Condens. Matter* **15**, S2011.
- Nakashima, M., K. Tabata, A. Thamizhavel, T. Kobayashi, M. Hedo, Y. Uwatoko, K. Shimizu, R. Settai, and Y. Onuki, 2004, *J. Phys.: Condens. Matter* **16**, L255.
- Nakatsuji, S., K. Kuga, Y. Machida, T. Tayama, T. Sakakibara, Y. Karaki, H. Ishimoto, S. Yonezawa, Y. Maeno, E. Pearson, G. G. Lonzarich, L. Balicas, H. Lee, and Z. Fisk, 2008, *Nat. Phys.* **4**, 603.
- Nakatsuji, S., S. Yeo, L. Balicas, Z. Fisk, P. Schlottmann, P. G. Pagliuso, N. O. Moreno, J. L. Sarrao, and J. D. Thompson, 2002, *Phys. Rev. Lett.* **89**, 106402.
- Nicklas, M., R. Borth, E. Lengyel, P. G. P. J. L. Sarrao, V. A. Sidorov, G. Sparn, F. Steglich, and J. D. Thompson, 2001, *J. Phys.: Condens. Matter* **13**, L905.
- Nicklas, M., V. A. Sidorov, H. A. Borges, P. G. Pagliuso, C. Petrovic, Z. Fisk, J. L. Sarrao, and J. D. Thompson, 2003, *Phys. Rev. B* **67**, 020506.
- Nicklas, M., G. Sparn, R. Lackner, E. Bauer, and F. Steglich, 2005, *Physica B* **359-361**, 386.
- Nishioka, T., G. Motoyama, S. Nakamura, H. Kadoya, and N. K. Sato, 2002, *Phys. Rev. Lett.* **88**, 237203.
- Norman, M. R., 1993, *Phys. Rev. Lett.* **71**, 3391.
- Norman, M. R., W. E. Pickett, H. Krakauer, and C. S. Wang, 1987, *Phys. Rev. B* **36**, 4058.
- Normile, P. S., S. Heathman, M. Idiri, P. Boulet, J. Rebizant, F. Wastin, G. H. Lander, T. L. Bihan, and A. Lindbaum, 2005, *Phys. Rev. B* **72**, 184508.
- Oda, K., T. Kumada, K. Sugiyama, N. Sato, T. Komatsubara, and M. Date, 1994, *J. Phys. Soc. Jpn.* **63**, 3115.
- Oda, K., K. Sugiyama, N. K. Sato, T. Komatsubara, K. Kindo, and Y. Onuki, 1999, *J. Phys. Soc. Jpn.* **68**, 3115.
- Oeschler, N., P. Gegenwart, F. Weickert, I. Zerec, P. Thalmeier, F. Steglich, E. D. Bauer, N. A. Frederick, and M. B. Maple, 2004, *Phys. Rev. B* **69**, 235108.
- Ogita, N., *et al.*, 2008, *J. Phys. Soc. Jpn.* **77**, 251.
- Oh, Y. S., K. H. Kim, P. A. Sharma, N. Harrison, H. Amitsuka, and J. A. Mydosh, 2007, *Phys. Rev. Lett.* **98**, 016401.
- Ohashi, M., F. Honda, T. Eto, S. Kaji, I. Minamidake, G. Oomi, S. Koiwai, and Y. Uwatoko, 2002, *Physica B* **312-313**, 443.
- Ohishi, K., T. U. Ito, W. Higemoto, and R. H. Heffner, 2006, *J. Phys. Soc. Jpn. Suppl.* **75**, 53.
- Ohishi, K., *et al.*, 2007, e-print arXiv:0706.4367.
- Ohkawa, F. J., and H. Shimizu, 1999, *J. Phys.: Condens. Matter* **11**, L519.
- Ohta, T., Y. Nakai, Y. Ihara, K. Ishida, K. Deguchi, N. K. Sato, and I. Satoh, 2008, *J. Phys. Soc. Jpn.* **77**, 023707.
- Oikawa, K., T. Kamiyama, H. Asano, Y. Onuki, and M. Kohgi, 1996, *J. Phys. Soc. Jpn.* **65**, 3229.
- Okane, T., *et al.*, 2006, *J. Phys. Soc. Jpn.* **75**, 024704.
- Okazaki, R., Y. Kasahara, H. Shishido, M. Konczykowski, K. Behnia, Y. Haga, T. D. Matsuda, Y. Onuki, T. Shibauchi, and Y. Matsuda, 2008, *Phys. Rev. Lett.* **100**, 037004.
- Okuda, Y., *et al.*, 2007, *J. Phys. Soc. Jpn.* **76**, 044708.
- Okuno, Y., and K. Miyake, 1998, *J. Phys. Soc. Jpn.* **67**, 2469.
- Onishi, Y., and K. Miyake, 2000, *J. Phys. Soc. Jpn.* **69**, 3955.
- Onnes, H. K., 1911a, *Commun. Phys. Lab. Univ. Leiden* **120b**.
- Onnes, H. K., 1911b, *Commun. Phys. Lab. Univ. Leiden* **122b**.
- Onnes, H. K., 1911c, *Commun. Phys. Lab. Univ. Leiden* **124c**.
- Onodera, A., S. Tsuduki, Y. Ohishi, T. Watanuki, K. Ishida, Y. Kitaoka, and Y. Onuki, 2002, *Solid State Commun.* **123**, 113.
- Onuki, Y., 1993, *Phys. Prop. Act. Rare Earth Comp., JJAP Ser.* **8**, 149.
- Onuki, Y., and A. Hasegawa, 1995, *Fermi Surfaces of Intermetallic Compounds*, Handbook of the Physics and Chemistry of Rare Earths Vol. 20 (North-Holland, Amsterdam).
- Onuki, Y., R. Settai, K. Sugiyama, T. Takeuchi, T. C. Kobayashi, Y. Haga, and E. Yamamoto, 2004, *J. Phys. Soc. Jpn.* **73**, 769.
- Onuki, Y., I. Ukon, S. W. Yun, I. Umehara, K. Satoh, T. Kukurahara, H. Sato, S. Takayanagi, M. Shikama, and A. Ochiai, 1992, *J. Phys. Soc. Jpn.* **61**, 293; note that the crystal structure is incorrect.
- Oomi, G., K. Kagayama, K. Nishimura, S. W. Yun, and Y. Onuki, 1995, *Physica B* **206-207**, 515.
- Oomi, G., K. Nishimura, Y. Onuki, and S. W. Yun, 1993, *Physica B* **186-188**, 758.
- Opahle, I., S. Elgazzar, K. Koepernik, and P. M. Oppeneer, 2004, *Phys. Rev. B* **70**, 104504.
- Opahle, I., and P. M. Oppeneer, 2003, *Phys. Rev. Lett.* **90**, 157001.
- Oppeneer, P. M., S. Lesbégue, O. Eriksson, I. Ophale, and A. B. Shick, 2006, *J. Phys. Soc. Jpn.* **75**, 215.

- Ormeno, R. J., A. Sibley, C. E. Gough, S. Sebastian, and I. R. Fisher, 2002, *Phys. Rev. Lett.* **88**, 047005.
- Osheroff, D. D., R. C. Richardson, and D. M. Lee, 1972, *Phys. Rev. Lett.* **28**, 885.
- Ott, H. R., E. Felder, C. Bruder, and T. M. Rice, 1987, *Europhys. Lett.* **3**, 1123.
- Ott, H. R., H. Rudigier, E. Felder, Z. Fisk, and J. L. Smith, 1986, *Phys. Rev. B* **33**, 126.
- Ott, H. R., H. Rudigier, Z. Fisk, and J. L. Smith, 1983, *Phys. Rev. Lett.* **50**, 1595.
- Ott, H. R., H. Rudigier, Z. Fisk, and J. L. Smith, 1984, *Moment Formation in Solids* (Plenum, New York).
- Ott, H. R., H. Rudigier, T. M. Rice, K. Ueda, Z. Fisk, and J. L. Smith, 1984, *Phys. Rev. Lett.* **52**, 1915.
- Otzsch, K., T. Mizukami, T. Hinouchi, J. Shimoyama, and K. Kishio, 1999, *J. Low Temp. Phys.* **117**, 885.
- Özcan, S., D. M. Broun, B. Morgan, R. K. W. Haselwimmer, J. L. Sarrao, S. Kamal, C. P. Bidinosti, P. J. Turner, M. Raudsepp, and J. R. Waldram, 2003, *Europhys. Lett.* **62**, 412.
- Paglione, J., P.-C. Ho, M. B. Maple, M. A. Tanatar, L. Taillefer, Y. Lee, and C. Petrovic, 2008, *Phys. Rev. B* **77**, 100505.
- Paglione, J., T. A. Sayles, P.-C. Ho, J. R. Jeffries, and M. B. Maple, 2007, *Nat. Phys.* **3**, 703.
- Paglione, J., M. A. Tanatar, D. G. Hawthorn, E. Boaknin, R. W. Hill, F. Ronning, M. Sutherland, L. Taillefer, C. Petrovic, and P. C. Canfield, 2003, *Phys. Rev. Lett.* **91**, 246405.
- Pagliuso, P., N. Curro, N. Moreno, M. F. Hundley, J. D. Thompson, J. L. Sarrao, and Z. Fisk, 2002, *Physica B* **320**, 370.
- Pagliuso, P., R. Movshovich, A. Bianchi, M. Nicklas, N. Moreno, J. Thompson, M. Hundley, J. Sarrao, and Z. Fisk, 2002, *Physica B* **312-313**, 129.
- Pagliuso, P. G., N. O. Moreno, N. J. Curro, J. D. Thompson, M. F. Hundley, J. L. Sarrao, Z. Fisk, A. D. Christianson, A. H. Lacerda, B. E. Light, and A. L. Cornelius, 2002, *Phys. Rev. B* **66**, 054433.
- Pagliuso, P. G., C. Petrovic, R. Movshovich, D. Hall, M. F. Hundley, J. L. Sarrao, J. D. Thompson, and Z. Fisk, 2001, *Phys. Rev. B* **64**, 100503.
- Palstra, T., A. A. Menovsky, J. Vandenberg, A. J. Dirkmaat, P. H. Kes, G. J. Nieuwenhuys, and J. A. Mydosh, 1985, *Phys. Rev. Lett.* **55**, 2727.
- Paolasini, L., J. A. Paixao, G. Lander, A. Delapalme, N. Sato, and T. Komatsubara, 1993, *J. Phys.: Condens. Matter* **5**, 8905.
- Park, J.-G., K. A. McEwen, S. deBrion, G. Chouteau, H. Amitsuka, and T. Sakakibara, 1997, *J. Phys.: Condens. Matter* **9**, 3065.
- Park, T., F. Ronning, H. Yuan, M. Salamon, R. Movshovich, J. Sarrao, and J. Thompson, 2006, *Nature (London)* **440**, 65.
- Park, W. K., J. L. Sarrao, J. D. Thompson, and L. H. Greene, 2008, *Phys. Rev. Lett.* **100**, 177001.
- Parks, R. D., 1969, Ed., *Superconductivity* (Dekker, New York).
- Pearson, W. B., 1958, *Handbook of Lattice Spacings and Structures of Metals* (Pergamon, New York), Vol. 3.
- Petersen, T., T. E. Mason, G. Aeppli, A. P. Ramirez, E. Bucher, and R. N. Kleinman, 1994, *Physica B* **119-200**, 151.
- Petrovic, C., R. Movshovich, M. Jaime, P. G. Pagliuso, M. F. Hundley, J. L. Sarrao, Z. Fisk, and J. D. Thompson, 2001, *Europhys. Lett.* **53**, 354.
- Petrovic, C., P. G. Pagliuso, M. F. Hundley, R. Movshovich, J. L. Sarrao, J. D. Thompson, Z. Fisk, and P. Monthoux, 2001, *J. Phys.: Condens. Matter* **13**, L337.
- Pfeleiderer, C., 2005, *J. Phys.: Condens. Matter* **17**, 887.
- Pfeleiderer, C., E. Bedin, and B. Salce, 1997, *Rev. Sci. Instrum.* **68**, 3120.
- Pfeleiderer, C., R. H. Friend, G. G. Lonzarich, N. R. Bernhoeft, and J. Flouquet, 1993, *Int. J. Mod. Phys. B* **7**, 887.
- Pfeleiderer, C., and R. Hackl, 2007, *Nature (London)* **450**, 492.
- Pfeleiderer, C., and A. D. Huxley, 2002, *Phys. Rev. Lett.* **89**, 147005.
- Pfeleiderer, C., A. D. Huxley, and S. M. Hayden, 2005, *J. Phys.: Condens. Matter* **17**, S3111.
- Pfeleiderer, C., S. R. Julian, and G. G. Lonzarich, 2001, *Nature (London)* **414**, 427.
- Pfeleiderer, C., G. J. McMullan, S. R. Julian, and G. G. Lonzarich, 1997, *Phys. Rev. B* **55**, 8330.
- Pfeleiderer, C., J. A. Mydosh, and M. Vojta, 2006, *Phys. Rev. B* **74**, 104412.
- Pfeleiderer, C., D. Reznik, L. Pintschovius, H. v. Löhneysen, M. Garst, and A. Rosch, 2004, *Nature (London)* **427**, 227.
- Pfeleiderer, C., R. Ritz, S. Mühlbauer, P. Niklowitz, T. Keller, E. M. Forgan, M. Laver, J. White, R. Cubitt, and E. Bauer, 2008, unpublished.
- Pfeleiderer, C., M. Uhlarz, S. M. Hayden, R. Vollmer, H. v. Löhneysen, N. R. Bernhoeft, and G. G. Lonzarich, 2001, *Nature (London)* **412**, 58.
- Pham, L. D., T. Park, S. Maquilon, J. D. Thompson, and Z. Fisk, 2006, *Phys. Rev. Lett.* **97**, 056404.
- Phillips, N. E., and B. T. Matthias, 1961, *Phys. Rev.* **121**, 105.
- Piekarz, P., K. Parlinski, P. T. Jochym, A. M. Oleś, J.-P. Sanchez, and J. Rebizant, 2005, *Phys. Rev. B* **72**, 014521.
- Ponchet, A., J. M. Mignot, A. de Visser, J. J. M. Franse, and A. Menovsky, 1986, *J. Magn. Magn. Mater.* **54-57**, 399.
- Pourovskii, L. V., M. I. Katsnelson, and A. I. Lichtenstein, 2006, *Phys. Rev. B* **73**, 060506.
- Prokes, K., T. Tahara, Y. Echizen, T. Takabatake, T. Fujita, I. H. Hagemus, J. C. P. Klaasse, E. Brück, F. R. de Boer, M. Divis, and V. Sechovsky, 2002, *Physica B* **311**, 220.
- Qian, Y. J., M.-F. Xu, A. Schenstrom, H.-P. Baum, J. B. Ketterson, D. Hinks, M. Levy, and B. K. Sarma, 1987, *J. Phys.: Condens. Matter* **63**, 599.
- Radovan, H. A., R. Movshovich, I. Vekhter, P. G. Pagliuso, and J. L. Sarrao, 2003, *Nature (London)* **425**, 51.
- Rashba, E. I., 1960, *Sov. Phys. Solid State* **2**, 1109.
- Rauchschwalbe, U., U. Ahlheim, F. Steglich, D. Rainer, and J. J. M. Franse, 1985, *Z. Phys. B: Condens. Matter* **60**, 379.
- Rauchschwalbe, U., W. Lieke, C. D. Bredl, F. Steglich, J. Aarts, K. M. Martini, and A. C. Mota, 1982, *Phys. Rev. Lett.* **49**, 1448.
- Rauchschwalbe, U., F. Steglich, G. R. Stewart, A. L. Giorgi, P. Fulde, and K. Maki, 1987, *Europhys. Lett.* **3**, 751.
- Raymond, S., and D. Jaccard, 2000, *Phys. Rev. B* **61**, 8679.
- Raymond, S., G. Knebel, D. Aoki, and J. Flouquet, 2008, *Phys. Rev. B* **77**, 172502.
- Raymond, S., K. Kuwahara, K. Kaneko, K. Iwasa, M. Kohgi, A. Hiess, M.-A. Measson, J. Flouquet, N. Metoki, H. Sugawara, Y. Aoki, and H. Sato, 2008, *J. Phys. Soc. Jpn.* **77**, 25.
- Raymond, S., P. Piekarz, J. P. Sanchez, J. Serrano, M. Krisch, B. Janoušová, J. Rebizant, N. Metoki, K. Kaneko, P. T. Jochym, A. M. Oleś, and K. Parlinski, 2006, *Phys. Rev. Lett.* **96**, 237003.
- Remenyi, G., D. Jaccard, J. Flouquet, A. Briggs, Z. Fisk, J. L. Smith, and H. R. Ott, 1986, *J. Phys. (France)* **47**, 367.
- Riblet, G., and K. Winzer, 1971, *Solid State Commun.* **9**, 1663.
- Roehler, J., J. Klug, and K. Keularz, 1988, *J. Math. Mech.* **76**,

- 77, 340.
- Ronning, F., C. Capan, A. Bianchi, R. Movshovich, A. Lacerda, M. F. Hundley, J. D. Thompson, P. G. Pagliuso, and J. L. Sarrao, 2005, *Phys. Rev. B* **71**, 104528.
- Rößler, U. K., A. N. Bogdanov, and C. Pfeleiderer, 2006, *Nature (London)* **442**, 797.
- Rotundu, C. R., H. Tsujii, Y. Takano, B. Andraka, H. Sugawara, Y. Aoki, and H. Sato, 2004, *Phys. Rev. Lett.* **92**, 037203.
- Rueff, J.-P., S. Raymond, A. Yaresko, D. Braithwaite, P. Leininger, G. Vankó, A. Huxley, J. Rebizant, and N. Sato, 2007, *Phys. Rev. B* **76**, 085113.
- Sa, D., 2002, *Phys. Rev. B* **66**, 140505.
- Sachdev, S., 1999, *Quantum Phase Transitions* (Cambridge University Press, Cambridge).
- Saint-James, D., G. Sarma, and E. J. Thomas, 1969, Eds., *Type II Superconductivity* (Pergamon, New York).
- Sakai, H., K. Yoshimura, H. Ohno, H. Kato, S. Kambe, R. Walstedt, T. Matsuda, and Y. Haga, 2001, *J. Phys.: Condens. Matter* **13**, L785.
- Sakai, H., *et al.* 2005, *J. Phys. Soc. Jpn.* **74**, 1710.
- Sakai, H., *et al.* 2006, *Physica B* **378-380**, 1005.
- Sakakibara, T., A. Yamada, J. Custers, K. Yano, T. Tayama, H. Aoki, and K. Machida, 2007, *J. Phys. Soc. Jpn.* **76**, 051004.
- Sakarya, S., N. H. van Dijk, and E. Brück, 2005, *Phys. Rev. B* **71**, 174417.
- Sakarya, S., N. H. van Dijk, A. de Visser, and E. Brück, 2003, *Phys. Rev. B* **67**, 144407.
- Sakon, T., K. Imamura, N. Koga, N. Sato, and T. Komatsubara, 1994, *Physica B* **119-200**, 154.
- Sakon, T., K. Imamura, N. Takeda, N. Sato, and T. Komatsubara, 1993, *Physica B* **186-188**, 297.
- Sakon, T., T. Namiki, and M. Motokawa, 2001, *J. Phys. Soc. Jpn.* **70**, 3046.
- Sales, B. C., 2003, *Filled Skutterudites*, Handbook of the Physics and Chemistry of Rare Earths Vol. 33 (Elsevier Science, Amsterdam), pp. 1–34.
- Samokhin, K. V., 2002, *Phys. Rev. B* **66**, 212509.
- Samokhin, K. V., 2004, *Phys. Rev. B* **70**, 104521.
- Samokhin, K. V., and M. B. Walker, 2002, *Phys. Rev. B* **66**, 174501.
- Samokhin, K. V., E. S. Zijlstra, and S. K. Bose, 2004, *Phys. Rev. B* **69**, 094514.
- Sandeman, K., G. G. Lonzarich, and A. J. Schofield, 2003, *Phys. Rev. Lett.* **90**, 167005.
- Sandratskii, L. M., J. Kübler, P. Zahn, and I. Mertig, 1994, *Phys. Rev. B* **50**, 15834.
- Santini, P., and G. Amoretti, 1994, *Phys. Rev. Lett.* **73**, 1027.
- Santini, P., G. Amoretti, R. Caciuffo, F. Bourdarot, and B. Fåk, 2000, *Phys. Rev. Lett.* **85**, 654.
- Sarrao, J. L., L. A. Morales, J. D. Thompson, B. L. Scott, G. R. Stewart, F. Wastin, J. Rebizant, P. Boulet, E. Colineau, and G. H. Lander, 2002, *Nature (London)* **420**, 297.
- Sarrao, J. L., and J. D. Thompson, 2007, *J. Phys. Soc. Jpn.* **76**, 051013.
- Sato, H., D. Kikuchi, K. Tanaka, H. Aoki, K. Kuwahara, Y. Aoki, M. Kohgi, H. Sugawara, and K. Iwasa, 2007, *J. Magn. Mater.* **310**, 188.
- Sato, H., H. Sugawara, T. Namiki, S. R. Saha, S. Osaki, T. T. Matsuda, Y. Aoki, Y. Inada, H. Shishido, R. Settai, and Y. Onuki, 2003, *J. Phys.: Condens. Matter* **15**, S2063.
- Sato, N., 1999, *Physica B* **259-261**, 634.
- Sato, N., N. Aso, G. H. Lander, B. Roessli, T. Komatsubara, and Y. Endoh, 1997a, *J. Phys. Soc. Jpn.* **66**, 2981.
- Sato, N., N. Aso, G. H. Lander, B. Roessli, T. Komatsubara, and Y. Endoh, 1997b, *J. Phys. Soc. Jpn.* **66**, 1884.
- Sato, N., K. Imamura, T. Sakon, Y. Inada, A. Sawada, T. Komatsubara, H. Matsui, and T. Goto, 1994, *Physica B* **119-200**, 122.
- Sato, N., N. Koga, and T. Komatsubara, 1996, *J. Phys. Soc. Jpn.* **65**, 1555.
- Sato, N., T. Sarkon, N. Takeda, T. Komatsubara, C. Geibel, and F. Steglich, 1992, *J. Phys. Soc. Jpn.* **61**, 32.
- Sato, N. K., N. Aso, K. Miyake, R. Shiina, P. Thalmeier, G. Varelogiannis, C. Geibel, F. Steglich, P. Fulde, and T. Komatsubara, 2001, *Nature (London)* **410**, 340.
- Sauls, J. A., 1994, *Adv. Phys.* **43**, 113.
- Saxena, S. S., and P. B. Littlewood, 2001, *Nature (London)* **412**, 290.
- Saxena, S. S., *et al.* 2000, *Nature (London)* **406**, 587.
- Scheffler, M., M. Drssell, M. Jourdan, and H. Adrian, 2005, *Nature (London)* **438**, 1135.
- Scheidt, E. W., F. Mayr, G. Eickerling, P. Rogl, and E. Bauer, 2005, *J. Phys.: Condens. Matter* **17**, L121.
- Schenck, A., D. Andreica, F. N. Gygax, D. Aoki, and Y. Onuki, 2002, *Phys. Rev. B* **66**, 144404.
- Schenck, A., N. K. Sato, G. Solt, D. Andreica, F. N. Gygax, M. Pinkpank, and A. Amato, 2000, *Eur. Phys. J. B* **13**, 245.
- Schenstrom, A., *et al.* 1989, *Phys. Rev. Lett.* **62**, 332.
- Schlabitz, W., J. Baumann, B. Pollit, U. Rauchschwalbe, H. M. Mayer, U. Ahlheim, and C. D. Bredl, 1984, unpublished.
- Schlabitz, W., J. Baumann, B. Pollit, U. Rauchschwalbe, H. M. Mayer, U. Ahlheim, and C. D. Bredl, 1986, *Z. Phys. B: Condens. Matter* **62**, 171.
- Schlottmann, P., 1989, *Phys. Rep.* **181**, 1.
- Schmidt, F. A., and O. N. Carlson, 1976, *Metall. Trans. A* **7A**, 127.
- Schröder, A., J. G. Lussier, B. D. Gaulin, J. D. Garrett, W. J. L. Buyers, L. Rebelsky, and S. M. Shapiro, 1994, *Phys. Rev. Lett.* **72**, 136.
- Sechovsky, V., and L. Havella, 1998, *Handbook of Magnetic Materials* (North-Holland, Amsterdam), Vol. 11, p. 7.
- Sekine, C., T. Uchiumi, I. Shirotnani, and T. Yagi, 1997, *Phys. Rev. Lett.* **79**, 3218.
- Settai, R., T. Kubo, T. Shirmoto, D. Honda, H. Shishido, K. Sugiyama, Y. Haga, T. Matsuda, K. Betsuyaku, H. Harima, T. Kobayashi, and Y. Onuki, 2005, *J. Phys. Soc. Jpn.* **74**, 3016.
- Settai, R., A. Misawa, S. Araki, M. Kosaki, K. Sugiyama, T. Takeuchi, K. Kindo, Y. Haga, E. Yamamoto, and Y. Onuki, 1997, *J. Phys. Soc. Jpn.* **66**, 2260.
- Settai, R., Y. Miyauchi, T. Takeuchi, F. Levy, I. Sheikin, and Y. Onuki, 2008, *J. Phys. Soc. Jpn.* **77**, 073705.
- Settai, R., Y. Okuda, I. Sugitani, Y. Onuki, T. D. Matsuda, Y. Haga, and H. Harima, 2007, *Int. J. Mod. Phys. B* **21**, 3238.
- Settai, R., H. Shishido, S. Ikeda, Y. Murakawa, M. Nakashima, D. Aoki, Y. Haga, H. Harima, and Y. Onuki, 2001, *J. Phys.: Condens. Matter* **13**, L627.
- Settai, R., T. Takeuchi, and Y. Onuki, 2007, *J. Phys. Soc. Jpn.* **76**, 051003.
- Seyfarth, G., J. P. Brison, G. Knebel, D. Aoki, G. Lapertot, and J. Flouquet, 2008, *Phys. Rev. Lett.* **101**, 046401.
- Seyfarth, G., J. P. Brison, M.-A. Méasson, D. Braithwaite, G. Lapertot, and J. Flouquet, 2006, *Phys. Rev. Lett.* **97**, 236403.
- Seyfarth, G., J. P. Brison, M.-A. Méasson, J. Flouquet, K. Izawa, Y. Matsuda, H. Sugawara, and H. Sato, 2005, *Phys. Rev. Lett.* **95**, 107004.

- Shakeripour, H., M. A. Tanatar, S. Y. Li, C. Petrovic, and L. Taillefer, 2007, *Phys. Rev. Lett.* **99**, 187004.
- Sharma, P. A., N. Harrison, M. Jaime, Y. S. Oh, K. H. Kim, C. D. Batista, J. A. Mydosh, and H. Amitsuka, 2005, e-print arXiv:cond-mat/0507545.
- Sheikin, I., E. Steep, D. Braithwaite, J. P. Brison, S. Raymond, D. Jaccard, and J. Flouquet, 2001, *J. Low Temp. Phys.* **122**, 591.
- Shick, A. B., 2002, *Phys. Rev. B* **65**, 180509.
- Shick, A. B., V. Janiš, V. Drchal, and W. E. Pickett, 2004, *Phys. Rev. B* **70**, 134506.
- Shick, A. B., V. Janiš, and P. M. Oppeneer, 2005, *Phys. Rev. Lett.* **94**, 016401.
- Shick, A. B., and W. E. Pickett, 2001, *Phys. Rev. Lett.* **86**, 300.
- Shiina, R., 2004, *J. Phys. Soc. Jpn.* **73**, 2257.
- Shiina, R., and Y. Aoki, 2004, *J. Phys. Soc. Jpn.* **73**, 541.
- Shimahara, H., 1994, *Phys. Rev. B* **50**, 12760.
- Shimahara, H., 1998, *J. Phys. Soc. Jpn.* **67**, 736.
- Shimahara, H., S. Matsuo, and K. Nagai, 1996, *Phys. Rev. B* **53**, 12284.
- Shimahara, H., and D. Rainer, 1997, *J. Phys. Soc. Jpn.* **66**, 3591.
- Shimizu, K., T. Kimura, S. Furomoto, K. Takeda, K. Kontani, Y. Onuki, and K. Amaya, 2001, *Nature (London)* **412**, 316.
- Shirotani, I., T. Uchiumi, K. Ohno, C. Sekine, Y. Nakazawa, K. Kanoda, S. Todo, and T. Yagi, 1997, *Phys. Rev. B* **56**, 7866.
- Shishido, H., R. Settai, H. Harima, and Y. Onuki, 2005, *J. Phys. Soc. Jpn.* **74**, 1103.
- Shishido, H., T. Ueda, S. Hashimoto, T. Kubo, R. Settai, H. Harima, and Y. Onuki, 2003, *J. Phys.: Condens. Matter* **15**, L499.
- Shishido, H., E. Yamamoto, Y. Haga, S. Ikeda, M. Nakashima, R. Settai, and Y. Onuki, 2006, *J. Phys. Soc. Jpn.* **75**, 119.
- Shivaram, B. S., Y. H. Jeong, T. F. Rosenbaum, and D. G. Hinks, 1986, *Phys. Rev. Lett.* **56**, 1078.
- Sidorov, V. A., M. Nicklas, P. G. Pagliuso, J. L. Sarrao, Y. Bang, A. V. Balatsky, and J. D. Thompson, 2002, *Phys. Rev. Lett.* **89**, 157004.
- Sigrist, M., 2005, *AIP Conf. Proc.* **789**, 165.
- Sigrist, M., and T. M. Rice, 1989, *Phys. Rev. B* **39**, 2200.
- Sigrist, M., and K. Ueda, 1991, *Rev. Mod. Phys.* **63**, 239.
- Singh, S., C. Capan, M. Nicklas, M. Rams, A. Gladun, H. Lee, J. F. DiTusa, Z. Fisk, F. Steglich, and S. Wirth, 2007, *Phys. Rev. Lett.* **98**, 057001.
- Singleton, J., J. A. Symington, M.-S. Nam, A. Ardavan, M. Kurmoo, and P. Day, 2001, *Physica B* **294-295**, 418.
- Söderlind, P., 2004, *Phys. Rev. B* **70**, 094515.
- Sonin, E. B., 2002, *Phys. Rev. B* **66**, 100504(R).
- Sonin, E. B., and I. Felner, 1998, *Phys. Rev. B* **57**, R14000.
- Souptel, D., W. Loser, and G. Behr, 2007, *J. Cryst. Growth* **300**, 538.
- Spalek, J., 2001, *Phys. Rev. B* **63**, 104513.
- Sparn, G., R. Borth, E. Lengyel, P. G. Pagliuso, J. Sarrao, F. Steglich, and J. Thompson, 2002, *Physica B* **319**, 262.
- Sparn, G., O. Stockert, F. Grosche, H. Yuan, E. Faulhaber, C. Geibel, M. Deppe, H. Jeevan, M. Loewenhaupt, G. Zwicknagl, and F. Steglich, 2006, *J. Phys. Chem. Solids* **67**, 529.
- Steele, R. A., E. Frikkee, R. B. Helmholdt, A. A. Menovsky, J. van den Berg, G. J. Nieuwenhuys, and J. A. Mydosh, 1988, *Solid State Commun.* **66**, 103.
- Steglich, F., J. Aarts, C. D. Bredl, W. Lieke, D. Meschede, W. Franz, and H. Schäfer, 1979, *Phys. Rev. Lett.* **43**, 1892.
- Steglich, F., P. Gegenwart, C. Geibel, P. Hinze, M. Lang, C. Langhammer, G. Sparn, T. Tayama, O. Trovarelli, N. Sato, T. Dahm, and G. Varelogiannis, 2001, *More is Different—Fifty Years of Condensed Matter Physics* (Princeton University Press, Princeton).
- Steglich, F., *et al.* 1996, *Physica C* **263**, 498.
- Stewart, G. R., 2001, *Rev. Mod. Phys.* **73**, 797.
- Stewart, G. R., 2006, *Rev. Mod. Phys.* **78**, 743.
- Stewart, G. R., Z. Fisk, J. O. Willis, and J. L. Smith, 1984, *Phys. Rev. Lett.* **52**, 679.
- Stock, C., C. Broholm, J. Hudis, H. J. Kang, and C. Petrovic, 2008, *Phys. Rev. Lett.* **100**, 087001.
- Stockert, O., E. Faulhaber, G. Zwicknagl, N. Stüßer, M. Deppe, R. Borth, R. Kuchler, M. Loewenhaupt, C. Geibel, and F. Steglich, 2004, *Phys. Rev. Lett.* **92**, 136401.
- Suderow, H., J. P. Brison, A. Huxley, and J. Flouquet, 1997, *J. Low Temp. Phys.* **108**, 11.
- Suderow, H., S. Vieira, J. D. Strand, S. Bud'ko, and P. C. Canfield, 2004, *Phys. Rev. B* **69**, 060504.
- Sugawara, H., M. Kobayashi, S. Osaki, S. R. Saha, T. Namiki, Y. Aoki, and H. Sato, 2005, *Phys. Rev. B* **72**, 014519.
- Sugawara, H., S. Osaki, S. R. Saha, Y. Aoki, H. Sato, Y. Inada, H. Shishido, R. Settai, Y. Onuki, H. Harima, and K. Oikawa, 2002, *Phys. Rev. B* **66**, 220504.
- Sugawara, H., *et al.*, 2008, *J. Phys. Soc. Jpn.* **77**, 108.
- Suginishi, Y., and H. Shimahara, 2006, *Phys. Rev. B* **74**, 024518.
- Sugiyama, K., T. Inoue, T. Ikeda, N. Sato, T. Komatsubara, A. Yamagishi, and M. Date, 1993, *Physica B* **186-188**, 723.
- Sugiyama, K., T. Inoue, K. Oda, T. Kumada, N. Sato, T. Komatsubara, A. Yamagishi, and M. Date, 1994, *Physica B* **119-200**, 227.
- Suhl, H., 2001, *Phys. Rev. Lett.* **87**, 167007.
- Suhl, H., and B. T. Matthias, 1959, *Phys. Rev.* **114**, 977.
- Süllow, S., B. Becker, A. de Visser, M. Mihalik, G. J. Nieuwenhuys, A. A. Menovsky, and J. A. Mydosh, 1997, *J. Phys.: Condens. Matter* **9**, 913.
- Süllow, S., B. Janossy, G. L. E. van Vliet, G. J. Nieuwenhuys, A. A. Menovsky, and J. A. Mydosh, 1996, *J. Phys.: Condens. Matter* **8**, 729.
- Sun, Y., and K. Maki, 1995, *Europhys. Lett.* **32**, 355.
- Suzumura, Y., and K. Ishino, 1983, *Prog. Theor. Phys.* **70**, 654.
- Szajek, A., and J. A. Morkowski, 2003, *J. Phys.: Condens. Matter* **15**, L155.
- Tachiki, M., S. Takahashi, P. Gegenwart, M. Weiden, M. Lang, C. Geibel, F. Steglich, R. Modler, C. Paulsen, and Y. Onuki, 1996, *Z. Phys. B: Condens. Matter* **100**, 369.
- Taillefer, L., and G. G. Lonzarich, 1988, *Phys. Rev. Lett.* **60**, 1570.
- Taillefer, L., R. Newbury, G. G. Lonzarich, Z. Fisk, and J. L. Smith, 1987, *J. Magn. Magn. Mater.* **63-64**, 372.
- Takada, S., and T. Izuyama, 1969, *Prog. Theor. Phys.* **41**, 635.
- Takahashi, S., M. Tachiki, R. Modler, P. Gegenwart, M. Lang, and F. Steglich, 1996, *Physica C* **263**, 30.
- Takahashi, T., N. Sato, T. Yokoya, A. Chainani, T. Morimoto, and T. Komatsubara, 1995, *J. Phys. Soc. Jpn.* **65**, 156.
- Takegahara, K., H. Harima, and T. Kasuya, 1986, *J. Phys. F: Met. Phys.* **16**, 1691.
- Takegahara, M., and H. Harima, 2000, *Physica B* **282**, 764.
- Takeuchi, T., T. Inoue, K. Sugiyama, D. Aoki, Y. Tokiwa, Y. Haga, K. Kindo, and Y. Onuki, 2001, *J. Phys. Soc. Jpn.* **70**, 877.
- Takeuchi, T., T. Yasuda, M. Tsujino, H. Shishido, R. Settai, H. Harima, and Y. Onuki, 2007, *J. Phys. Soc. Jpn.* **76**, 014702.
- Takeuchi, T., *et al.*, 2005, *J. Phys.: Condens. Matter* **16**, L333.
- Tanatar, M. A., J. Paglione, S. Nakatsuji, D. G. Hawthorn, E.

- Boaknin, R. W. Hill, F. Ronning, M. Sutherland, L. Taillefer, C. Petrovic, P. C. Canfield, and Z. Fisk, 2005, *Phys. Rev. Lett.* **95**, 067002.
- Tateiwa, N., Y. Haga, T. D. Matsuda, S. Ikeda, E. Yamamoto, Y. Okuda, Y. Miyauchi, R. Settai, and Y. Onuki, 2007, e-print arXiv:0706.4398.
- Tateiwa, N., Y. Haga, T. D. Matsuda, S. Ikeda, T. Yasuda, T. Takeuchi, R. Settai, and Y. Onuki, 2005, *J. Phys. Soc. Jpn.* **74**, 1903.
- Tateiwa, N., K. Hanazono, T. C. Kobayashi, K. Amaya, T. Inoue, K. Kindo, Y. Koike, N. Metoki, Y. Haga, R. Settai, and Y. Onuki, 2001, *J. Phys. Soc. Jpn.* **70**, 2876.
- Tateiwa, N., T. C. Kobayashi, K. Amaya, Y. Haga, R. Settai, and Y. Onuki, 2004, *Phys. Rev. B* **69**, 180513.
- Tateiwa, N., T. C. Kobayashi, K. Hanazono, K. Amaya, Y. Haga, R. Settai, and Y. Onuki, 2001, *J. Phys.: Condens. Matter* **13**, L17.
- Tateiwa, N., N. Sato, and T. Komatsubara, 1998, *Phys. Rev. B* **58**, 11131.
- Tayama, T., A. Harita, T. Sakakibara, Y. Haga, H. Shishido, R. Settai, and Y. Onuki, 2002, *Phys. Rev. B* **65**, 180504.
- Tayama, T., Y. Namai, T. Sakakibara, M. Hedo, Y. Uwatoko, H. Shishido, R. Settai, and Y. Onuki, 2005, *J. Phys. Soc. Jpn.* **74**, 1115.
- Tayama, T., T. Sakakibara, H. Sugawara, Y. Aoki, and H. Sato, 2003, *J. Phys. Soc. Jpn.* **72**, 1516.
- Tenya, K., I. Kawasaki, K. Tameyasu, S. Yasuda, M. Yokoyama, H. Amitsuka, N. Tateiwa, and T. C. Kobayashi, 2005, *Physica B* **359-361**, 1135.
- Tenya, K., K. Kuwahara, H. Amitsuka, T. Sakakibara, H. Ohkuni, Y. Inada, E. Yamamoto, Y. Haga, and Y. Onuki, 2000, *Physica B* **281-282**, 991.
- Terashima, T., K. Enomoto, T. Konoike, T. Matsumoto, S. Uji, N. Kimura, M. Endo, T. Komatsubara, H. Aoki, and K. Maezawa, 2006, *Phys. Rev. B* **73**, 140406.
- Terashima, T., C. Haworth, M. Takashita, H. Aoki, N. Sato, and T. Komatsubara, 1997, *Phys. Rev. B* **55**, R13369.
- Terashima, T., T. Matsumoto, C. Terakura, S. Uji, N. Kimura, M. Endo, T. Komatsubara, and H. Aoki, 2001, *Phys. Rev. Lett.* **87**, 166401.
- Terashima, T., T. Matsumoto, C. Terakura, S. Uji, N. Kimura, M. Endo, T. Komatsubara, H. Aoki, and K. Maezawa, 2002, *Phys. Rev. B* **65**, 174501.
- Thalmeier, P., and B. Lüthi, 1991, *The Electron Phonon Interaction in Intermetallic Compounds*, Handbook of the Physics and Chemistry of Rare Earths Vol. 14 (North-Holland, Amsterdam).
- Thalmeier, P., and G. Zwicknagl, 2005, *Unconventional Superconductivity and Magnetism in Lanthanide and Actinide Intermetallic Compounds*, Handbook of the Physics and Chemistry of Rare Earths Vol. 34 (North-Holland, Amsterdam), Chap. 219.
- Thalmeier, P., G. Zwicknagl, O. Stockert, G. Sparn, and F. Steglich, 2005, *Unconventional Superconductivity and Magnetism in Lanthanide and Actinide Intermetallic Compounds*, Frontiers in Magnetic Materials/Frontiers in Superconductive Materials Vol. XXXII (Springer Verlag, Berlin), Chaps. 109–182.
- Thomas, F., J. Thomasson, C. Ayache, C. Geibel, and F. Steglich, 1993, *Physica B* **186-188**, 303.
- Thomas, F., B. Wand, T. Lühmann, P. Gegenwart, G. R. Stewart, F. Steglich, J. P. Brison, A. Buzdin, L. Glémont, and J. Flouquet, 1996, *J. Low Temp. Phys.* **102**, 117.
- Thompson, J. D., A. A. Ekimov, V. A. Sidorov, E. D. Bauer, L. A. Morales, F. Wastin, and J. L. Sarrao, 2006, *J. Phys. Chem. Solids* **67**, 557.
- Thompson, J. D., M. Nicklas, V. A. Sidorov, E. D. Bauer, R. Movshovich, N. J. Curro, and J. L. Sarrao, 2006, *J. Alloys Compd.* **408**, 16.
- Thompson, J. D., T. Park, N. J. Curro, and J. L. Sarrao, 2006, *J. Phys. Soc. Jpn.* **75**, 1.
- Thompson, J. D., R. D. Parks, and H. Borges, 1986, *J. Magn. Magn. Mater.* **54-57**, 377.
- Thompson, J. D., J. L. Sarrao, L. A. Morales, F. Wastin, and P. Boulet, 2004, *Physica C* **412-414**, 10.
- Tinkham, M., 1969, *Introduction to Superconductivity* (Dekker, New York).
- Togano, K., P. Badica, Y. Nakamori, S. Orimo, H. Takeya, and K. Hirata, 2004, *Phys. Rev. Lett.* **93**, 247004.
- Tokiwa, Y., R. Movshovich, F. Ronning, E. D. Bauer, P. Papin, A. D. Bianchi, J. F. Rauscher, S. M. Kauzlarich, and Z. Fisk, 2008, *Phys. Rev. Lett.* **101**, 037001.
- Tou, H., Y. Kitaoka, K. Asayama, N. Kimura, Y. Onuki, E. Yamamoto, and K. Maezawa, 1996, *Phys. Rev. Lett.* **77**, 1374.
- Tou, H., Y. Kitaoka, T. Kamatsuka, K. Asayama, C. Geibel, C. Schank, F. Steglich, S. Süllow, and J. Mydosh, 1997, *Physica B* **230-232**, 360.
- Tran, V. H., S. Paschen, R. Troc, M. Baenitz, and F. Steglich, 2004, *Phys. Rev. B* **69**, 195314.
- Tran, V. H., R. Troc, and G., andré, 1998, *J. Magn. Magn. Mater.* **186**, 81.
- Trappmann, T., H. v. Löhneysen, and L. Taillefer, 1991, *Phys. Rev. B* **43**, 13714.
- Trovarelli, O., M. Weiden, R. Müller-Reisener, M. Gómez-Berisso, P. Gegenwart, M. Deppe, C. Geibel, J. G. Sereni, and F. Steglich, 1997, *Phys. Rev. B* **56**, 678.
- Turel, C. S., J. Y. T. Wei, W. Yuhasz, R. Baumbach, and M. B. Maple, 2008, *J. Phys. Soc. Jpn.* **77**, 21.
- Uemura, S., G. Motoyama, Y. Oda, T. Nishioka, and N. K. Sato, 2005, *J. Phys. Soc. Jpn.* **74**, 2667.
- Urbano, R. R., B.-L. Young, N. J. Curro, J. D. Thompson, L. D. Pham, and Z. Fisk, 2007, *Phys. Rev. Lett.* **99**, 146402.
- Ushida, Y., H. Nakane, T. Nishioka, G. Motoyama, S. Nakamura, and N. K. Sato, 2003, *Physica C* **388**, 525.
- v. Löhneysen, H., A. Rosch, M. Vojta, and P. Wölfle, 2007, *Rev. Mod. Phys.* **79**, 1015.
- van Daal, H. J., and K. H. L. Buschow, 1969, *Solid State Commun.* **7**, 217.
- van Dijk, N. H., B. Fåk, T. Charvolin, P. Lejay, and J. M. Mignot, 2000, *Phys. Rev. B* **61**, 8922.
- van Dijk, N. H., A. de Visser, J. J. M. Franse, and A. A. Menovsky, 1995, *Phys. Rev. B* **51**, 12665.
- van Dijk, N. H., A. de Visser, J. J. M. Franse, and L. Taillefer, 1993, *J. Low Temp. Phys.* **93**, 101.
- Vargoz, E., D. Jaccard, J. Y. Genoud, J. P. Brison, and J. Flouquet, 1998, *Solid State Commun.* **106**, 631.
- Varma, C. M. and L. Zhu, 2006, *Phys. Rev. Lett.* **96**, 036405.
- Vekhter, I. and A. Houghton, 1999, *Phys. Rev. Lett.* **83**, 4626.
- Villaume, A., D. Aoki, Y. Haga, G. Knebel, R. Boursier, and J. Flouquet, 2008, *J. Phys.: Condens. Matter* **20**, 015203.
- Vincent, E., J. Hammann, L. Taillefer, K. Behnia, and N. Keller, 1991, *J. Phys.: Condens. Matter* **3**, 3517.
- Vojta, M., 2003, *Rep. Prog. Phys.* **66**, 2069.
- Vollhardt, D. and P. Wölfle, 1990, *The Superfluid Phases of ³He* (Taylor & Francis, New York).
- Vollmer, R., A. Faisst, C. Pfeleiderer, H. von Löhneysen, E. D.

- Bauer, P. C. Ho, V. Zapf, and M. B. Maple, 2003, *Phys. Rev. Lett.* **90**, 057001.
- Vollmer, R., C. Pfeleiderer, H. v. Löhneysen, E. D. Bauer, and M. B. Maple, 2002, *Physica B* **312-313**, 112.
- Volovik, G. E., 1993, *JETP Lett.* **58**, 469.
- Waldram, J. R., 1996, *Superconductivity of Metals and Cuprates* (IOP, London).
- Walker, I. R., F. M. Grosche, D. M. Freye, and G. G. Lonzarich, 1997, *Physica C* **282-287**, 303.
- Wang, Q., H.-Y. Chen, C.-R. Hu, and C. S. Ting, 2006, *Phys. Rev. Lett.* **96**, 117006.
- Wassermann, A. and M. Springford, 1994, *Physica B* **194-199**, 1801.
- Wastin, F., P. Boulet, J. Rebizant, E. Colineau, and G. H. Lander, 2003, *J. Phys.: Condens. Matter* **15**, S2279.
- Wastin, F., E. Colineau, P. Javorsky, and J. Rebizant, 2006, *J. Phys. Soc. Jpn.* **75**, 10.
- Watanabe, S. and K. Miyake, 2002, *J. Phys. Soc. Jpn.* **71**, 2489.
- Watanabe, T., K. Izawa, Y. Kasahara, Y. Haga, Y. Onuki, P. Thalmeier, K. Maki, and Y. Matsuda, 2004, *Phys. Rev. B* **70**, 184502.
- Watanabe, T., Y. Kasahara, K. Izawa, T. Sakakibara, Y. Matsuda, C. J. van der Beek, T. Hanaguri, H. Shishido, R. Settai, and Y. Onuki, 2004, *Phys. Rev. B* **70**, 020506.
- Wei, W., Z. Tun, W. J. L. Buyers, B. D. Gaulin, T. E. Mason, J. D. Garrett, and E. D. Isaacs, 1992, *J. Magn. Magn. Mater.* **108**, 77.
- Weickert, F., P. Gegenwart, H. Won, D. Parker, and K. Maki, 2006, *Phys. Rev. B* **74**, 134511.
- Werthamer, N. R., E. Helfand, and P. C. Hohenberg, 1966, *Phys. Rev.* **147**, 295.
- Wheatley, J. C., 1975, *Rev. Mod. Phys.* **47**, 415.
- White, R. M. and T. H. Geballe, 1979, *Long Range Order in Solids* (Academic, New York).
- Wiebe, C. R., J. A. Janik, G. J. MacDougall, G. M. Luke, J. D. Garrett, H. D. Zhou, Y.-J. Jo, L. Balicas, Y. Qiu, J. R. D. Copley, Z. Yamani, and W. J. L. Buyers, 2007, *Nat. Phys.* **3**, 96.
- Wilhelm, H., S. Raymond, D. Jaccard, O. Stockert, H. von Löhneysen, and A. Rosch, 2001, *J. Phys.: Condens. Matter* **13**, L329.
- Willis, J. O., J. D. Thompson, Z. Fisk, A. de Visser, J. J. M. Franse, and A. Menovsky, 1985, *Phys. Rev. B* **31**, 1654.
- Wolfer, W. G., 2000, *Los Alamos Sci.* **26**, 274.
- Wüchner, S., N. Keller, J. L. Tholence, and J. Flouquet, 1993, *Solid State Commun.* **85**, 355.
- Xiao, H., T. Hu, C. C. Almasan, T. A. Sayles, and M. B. Maple, 2008, *Phys. Rev. B* **78**, 014510.
- Yamagami, H., D. Aoki, Y. Haga, and Y. Onuki, 2008, *J. Phys. Soc. Jpn.* **083702**, 76.
- Yanase, Y., and M. Sigrist, 2007, *J. Phys. Soc. Jpn.* **76**, 043712.
- Yang, K., and A. H. MacDonald, 2004, *Phys. Rev. B* **70**, 094512.
- Yang, S.-H., H. Kumigashira, T. Yokoyama, A. Chainani, T. Takahashi, S.-J. Oh, N. Sato, and T. Komatsubara, 1996, *J. Phys. Soc. Jpn.* **65**, 2685.
- Yano, K., T. Sakakibara, T. Tayama, M. Yokoyama, H. Amitsuka, Y. Homma, P. Miranovic, M. Ichioka, Y. Tsutsumi, and K. Machida, 2008, *Phys. Rev. Lett.* **100**, 017004.
- Yaouanc, A., P. Dalmas de Réotier, G. van der Laan, A. Hiess, J. Goulon, C. Neumann, P. Lejay, and N. Sato, 1998, *Phys. Rev. B* **58**, 8793.
- Yashima, M., S. Kawasaki, Y. Kawasaki, G. q. Zheng, Y. Kitaoka, H. Shishido, R. Settai, Y. Haga, and Y. Onuki, 2004, *J. Phys. Soc. Jpn.* **73**, 2073.
- Yasuda, T., H. Shishido, T. Ueda, S. Hashimoto, R. Settai, T. Takeuchi, T. D. Matsuda, Y. Haga, and Y. Onuki, 2004, *J. Phys. Soc. Jpn.* **73**, 1657.
- Yelland, E. A., S. M. Hayden, S. J. C. Yates, C. Pfeleiderer, M. Uhlarz, R. Vollmer, H. v. Löhneysen, N. R. Bernhoeft, R. P. Smith, S. S. Saxena, and N. Kimura, 2005, e-print arXiv:cond-mat/0502341.
- Yin, G. and K. Maki, 1993, *Phys. Rev. B* **48**, 650.
- Yogi, M., Y. K. S. Hashimoto, T. Yasuda, R. Settai, T. D. Matsuda, Y. Haga, Y. Onuki, P. Rogl, and E. Bauer, 2004, *Phys. Rev. Lett.* **93**, 027003.
- Yogi, M., H. Mukuda, Y. Kitaoka, S. Hashimoto, T. Yasuda, R. Settai, T. D. Matsuda, Y. Haga, Y. Onuki, P. Rogl, and E. Bauer, 2006, *J. Phys. Soc. Jpn.* **75**, 013709.
- Yogi, M., T. Nagai, Y. Imamura, H. Mukuda, Y. Kitaoka, D. Kikuchi, H. Sugawara, Y. Aoki, H. Sato, and H. Harima, 2008, *J. Phys. Soc. Jpn.* **77**, 31.
- Yokoyama, M., H. Amitsuka, K. Tenya, K. Watanabe, S. Kawarazaki, H. Yoshizawa, and J. A. Mydosh, 2005, *Phys. Rev. B* **72**, 214419.
- Yokoyama, M., H. Amitsuka, K. Watanabe, S. Kawarazaki, H. Yoshizawa, and J. A. Mydosh, 2002, *J. Phys. Soc. Jpn. Suppl.* **71**, 264.
- Yokoyama, M., N. Oyama, H. Amitsuka, S. Oinuma, I. Kawasaki, K. Tenya, M. Matsuura, K. Hirota, and T. J. Sato, 2008, *Phys. Rev. B* **77**, 224501.
- Young, B.-L., R. R. Urbano, N. J. Curro, J. D. Thompson, J. L. Sarrao, A. B. Vorontsov, and M. J. Graf, 2007, *Phys. Rev. Lett.* **98**, 036402.
- Young, D. P., M. Moldovan, X. S. Wu, P. W. Adams, and J. Y. Chan, 2005, *Phys. Rev. Lett.* **94**, 107001.
- Yuan, H. Q., D. F. Agterberg, N. Hayashi, P. Badica, D. Vandervelde, K. Togano, M. Sigrist, and M. B. Salamon, 2006, *Phys. Rev. Lett.* **97**, 017006.
- Yuan, H. Q., F. M. Grosche, M. Deppe, C. Geibel, G. Sparn, and F. Steglich, 2003, *Science* **302**, 2104.
- Zapf, V. S., E. J. Freeman, E. D. Bauer, J. Petricka, C. Sirvent, N. A. Frederick, R. P. Dickey, and M. B. Maple, 2001, *Phys. Rev. B* **65**, 014506.
- Zheng, G., N. Yamaguchi, H. Kan, Y. Kitaoka, J. L. Sarrao, P. G. Pagliuso, N. O. Moreno, and J. D. Thompson, 2004, *Phys. Rev. B* **70**, 014511.
- Zheng, G.-q., K. Tanabe, T. Mito, S. Kawasaki, Y. Kitaoka, D. Aoki, Y. Haga, and Y. Onuki, 2001, *Phys. Rev. Lett.* **86**, 4664.
- Zwicknagl, G., and U. Pulst, 1993, *Physica B* **186-188**, 895.
- Zwicknagl, G., A. N. Yaresko, and P. Fulde, 2002, *Phys. Rev. B* **65**, 081103.